Development of a UHPLC/MS method for the analysis of triacylglycerols in oils, fats and milk products

Marina Chanidou

A thesis submitted to the University of York in fulfilment of the requirements for the degree of Doctor of Philosophy

University of York

Department of Chemistry

September 2018

Abstract

A two-stage reversed-phase ultra high performance liquid chromatography (UHPLC) separation coupled with Orbitrap-MS was developed for the separation of triacylglycerols (TAGs) in milk, animal fats and vegetable oils. The method constitutes a significant improvement compared with existing methods, achieving separation of positional isomers and identifying a great number of TAGs with equivalent carbon numbers (ECNs) ranging between 26 and 56. This is achieved in a third of the time of the method most highly cited in the literature.

Unlike previously developed methods, the UHPLC-MS method is appropriate for the analysis of samples of a wide range of biological sources. A total of 90 samples analysed with the method include 37 fats from meat products, 37 oils and fats from plant material, 6 milk fat extracts, 2 infant formula milk fat extracts and 6 forensic samples suspected to contain residues of infant formula milk. Statistical analysis of the results resulted in groups of samples with the same or similar origins. Separate groups of olive oil, sunflower oil, sesame seed oil, soya, pork and cow milk samples were produced, along with a group including both beef and lamb samples and a group including different types of poultry samples (chicken, duck and goose). Milk and infant formula milk were categorised in two different groups, although the brand of infant milk formula could not be positively determined.

TAGs important for the discrimination between species were identified. Most abundant peaks for each type of sample were identified and were usually the most important variables between different types of samples. In olive oil those peaks were identified as OOO and OOP*, in rapeseed oil OOO and OOL*. In both sunflower and sesame seed oil the two most abundant TAGs were LLL and LLO, with LLL being the highest one in sunflower and LLO in sesame seed. The most abundant TAGs in beef and lamb were OOP*, POP* and OOS, while in pork they were OPO*, LPO and SPO*. For all three types of poultry analysed OOP* and OOO were amongst the highest abundance TAGs. Milk fat samples had significantly more TAG components than oils and animal fats, but all cow milk samples had higher abundances for PPC_4, PMC_4 and OPP. The TAGs with the highest abundance for goat milk were PPC_4, PPCa and OPO. Positional isomers of TAGs are another indicator for the identity of samples, especially in the case of animal fats. Beef and lamb fat samples have very similar TAG distributions, but beef fat contains only the SOS* isomer while lamb fat contains both SOS* and SSO* and pork and poultry contain only SSO*.

This work shows that a single UHPLC method can be applied for the analysis and identification of TAGs in oils and fats of plant and animal origin and the variations of TAG distribution and relative abundances are sufficient for the identification of the sample's origin in most cases.

Contents

Abstract 2

List of tables 6

List of figures 10

ACKNOWLEDGEMENTS 18

AUTHOR'S DECLARATION 19

1 Introduction 20

1.1 Triacylglycerols 20

1.1.1 Structure and properties 20

1.2 Developments in TAG analysis for food chemistry 22

1.2.1 Charged Aerosol Detector (CAD) 23

1.2.2 Orbitrap 25

1.2.3 Coupling UHPLC and Orbitrap 25

1.3 Aims and objectives 26

2 Experimental 27

2.1 Samples 27

2.2 Sample preparation 28

2.2.1 Open column fractionation 28

2.2.2 Fraction collection according to ECN 29

2.3 Separation techniques 30

2.3.1 UHPLC method 30

2.3.1.1 Mass spectrometry 31

2.3.2 Two stage separation 31

2.3.2.1 Method ECN 26-40 31

2.3.2.2 Method ECN 42-56 32

3 Development of a single stage RP UHPLC separation of TAGs in various milk samples 33

3.1 Introduction 33

3.2 Results and discussion 35

3.2.1 Method development 35

3.2.2 51

3.2.3 Mass spectrometric analysis of milk TAGs 55

3.3 Conclusions 78

4 Development of two stage separation method for TAGs 80

4.1 Introduction 80

4.2 Results and discussion 81

4.2.1 Method development 81

4.2.1.1 Two stage separation 81

4.2.1.2 UHPLC separation in two stages 91

4.2.2 Separation of cow's milk TAGs with methods ECN26-40 and ECN42-56 96

4.2.3 PCA of results 105

4.3 Conclusions 109

5 Application of RP UHPLC separation of TAGs to fat and oil samples 110

5.1 Introduction 110

5.2 Results and discussion 111

5.2.1 Chromatograms of vegetable oils 111

5.2.2 Chromatograms of animal fats 118

5.2.3 PCA of oils and fats 121

5.2.4 PCA of vegetable oils, animal fats and milk samples 130

5.3 Chapter conclusions/overview 132

6 Application of two stage method on forensic case 133

6.1 Introduction 133

6.2 Results and discussion 134

6.2.1 Forensic case, baby gro experiment 134

6.2.2 PCA of samples 139

6.2.3 PCA of results from all chapters 141

6.3 Chapter conclusions/overview 144

7 Conclusions and further work 145

7.1 Conclusions 145

7.2 Further work 146

Appendix A 147

Appendix B 148

Appendix C 151

Abbreviations 168

References 169

List of tables

Table 2.1: Number of samples for each type of fat 27

Table 2.2: Number of samples for each type of oil 27

Table 2.3: Mobile phase gradient of fraction collection method for HPLC separation of TAGs and collection of fractions. Flow rate 1 mL/min. 29

Table 2.4: Program parameters for collecting sample fractions with TIME PROG mode of 201 Gilson fraction collector. 29

Table 2.5: Fraction collection times for fraction collection method (Table 2.3) 30

Table 2.6: Mobile phase gradient for UHPLC separation of TAGs (Method S) 30

Table 2.7: Mass range for the selection of the most abundant ion for MS^2 (Method S) 31

Table 2.8: Mobile phase gradient for UHPLC separation of TAGs (Method ECN 26-40) 31

Table 2.9: Mass range for the selection of the most abundant ion for MS^2 (Method ECN 26-40) 32

Table 2.10: Mobile phase gradient for UHPLC separation of TAGs (Method ECN 42-56) 32

Table 2.11: Mass range for the selection of the most abundant ion for MS^2 (Method ECN 42-56) 32

Table 3.1: Mobile phase gradient of Method J (Hasan, 2010) for HPLC separation of TAGs. Flow rate 1 mL/min. 35

Table 3.2: Response factors (RFs) of 19 single acid triacyglycerol (TAG) standards using charged aerosol detection (CAD) and atmospheric pressure chemical ionisation (APCI) in relation to triolein (C18:1 C18:1 C18:1) which is set to 1.00. 38

Table 3.3: Mobile phase gradient of Method A for UHPLC separation of TAGs. Flow rate 0.7 mL/min. Temperature controlled at 60°C. 39

Table 3.4: Percentage of method time where ranges of TAGs elute for Methods C and D. 42

Table 3.5: Mobile phase gradient of Methods D, E and F for UHPLC separation of TAGs. Flow rate 0.3 mL/min. Temperature controlled at 40°C. 42

Table 3.6: Mobile phase gradient of Methods F, G and H for UHPLC separation of TAGs. Flow rate 0.3 mL/min. Temperature controlled at 40°C. 44

Table 3.7: Flow rate and temperature conditions for methods I, J and K. The eluent composition and gradient is the same for all three methods and the same with method H (.. 45

Table 3.8: Mobile phase gradient of Methods M, N and O for UHPLC separation of TAGs. Flow rate 0.45 mL/min. Temperature controlled at 50°C. The solvents used were A: Methanol (95%) and ammonium acetate in methanol (10 mM; 5%), B: Acetonitrile, C: Dichloromethane and D: Water. The changes made to dichloromethane and acetonitrile are highlighted. Percentages are rounded to 2 significant figures. 48

Table 3.9: Mobile phase gradient of Methods P and Q for UHPLC separation of TAGs. Flow rate 0.45 mL/min. Temperature controlled at 50°C. The solvents used were A: Methanol (95%) and ammonium acetate in methanol (10 mM; 5%), B: Acetonitrile, C: Dichloromethane and D: Water. The changes made to dichloromethane and acetonitrile are highlighted. Percentages are rounded to 2 significant figures. 50

Table 3.10: Mobile phase gradient of Method R for UHPLC separation of TAGs. Flow rate 0.45 mL/min. Temperature controlled at 50°C. The solvents used were A: Methanol (95%) and ammonium acetate in methanol (10 mM; 5%), B: Acetonitrile, C: Dichloromethane and D: Water. The changes made to dichloromethane and acetonitrile are highlighted. Percentages are rounded to 2 significant figures. 51

Table 3.11: Mobile phase gradient of Method S for UHPLC separation of TAGs. Flow rate 0.45 mL/min. Temperature controlled at 46°C. The solvents used were A: Methanol (90%) and ammonium acetate in methanol (10 mM; 10%), B: Acetonitrile, C: Dichloromethane and D: Water. Percentages are rounded to 2 significant figures. 54

Table 3.12: TAGs identified in cow milk analysed using Method S (Table 3.11; Figure 3.18) giving *m*/*z* values of ammonium adduct ions, $[M+NH_4]^+$, proton adduct ions, $[M+H]^+$, and DAG product ions, $[M-RCO_2]^+$. Tentative TAG identifications are enclosed in using brackets. Multiple positional isomers of the TAGs could not be distinguished apart from a small number of cases where the TAG in question is labelled as ABC*, meaning the acyl group in position sn-2 is B and positions sn-1 and sn-3 are occupied by either A or C. The abbreviations used for the acyl groups are explained in Abbreviations. 59

Table 3.13: TAGs identified in Beccaria et al. (2014) and in the present study. No positional isomers were identified in Beccaria et al. (2014). 76

Table 4.1: Mobile phase gradient of fraction collection method for HPLC separation of TAGs and collection of fractions. Flow rate 1 mL/min. 81

Table 4.2: Fraction numbers and the corresponding ECN of TAGs collected. 81

Table 4.3: Eluent composition of Method S at the retention time windows for components of different ECNS regions where separation of TAGs was incomplete, i.e. ECNs 42, 44, 46 and 48. 83

Table 4.4: Mobile phase gradient of Methods ECN42-56_A and ECN42-56 for UHPLC separation of TAGs. Flow rate 0.55 mL/min. Temperature controlled at 40°C. The solvents used were A: Acetonitrile, B: Dichloromethane and C: Ammonium acetate in methanol (10 mM; 10%). 92

Table 4.5: Mobile phase gradient of Methods ECN26-40_A, ECN26-40_B and ECN26-40 for UHPLC separation of TAGs. Flow rate 0.45 mL/min. Temperature controlled at 40°C for ECN26-40_A and at 50°C for ECN26-40_B and ECN26-40. The solvents used were A: Methanol (90%) and ammonium acetate in methanol (10 mM; 10%), B: Acetonitrile, C: Dichloromethane and D: Water 94

Table 4.6: TAGs identified in cow milk analysed using Methods ECN26-40 (Table 4.5, Figure 4.14) and ECN42-56 (Table 4.4, Figure 4.13) giving m/z values of ammonium adduct ions, [M+NH4]+, proton adduct ions, [M+H]+, and DAG product ions, [M-RCO2]+. Tentative TAG identifications are enclosed in brackets. Multiple positional isomers of the TAGs could not be distinguished apart from a small number of cases where the TAG in question is labelled as ABC*, meaning the acyl group in position sn-2 is B and positions sn-1 and sn-3 are occupied by either A or C. The abbreviations used for the acyl groups are explained in Abbreviations 97

Table 4.7: TAG identification for peaks of Figure 4.15. 102

Table 4.8: TAGs identified with Method S and TAGs identified with the two stage approach. 103

Table 5.1: TAGs identified in different products of plant origin using in base peakchromatographs using Method ECN42-56 (Table 4.4). The TAGs are listed in retention time order. The relative abundance of peaks corresponding to TAGs identified was used as a second component for the identification of samples. The values given in the table below are averages for the relative abundance of the same peak for samples of the same type. Only TAGs corresponding to peaks with relative abundances higher than 0.1 are listed. 115

Table 5.2: TAGs identified in different products of plant origin using in base peakchromatographs using Method ECN42-56 (Table 4.4). The TAGs are listed in retention

time order. The relative abundance of peaks corresponding to TAGs identified was used as a second component for the identification of samples. The values given in the table below are averages for the relative abundance of the same peak for samples of the same type. Only TAGs corresponding to peaks with relative abundances higher than 0.1 are listed. 120

Table 6.1: Weight of sample extracted from each sampling position that was consequently dissolved in appropriate organic solvent for analysis..... 135

Table 6.2: TAGs identified in infant milk samples in base peakchromatographs Methods ECN26-40 (Table 4.5, Figure 4.14) and ECN42-56 (Table 4.4, Figure 4.13). The TAGs are listed in retention time order. The relative abundance of peaks corresponding to TAGs identified was used as a second component for the identification of samples. Only TAGs corresponding to peaks with relative abundances higher than 0.1 are listed. 138

List of figures

Figure 1.1: Structure of triacylglycerol with all three acyl groups having 18 carbons and no double bonds. The glycerol backbone is highlighted by the blue box and one of the three acyl chains by a red box. The three carbons on the glycerol backbone are numbered and the positions of the acyl chains are named sn1, sn2 and sn3. The common abbreviation for this triacylglycerol is SSS, since it contains three residues of stearic acid..... 20

Figure 1.2: Schematic of Charged Aerosol Detector (CAD)..... 24

Figure 3.1: Partial base peak RP LC-APCI MS chromatogram of commercial full fat cow milk sample analysed with Method J (Table 3.1) developed by Hasan (2010). Regions are assigned according to ECN..... 36

Figure 3.2: Total ion current NARP LC-APCI MS chromatogram of cow milk sample on three serially coupled Ascentis Express C18 columns, with mobile phase flow rate 1 mL/min and mobile phase gradient: 0 min, 100% acetonitrile; 150 min, 30% acetonitrile, 70% isopropanol (hold for 15 min); 168 min, 100% acetonitrile. Regions are assigned according to ECN. (Modified from Beccaria et al., 2014)..... 36

Figure 3.3: Partial RP UHPLC-CAD chromatogram of commercial full fat cow milk sample analysed with Method A (Beccaria et al., 2014) Regions are assigned according to ECN..... 39

Figure 3.4: Partial RP UHPLC-CAD chromatogram of commercial full fat cow milk sample analysed with Method B (temperature controlled at 40^{o}C; flow rate = 0.45 mL/min; isocratic elution MeOH 90%, DCM 10%). Regions are assigned according to ECN..... 40

Figure 3.5: Partial RP UHPLC-CAD chromatogram of commercial full fat cow milk sample analysed with Method C (temperature controlled at 40^{o}C; flow rate = 0.45 mL/min; isocratic elution methanol 80%, dichloromethane 10% , acetonitrile 10%). Regions are assigned according to ECN..... 41

Figure 3.6: Partial RP UHPLC-CAD chromatogram of commercial full fat cow milk sample analysed with Method D (temperature controlled at 40^{o}C; flow rate = 0.3 mL/min; 78% methanol, 10% acetonitrile, 10% dichloromethane, 2% water, composition at 10 min: 80% methanol, 10% acetonitrile, 10% dichloromethane). Regions are assigned according to ECN.. 41

Figure 3.7: Partial RP UHPLC-CAD chromatograms of commercial full fat cow milk sample analysed with Methods D (10% acetonitrile), E (5% acetonitrile) and F (15% acetonitrile) (Table

3.5). Red square boxes include TAGs with ECN 38, blue rectangle boxes include TAGs with ECN 44 and blue ovals include TAGs with ECN 48. 43

Figure 3.8: Partial RP UHPLC-CAD chromatograms of commercial full fat cow milk sample analysed with Methods F, G and H (Beccaria et al., 2014). Blue rectangle boxes include TAGs with ECN 46. 44

Figure 3.9: Partial RP UHPLC-APCI MS base peak chromatograms of commercial full fat cow milk sample analysed with Methods I, J and K (Table 3.7). Regions are assigned according to ECN. 46

Figure 3.10: Partial RP UHPLC-APCI MS base peak chromatograms of commercial full fat cow milk sample analysed with Methods K (Table 3.7) and L (same as Method K, with dichloromethane lowered to 7%) during time ranges: a) 3.5 to 10 min and b) 12 to 30 min. Regions are assigned according to ECN. 47

Figure 3.11: Partial RP UHPLC-APCI MS base peak chromatograms of commercial full fat cow milk sample analysed with Methods M, N and O (Table 3.8 48

Figure 3.12: Partial RP UHPLC-APCI MS base peak chromatograms of commercial full fat cow milk sample analysed with Methods P and Q (Beccaria et al., 2014). Regions are assigned according to ECN. 50

Figure 3.13: Partial RP UHPLC-APCI MS base peak chromatogram of commercial full fat cow milk sample analysed with Method R (Table 3.10). Regions are assigned according to ECN..... 52

Figure 3.14: APCI-MS spectrum of peak at 19.72 min of Figure 3.13. 53

Figure 3.15: Orbitrap MS detector Partial RP UHPLC-APCI MS base peak chromatograms of commercial full fat cow milk sample analysed with Methods R_a, R_b and R_c (Methods described in Table 3.10 with solvent A: methanol 100% for method R_a; methanol 90%, ammonium acetate [in methanol 10mM] 10% for method R_b; ammonium acetate [in methanol 10mM] 100% for method R_c) 53

Figure 3.16: Partial RP UHPLC-APCI MS base peak chromatogram of commercial full fat cow milk sample analysed with Method S (Table 3.11). Regions are assigned according to ECN. 54

Figure 3.17: Partial RP UHPLC-APCI MS base peak chromatogram of a commercial full fat cow milk sample analysed with Method S (Table 3.11). Regions are assigned according to ECN. Peaks are labelled with *m/z* value of the ammonium adduct ion. 56

Figure 3.18 Partial RP UHPLC-APCI MS base peak chromatogram of a commercial full fat cow milk sample analysed with Method S (Table 3.11). Regions are assigned according to ECN. Peaks are labelled with *m*/*z* value of the ammonium adduct ion. 57

Figure 3.19: APCI-MS spectrum summed over peak 55 (..... 63

Figure 3.20: MS^2 spectrum from proton adduct ion at *m*/*z* 885.79 summed over peak 55 (.... 63

Figure 3.21: APCI-MS spectrum across peak 56 (..... 65

Figure 3.22: MS^2 spectrum from proton adduct ion at *m*/*z* 859.78 across peak 56 (..... 65

Figure 3.23: APCI-MS spectrum across peak 20 (..... 66

Figure 3.24: MS^2 spectrum from ammonium adduct ion at *m*/*z* 628.55 across peak 20 (..... 66

Figure 3.25: APCI-MS spectrum across peak 14 (..... 67

Figure 3.26: MS^2 spectrum from ammonium adduct ion at *m*/*z* 600.52 across peak 14 (..... 68

Figure 3.27: APCI-MS spectrum across peak 39 (..... 69

Figure 3.28: MS^2 spectrum from ammonium adduct ion at *m*/*z* 684.61 across peak 39 (..... 69

Figure 3.29: MS^2 spectrum from ammonium adduct ion at *m*/*z* 710.63 across peak 39 (Table 3.12 70

Figure 3.30: APCI-MS spectrum across peak 45 (..... 71

Figure 3.31: MS^2 spectrum from ammonium adduct ion at *m*/*z* 712.65 across peak 45 (..... 71

Figure 3.32: MS^2 spectrum from ammonium adduct ion at *m*/*z* 738.66 across peak 45 (Table 3.12 72

Figure 3.33: APCI-MS spectrum across peak 67 (..... 73

Figure 3.34: Correlation between the relative abundance of the proton adduct ion of a peak and the number of double bonds of the TAG suspected to elute. The circled data points represent TAGs that exhibited proton adduct ion peaks smaller than expected from the literature and the number of double bonds present. 1) LMC4 2) LPC4 and OPoC4 3) LPC4 4) LPP 5) OPMo 6) OOO and 7) OOMa..... 74

Figure 3.35: Correlation between the percentage of Solvent A (Methanol (90%) and ammonium acetate in methanol (10 mM; 10%; Table 3.11) in the mobile phase and the relative abundance of the ammonium adduct ion detected in the MS spectrum of the peak. 75

Figure 4.1: Partial base peak RP LC-APCI MS chromatogram of olive oil sample analysed with fraction collection method (Table 2.3). Regions represent fractions collected (Table 2.5). 82

Figure 4.2: Partial RP UHPLC-APCI MS base peak chromatogram of olive oil sample analysed with Method S (Table 3.11). Regions are assigned according to ECN. 82

Figure 4.3: Partial RP UHPLC-APCI MS base peak chromatogram of fraction 6 (Table 2.5) of olive oil sample analysed with Method ECN48_A (isocratic elution, acetonitrile (70%), dichloromethane (25%) and ammonium acetate in methanol (10 mM; 10%) (5%), temperature 50^{o}C, flow rate: 0.45 mL/min). TAGs OOO, OOP, OPP and OOG were identified with MS and the peaks are labelled accordingly. 83

Figure 4.4: Partial RP UHPLC-APCI MS base peak chromatogram of fraction 6 (Table 2.5) of olive oil sample analysed with Method ECN48_B (isocratic elution, acetonitrile (70%), dichloromethane (25%) and ammonium acetate in methanol (10 mM; 10%) (5%), temperature 50^{o}C, flow rate: 0.65 mL/min). TAGs OOO, OOP, OPP and OOG were identified with MS and the peaks are labelled accordingly. 84

Figure 4.5: Partial RP UHPLC-APCI MS base peak chromatogram of fraction 6 (Table 2.5) of olive oil sample analysed with Method ECN48_C (isocratic elution, acetonitrile (70%), dichloromethane (25%) and ammonium acetate in methanol (10 mM; 10%) (5%), temperature 40^{o}C, flow rate: 0.45 mL/min). TAGs OOO, OOP, OPP and OOG were identified with MS and the peaks are labelled accordingly. 85

Figure 4.6: Partial RP UHPLC-APCI MS base peak chromatogram of fraction 6 (Table 2.5) of olive oil sample analysed with Method ECN48_D (isocratic elution, acetonitrile (70%), dichloromethane (25%) and ammonium acetate in methanol (10 mM; 10%) (5%), temperature 40^{o}C, flow rate: 0.60 mL/min). TAGs OOO, OOP, OPP and OOG were identified with MS and the peaks are labelled accordingly. 86

Figure 4.7: Partial RP UHPLC-APCI MS base peak chromatogram of fraction 4 (Table 2.5) of olive oil sample analysed with Method ECN44_A (isocratic elution, acetonitrile (75%), dichloromethane (20%) and ammonium acetate in methanol (10 mM; 10%) (5%), temperature 40^{o}C, flow rate: 0.55 mL/min). TAGs LLO, LnOO and LnOP were identified with MS and the peaks are labelled accordingly. 87

Figure 4.8: Partial RP UHPLC-APCI MS base peak chromatogram of fraction 4 (Table 2.5) of olive oil sample analysed with Method ECN44_B (isocratic elution, acetonitrile (75%), dichloromethane (15%) and ammonium acetate in methanol (10 mM; 10%) (10%), temperature 40°C, flow rate: 0.55 mL/min). TAGs LLO, LnOO and LnOP were identified with MS and the peaks are labelled accordingly. 88

Figure 4.9: Partial RP UHPLC-APCI MS base peak chromatogram of fraction 3 (Table 2.5) of olive oil sample analysed with Method ECN42_A (isocratic elution, acetonitrile (70%), dichloromethane (20%) and ammonium acetate in methanol (10 mM; 10%) (10%), temperature 40°C, flow rate: 0.60 mL/min). TAGs LLL, OLLn and PLLn were identified with MS and the peaks are labelled accordingly. 89

Figure 4.10: Partial RP UHPLC-APCI MS base peak chromatogram of fraction 5 (Table 2.5) of olive oil sample analysed with Method ECN46_A (isocratic elution, acetonitrile (60%), dichloromethane (35%) and ammonium acetate in methanol (10 mM; 10%) (5%), temperature 40°C, flow rate: 0.60 mL/min). TAGs OOL, OOPo, OLP and OPPo were identified with MS and the peaks are labelled accordingly. TAG OLP co-elutes with OOPo at peak with apex RT 1.85 min and with OPPo at peak with apex RT 1.92 min. 90

Figure 4.11: Partial RP UHPLC-APCI MS base peak chromatogram of fraction 5 (Table 2.5) of olive oil sample analysed with Method ECN46_B (isocratic elution, acetonitrile (65%), dichloromethane (30%) and ammonium acetate in methanol (10 mM; 10%) (5%), temperature 40°C, flow rate: 0.60 mL/min). TAGs OOL, OLP, PPL and OPPo were identified with MS and the peaks are labelled accordingly. TAGs PPL and OPPo co-elute. 91

Figure 4.12: Partial RP UHPLC-APCI MS base peak chromatograms of olive oil sample analysed with Methods ECN42-56_A (top) and ECN42-56 (bottom) (Table 4.4). 93

Figure 4.13: Partial RP UHPLC-APCI MS base peak chromatograms of cow milk sample analysed with Methods ECN42-56_A (top) and ECN42-56 (bottom) (Table 4.4). 93

Figure 4.14: Partial RP UHPLC-APCI MS base peak chromatograms of cow milk sample analysed with Methods ECN26-40_A (top) ECN26-40_B (middle) and ECN26-40 (bottom) (Table 4.5)... 95

Figure 4.15: Partial RP UHPLC-APCI MS base peak chromatograms of cow milk sample analysed with Methods S (Table 3.11) (top) and ECN26-40 (Table 4.5) (bottom) (Table 4.5). The region depicted in both chromatograms shows the peaks attributed to TAGs with ECN 38 and the integration of the peaks is shown as well. The numbers above each peak correspond to the

identification of the TAGs of each peak with can be found in Table 3.12 for Method S (top) and in Table 4.6 for Method ECN26-40 (bottom). 101

Figure 4.16: PCA plot of unscaled data for milk samples. PC1 contribution to variance 80.8%. PC2 contribution to variance 8.9%. GM01 is a goat milk sample and CM01-CM05 are cow milk samples. More details on all samples can be found in Appendix B. Scree plot and loading plots can be found in Appendix C (pages 149, 152 and 153)..... 106

Figure 4.17: PCA plot of scaled data for milk samples. PC1 contribution to variance 61.7%. PC2 contribution to variance 16.8%. GM01 is a goat milk sample and CM01-CM05 are cow milk samples. More details on all samples can be found in Appendix B. 107

Figure 4.18: Dendrogram of milk samples. GM01 is a goat milk sample and CM01-CM05 are cow milk samples. More details on all samples can be found in Appendix B. 108

Figure 5.1: Partial RP UHPLC-APCI MS base peak chromatograms of almond milk, rice bran oil, rice milk, groundnut oil and corn oil samples analysed with Method ECN42-56 (Table 4.4). Regions are assigned according to ECN. 112

Figure 5.2: Partial RP UHPLC-APCI MS base peak chromatograms of walnut oil, grapeseed oil, coconut milk, soya milk and sesame seed oil samples analysed with Method ECN42-56 (Table 4.4). Regions are assigned according to ECN. 113

Figure 5.3: Partial RP UHPLC-APCI MS base peak chromatograms of olive oil, sunflower oil, rapeseed oil and mix vegetable oil analysed with Method ECN42-56 (Table 4.4). Regions are assigned according to ECN. 114

Figure 5.4: Partial RP UHPLC-APCI MS base peak chromatograms of beef, lamb and pork fat samples analysed with Method ECN42-56 (Table 4.4). Regions are assigned according to ECN. 118

Figure 5.5: Partial RP UHPLC-APCI MS base peak chromatograms of chicken, duck and goose fat samples analysed with Method ECN42-56 (Table 4.4). Regions are assigned according to ECN. 119

Figure 5.6: PCA plot of unscaled data for oils and fats from products of plant origin. PC1 contribution to variance 71.7%. PC2 contribution to variance 12.4%. Samples O01-O08 are olive oil samples, S01-S07 are sunflower oil samples, R01-R06 are rapeseed oil samples, SE01-SE05 are sesame seed oil samples, MM01-MM05 are milk products of plant origin, CR01 is corn oil sample, GN01 is groundnut oil, GR01 is grapeseed oil, RB01 is rice bran oil, V01 is a mix

blend of vegetable oils and W01 is walnut oil. More details on all samples can be found in Appendix B. Scree plot and loading plots can be found in Appendix C (pages 149, 154 and 155). 122

Figure 5.7: Dendrogram of vegetable oil samples. Samples O01-O08 are olive oil samples, S01-S07 are sunflower oil samples, R01-R06 are rapeseed oil samples, SE01-SE05 are sesame seed oil samples, MM01-MM05 are milk products of plant origin, CR01 is corn oil sample, GN01 is groundnut oil, GR01 is grapeseed oil, RB01 is rice bran oil, V01 is a mix blend of vegetable oils and W01 is walnut oil More details on all samples can be found in Appendix B. 123

Figure 5.8: PCA plot of unscaled data for fats from products of animal origin. PC1 contribution to variance 73.5%. PC2 contribution to variance 13.4%. Samples P01-P18 are pork fat samples, B01-B05 are beef fat samples, L01 to L04 are lamb fat samples, C01-C04 are chicken fat samples, D01 to D04 are duck fat samples and G01 and G02 are goose fat samples. More details on all samples can be found in Appendix B. Scree plots and loading plots can be found in Appendix C (pages 150, 156 and 157)..... 125

Figure 5.9: PCA plot of unscaled data for fats from products of animal origin. PC1 contribution to variance 38.6%. PC3 contribution to variance 10.4%. Samples P01-P18 are pork fat samples, B01-B05 are beef fat samples, L01 to L04 are lamb fat samples, C01-C04 are chicken fat samples, D01 to D04 are duck fat samples and G01 and G02 are goose fat samples. More details on all samples can be found in Appendix B. Scree plots and loading plots can be found in Appendix C (pages 150, 156 and 158)..... 126

Figure 5.10: Dendrogram of fats from products of animal origin. Samples P01-P18 are pork fat samples, B01-B05 are beef fat samples, L01 to L04 are lamb fat samples, C01-C04 are chicken fat samples, D01 to D04 are duck fat samples and G01 and G02 are goose fat samples. More details on all samples can be found in Appendix B..... 127

Figure 5.11: Dendrogram of pork fat samples from different anatomical positions. Pink: leg, Black: shoulder, Blue: unknown, Aqua: belly, Brown: loin 128

Figure 5.12: Dendrogram of pork fat samples from different types of fat. Blue: unknown, Black: subcutaneous, Pink: intramuscular..... 129

Figure 5.13: Dendrogram of pork fat samples from different pigs. Blue: unknown, Black: pig A, Green: pig B, Brown: pig C 129

Figure 5.14: PCA plot of unscaled data for oils and fats from products of plant and animal origin including milks. PC1 contribution to variance 34.3%. PC2 contribution to variance 31.8%.

Sample codes as previously. More details on all samples can be found in Appendix B. Scree plots and loading plots can be found in Appendix C (pages 150, 159, 160 and 161). 130

Figure 5.15: Dendogram of oils and fats from products of plant and animal origin including milks. Sample codes as previously. More details on all samples can be found in Appendix B. 131

Figure 6.1: Sampling positions for forensic samples IM01 to IM06..... 134

Figure 6.2: Partial RP UHPLC-APCI MS base peak chromatograms of infant milk samples analysed with Method ECN28-40 (Table 4.5). IM01 is the forensic sample from sampling point 1, IM07 is the experimental sample created in the lab, IM09 and IM10 are two commercial brands of infant milk. Regions are assigned according to ECN..... 136

Figure 6.3: Partial RP UHPLC-APCI MS base peak chromatograms of infant milk samples samples analysed with Method ECN42-56 (Table 4.4). IM01 is the forensic sample from sampling point 1, IM07 is the experimental sample created in the lab, IM09 and IM10 are two commercial brands of infant milk. Regions are assigned according to ECN..... 137

Figure 6.4: PCA plot of unscaled data for milks and infant milks. PC1 contribution to variance 77.6%. PC2 contribution to variance 10.3%. More details on all samples can be found in Appendix B. 140

Figure 6.5: Dendogram of milk and infant milk samples. 141

Figure 6.6: PCA plot of unscaled data for oils and fats from products of plant and animal origin including milks and infant milks. PC1 contribution to variance 32.9%. PC2 contribution to variance 30.6%. Sample codes as previously. More details on all samples can be found in Appendix B. Scree plots and loading plots can be found in Appendix C (pages 151, 162, 163, 164 and 165). 142

Figure 6.7: Dendogram of samples of oils and fats from products of plant and animal origin including milks and infant milks. More details on all samples can be found in Appendix B. ... 143

ACKNOWLEDGEMENTS

I would firstly like to thank the Department of Chemistry for providing me with the funding without which I would not have been able to undertake and complete this research.

My thanks also go to my supervisor Brendan Keely for trusting me with this project, believing in me when I didn't and supporting me through good and hard times.

My gratitude to Matt Pickering, Ed Bergstrom and Julie Wilson for providing me with much needed training in a number of techniques. Thanks go also to Elizabeth Dickinson and Kirsty High for discussing my research with me and giving me valuable advice and encouragement. I would also like to thank my office mates Adam, Cezary and Scott for all the times we spend together, even though they drove me mad half the time.

Enormous thanks and gratitude go especially to Martina, Natta and Marianna. They made the last year of my PhD bearable, even enjoyable at times! I will miss our special tea and cake breaks more than anything. You have all been extremely encouraging and supportive.

I would also like to give special thanks to Kirsty Penkman for the advice and support she has provided me in her capacity of Chair of the Graduate School.

On a more personal note, I would like to thank all the health professionals who supported me during this journey, especially the people at York Mind. I would not have made it through without you. Thank you to all the people who came into my life during this journey, even the ones who have left before its end.

My deepest and most heartfelt thanks go to my friends, especially Emi and my moon circle, and to my family, especially to my wonderful mother Sophia to whom I own who I am today.

To my husband Mike, always.

AUTHOR'S DECLARATION

I hereby declare that the work described in this thesis is my own, except where otherwise acknowledged, and has not been submitted previously for a degree at this or any other university.

Marina Chanidou

1 Introduction

1.1 Triacylglycerols

The identification of triacylglycerols (TAGs) is of interest to many scientific fields, such as Food Chemistry where it is applied to characterize and authenticate fats and oils in food (Dugo et al., 2008; Herrero et al., 2009; Bosque-Sendra et al., 2012). The information obtained from this type of analysis is used to determine animal or plant species, geographical origin and the presence of adulterants (Bosque-Sendra et al., 2012). Archaeological studies focus on the detection of lipids to collect information about their use by past human societies (Regert, 2011). Finally, the field of lipidomics is concerned with the detailed analysis of lipids in a living organism (Harkewicz and Dennis, 2011).

1.1.1 Structure and properties

Triacylglycerols (TAGs) are a group of molecules that consist of a glycerol backbone and three fatty acid chains (FA). They are the main forms of stored energy for vertebrates and most lipids in human diet are TAGs. Fats and oils are mixtures of different TAGs found in human diet and fats are solid at body temperature while oils are liquid. Naturally occurring fats and oils can contain 20 to 30 different TAGs. The difference between these molecular species is the fatty acid chains attached to the glycerol backbone. Each fatty acid chain can have a different number of carbon atoms, with or without double bonds at different positions. Another difference is the position on the glycerol backbone that each chain is attached to (Figure 1.1).

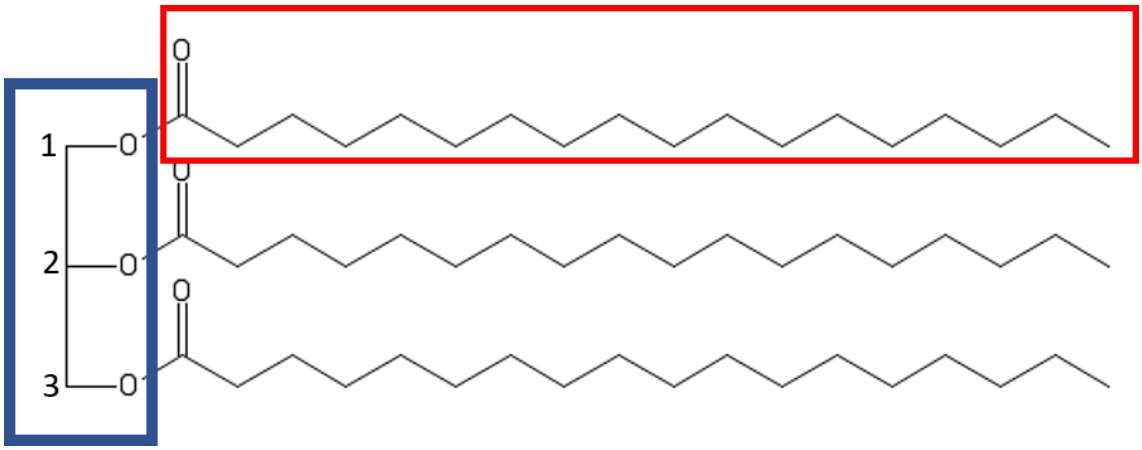

Figure 1.1: Structure of triacylglycerol with all three acyl groups having 18 carbons and no double bonds. The glycerol backbone is highlighted by the blue box and one of the three acyl chains by a red box. The three carbons on the glycerol backbone are numbered and the positions of the acyl chains are named sn1, sn2 and sn3. The common abbreviation for this triacylglycerol is SSS, since it contains three residues of stearic acid.

Most fatty acids have an even number of carbons which is a result of the biosynthesis mechanism. Enzymes in plants and mammals attach two carbon units to an acyl group so the resulting acyl chains are even numbered. Odd numbered acyl chains can be found in animal fats, because bacteria in stomachs of ruminants produce odd numbered chains.

The number of carbons and double bonds in each FA chain, the position of the double bonds in each chain and also the position of each chain on the glycerol backbone (sn1/sn3 or sn2) define an individual TAG molecule (Coultate and Davies, 2001). This leads to a large number of potential TAGs that can be present in a sample, but also allows the identification of the origin of the sample, because of the unique profile of TAGs in different fats and oils. TAGs can be categorised according to their equivalent carbon number (ECN) which can be calculated as follows:

$$ECN = CN + 2DB$$

where CN= number of carbon atoms in the molecule and DB= number of double bonds in the FA chains.

Animal fat comprises mostly of TAGs; adipose tissue is 90% TAGs (Ruiz-Gutiérrez and Barron, 1995).

1.1.2 Nomenclature

TAGs are named using abbreviated forms of the names of the fatty acids whose acyl moieties are attached to the glycerol backbone of each TAG. For example, stearic acid is the trivial name for octadecanoic acid, a fatty acid with 18 carbon atoms and no double bonds (Table 1.1). Tristearin or tristearoylglycerol is a TAG that consists of three acyl moieties with 18 carbon atoms each and no double bonds connected to the glycerol backbone and it is usually represented as SSS, for the three stearic moieties present in the molecule. All TAGs can be named in this way, using the abbreviated form of the fatty acid names. The order of the abbreviated forms in this nomenclature of the TAGs does not indicate the position of each acyl chain on the glycerol backbone. In this work, where the position of the acyl chain is known, the abbreviated form for the TAG will be followed by an asterisk (*). For example, a TAG with one oleic acyl chain and two stearic acid chains can be represented with the letter O and two S in any order without indicating position of the chain on the glycerol backbone, so OSS and SOS can both be used. On the other hand, if OSS* is mentioned, it refers to the TAG with a stearic acyl chain in the sn-2 position and either oleic or stearic chain in each of the sn-1/sn-3 positions and it is a different isomer from SOS*. Separation of this type of positional isomers is not always achieved for all TAGs (Mottram and Evershed, 1996; Gotoh et al., 2011).

Table 1.1 Fatty acids whose acyl moieties were detected in TAGs in the present work and their abbreviations used throughout.

Systemic name	Trivial name	Abbreviation	No of carbon atoms	No of Double bonds
butanoic	butyric	C_4	4	0
hexanoic	caproic	C_6	6	0
octanoic	caprylic	C	8	0
decanoic	capric	Ca	10	0
decenoic		$C_{10:1}$	10	1
dodecanoic	lauric	La	12	0
tetradecanoic	myristic	M	14	0
tetradecenoic	myristoleic	My	14	1
pentadecanoic		Pt	15	0
hexadecanoic	palmitic	P	16	0
hexadecenoic	palmitoleic	Po	16	1
heptadecanoic	margaric	Ma	17	0
heptadecenoic		Mo	17	1
octadecanoic	stearic	S	18	0
octadecenoic	oleic	O	18	1
octadecadienoic	linoleic	L	18	2
octadecatrienoic	linolenic	Ln	18	3
eicosenoic	gadoleic	G	20	1
eicosanoic	arachidic	C_{20}	20	0
docosanoic	behenic	$C_{22:0}$	22	0
docosenoic		$C_{22:1}$	22	1
tetracosanoic	lignoceric	C_{24}	24	0
tetracosenoic		$C_{24:1}$	24	1
hexacosanoic	cerotic	C_{26}	26	0

1.2 Developments in TAG analysis for food chemistry

1.2.1 Previous work/ existing literature

The application of HPLC to the separation of TAGs has been widely studied and is considered the most appropriate method for these types of molecules (Kuksis and Itabashi, 2005; Dugo et al., 2008; Herrero et al., 2009; Kalo and Kemppinen, 2012).

There are a number of reviews on the subject. Kuksis and Itabashi (2005) review the different liquid chromatography methods for the separation of regioisomers and stereoisomers of glycerolipids. They provide examples of separations, proposing different methods for the separation of different types of isomers, reverse phase HPLC to separate regioisomers, normal phase for diastereomers and chiral phase HPLC for enantiomers. Two reviews focus specifically on the use of multidimensional chromatography techniques for the analysis of various food samples (Dugo *et al.*, 2008; Herrero *et al.*, 2009). With regards to lipids, both reviews look at

off-line methods that combine silver ion HPLC (Ag-HPLC) with non-aqueous reverse phase HPLC (NARP-HPLC) in both the 1st and the 2nd dimension. There is also special mention of comprehensive LC x LC methods. The advantages and disadvantages of off-line, on-line and comprehensive systems are listed by Dugo *et al.* (2008).

A large number of studies over the past years have been dedicated to the study of the separation of TAGs using different HPLC methods. The majority of studies concern applications in food science and only a few deal with the application in archaeological science (Mottram et al., 2001; Evershed et al., 2002; Saliu et al., 2011). Most of the 2D methods reported are combinations of RP-HPLC and Ag-HPLC. A different approach combining RP-HPLC with UHPLC could have the potential to separate TAGs satisfactorily and in shorter time scales. Such an approach has not been explored in either of these areas of application.

Another topic insufficiently explored in the literature is TAGs with odd numbered fatty acids, which also means odd ECN. Few studies have detected TAGs with odd ECN (Lísa et al., 2011; Dugo et al., 2012, 2013; Beccaria et al., 2014) and those are very recent. Earlier studies of samples which are shown in this report to have TAGs with odd ECN (beef fat) have not reported those TAGs. For example Dugo *et al.* (2006), in the FA analysis report Pt, Ma and Mo (odd numbered FA) but no TAGs in the HPLC analysis contains these FA. Also, Kalo *et al.* (2004) analyse butterfat but report no TAGs with odd ECN. This is an area where further study is warranted.

Milk samples are of particular interest due to their complex nature. Also, differences between human breast milk and cow milk can be of forensic interest. There has been a number of very recent studies on this subject(Lopez et al., 2013; X. Zou et al., 2013a, 2013b; X.-Q. Zou et al., 2013; Linderborg et al., 2014; Villaseñor et al., 2014), but the development of a detailed and short method is still not achieved. The method used by Zou (X.-Q. Zou et al., 2013) is very similar to the method developed by Hasan (2010).

TAGs are increasingly being considered as molecular biomarkers for the discrimination of animal fats in archaeological samples, with HPLC especially coupled with APCI-MS as one of the main techniques for their analysis (Regert, 2011). An obvious gap in research is in the application of multidimensional techniques for TAG analysis in archaeological investigations. This could provide a wealth of information that is not currently available.

1.2.2 Charged Aerosol Detector (CAD)

Charged Aerosol Detectors (CAD) are an alternative to UV and ELSD detectors that are particularly suited for the detection of TAGs. TAGs do not usually have a chromophore group in their structure and so UV detectors are not appropriate. A CAD can be used for the detection

of non-volatile or semi-volatile molecules with no chromophores, so it has potential to be a good detector for TAG applications. The operating principle of this detector is an initial phase of nebulisation of the chromatographic eluent, during which the mobile phase is evaporated and dry particles of the analyte are formed. More analyte present results in larger particles formed. A stream of nitrogen gas ions, charged by a high voltage corona wire, collides with the analyte particles and the charge is transferred to them. The larger the particles of the analyte, the more surface for the electric charge. During the last phase, the charged analyte particles are collected and their charge is measured by a highly sensitive electrometer. The signal generated is directly proportional to the charge, which in turn is proportional to the amount of analyte.

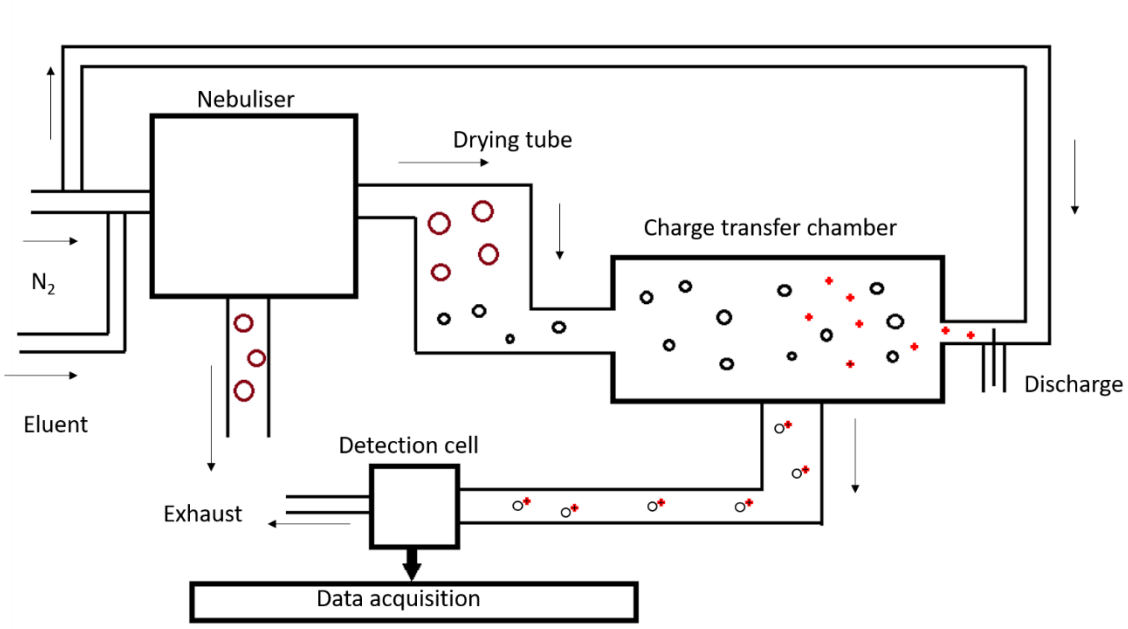

Figure 1.2: Schematic of Charged Aerosol Detector (CAD)

The principle of the detection method is not dependant on the structure or characteristics of the molecules analysed and the response signal is not affected by these factors, meaning that peak areas of different analytes are directly comparable. This is especially useful for quantification or relative quantification of unknown analytes or when standards are not available. The CAD also benefits from good linearity and range of detection.

Detection can be affected by the mobile phase, especially for gradient elution, but this can be solved with mobile phase compensation after the chromatographic column but before the detector. Additives to the mobile phase, such as buffers in high concentrations, can decrease the s/n ratio for CAD (Vehovec and Obreza, 2010).

1.2.3 Orbitrap

The principle of operation for the Orbitrap MS analyser was first described in 2000 and in 2005 the first analyser of this type became available and quickly developed into a mainstream technique.

The common feature of Orbitrap analysers is the use of an injection device trapping ions in an RF-only, gas-filled quadrupole called C-trap. The C-trap allows the accumulation of ions and then injection to the mass analyser in a short pulse. Ions with the same mass to charge ratio form a sub-microsecond pulse and are directed to the Orbitrap analyser. The process that follows is called "excitation by injection" and can be briefly described as follows. The Orbitrap analyser comprises of an outer curved electrode and a curved central electrode sustained at high voltage. The ions enter the space between the two electrodes at an angle and the strong electrical field inside the trap pushes them away from the external electrode, which leads to axial oscillations of the ions, while the ions are also rotating around the central electrode. This rotation keeps the ions from falling into the central electrode. The rotation depends on ion energies, angles and initial positions, which forces each ion packet (ions with same mass to charge ratio) to spread forming a thin rotating ring around the central electrode. The ring oscillates harmonically, proportionally to $(m/z)^{1/2}$ and an image current is produced on the outer electrode. The detection of this signal is followed by a Fourier Transformation (FT) (Makarov and Scigelova, 2010).

The Orbitrap analyser combines the use of a continuous ionisation source, such as APCI, with an accumulation device (C-trap) so that a higher number of ions can be detected. In this way, sensitivity is not as dependant on detection time as for other analysers. The C-trap also allows integration with additional devices, such as collision cells, for simultaneous experiments.

1.2.4 Coupling UHPLC and Orbitrap

Reversed phase columns packed with sub-2µm particles in UHPLC have been developed to deliver high efficiency in short times to face the demands of high sample throughput. Coupling UHPLC with MS analysers can cause problems because of differences in the mode of operation (Rodriguez *et al*, 2013). UHPLC chromatography usually performs optimally with flow rates of 0.5 to 1 mL/min, while mass analysers need much lower flow rates to achieve acceptable ionisation yields. APCI sources can be employed to mitigate this issue, because the ionisation technique is mass dependent and so the sensitivity increases with increased flow rates. Another issue is band broadening that has been associated with MS analysers. Lastly, the data acquisition rate of most MS analysers is not sufficient to acquire the recommended points per peak for quantification and suitable performance, since UHPLC peak widths can be as short as

2-4 s. This issue can be mitigated with the use of an Orbitrap analyser. As discussed in section 1.2.3, the sensitivity of the Orbitrap does not decrease significantly with increased acquisition points. The coupling of Orbitrap with UHPLC allows faster analysis without compromising resolution (Núñez *et al*, 2012). This can lead to increased number of analyses for samples with high complexity.

1.3 Aims and objectives

The aim of this work was to improve on existing methods of TAG separation and identification, while reducing the analysis time and producing a method that could be universally applied to all types of samples for the identification of TAGs. The method needed to work with complex samples, such as milk fats, that have been the most challenging for researchers. The potential applications of such a method to forensic and archaeological contexts was also of interest. Another aim was the determination of the TAG components characteristic for different types of samples.

Based on the aims detailed above, the following objectives were formulated:

- To develop a TAG separation method that is comparable or better than existing methods in terms of TAG separation, but also has shorter run time.
- To evaluate a multi-stage approach compared to a single stage separation.
- To analyse samples of different origins with the separation method developed and determine the efficacy of the method in identifying the type of sample analysed.
- To use the method to attempt to answer the questions posed by authorities in a forensic case and evaluate its potential for use in similar cases.

2 Experimental

2.1 Samples

All vegetable oil and animal fat samples were purchased from local stores (Table 2.1, Table 2.2). Different types of cow milk (full fat, semi-skimmed, skimmed), goat milk, coconut and almond milk, as well as baby formula milks were also purchased from supermarkets (details of samples reported in Appendix B).

Table 2.1: Number of samples for each type of fat

Type of fat	Number of samples
Pork	18
Beef	5
Lamb	4
Chicken	4
Duck	4
Goose	2
Cow milk	5
Goat milk	1
Infant milk	2

Table 2.2: Number of samples for each type of oil

Type of oil	Number of samples
Olive	8
Sunflower	7
Rapeseed	6
Sesame seed	5
Corn	1
Groundnut	1
Grapeseed	1
Rice bran	1
Walnut	1
Mix blend	1
Coconut milk	1
Almond milk	1
Rice milk	1
Soya milk	2

2.2 Sample preparation

Vegetable oils were dissolved in an appropriate solvent mix immediately prior to HPLC analysis. Animal fat samples (5 g) were macerated, submerged in a 2:1 mixture of $CHCl_3$:MeOH (20 ml:10 mL) and left for 24 h. The solution was filtered through cellulose filters and solvent was removed using a rotary evaporator. The dry extract was dissolved in hexane (5 ml) and washed with water (4 ml). The solution was allowed to separate and the organic phase was collected and filtered through DCM washed cotton wool. The remaining solvent was removed under a gentle stream of N_2. The extract was stored in the freezer (-20^{o}C) until it was analysed.

Store bought milk samples, cow, goat and infant milk, were prepared according to the method of Romeu-Nadal *et al.* (2004). Briefly, milk samples (3 mL) were mixed with DCM/MeOH (27 mL, 2:1 v/v) in centrifuge vials. The vials were shaken (15 min) and centrifuged at 2500 x g for 8 min at 6^{o}C. Distilled water (8 mL) was added to the vials prior to shaking and centrifugation as before. The upper, aqueous, layer was removed by pipette and the organic layer was washed with saturated NaCl (8 mL) before being shaken and centrifuged. The samples were transferred to a separating funnel and the organic (lower) layer was collected in pre-weighed vials. The solvent was removed using a Christ rotary vacuum centrifuge (RVC; 60 min). The extracted fat was stored in the freezer (-20^{o}C) until it was analysed.

2.2.1 Open column fractionation

Milk samples were subjected to open column chromatography fractionation to ensure that only TAGs were present in samples analysed. The method used for fractionation is described in Pickering et al. (2018). The extracted fat (10 mg) was dissolved in DCM (200 µL) and the solution was added to silica gel 60 (c. 50 mg) and dried using a rotary vacuum evaporator (RVC). Small scale silica chromatography columns (10 mm i.d., 90 mm height) were dry packed and washed by successive elution with DCM: MeOH (2:1 v/v, 6 mL), DCM (3 mL) and finally hexane: toluene (10:1, v/v, 6 mL). The extract impregnated silica was loaded onto a small scale column and fraction F1 was collected by elution with hexane:toluene (10:1, v/v, 3.5 mL), fraction F2 by elution with hexane: ethyl acetate (4:1, v/v, 3.5 mL) and fraction F3 by elution with DCM: MeOH (1:1, v/v, 3.5 mL). Fractions were collected in pre-weighed vials, the solvent was removed by RVC and the masses were recorded. Fraction F2, containing TAGs, was subjected to analysis.

2.2.2 Fraction collection according to ECN

The olive oil fractions were collected by splitting the HPLC outlet between the detector and a 201 Gilson fraction collector. The column used was a Waters XBRIDGE C18 column (4.6 mm x 150 mm, 5 µm, 18% C loading) and the mobile phase consisted of acetonitrile and isopropanol (Table 2.3). The column was maintained at 35°C, samples (20 µL) were dissolved in a hexane: acetonitrile: isopropanol mixture (980 µl, 1:1:1 v/v/v) and the injection volume was 20 µL. The fraction collector operated under TIME PROG mode (Table 2.4) to allow collection at pre-programmed time periods (Table 2.5). After fractions were collected, the solvent was removed using a Christ rotary vacuum centrifuge for appropriate time periods according to the amount of solvent in each fraction.

Table 2.3: Mobile phase gradient of fraction collection method for HPLC separation of TAGs and collection of fractions. Flow rate 1 mL/min.

Time (min)	% acetonitrile	% isopropanol
0	70	30
15	60	40
25	45	55
38	30	70
45	30	70

Table 2.4: Program parameters for collecting sample fractions with TIME PROG mode of 201 Gilson fraction collector.

Parameter	Value	Unit
Rack code	10	
Waste	0	Minute
Inject	0	Minute
Wait	0	Minute
No Collections	1	
Drain	*	Minute
Collect	*	Minute
Safety	0	Peak No
Negative peak	0	
Level	-	%
T. min	-	Minute
T. max	-	Minute
Rinse	0	Minute
Number of cycles	1	

Table 2.5: Fraction collection times for fraction collection method (Table 2.3)

Fraction No	Start Time	Finish Time	Corresponding ECN
1	1.5	4.2	-
2	5.4	6.8	-
3	6.9	8.4	42
4	9.6	11.4	44
5	11.4	13.7	46
6	13.7	17.1	48
7	17.1	19.0	50
8	19.0	21.6	52
9	21.6	25.4	54

2.3 Separation techniques

A Dionex UltiMate 3000 HPLC was used for liquid chromatography separations.

2.3.1 UHPLC method

An ultra high performance liquid chromatography (UHPLC) method was developed using a Waters Acquity UPLC BEH C18 column (2.1 mm x 150 mm, 1.7 µm, 18% C loading). This method is used in Chapter 3. The mobile phase consisted of A: methanol (90%) and ammonium acetate in methanol (10mM; 10%), B: acetonitrile, C: dichloromethane and D: water, according to the gradient shown in Table 2.6. The column was maintained at 46°C. The samples (1 mg if solid, 1mL if liquid) were dissolved in a hexane: acetonitrile: isopropanol mixture (1 mL, 1:1:1 v/v/v) and the injection volume was 1 µL.

Table 2.6: Mobile phase gradient for UHPLC separation of TAGs (Method S)

Time (min)	Flow rate (mL/min)	% A	% B	% C	% D
0	0.45	79	15	3	3
2	0.45	79	15	3	3
8	0.45	80.6	15	3	1.4
11	0.45	45.5	51	3	0.5
13	0.45	5	75	20	0
18	0.45	5	65	30	0
24	0.45	5	65	30	0
25	0.45	79	15	3	3
30	0.45	79	15	3	3

2.3.1.1 Mass spectrometry

The detector used was a Thermo Scientific Orbitrap Fusion. The source used was APCI with sheath gas set at 50 (arbitrary units), auxilary gas at 10 and sweep gas at 5. The ion transfer tube temperature was set at 275°C and the vaporiser at 425°C. The positive ion discharge current was set at 4.5 µA and the negative ion discharge current at 10 µA. The Orbitrap detector was used for MS at 15000 resolution, scanning the mass range 230-1100 *m/z*. This relatively low resolution was selected to increase the data points collected in a short amount of time and to enable collection of MS^2 spectra for multiple precursor ions. Quadrupole isolation was used to select the most abundant ion from a pre-set mass range (Table 2.7) and MS^2 spectra were generated by collision- induced dissociation of that ion, using an isolation width of 1.6 *m/z* and a collision energy of 30%.

Table 2.7: Mass range for the selection of the most abundant ion for MS^2 (Method S)

Start (min)	Stop (min)	Scan range (*m/z*)
0	16	490-790
16	30	720-940

2.3.2 Two stage separation

The following two methods were employed in Chapters 4, 5 and 6.

2.3.2.1 Method ECN 26-40

The column, solvents, sample preparation and injection volume are the same for this method as described in 2.3.1. The column was maintained at 50°C and the gradient for the mobile phase is shown in Table 2.8

Table 2.8: Mobile phase gradient for UHPLC separation of TAGs (Method ECN 26-40)

Time (min)	Flow rate (mL/min)	% A	% B	% C	% D
0	0.45	79	3	3	15
11	0.45	79	3	3	15
13	0.45	62	20	3	15
18	0.45	52	30	3	15
24	0.45	52	30	3	15
25	0.45	79	3	3	15
30	0.45	79	3	3	15

The detector and all the settings are the same as described in 0, except for the mass range used for the selection of an ion for MS^2 which is given in Table 2.9.

Table 2.9: Mass range for the selection of the most abundant ion for MS^2 (Method ECN 26-40)

Start (min)	Stop (min)	Scan range (*m/z*)
0	15	490-790
15	30	720-940

2.3.2.2 Method ECN 42-56

The column, sample preparation and injection volume are the same for this method as described in 2.3.1. The mobile phase consisted of A: acetonitrile, B: dichloromethane and C: ammonium acetate in methanol (10mM), according to the gradient shown in Table 2.10. The column was maintained at 40°C.

Table 2.10: Mobile phase gradient for UHPLC separation of TAGs (Method ECN 42-56)

Time (min)	Flow rate (mL/min)	% A	% B	% C
0	0.55	85	10	5
15	0.55	70	25	5
18	0.55	65	30	5
20	0.55	60	35	5
21	0.55	85	10	5
26	0.55	85	10	5

The detector and all the settings are the same as described in 0, except for the mass range used for the selection of an ion for MS^2 which is given in Table 2.11.

Table 2.11: Mass range for the selection of the most abundant ion for MS^2 (Method ECN 42-56)

Start (min)	Stop (min)	Scan range (*m/z*)
0	7.5	490-790
7.5	26	720-940

3 Development of a single stage RP UHPLC separation of TAGs in various milk samples

3.1 Introduction

Milk and its products are important in the human diet. Cow, buffalo, sheep and goat are the most popular species, with cow milk production being five times greater than that of the other three combined (Belitz et al., 2009). More than 415 million metric tons of cow milk was produced globally in 2016, an estimated 17% being liquid milk, 37% cheese, 5% whole milk powder and 10% skimmed milk powder. Milk contains a complex mixture of a large number of different TAG components and their identification has been a challenge (Liu et al., 2018). Nevertheless, the importance of milk and dairy products has led to a number of studies trying to determine its lipid composition and the variables that affect it. One of the earliest studies utilising HPLC analysis examined cow, sheep and goat milk and identified differences in the distribution of TAGs by partition number among the three types of milk (Barron et al., 1990). Notably, the identification of the components had to be performed by GLC analysis of the main fatty acids of different fractions collected after the HPLC separation. Since then, the advances in column technology and mass spectrometry have allowed further study and discrimination of milk samples of different origins, including cow, goat, human and donkey milk (Mottram and Evershed, 2001; Dugo et al., 2005; Mirabaud et al., 2007; Gastaldi et al., 2011; Beccaria et al., 2014; Ten-Doménech et al., 2015) and other dairy products, mainly different types of cheese (A. I. Nájera et al., 1998; Beccaria et al., 2014).

Several studies focused on the ageing of different cheese products and its effect on the TAG composition, with longer ripening processes up to 1 year decreasing the amount of short-chain TAGs that could be involved in hydrolysis reactions (Ana I. Nájera et al., 1998). Notably, analysis of products from fresh until after their best-by-date (around 50 days) revealed no significant changes in lipid fraction for the products examined (Beccaria et al., 2016). A number of other parameters can affect the lipid composition of milk and dairy products, such as the different commercial treatment processes, as evidenced by the study from Gastaldi *et al.* (2011) in which significant differences between untreated and commercial goat milk were identified. The commercial milk featuring a higher abundance of DAGs, while the same phenomenon was not observed for untreated and commercial cow milk. Another important factor affecting TAG composition is the diet of the animals producing the milk. A study compared the nutritional quality of the fat of milk produced by flocks of sheep grazing in different areas of Spain (Bravo-Lamas et al., 2018). The flocks raised in mountain farms

produced milk richer in α-linolenic acid, long-chain saturated, branched-chain, and cis-monounsaturated fatty acids than flocks in valley farms.

Milk is also very important in infant diet, with human breast milk considered preferable to the range of available commercial products, mostly cow milk-based formula. The lipid composition of human breast milk have been studied widely as have the variables that affect the composition. Variations in weight and diet of breastfeeders (Koletzko et al., 2001; Linderborg et al., 2014), geographical location (Smit et al., 2002; Tu et al., 2017) and lactation stage (Koletzko et al., 2001; Sala-Vila et al., 2005; Tu et al., 2017) have all been examined with regards to their effect on the TAG composition of human breast milk. The identification of the TAG compositions of human breast milk is highly important to the development of infant supplements or replacement milk products with the highest possible resemblance to human breast milk (Morera et al., 2003; Long et al., 2013; Pande et al., 2013; X. Zou et al., 2013b; X.-Q. Zou et al., 2013; Sun et al., 2018).

The interest in the nutritional properties of milk and in particular in the role of its lipid composition leads to the need for an accurate and quick method to determine the lipid compositions. Such a method could also offer the potential to detect adulteration of milk and milk based products. The aim of the work presented in this chapter was to develop a single stage UHPLC method with the capacity to separate and identify the wide range of TAGs expected in milk and allow the characterisation of the TAG profiles in a shorter timeframe than that previously achieved.

3.2 Results and discussion

3.2.1 Method development

The HPLC method developed by Hasan (2010) for the separation of animal fats from raw meat and cooked meat products (Table 3.1) was selected as the starting point in the establishment of a method applicable to milk from various animals as well as commercial milk products. The method was first evaluated using a full fat milk sample obtained from a local supermarket. The separation was performed using two columns in series, Spherisorb ODS2 (4.6 mm x 150 mm, 3 µm, 11.5% C loading) and Waters X Select CSH C18 (4.6 mm x 150 mm, 3.5 µm, 15% C loading) and with detection using a CAD detector (Figure 3.1).

Table 3.1: Mobile phase gradient of Method J (Hasan, 2010) for HPLC separation of TAGs. Flow rate 1 mL/min.

Time (min)	% acetonitrile	% dichloromethane	% ammonium acetate in methanol (10 mmol)
0	76	20	4
82	75	21	4
145	61	35	4

The total analysis time of approximately 130 min is similar to other methods reported in the literature, for example the method of Beccaria et al. (2014) extends to 160 min. Although the method of Hasan (2010; Figure 3.1) shows the separation of TAGs over a broad range of ECN, it does not discriminate TAGs of ECN between 26 and 38 as well as does the method of Beccaria et al. (2014; Figure 3.2). The difference reflects the difference in purpose for which the two methods were developed: Hasan (2010) for animal fats and Beccaria et al. (2014) specifically for milks. The higher use of 100% acetonitrile at the start of the method of Beccaria et al. (2014) is more suitable for the more polar components (ECN= 26-38) that are prominent in milk , whereas the gradient employed by Hasan (2010) has a much less polar initial eluent composition (76% acetonitrile).

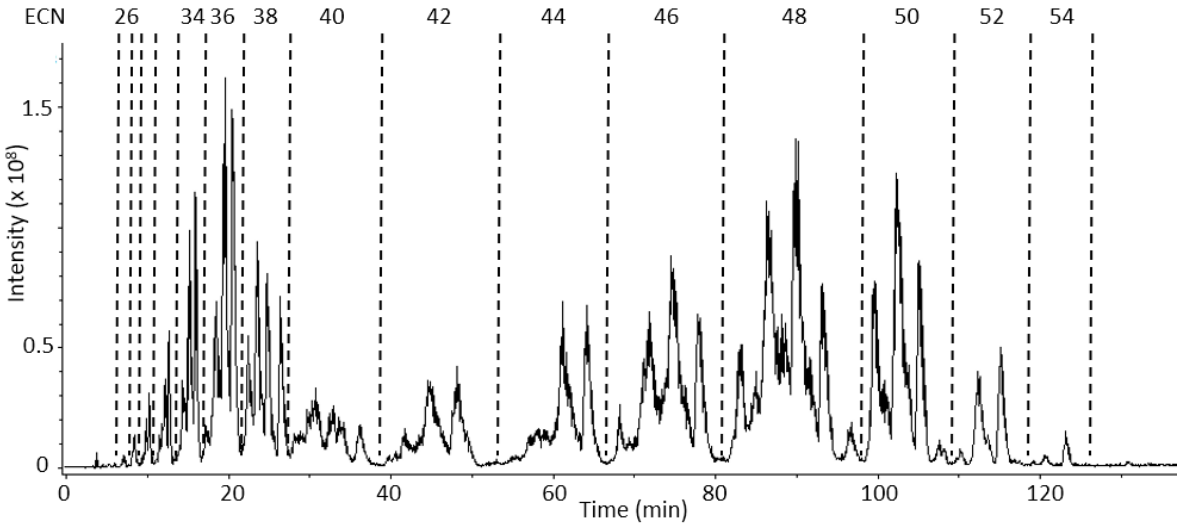

Figure 3.1: Partial base peak RP LC-APCI MS chromatogram of commercial full fat cow milk sample analysed with Method J (Table 3.1) developed by Hasan (2010). Regions are assigned according to ECN.

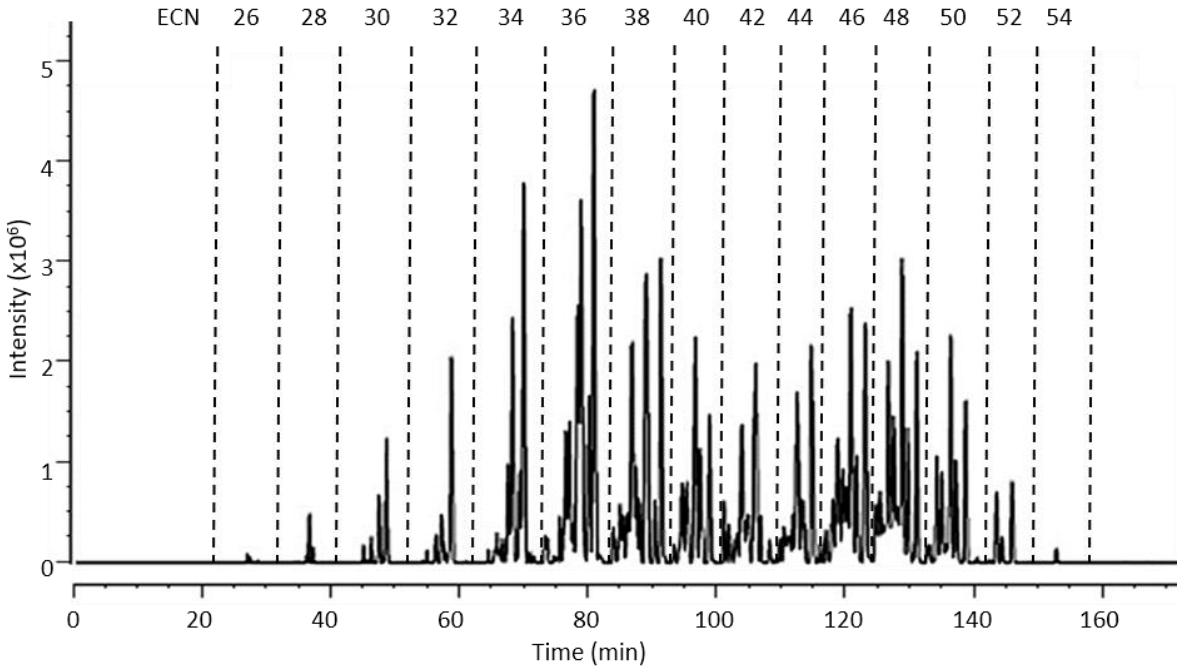

Figure 3.2: Total ion current NARP LC-APCI MS chromatogram of cow milk sample on three serially coupled Ascentis Express C18 columns, with mobile phase flow rate 1 mL/min and mobile phase gradient: 0 min, 100% acetonitrile; 150 min, 30% acetonitrile, 70% isopropanol (hold for 15 min); 168 min, 100% acetonitrile. Regions are assigned according to ECN. (Modified from Beccaria et al., 2014)

In addition to the more polar initial eluent composition, Beccaria et al. (2014) used fused-core technology columns with 2.7 µm particle size rather than the porous silica 3 µm particles used by Hasan (2010). In fused-core technology columns only a section of the particle is porous and interacts with the eluent, making the effective diameter of the particles even smaller. The technology of the columns and particle size effects the efficiency of the separation, with smaller particle sizes resulting in better peak shapes and resolution. This difference between the columns would also explain why the two methods have similar analysis times despite using

the same flow rate (1 mL/min) with different total column lengths: 300 mm for Hasan (2010) compared with 450 mm for Beccaria et al. (2014).

The difference in relative response of TAGs with higher ECN between the two methods can be attributed to the different detectors used. CAD detectors (used for the chromatogram in Figure 3.1: Partial base peak RP LC-APCI MS chromatogram of commercial full fat cow milk sample analysed with Method J (Table 3.1) developed by Hasan (2010). Regions are assigned according to ECN.Figure 3.1) have better response factors for unsaturated and saturated TAGs with longer chain lengths and much lower response factors for saturated TAGs with shorter chain lengths than APCI-MS (which was used by Beccaria et al. (2014)) (Holčapek et al., 2005; Lísa et al., 2007; Table 3.2).

Table 3.2: Response factors (RFs) of 19 single acid triacyglycerol (TAG) standards using charged aerosol detection (CAD) and atmospheric pressure chemical ionisation (APCI) in relation to triolein (C18:1 C18:1 C18:1) which is set to 1.00.

TAGs	RFs-CAD[a]	RFs-APCI[b]
C7:0 C7:0 C7:0	0.54	97.20
C8:0 C8:0 C8:0	0.74	74.44
C9:0 C9:0 C9:0	0.83	38.91
C10:0 C10:0 C10:0	0.86	17.62
C11:0 C11:0 C11:0	0.89	10.85
C12:0 C12:0 C12:0	0.94	6.04
C13:0 C13:0 C13:0	0.97	4.31
C14:0 C14:0 C14:0	0.95	2.77
C15:0 C15:0 C15:0	0.98	1.75
C16:0 C16:0 C16:0	1.01	1.32
C17:0 C17:0 C17:0	1.01	0.81
C18:3 C18:3 C18:3	0.92	0.40
C18:2 C18:2 C18:2	0.98	0.57
C18:1 C18:1 C18:1	**1.00**	**1.00**
C18:0 C18:0 C18:0	1.02	0.61
C19:0 C19:0 C19:0	1.05	0.49
C20:0 C20:0 C20:0	1.11	0.40
C21:0 C21:0 C21:0	1.27	0.39
C22:0 C22:0 C22:0	1.38	0.46

[a]Data from (Lísa et al., 2007)
[b]Data from (Holčapek et al., 2005)

Careful consideration of both separations enabled identification of aspects that could be improved. Both methods are more than two hours long and use more than one column, increasing the cost. The Hasan (2010) method resolves a number of isomers whereas the Beccaria et al. (2014) method gives better separation of TAGs with lower ECNs. The method developed by Hasan (2010) was used as the starting point for the UHPLC method development, because of the technological advantages of UHPLC columns compared to fused core ones.

The efficiencies of UPLC columns are around 20% greater than fused-core columns (Abrahim et al., 2010), providing the potential for shorter column length to be used, decreasing analysis time and cost while not compromising the quality of the separation. Hence, the two HPLC columns used in Hasan's method (Figure 3.1) were replaced with a single Waters Acquity UPLC BEH (150 mm x 2.1 mm, 1.7 µm). To avoid excessively high backpressures caused by the small internal diameter and the small particle size of the column, a lower flow rate of 0.7 mL/min was used. In order to regulate the separation and reduce overall analysis time, the column was temperature controlled at 60°C. Based on its widespread use in previous methods reported in the literature, acetonitrile was selected as the main organic solvent. A modifier is used in the mobile phase to improve the solubility of TAGs in the eluent, change the polarity of

the eluent and increase peak selectivity (Ruiz-Gutiérrez and Barron, 1995). Hasan (2010) examined isopropanol, chloroform and dichloromethane as potential organic modifiers and concluded that dichloromethane was superior at solubilising TAGs and provided better peak resolution. For this reason, dichloromethane was selected as the modifier for this study. In addition, to maintain a greater polar character during the early part of the separation, the proportion of dichloromethane in the initial eluent was decreased and the gradient adjusted (Method A, Table 3.3) from that used by Hasan (2010).

Table 3.3: Mobile phase gradient of Method A for UHPLC separation of TAGs. Flow rate 0.7 mL/min. Temperature controlled at 60°C.

Time (min)	% acetonitrile	% dichloromethane	% ammonium acetate in methanol (10 mmol)
0	94	5	1
5	94	5	1
45	79	20	1
52	64	35	1
60	94	5	1

The analysis time for the method, 20 min, is considerably less than the 130 min for Hasan's method, despite the reduced flow rate (Figure 3.3). This can be partly attributed to the change in total column length, from 300 mm to 150 mm, but is also due to the higher efficiency of the UPLC column. Furthermore, the groups of TAGs with different equivalent carbon numbers were more clearly separated, although separation within groups of the same ECN was minimal, especially within the early part of the chromatogram.

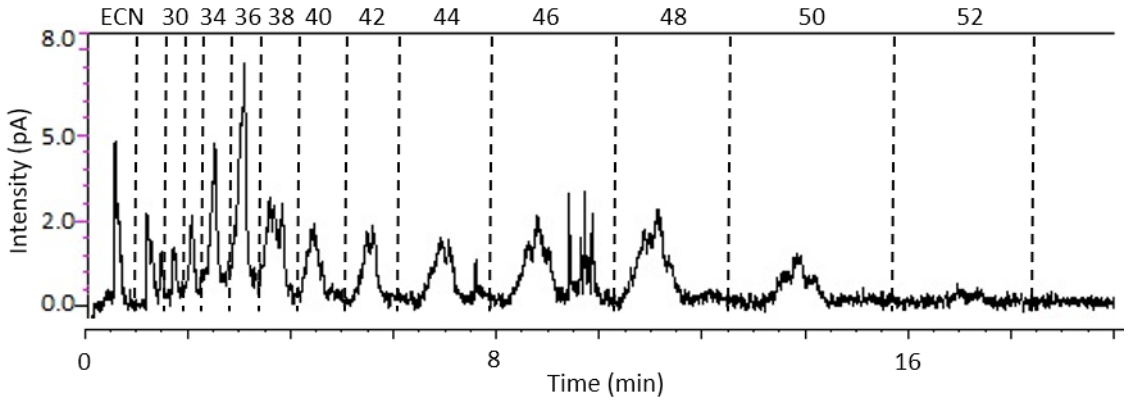

Figure 3.3: Partial RP UHPLC-CAD chromatogram of commercial full fat cow milk sample analysed with Method A (Beccaria et al., 2014) **Regions are assigned according to ECN.**

To enable a broader range of polarities to be explored, and also to reduce cost, acetonitrile was replaced with a more polar solvent, methanol. The temperature control for the column was lowered from 60°C to 40°C to achieve sharper peaks. The decrease in temperature caused an increase in backpressure, necessitating a decrease in flow rate (0.45 mL/min) to maintain

the pressure within the acceptable limits and allow the analytes to interact longer with the column. The separation was carried out with isocratic elution (MeOH 90%, DCM 10%; Method B, Figure 3.4) to allow for the maximum expression of the separation capacity of the column and for simplicity.

The separation of TAGs with different ECNs is similar to that observed with method A (Figure 3.3, Table 3.3), though separation within the ECN range 36 to 38 improved: two peaks are evident where one broad peak was observed previously. In addition, a number of minor peaks that were not observed previously are evident within the ranges ECN 42, 44, 46 and 48.

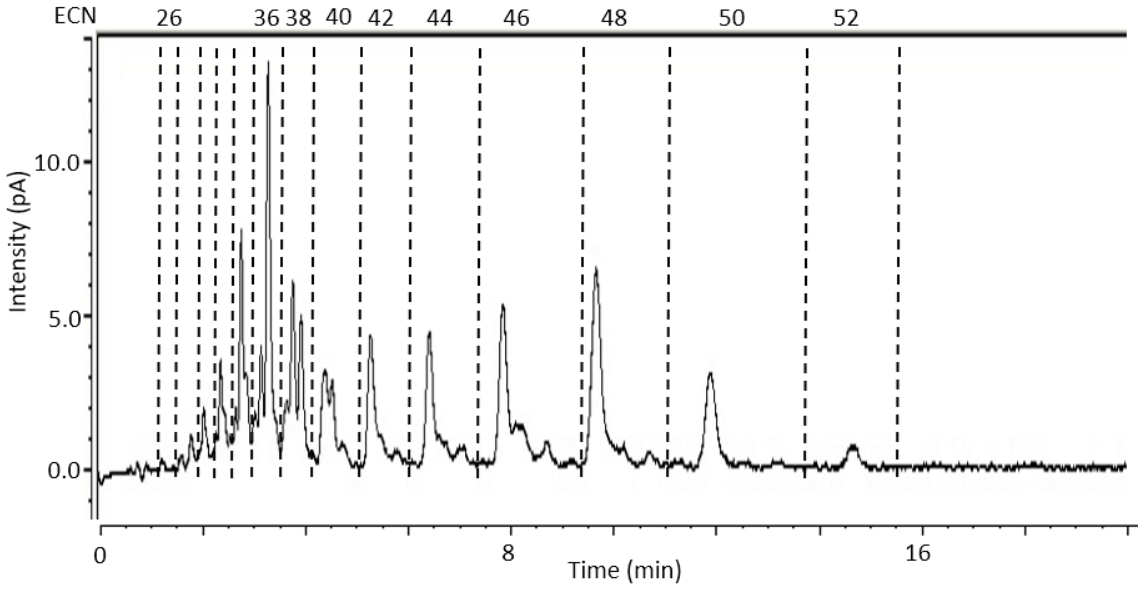

Figure 3.4: Partial RP UHPLC-CAD chromatogram of commercial full fat cow milk sample analysed with Method B (temperature controlled at 40°C; flow rate = 0.45 mL/min; isocratic elution MeOH 90%, DCM 10%). Regions are assigned according to ECN.

In an attempt to achieve greater discrimination in the interactions of the analytes with the column a more subtle change in polarity was evaluated by adding a small amount of acetonitrile while maintaining the amount of dichloromethane in the mobile phase. The temperature and flow rate were not altered and the mobile phase comprised methanol 80%, dichloromethane 10% and acetonitrile 10% (Method C, Figure 3.5). Comparison of Methods B and C (Figure 3.4 and Figure 3.5, respectively) reveals some obvious improvements in the latter, in the regions representing ECNs 42 to 48. The shoulders on the major peaks in that region in method B are resolved as separate peaks in Method C (for example region ECN 46). The small changes in relative peak height can also be attributed to the greater degree of separation.

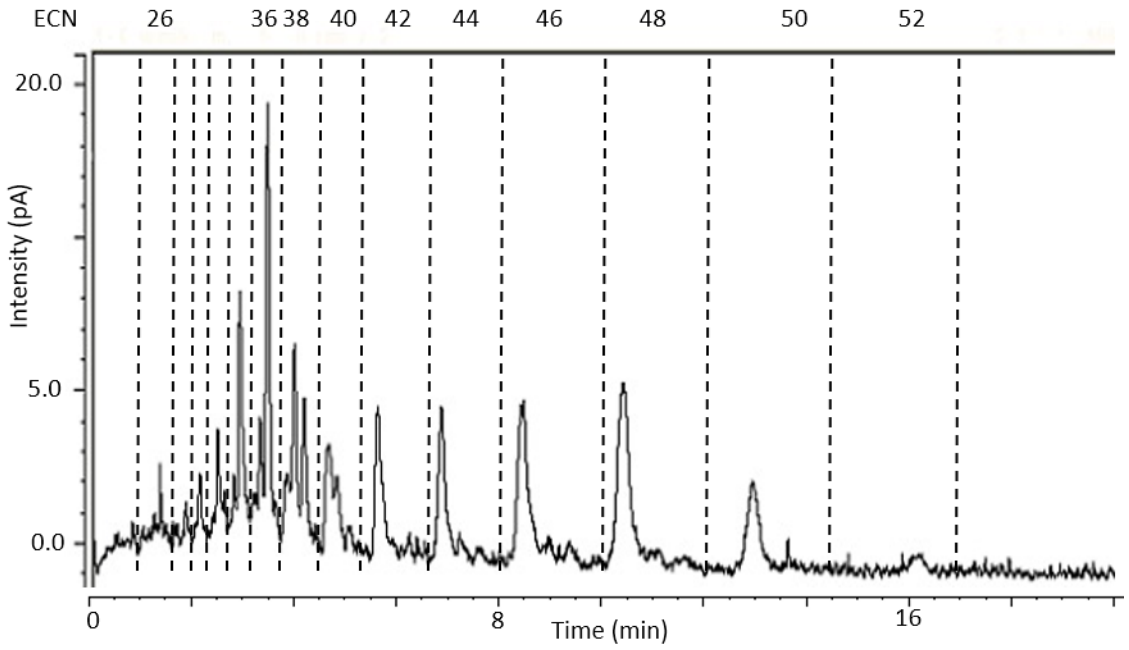

Figure 3.5: Partial RP UHPLC-CAD chromatogram of commercial full fat cow milk sample analysed with Method C (temperature controlled at 40°C; flow rate = 0.45 mL/min; isocratic elution methanol 80%, dichloromethane 10% , acetonitrile 10%). Regions are assigned according to ECN.

The addition of acetonitrile improved the separation for some of the longer chain length saturated TAGs while not affecting the earlier part of the separation where ECNs 26-38 elute. Given the inability of isocratic methods B and C to resolve components across the polarity range, it was deemed necessary to move to a gradient elution. Addition of water over the first few minutes of the separation (starting composition: 78% methanol, 10% acetonitrile, 10% dichloromethane, 2% water, composition at 10 min: 80% methanol, 10% acetonitrile, 10% dichloromethane) effected greater separation among groups of ECNs 30, 32, 34 and 36 (Method D, Figure 3.6). It did, however, cause an increase in backpressure, requiring the flow rate to be lowered further, to 0.3 mL/min.

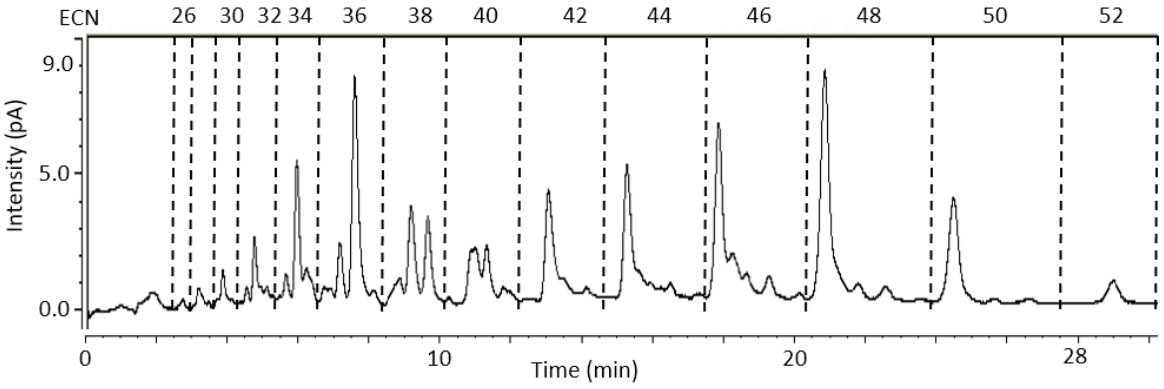

Figure 3.6: Partial RP UHPLC-CAD chromatogram of commercial full fat cow milk sample analysed with Method D (temperature controlled at 40°C; flow rate = 0.3 mL/min; 78% methanol, 10% acetonitrile, 10% dichloromethane, 2% water, composition at 10 min: 80% methanol, 10% acetonitrile, 10% dichloromethane). Regions are assigned according to ECN.

TAGs of 14 different ECNs were observed in the chromatograms of Method B-D, though efficiency is not the same among all ECN numbers. Method D achieves separation over a greater extent of the analysis time: the dead time of the method is significantly reduced and the time ranges over which different ECN groups elute is more evenly distributed, though it increases with analysis time (Table 3.4). The separation of a number of peaks, for example those with ECN 36, exhibit near baseline resolution for the two largest peaks, which was not observed previously. Furthermore, a number of additional peaks appear, such as a fifth peak in the group for ECN 46 which was not seen using Method C.

Table 3.4: Percentage of method time where ranges of TAGs elute for Methods C and D.

Method	ECN 26-38 (%)	ECN 40-52(%)	Dead time (%)
C	17.5	65	17.5
D	27	67	6

Different concentrations of acetonitrile were tested, 5%, 10% and 15% (Table 3.5, Figure 3.7), to assess the impact of acetonitrile on the separation after the addition of water.

Table 3.5: Mobile phase gradient of Methods D, E and F for UHPLC separation of TAGs. Flow rate 0.3 mL/min. Temperature controlled at 40°C.

Method	Solvents	Eluent composition at 0 min (%)	Eluent composition at 10 min (%)
D	Methanol	78	80
	Acetonitrile	10	10
	Dichloromethane	10	10
	Water	2	0
E	Methanol	83	85
	Acetonitrile	5	5
	Dichloromethane	10	10
	Water	2	0
F	Methanol	73	75
	Acetonitrile	15	15
	Dichloromethane	10	10
	Water	2	0

The increase of acetonitrile improved peak shape and separation across the range of ECNs. The region corresponding to ECN 38 gave sharper peaks and improved separation (red squares, Figure 3.7), while in the region corresponding to ECN 44 more peaks were baseline separated (blue rectangles, Figure 3.7). Peaks also appear closer to the ideal Gaussian distribution, for example tailing and co-elution of the largest peak at ECN 48 was reduced with higher concentrations of acetonitrile, giving rise to complete resolution (blue ovals, Figure 3.7).

The improvements to peak shape and separation can be attributed to the decrease in the polarity of the eluent; the increase in acetonitrile in place of methanol, the more polar of the two. Trying to get the same result by increasing dichloromethane would not achieve the same effect because dichloromethane is much less polar than acetonitrile and would significantly reduce retention times and cause co-elution of peaks, especially for TAGs with ECNs between 26 and 38. On the other hand, replacing dichloromethane with acetonitrile would reduce the solubility of TAGs in the eluent, especially TAGs with ECNs higher than 46. Thus, method F and 15% acetonitrile were selected for further development.

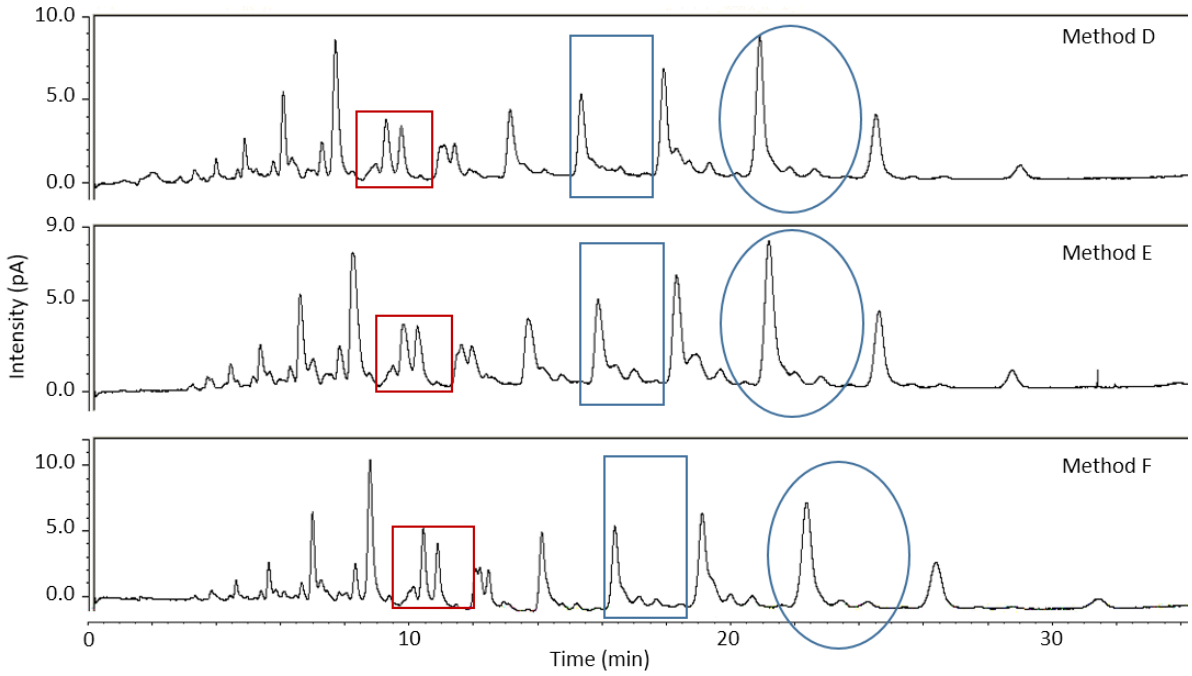

Figure 3.7: Partial RP UHPLC-CAD chromatograms of commercial full fat cow milk sample analysed with Methods D (10% acetonitrile), E (5% acetonitrile) and F (15% acetonitrile) (Table 3.5). Red square boxes include TAGs with ECN 38, blue rectangle boxes include TAGs with ECN 44 and blue ovals include TAGs with ECN 48.

The water content and the gradient for its decrease in the mobile phase were explored in order to maximise the impact on the peaks that were most positively affected by the higher polarity of the mobile phase (Table 3.6, Figure 3.8). The differences between the three methods were marginal, but better separation for ECN 46 was observed with Method H and so it was selected for further development (Figure 3.8).

Table 3.6: Mobile phase gradient of Methods F, G and H for UHPLC separation of TAGs. Flow rate 0.3 mL/min. Temperature controlled at 40°C.

Method	Solvents	Eluent composition at 0 min (%)	Eluent composition at 10 min (%)	Eluent composition at 15 min (%)
F	Methanol	73	75	75
	Acetonitrile	15	15	15
	Dichloromethane	10	10	10
	Water	2	0	0
G	Methanol	72	75	75
	Acetonitrile	15	15	15
	Dichloromethane	10	10	10
	Water	3	0	0
H	Methanol	72	74	75
	Acetonitrile	15	15	15
	Dichloromethane	10	10	10
	Water	3	1	0

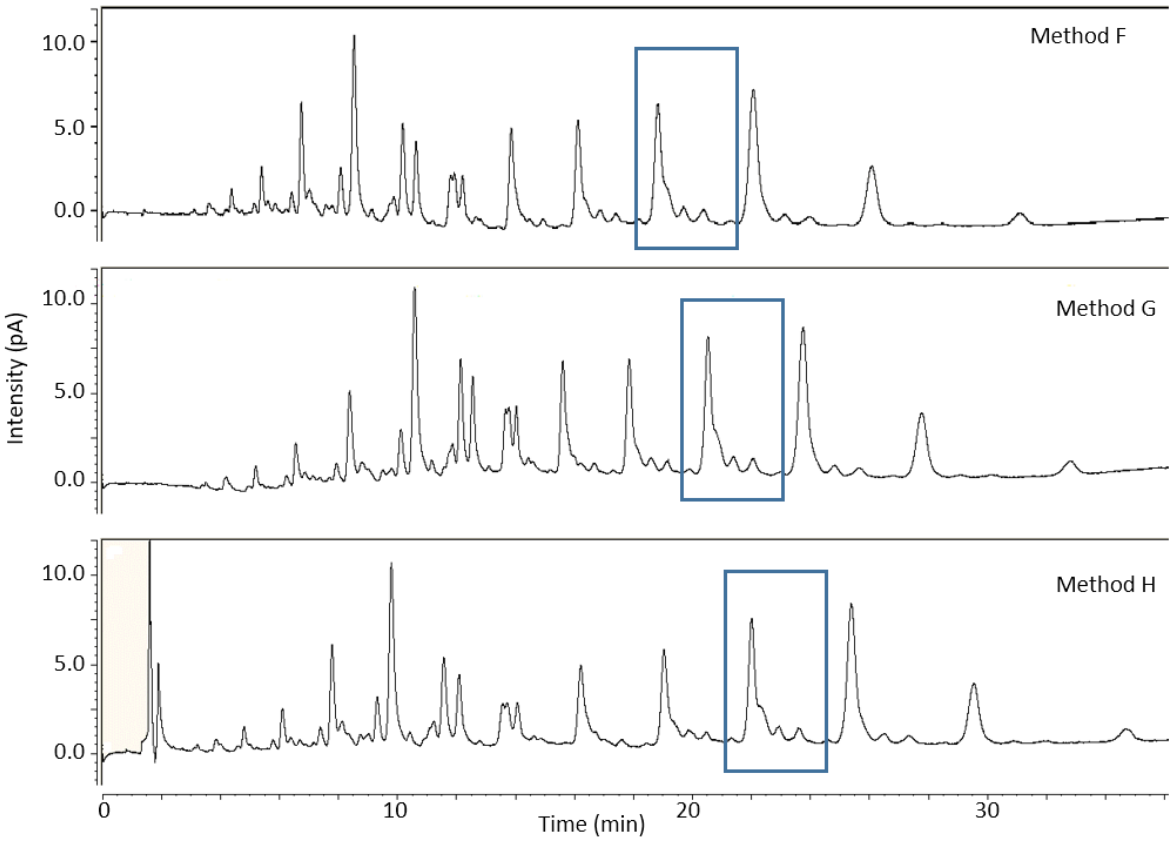

Figure 3.8: Partial RP UHPLC-CAD chromatograms of commercial full fat cow milk sample analysed with Methods F, G and H (Beccaria et al., 2014)**. Blue rectangle boxes include TAGs with ECN 46.**

At this point in the method development the Thermo Orbitrap Fusion mass spectrometer became available. Even though the CAD has more consistent response factors across TAGs of different saturation and chain length (Holčapek et al., 2005; Lísa et al., 2007; Table 3.2), a mass spectrometer can provide information for the identification of each of TAGs and enable deconvolution of closely eluting components based on mass differences. Identification of the different component TAGs was considered important at this stage of method development, hence mass spectrometric detection was used from this point forward.

As discussed previously, ammonium acetate aids ionisation of TAGs, forming ammonium adduct ions which can be detected even when proton adducts ions are not. since the LC system being used has a limit of four solvent reservoirs, the appropriate amount of ammonium acetate as determined by Hasan (2010) was dissolved in methanol. Thus, from this point forward the methanol component of the eluent comprises methanol (95%) and ammonium acetate dissolved in methanol (10mM; 5%).

With the adjustments made to the separation conditions the total analysis time for method H exceeded 30 min. Given the desire for a rapid method, changes to the temperature and flow rate were explored (Table 3.7, Figure 3.9). The combination of a temperature of 50^{o}C and a flow rate of 0.45 mL/min (Method K, Table 3.7, Figure 3.9) gave an appreciable improvement in total analysis time, to less than 25 min, while maintaining separation of the components previously observed and also allowing the observation of a new peak that was not previously detected (ECN 54, Figure 3.9)

Table 3.7: Flow rate and temperature conditions for methods I, J and K. The eluent composition and gradient is the same for all three methods and the same with method H (

Table 3.6), with the only difference being the addition of ammonium acetate in the methanol. Thus, where for method H it was methanol, for methods I, J and K it is methanol (95%) and ammonium acetate dissolved in methanol (10mM; 5%).

Method	Flow rate (mL/min)	Temperature (^{o}C)
I	0.3	40
J	0.3	50
K	0.45	50

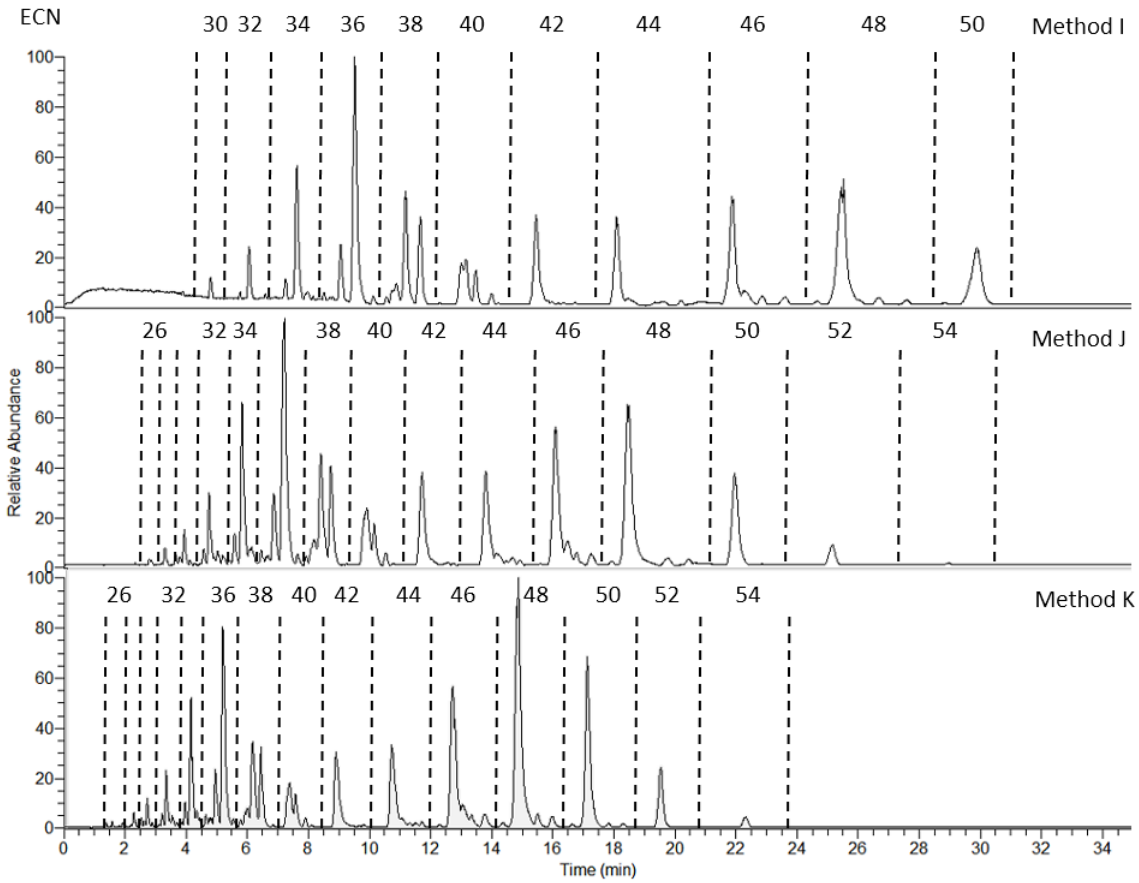

Figure 3.9: Partial RP UHPLC-APCI MS base peak chromatograms of commercial full fat cow milk sample analysed with Methods I, J and K (Table 3.7). Regions are assigned according to ECN.

In an effort to further improve the separation of TAGs with lower ECNs (<40), the percentage of dichloromethane was lowered from 10% (Table 3.7, method K) to 7% (Method L) to increase the polarity at the beginning of the separation. Although the change revealed some co-eluting peaks towards the start of the chromatogram (Figure 3.10a), it led to a decrease in the separation of later eluting analytes (Figure 3.10b). Notably, within ECNs 34 to 40 some peaks appear to be split, revealing co-eluting components (Figure 3.10a), while peaks at higher ECNs are lost, most importantly ECN 54 is no longer detected (Figure 3.10b). The decrease in dichloromethane and subsequent increase in polarity benefitted more separation of polar TAGs with lower ECNs but decreased the detectability of more apolar TAGs. The effect on more apolar TAGs could also be a result of reduced solubility in the eluent after the decrease of dichloromethane present.

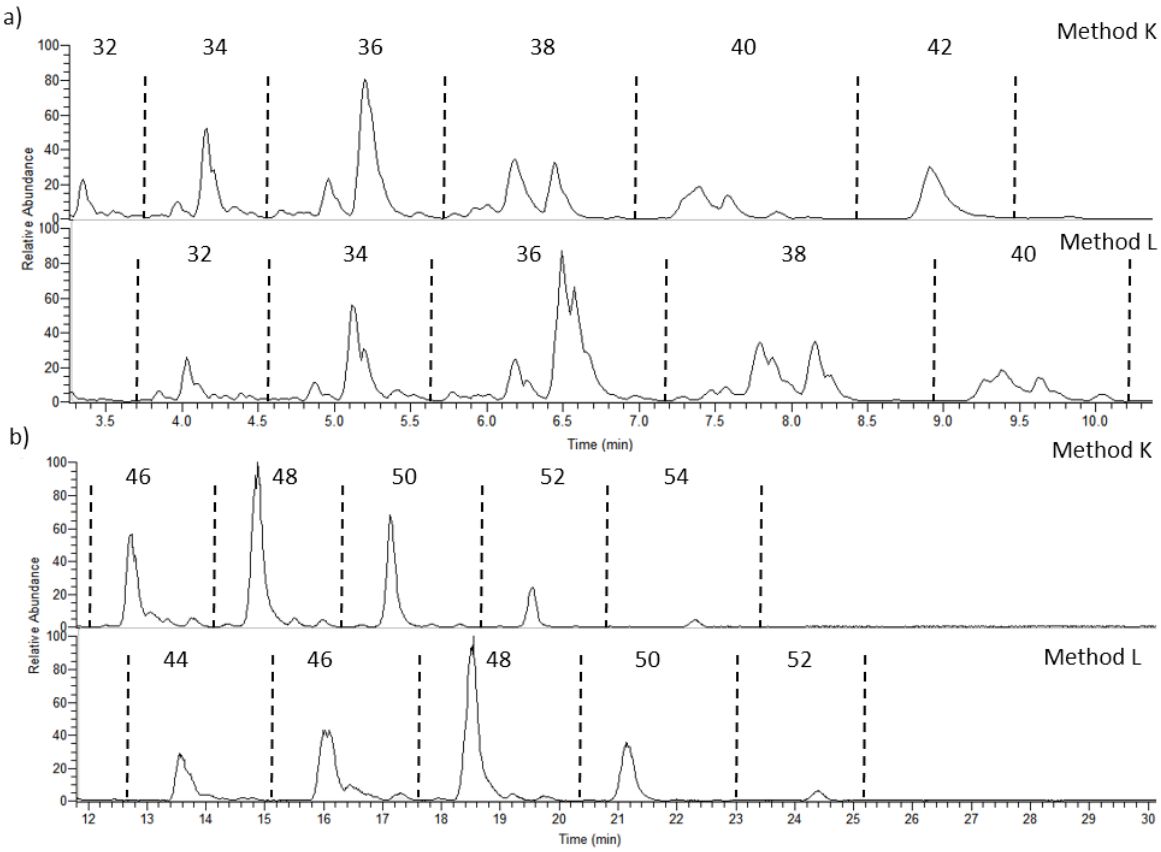

Figure 3.10: Partial RP UHPLC-APCI MS base peak chromatograms of commercial full fat cow milk sample analysed with Methods K (Table 3.7) and L (same as Method K, with dichloromethane lowered to 7%) during time ranges: a) 3.5 to 10 min and b) 12 to 30 min. Regions are assigned according to ECN.

Different gradients were evaluated in an effort to retain the positive impact of lower dichloromethane percentage at the start of the analysis, while mitigating negative effects on the more apolar TAGs (Table 3.8). Thus, acetonitrile was reduced from 15% to 10%. Increasing dichloromethane at 10 min from 7% to 10%, 15% and 20% was evaluated (methods M, N and O; Table 3.8)). Additionally, the polarity was further reduced in method O by decreasing acetonitrile from 10% at 10 min to 7% at 20 min. Out of the three methods tested, only method O detected TAGs with ECN 54 (Figure 3.11), so the higher percentage of dichloromethane is necessary for the detection of that peak. Nevertheless, method O still did not achieve the desirable degree of separation for TAGs with ECNs 42 and above by comparison with the methods of Hasan (2010) and Beccaria *et al.* (2014).

Table 3.8: Mobile phase gradient of Methods M, N and O for UHPLC separation of TAGs. Flow rate 0.45 mL/min. Temperature controlled at 50°C. The solvents used were A: Methanol (95%) and ammonium acetate in methanol (10 mM; 5%), B: Acetonitrile, C: Dichloromethane and D: Water. The changes made to dichloromethane and acetonitrile are highlighted. Percentages are rounded to 2 significant figures.

		Eluent composition (%)				
Method	Solvents	at 0 min	at 2 min	at 10 min	at 15 min	20 min
M	A	80	80	82	82	80
	B	10	10	10	10	10
	C	7.0	7.0	7.0	8.5	10
	D	3.0	3.0	1.2	0.0	0.0
N	A	80	80	82	79	75
	B	10	10	10	10	10
	C	7.0	7.0	7.0	11	15
	D	3.0	3.0	1.2	0.0	0.0
O	A	80	80	82	78	73
	B	10	10	10	8.5	7.0
	C	7.0	7.0	7.0	14	20
	D	3.0	3.0	1.2	0.0	0.0

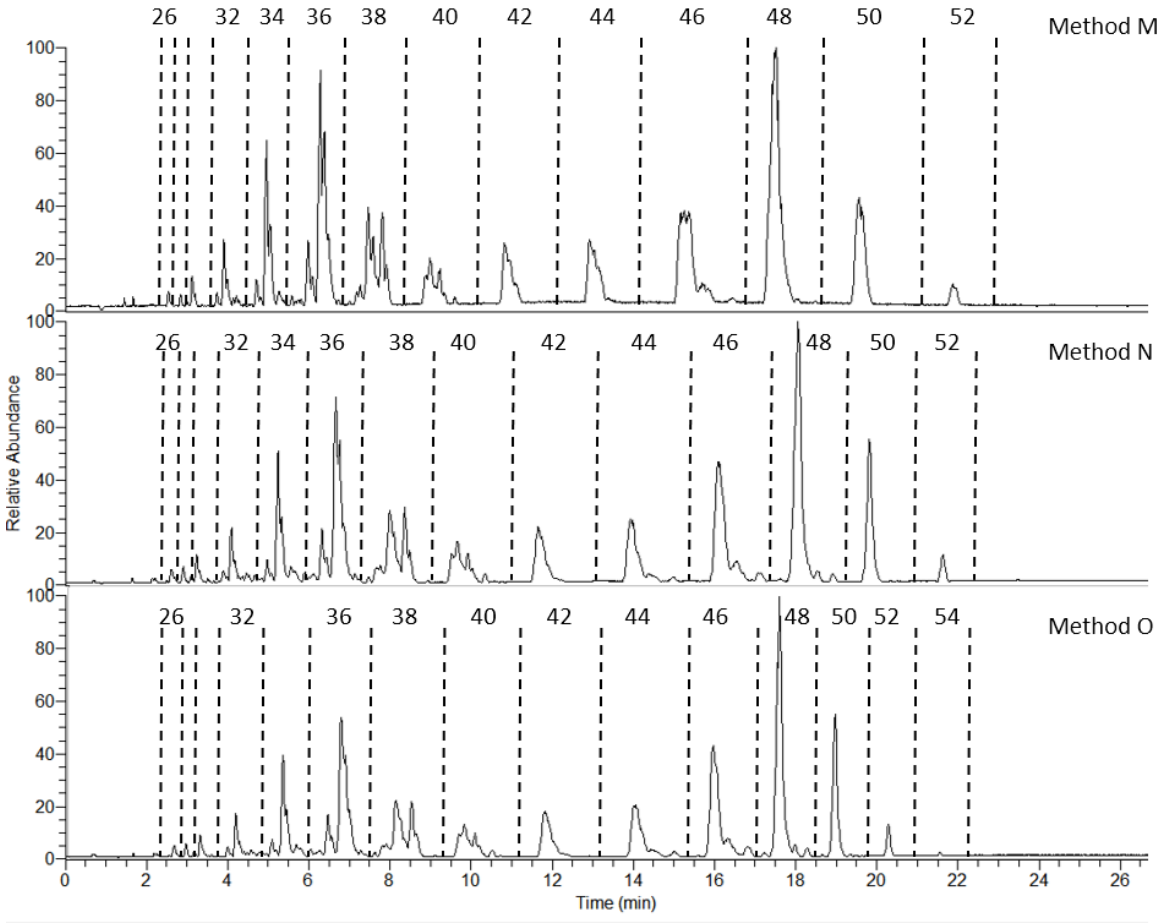

Figure 3.11: Partial RP UHPLC-APCI MS base peak chromatograms of commercial full fat cow milk sample analysed with Methods M, N and O (Table 3.8). Regions are assigned according to ECN.

Comparison of the method by Hasan (Figure 3.1) with method O (Figure 3.11) reveals several improvements as well as some negative differences. The most obvious and drastic improvement is the decrease of analysis time from 180 min to less than 25 min. Furthermore, the separation of TAGs with ECNs from 26 to 40 is comparable: most peaks are identified in both methods. Nevertheless, the separation of peaks with ECN 42 and higher is very much worse for method O than for the Hasan method. For example, two distinct ECN 52 peaks are evident with Hasan's method whereas only one is detected with Method O and some peaks are barely detected, such as the peak at ECN 54. Hence, it is evident that the changes to the eluent at the beginning of the separation, the introduction of methanol and water, are beneficial for the separation of the more polar TAGs, but that changes should be made to the later part of the separation to resolve TAGs with higher ECNs.

In order to achieve better resolution for less polar TAGs with higher ECNs, the eluent needs to have a much less polar composition. Both methanol and acetonitrile are more polar than dichloromethane, but methanol is more polar than acetonitrile. Thus, a much less polar eluent should be employed after 10 min into the separation (i.e. when TAGs with ECNs higher than 40 start to elute) by lowering the percentage of methanol and replacing it with acetonitrile, while also increasing the percentage of dichloromethane. For this reason the acetonitrile content of the mobile phase was altered and a gradient was introduced to increase ACN from 10% at 8 min to 65% at 12min for method P and from 10% at 6 min to 75% at 10min for method Q (Table 3.9). In addition, the dichloromethane ramp from 7% to 20%, which was previously found to be beneficial (Table 3.8, Figure 3.11), was modified to occur over the range 15 min to 25 min for method P and 10 to 15 min for method Q (Table 3.9). The reason for this adaptation was to ensure the increase in dichloromethane occurs after TAGs with ECNs lower than 40 have already eluted. If dichloromethane was increased before that, it would affect the elution of those analytes and would lead to co-elution.

The changes made positively affected the separation of TAGs with higher ECNs (Figure 3.12). Both methods detected the peak for ECN 54, although it is very small, and both methods revealed two peaks at ECN 52 which were co-eluted in Method O (Figure 3.11). Method Q is superior to method P in the separation of ECN 50, since the single peak previously detected exhibits partial separation into three peaks. Nevertheless, ECNs 44, 46 and 48 do not exhibit any significant improvement.

Table 3.9: Mobile phase gradient of Methods P and Q for UHPLC separation of TAGs. Flow rate 0.45 mL/min. Temperature controlled at 50°C. The solvents used were A: Methanol (95%) and ammonium acetate in methanol (10 mM; 5%), B: Acetonitrile, C: Dichloromethane and D: Water. The changes made to dichloromethane and acetonitrile are highlighted. Percentages are rounded to 2 significant figures.

		Eluent composition (%)					
Method	Solvents	at 0 min	at 2 min	at 8 min	at 12 min	15 min	25 min
P	A	80	80	81	27	28	15
	B	10	10	10	65	65	65
	C	7.0	7.0	7.0	7.0	7.0	20
	D	3.0	3.0	1.6	0.7	0.0	0.0
		Eluent composition (%)					
Method	Solvents	at 0 min	at 2 min	at 6 min	at 10 min	15 min	
Q	A	80	80	81	17	5	
	B	10	10	10	75	75	
	C	7.0	7.0	7.0	7.0	20	
	D	3.0	3.0	2.1	1.2	0	

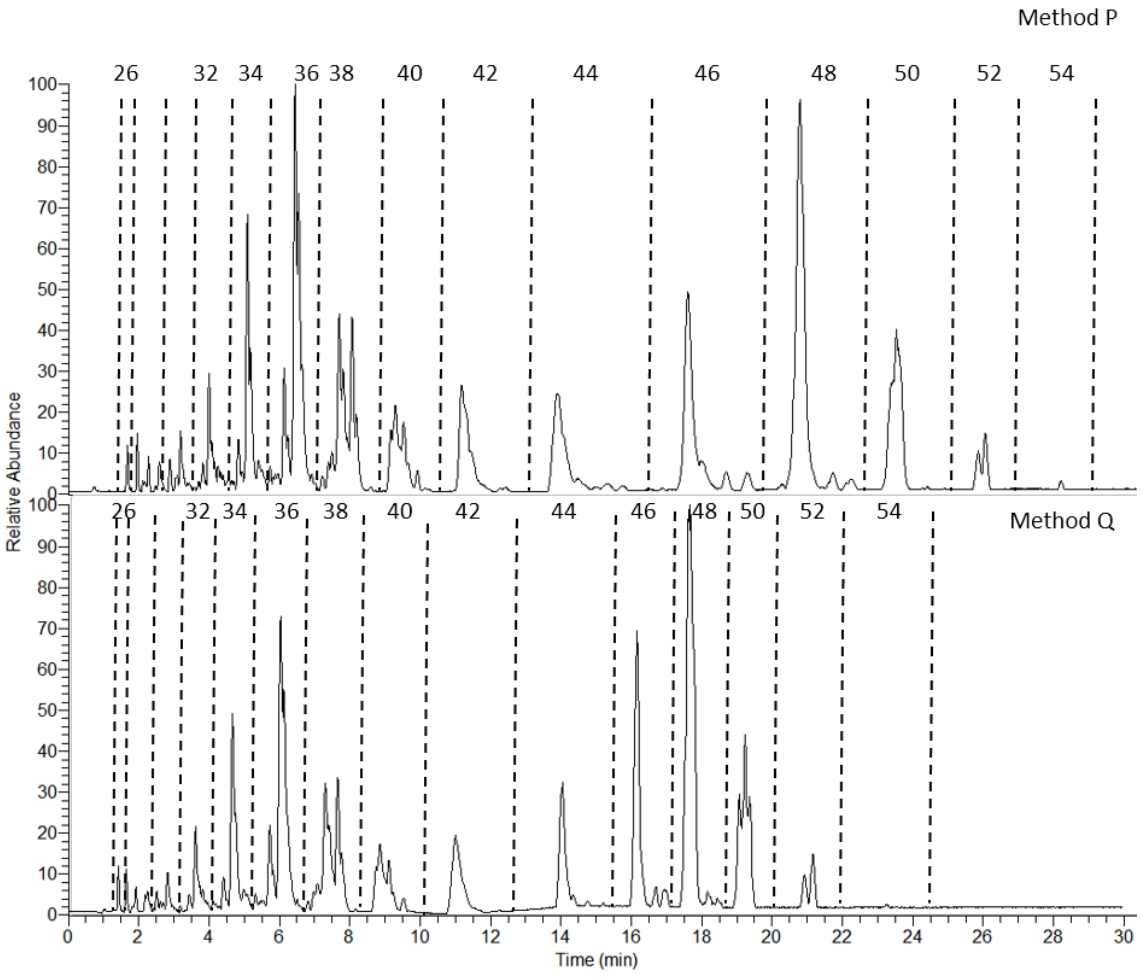

Figure 3.12: Partial RP UHPLC-APCI MS base peak chromatograms of commercial full fat cow milk sample analysed with Methods P and Q (Beccaria et al., 2014)**. Regions are assigned according to ECN.**

Assessment of method development and resulting method proposed

Based on all the previous observations, some basic principles that influence the separation can be identified. The separation of TAGs of ECNs 40 and lower benefits from a very polar eluent composition, with high methanol content and also some water. TAGs with higher ECNs benefit from much less polar eluent composition, no water, very little methanol and high acetonitrile and dichloromethane content. Furthermore, higher dichloromethane content increases the response of the peak at ECN 54, since longer chain TAGs have a lower response factors under APCI MS detection (Table 3.2). Taking all these principles into account, the following adaptations were implemented in Method R (Table 3.10, Figure 3.13). The initial dichloromethane content was reduced to 3% from 7% previously and acetonitrile increased to 15% (Table 3.10), both changes being made in an effort to increase the polarity of the initial eluent composition. As a result, TAGs with ECNs between 26 and 40 elute between 2 and 14 min, whereas previously they eluted between 1.5 and 10 min (Figure 3.13), resulting in improved resolution of the peaks in that time range. The decrease in water content from 3 - 0% was adjusted to reflect the change in elution times (from 2-15 min, Table 3.9, to 2-13 min, Table 3.10). A ramp to increase acetonitrile from 15 to 75% was introduced at 8 min to achieve the reduction in polarity of the eluent that is required to give better separation of the TAGs with higher ECNs. Furthermore, dichloromethane was increased from 3 to 20% between 11 and 13 min and then to 30% at 18 min. As a result of these changes, TAGs with ECNs between 42 and 54 elute between 14 and 21 min (Figure 3.13), decreasing the overall analysis time compared with previous methods. Separation of peaks in ranges for ECNs 50 and 52 is improved compared to method Q (Figure 3.12) and the peak at ECN 48 can be seen to begin to separate into four different peaks that were not observed previously (Figure 3.13). Also, the relative intensity of the peak at ECN 54 is greater. Despite all the improvements, the peaks at ECN 42, 44 and 46 remain unresolved.

Table 3.10: Mobile phase gradient of Method R for UHPLC separation of TAGs. Flow rate 0.45 mL/min. Temperature controlled at 50°C. The solvents used were A: Methanol (95%) and ammonium acetate in methanol (10 mM; 5%), B: Acetonitrile, C: Dichloromethane and D: Water. The changes made to dichloromethane and acetonitrile are highlighted. Percentages are rounded to 2 significant figures.

Time (min)		0	2	8	11	13	18
Solvents	A %	79	79	81	45	5.0	5.0
	B %	15	15	15	51	75	65
	C %	3.0	3.0	3.0	3.0	20	30
	D%	3.0	3.0	1.4	0.6	0.0	0.0

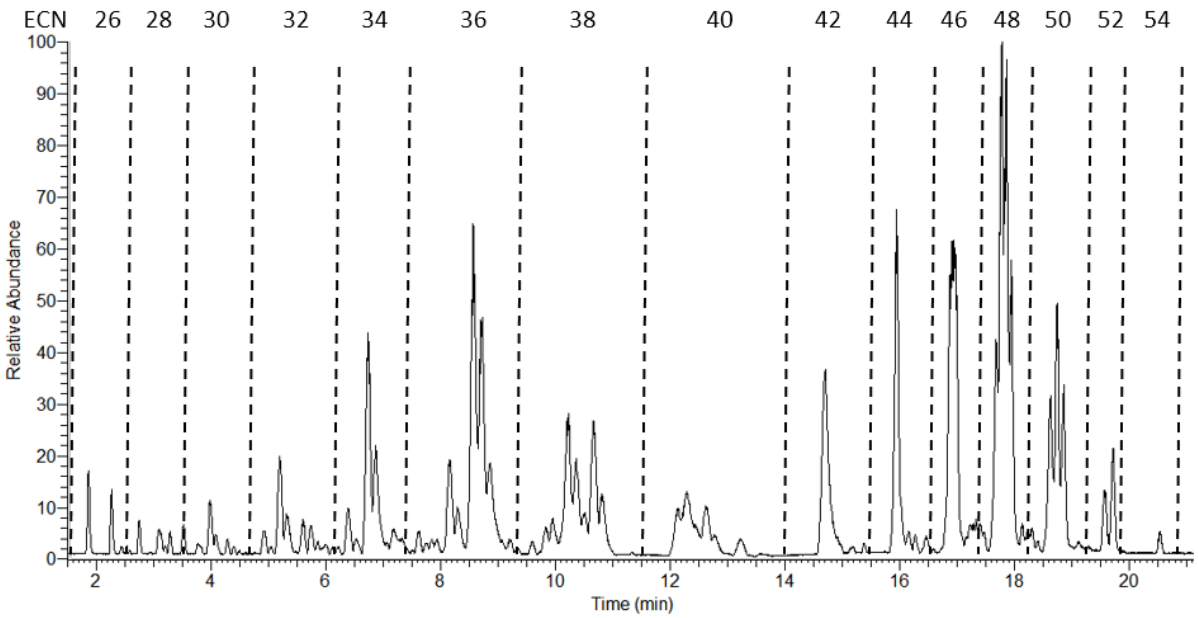

Figure 3.13: Partial RP UHPLC-APCI MS base peak chromatogram of commercial full fat cow milk sample analysed with Method R (Table 3.10). Regions are assigned according to ECN.

At this point the effect of the addition of ammonium acetate was investigated. Although for most TAGs the ammonium adduct, and in some of the cases the proton adduct ion, appear in the mass spectra, the spectra of some TAGs lack either adduct ion. Notably, those TAGs were ones with fully saturated carbon chains. For example, the mass spectrum of the second peak in the region of ECN 52 (19.72 min, Figure 3.13) shows peaks at *m*/*z* values corresponding to two protonated DAG ions (*m*/*z* 579.54 and *m*/*z* 607.57), but no corresponding ammonium or proton adduct ion (Figure 3.14). Knowing the DAG ions and the ECN, it can be concluded that the TAG is SSP. The presence of an ammonium adduct, expected at around *m*/*z* 880, would confirm the identification with greater certainty. Thus, different concentrations of ammonium acetate (solvent A; Table 3.10) were tested. Using only methanol in solvent A provided a base for comparison to determine whether the addition of ammonium acetate affected the separation (solvent A: methanol 100%, method R_a; Figure 3.15). Completely replacing methanol with ammonium acetate dissolved in methanol interfered with the quality of the chromatography by increasing the background noise over the time window 14-19 min of the analysis time (solvent A: ammonium acetate [in methanol 10mM] 100%, method R_c; Figure 3.15). As already discussed (Figure 3.14) 5% of ammonium acetate [in methanol 10mM] in solvent A is not adequate for the production of ammonium adducts from all TAG species. The percentage of ammonium acetate in solvent A was increased to 10%, which proved sufficient to form ammonium adducts without affecting the background noise in the chromatogram (solvent A: methanol 90%, ammonium acetate [in methanol 10mM] 10%, method R_b; Figure 3.15)

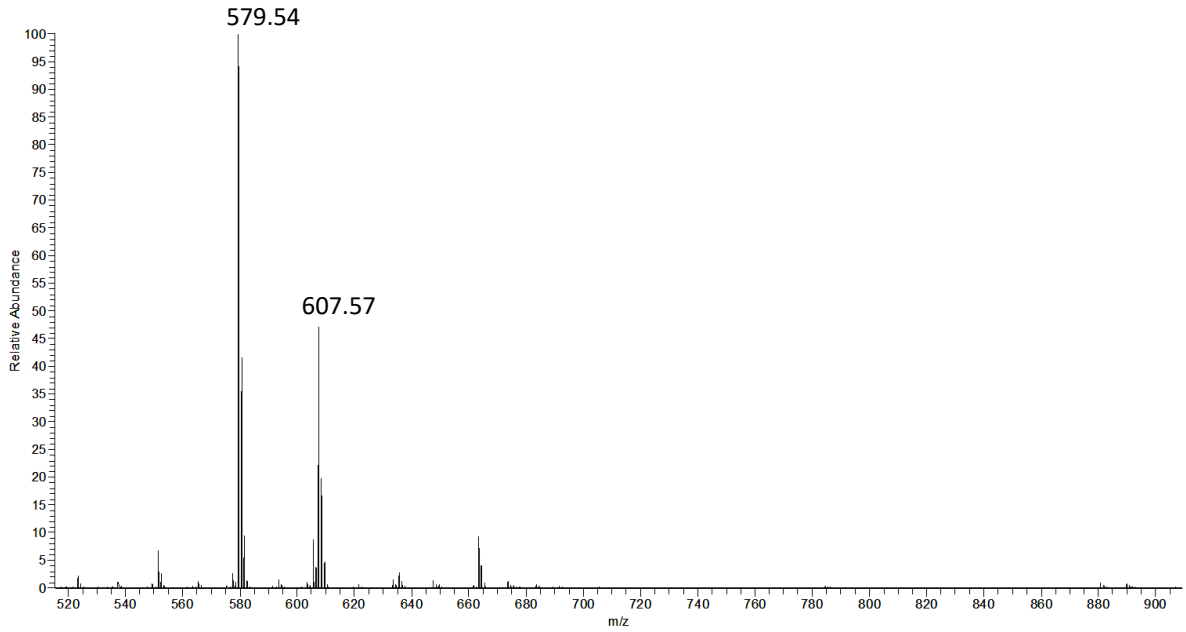

Figure 3.14: APCI-MS spectrum of peak at 19.72 min of Figure 3.13.

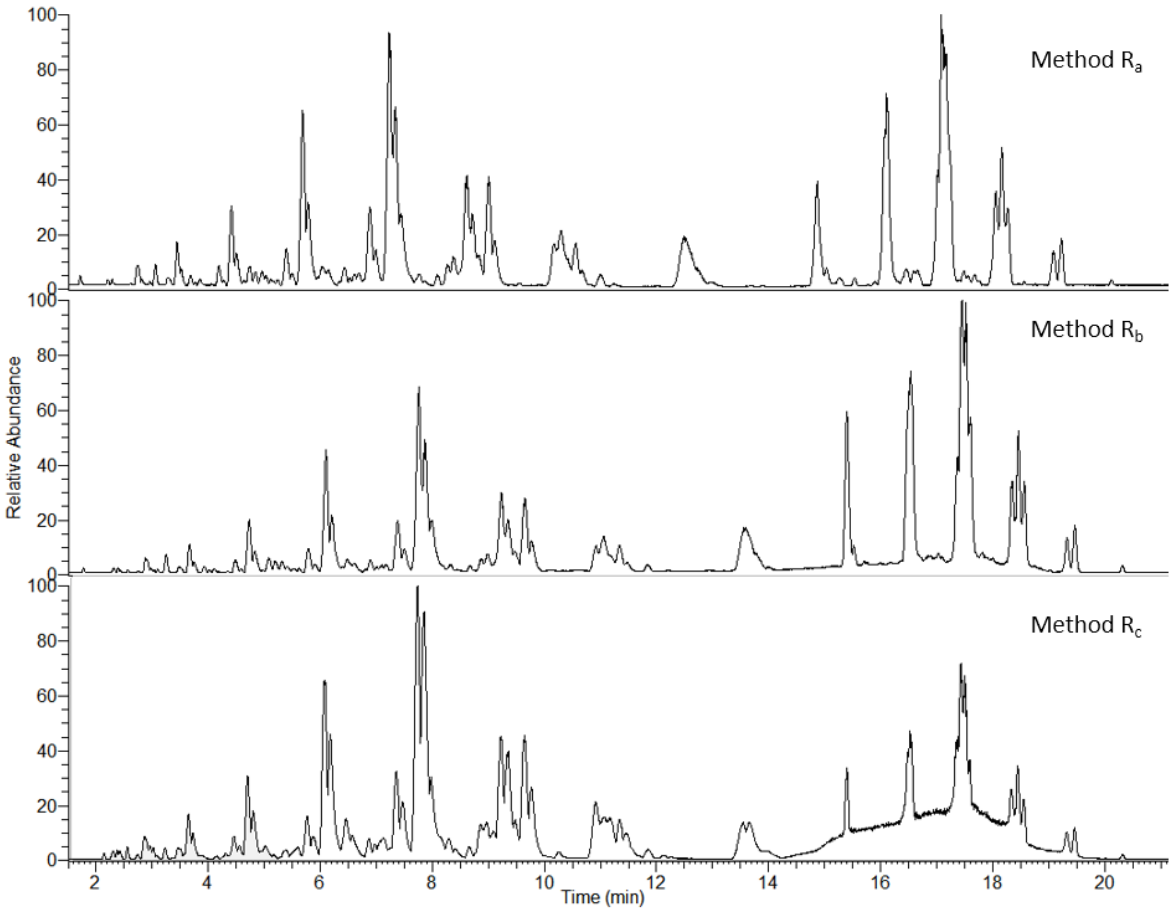

Figure 3.15: Orbitrap MS detector Partial RP UHPLC-APCI MS base peak chromatograms of commercial full fat cow milk sample analysed with Methods R_a, R_b and R_c (Methods described in Table 3.10 with solvent A: methanol 100% for method R_a; methanol 90%, ammonium acetate [in methanol 10mM] 10% for method R_b; ammonium acetate [in methanol 10mM] 100% for method R_c)

The final adjustment made was to decrease the temperature to 46°C from the previous 50°C. The reason for this change was to allow the analytes to interact longer with the column in

anticipation of achieving better separation without further adjustment of the eluent composition. The temperature could not be lowered any further due to the high backpressure of the UHPLC method. The temperature selected was the lowest one that would still allow the flow rate to remain the same and also to stay within the backpressure limitations of the UHPLC equipment. The resulting Method S has the same gradient as Method R with an additional six minutes for column equilibration to allow the eluent to return to the initial composition (Table 3.1). The percentage of ammonium acetate in solvent A was also adjusted to 10% according to the previous findings. The change in temperature led to a slight increase in the analysis time (last peak elutes at 21.7 min while previously it eluted at 20.5 min; Figure 3.16 and Figure 3.13 respectively) which is compensated for by a significant improvement in separation of for TAGs with ECN 46 and 48: a number of peaks of ECN 46 are partially separated while those of ECN 48 are better resolved than previously, although still not to baseline. Some definition of peaks for ECN 40 was lost.

Table 3.11: Mobile phase gradient of Method S for UHPLC separation of TAGs. Flow rate 0.45 mL/min. Temperature controlled at 46°C. The solvents used were A: Methanol (90%) and ammonium acetate in methanol (10 mM; 10%), B: Acetonitrile, C: Dichloromethane and D: Water. Percentages are rounded to 2 significant figures.

Time (min)		0	2	8	11	13	18	24	25	30
Solvents	A %	79	79	81	45	5.0	5.0	5.0	79	79
	B %	15	15	15	51	75	65	65	15	15
	C %	3.0	3.0	3.0	3.0	20	30	30	3.0	3.0
	D%	3.0	3.0	1.4	0.6	0.0	0.0	0.0	3.0	3.0

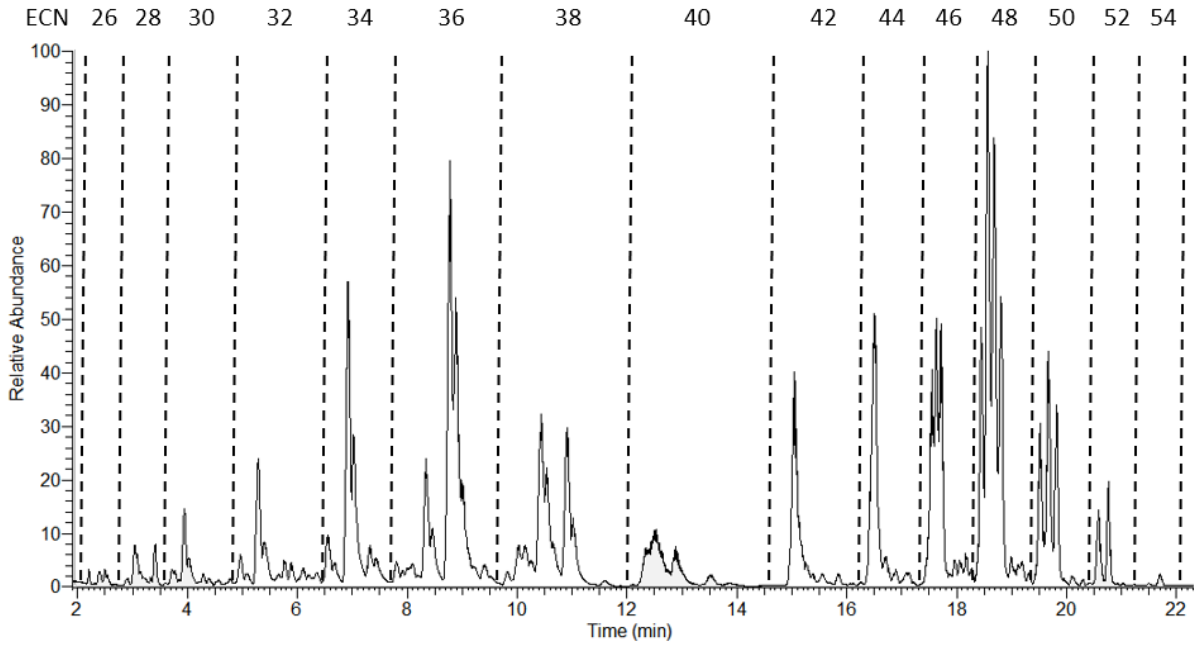

Figure 3.16: Partial RP UHPLC-APCI MS base peak chromatogram of commercial full fat cow milk sample analysed with Method S (Table 3.11). Regions are assigned according to ECN.

Overall, method S was deemed to be a suitable method to analyse the range of TAGs found in milk samples in a short time. Full separation of all TAGs was not achieved, with problems for groups of ECNs 42 and 44, but most of the components were separated and, most importantly, this was achieved in 22 min while all previous methods were longer than two hours, which can allow for rapid screening of a large number of samples for food analysis and authentication in a fraction of the time.

3.2.2 Mass spectrometric analysis of milk TAGs

Mass spectrometry was used to identify TAGs in the milk sample. Due to the narrow peak widths and complexity of the mixtures a short MS duty cycle was required for UHPLC method development. Furthermore, obtaining tandem mass spectra was crucial for the identification of the various acyl groups attached to the glycerol backbone of the TAGs and, in cases where possible, to identify different positional isomers of TAGs. The Thermo Orbitrap allows the scanning of ions with the Orbitrap detector at the same time as isolation of a precursor ion in quadrupole mode. Hence, collision- induced dissociation MS^n spectra can be generated rapidly, and without compromising the resolution of the MS spectra. The MS^2 spectra that are useful for the identification of the different acyl groups present are those produced by the dissociation of the molecular adduct ions. A precursor ion *m*/*z* range was selected to ensure that appropriate ions were selected for dissociation. The *m*/*z* values of the ammoni adducts for the milk TAGs range from *m*/*z* 516.43 to *m*/*z* 908.87, the TAGs with higher *m*/*z* values generally eluting later in the chromatogram. Thus, precursor scan ranges were set at *m*/*z* 490-790 for 0-16 min and *m*/*z* 720-940 for 16 to 30 min (Table 2.7, Chapter 2).

The base peak chromatogram of cow's milk shows the presence of TAGs with ECN values between 26 and 54 (Figure 3.17 and Figure 3.18). The complex chromatogram contained some peaks giving rise to only one ammonium adduct ion *m*/*z* value and others where the presence of more than one *m*/*z* value indicates co-elution of different TAGs. TAGs with ECNs 42 and 44 (time range 14.5-17 min, Figure 3.18) appear as single broad peaks and the ammonium adduct ions and thus the co-eluting TAGs could not be identified because of the complexity of the mass chromatogram.

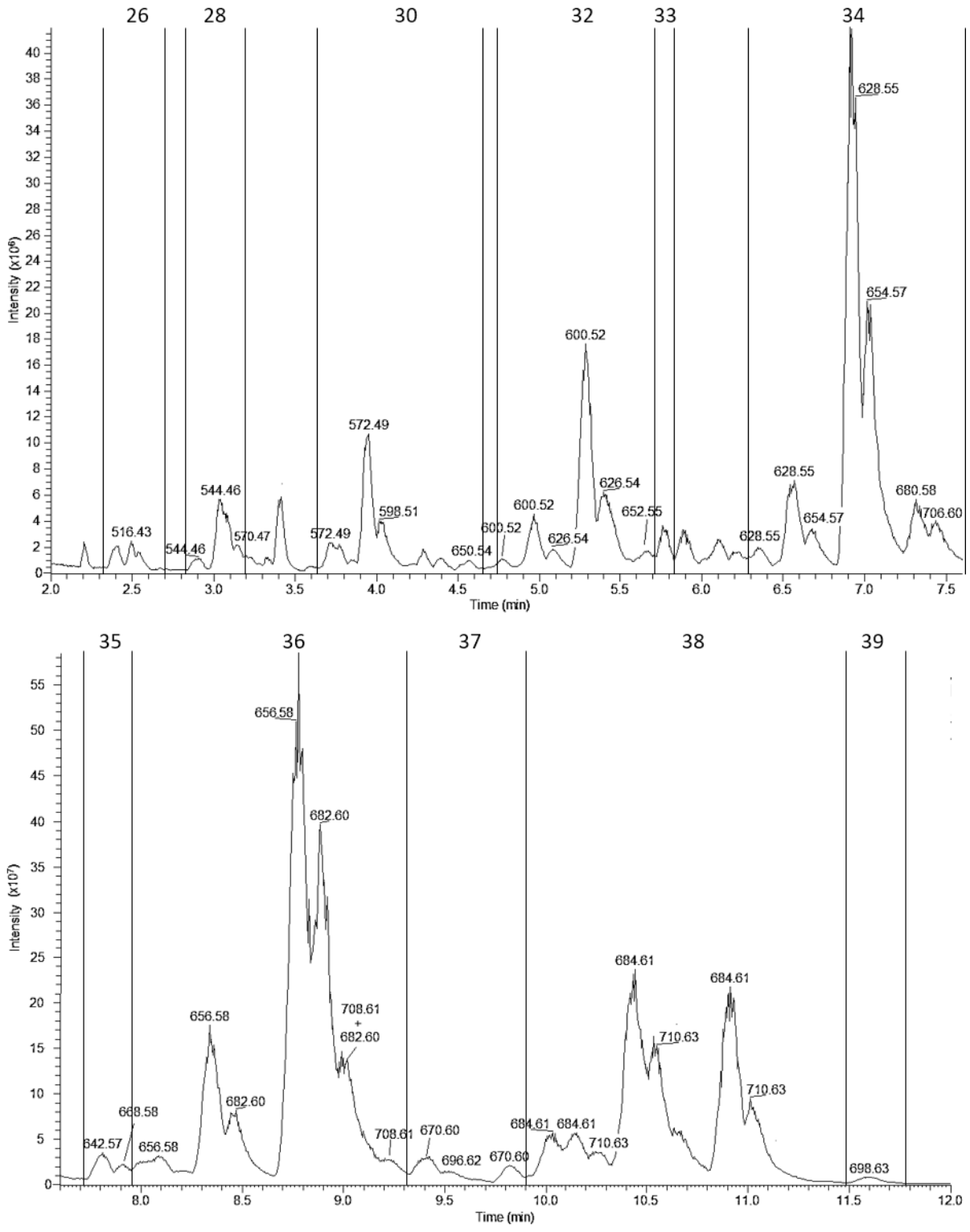

Figure 3.17: Partial RP UHPLC-APCI MS base peak chromatogram of a commercial full fat cow milk sample analysed with Method S (Table 3.11). Regions are assigned according to ECN. Peaks are labelled with *m/z* value of the ammonium adduct ion.

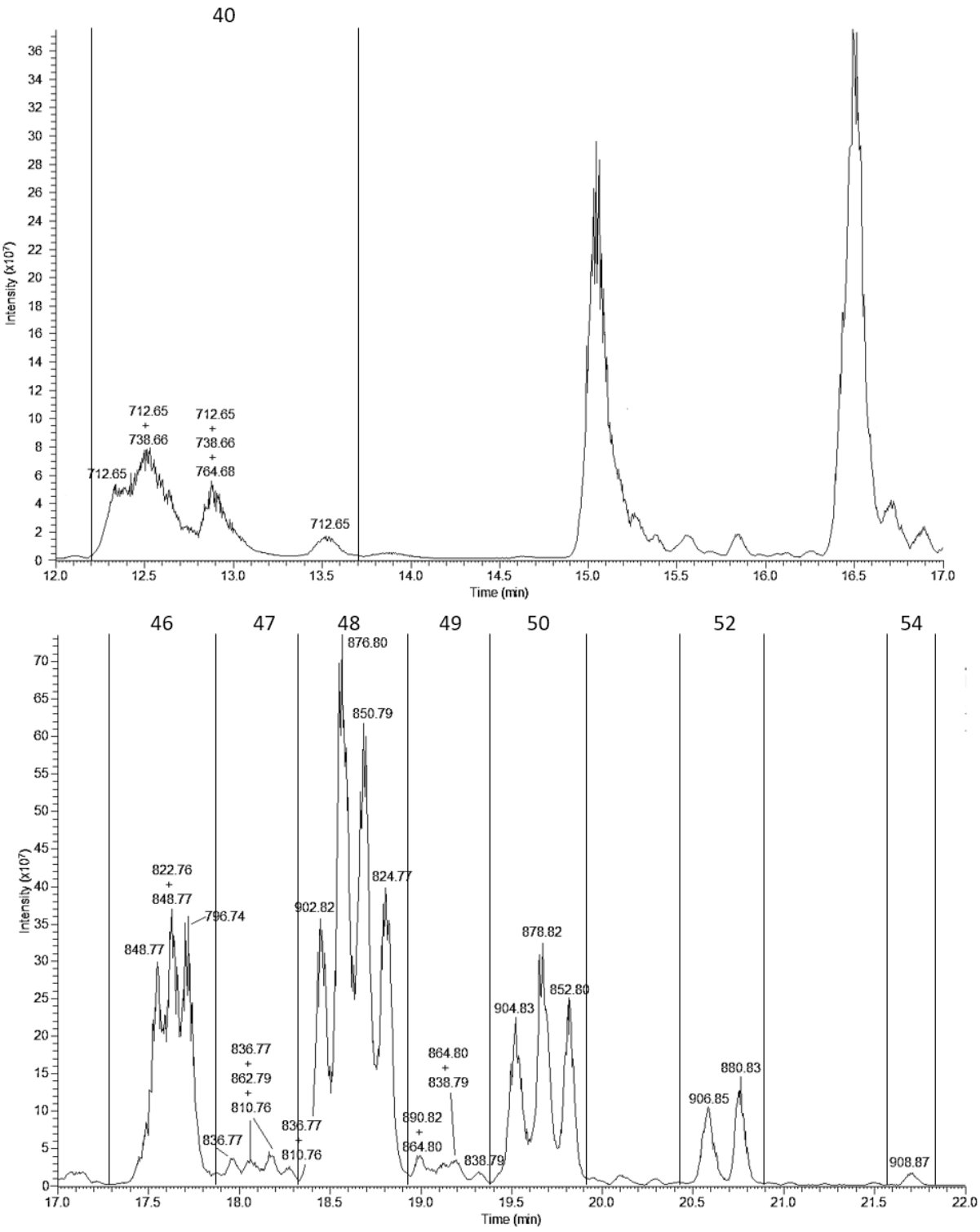

Figure 3.18 Partial RP UHPLC-APCI MS base peak chromatogram of a commercial full fat cow milk sample analysed with Method S (Table 3.11). Regions are assigned according to ECN. Peaks are labelled with *m/z* value of the ammonium adduct ion.

A total of 67 distinct peaks were recognised (Table 3.12), 27 of which correspond to single TAGs and 40 show evidence of coelution. The MS^2 spectra enabled identification of a total of 96 TAGs (27 separated and 69 coeluting) and a further 21 were identified tentatively. Isobaric TAGs presented a problem for identification with MS^2. When TAGs separate completely, they produce clean spectra containing ions corresponding to the ammonium and proton adduct ions and up to three DAG ions. TAGs having three different acyl chains generate 3 DAG ions, those with two different acyl chains, generate 2 DAG ions and those containing the same acyl chain on all three positions give 1 DAG ion. In cases where TAGs co-elute a number of ammonium and proton adduct ions and DAGs could be present. Using MS^2 on the different ammonium adduct ions can elucidate the TAG structures, unless the different co-eluting TAGs are isobaric, in which case, even the MS^2 spectrum will show more than three DAG ions making identification (especially for positional isomers) harder or not possible.

Table 3.12: TAGs identified in cow milk analysed using Method S (Table 3.11; Figure 3.18) giving *m/z* values of ammonium adduct ions, $[M+NH_4]^+$, proton adduct ions, $[M+H]^+$, and DAG product ions, $[M-RCO_2]^+$. Tentative TAG identifications are enclosed in using brackets. Multiple positional isomers of the TAGs could not be distinguished apart from a small number of cases where the TAG in question is labelled as ABC*, meaning the acyl group in position sn-2 is B and positions sn-1 and sn-3 are occupied by either A or C. The abbreviations used for the acyl groups are explained in Abbreviations.

Peak No	Apex RT min	$[M-RCO_2]^+$ *m/z*	$[M+NH_4]^+$ *m/z*	$[M+H]^+$ *m/z*	TAG identification	ECN
1	2.41	411.35, 355.28, 271.19	516.43	499.41	MCC_4	26
2	2.49	411.35, 383.32, 243.16	516.43	499.41	PC_6C_4	
3	2.54	437.36, 409.33, 243.16	542.44	525.42	OC_6C_4	
4	2.9	411.35, 383.32, 299.22	544.46	527.42	MCC_6	28
		411.35, 355.28, 327.25			$LaCaC_6$	
5	3.03	439.38, 355.28, 299.22	544.46	527.44	$MCaC_4$	
6	3.14	465.39, 409.33, 271.19	570.47	553.45	OCC_4	
		439.38, 383.32, 271.19	544.46	527.39	PCC_4	
7	3.71	439.38, 383.32, 327.25	572.49	555.46	$MCaC_6$	30
8	3.77	439.38, 411.35, 299.22	572.49	555.46	PCC_6	
9	3.95	467.41, 383.32, 299.22	572.49	555.47	$PCaC_4$	
		467.41, 355.28, 327.25			$MLaC_4$	
10	4.57	545.46, 405.30, 355.28	650.54	633.51	$LnMC_4$	
11	4.78	411.35, 383.32	600.52	583.44	LaCaCa	32
		439.38, 411.35, 355.28			MCaC	
12	4.96	439.38, 327.25	600.52	583.49	PCC	
		467.41, 383.32, 355.28			$MLaC_6$	
		467.41, 411.35, 327.25			$PCaC_6$	
13	5.08	493.43, 437.36, 327.25	626.54	609.51	$OCaC_6$	
14	5.29	495.44, 355.28	600.52	583.51	MMC_4	
		495.44, 383.32, 327.25			$PLaC_4$	
15	5.4	521.46, 409.33, 327.25	626.54	609.51	$OLaC_4$	
		521.46, 381.30, 355.28			$PoMC_4$	
		521.46, 383.32, 353.27			$PMyC_4$	
16	5.67	547.47, 407.32, 355.28	652.55	635.53	LMC_4	
17	5.76	509.46, 369.30, 355.28	614.54	597.49	$PtMC_4$	33
18	6.35	439.38, 383.32	628.55	611.52	[MCaCa]	34
		467.41, 439.38, 355.28			PCaC	
		439.38, 411.35			[LaLaCa]	
		467.41, 411.35, 383.32			[MLaC]	
19	6.57	495.44, 383.32	628.55	611.52	MMC_6	
		495.44, 411.35, 355.28			$PLaC_6$	
20	6.91	523.47, 383.32, 355.28	628.55	611.52	PMC_4	
21	7.01	549.49, 383.32, 381.30	654.57	637.54	$PPoC_4$	
		549.49, 409.33, 355.28			OMC_4	
22	7.32	575.50, 407.32, 383.32	680.58	663.56	LPC_4	
		575.50, 409.33, 381.30			$OPoC_4$	

Peak No	Apex RT min	$[M\text{-}RCO_2]^+$ *m/z*	$[M+NH_4]^+$ *m/z*	$[M+H]^+$ *m/z*	TAG identification	ECN
23	7.44	601.52, 409.33, 407.32	706.60	689.57	OLC_4	
		575.50, 407.32, 383.32	680.58	663.56	LPC_4	
24	7.81	537.49, 383.32, 369.30	642.57	625.56	$PPtC_4$	35
25	7.91	563.50, 409.33, 369.30	668.58	651.56	$OPtC_4$	
		563.50, 395.32, 383.32			$MoPC_4$	
26	8.09	467.41, 383.32	656.58	639.56	PCaCa	36
		495.44, 411.35			MMC	
		467.41, 439.38, 411.35			MLaCa	
27	8.34	523.47, 411.35, 383.32	656.58	639.56	PMC_6	
28	8.47	549.49, 411.35, 409.33	682.60	665.57	$PPoC_6$	
		549.49, 437.36, 383.32			OMC_6	
29	8.78	551.50, 383.32	656.58	639.56	PPC_4	
		551.50, 411.35, 355.28			SMC_4	
30	8.89	577.52, 409.33, 383.32	682.60	665.57	OPC_4	
31	9.02	603.54, 409.33	708.61	691.59	OOC_4	
		577.52, 409.33, 383.32	682.60	665.57	OPC_4	
32	9.25	603.54, 409.33	708.61	691.59	OOC_4	
		603.54, 411.35, 407.32			SLC_4	
33	9.42	537.49, 411.35, 397.33	670.60	653.56	$PPtC_6$	37
		565.52, 411.35, 369.30			$SPtC_4$	
		565.52, 397.33, 383.32			$MaPC_4$	
34	9.52	591.54, 409.33, 397.33	696.61	679.59	$OMaC_4$	
		563.50, 437.36, 397.33			$OPtC_6$	
		563.50, 423.35, 411.35			$MoPC_6$	
35	9.82	565.52, 411.35, 369.30	670.60	653.56	$SPtC_4$	
		565.52, 397.33, 383.32			$MaPC_4$	
36	10.03	467.41, 439.38	684.61	667.58	[MLaLa]	38
		495.44, 439.38			[MMCa]	
		495.44, 467.41, 411.35			PLaCa	
37	10.15	523.47, 439.38, 411.35	684.62	667.58	PMC	
		521.46, 493.43, 411.35	710.63	693.60	OLaCa	
38	10.28	549.49, 465.39, 411.35	710.63	693.60	OMC	
		523.47, 439.38, 411.35	684.62	667.58	PMC	
39	10.44	551.50, 411.35	684.61	667.59	PPC_6	
		551.50, 439.38, 383.32			SMC_6	
		577.52, 437.36, 411.35	710.63	693.60	OPC_6	
		523.47, 465.40, 437.37			$PMC_{10:1}$	
40	10.53	577.52, 437.36, 411.35	710.63	693.60	OPC_6	
		551.50, 411.35	684.62	-	PPC_6	
		603.54, 437.36	736.65	719.62	OOC_6	
41	10.91	579.54, 411.35, 383.32	684.61	667.60	SPC_4	
42	11.01	605.55, 411.35, 409.33	710.63	693.60	SOC_4	

Peak No	Apex RT min	$[M\text{-}RCO_2]^+$ *m/z*	$[M+NH_4]^+$ *m/z*	$[M+H]^+$ *m/z*	TAG identification	ECN
43	11.6	565.52, 425.36, 411.35	698.63	681.48	$MaPC_6$	39
		565.52, 439.38, 397.33			$SPtC_6$	
		593.55, 411.35, 397.33			$SMaC_4$	
44	12.34	495.44, 439.38	712.65	695.61	PLaLa	40
		523.47, 467.41, 439.38			PMCa	
45	12.53	495.44, 439.38	712.65	695.62	PLaLa	
		551.50, 467.41, 411.35			SMC	
		551.50, 439.38			PPC	
		523.47, 467.41, 439.38			PMCa	
		549.49, 493.43, 439.38	738.66	721.64	[OMCa]	
		549.49, 467.41, 465.39			PPoCa	
		521.46, 439.38			OLaLa	
		577.52, 465.39, 439.38			OPC	
		495.44, 493.43			MMMy	
46	12.88	603.54, 465.39	764.68	747.65	OOC	
		575.50, 491.41, 467.41			LPCa	
		605.55, 439.38, 437.36	738.66	721.64	SOC_6	
		551.50, 465.39			$PPC_{10:1}$	
		579.54, 439.38, 411.35	712.65	695.61	SPC_6	
47	13.52	607.57, 411.35	712.65	695.62	SSC_4	
48	17.55	523.47, 549.49, 577.52	822.76	805.73	[OPM]	46
		549.49, 603.54	848.77	831.75	OOM	
		549.49, 575.50, 577.52			OPPo	
49	17.63	523.47, 549.49, 577.52	822.76	805.73	[OPM]	
		551.50, 575.50	848.77	831.75	[LPP]	
50	17.72	495.44, 551.50	796.74	779.71	[SMM]	
		523.47, 551.50			[PPM]	
51	17.95	577.52, 563.50, 537.49	836.77	819.75	OPPt	47
52	18.06	577.52, 563.50, 537.49	836.77	819.75	[OPPt]	
		603.54, 563.50	862.79	845.76	[OOPt]	
		589.52, 577.52, 563.50			[OPMo]	
		565.52, 537.49, 523.47	810.76	793.73	[MaPM]	
		551.50, 537.49			[PPPt]	
53	18.16	577.52, 563.50, 537.49	836.77	819.75	[OPPt]	
		589.52, 577.52, 563.50	862.78	845.76	[OPMo]	
		565.52, 537.49, 523.47	810.75	-	[MaPM]	
		551.50, 537.49			[PPPt]	
54	18.28	577.52, 563.50, 537.49	836.77	819.75	[OPPt]	
		565.52, 537.49, 523.47	810.76	793.71	[MaPM]	
		551.50, 537.49			[PPPt]	
55	18.44	603.54	902.82	885.79	OOO	48
56	18.57	577.52, 603.54	876.80	859.77	OPO*	
57	18.68	551.50, 577.52	850.79	833.76	OPP*	

Peak No	Apex RT min	$[M\text{-}RCO_2]^+$ *m/z*	$[M+NH_4]^+$ *m/z*	$[M+H]^+$ *m/z*	TAG identification	ECN
58	18.81	523.47, 551.50, 579.53	824.77	807.74	SPM	
59	18.99	603.54, 591.54	890.81	873.79	[OOMa]	49
		591.54, 577.52, 565.52	864.80	847.78	[OMaP]	
		605.55, 565.52, 563.50			[SOPt]	
60	19.2	591.54, 577.52, 565.52	864.80	847.78	[OMaP]	
		605.55, 565.52, 563.50			[SOPt]	
		579.53, 565.52, 537.49	838.79	821.76	[SPPt]	
		565.52, 551.50			[MaPP]	
61	19.32	579.54, 565.52, 537.49	838.79	821.76	[SPPt]	
		565.52, 551.50			[MaPP]	
62	19.52	603.54, 605.55	904.83	887.81	SOO*	50
63	19.67	577.52, 579.53, 605.55	878.82	861.79	SPO*	
64	19.82	551.50, 579.54	852.80	835.77	SPP*	
65	20.58	605.55, 607.57	906.85	889.82	SSO*	52
66	20.76	579.54, 607.57	880.83	863.80	SPS*	
67	21.71	607.57	908.86	891.83	SSS	54
		579.54, 607.57, 635.60			$[SPC_{20}]$	
		551.50, 635.60			$[PPC_{22}]$	

Examples of the process of identifying TAGs from their MS spectra are shown below.

The mass spectrum for peak 55 shows a very small peak for the ammonium adduct ion (*m/z* 902.82), the major peaks in the spectrum corresponding to the proton adduct ion (*m/z* 885.79) and two peaks that could be from DAG ions (*m/z* 603.54 and 577.52) (Figure 3.19). The MS^2 spectrum of the proton adduct ion (being the largest peak in the precursor ion selection range) was examined to determine whether the peaks at *m/z* 603.54 and 577.52 correspond to DAG ions (Figure 3.20). Of the two peaks, only *m/z* 603.54 appears in the MS^2 spectrum indicating the TAG to have only one type of acyl group present, an oleyl group (derivative of oleic acid, C18:1) which can be determined by calculating its mass from the difference between the mass of the DAG and the TAG ions. The peak at *m/z* 867.77 can be attributed to the dehydration of the ion, but the ion *m/z* 886.77 is harder to attribute. The isolation width for the MS^2 analysis, 1.6 *m/z*, does not account for the presence of this peak, although it can account for the smaller peak at *m/z* 885.80.

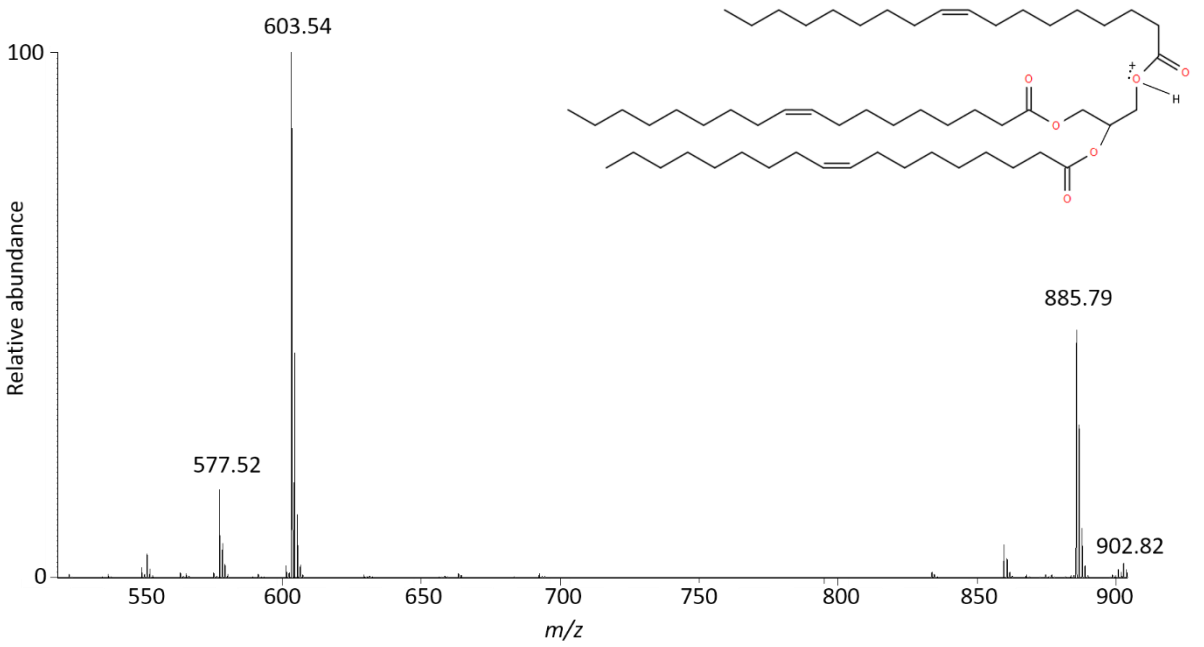

Figure 3.19: APCI-MS spectrum across peak 55 (Table 3.12), apex RT 18.44 (Figure 3.18). Structure of ($M+H^+$) with mass 885.79 shown

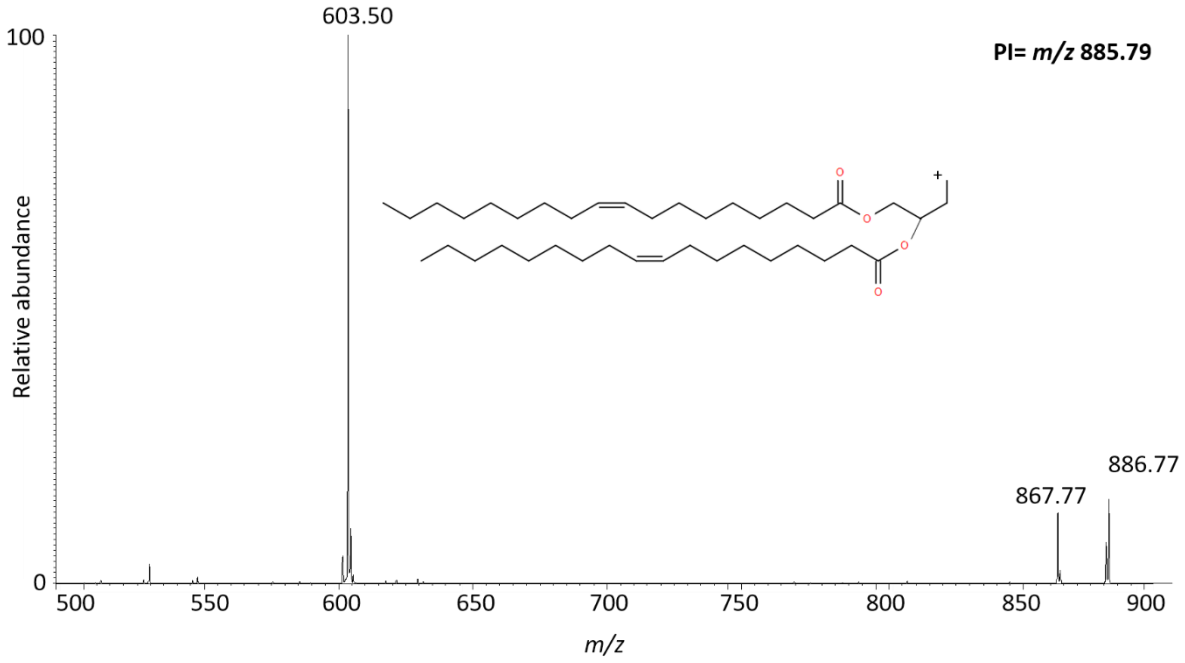

Figure 3.20: MS^2 spectrum from proton adduct ion at *m/z* 885.79 summed over peak 55 (Table 3.12) (PI=precursor ion). Structure of fragment with mass 603.50 shown

The spectrum for peak 56 is slightly more complicated. There are a number of ions in the *m*/*z* range where the ammonium and proton adduct ions are expected. Of those ions, *m*/*z* 859.77, being the most abundant, was automatically selected for MS^2. It can be surmised that one of the other ions, *m*/*z* 885.79, results from partial co-elution with the previous peak (peak 55, Figure 3.19), a factor that could be resolved with improved chromatographic separation. Assuming that *m*/*z* 885.79 is the proton adduct ion, the two most abundant ions in the spectrum, *m*/*z* 577.52 and 603.54, can be identified as [OP] and [OO] DAG ions, respectively. The MS^2 spectrum verifies the assumption (Figure 3.22) since both DAG ions are present, along with ions *m*/*z* 841.77 and 860.77, the first of which can be attributed to the dehydration of the proton adduct ion while the second one could not be attributed, as was also seen previously for the MS^2 of peak 55 (Figure 3.20). The MS^2 spectrum also provides important information about the stereochemistry of the TAG, specifically the positions of the different acyl moieties (Byrdwell and Neff, 2002; Holcapek et al., 2003; Hasan, 2010). If the MS spectrum was considered in isolation the ratio of the DAG peaks ([OP]/[OO]) would be taken to suggest that the isomer OPO* is present whereas analysis of the MS^2 spectrum indicates the isomer to be OOP*.

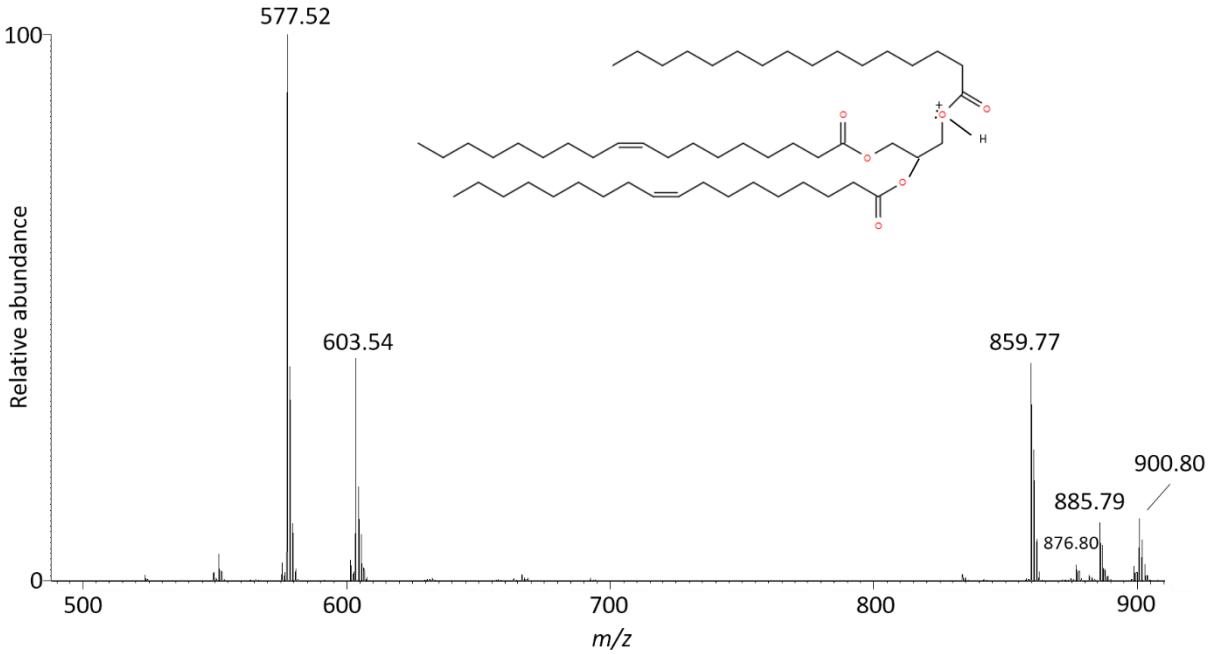

Figure 3.21: APCI-MS spectrum across peak 56 (Table 3.12), apex RT 18.57 (Figure 3.18). Structure of ($M+H^+$) with mass 859.77 shown

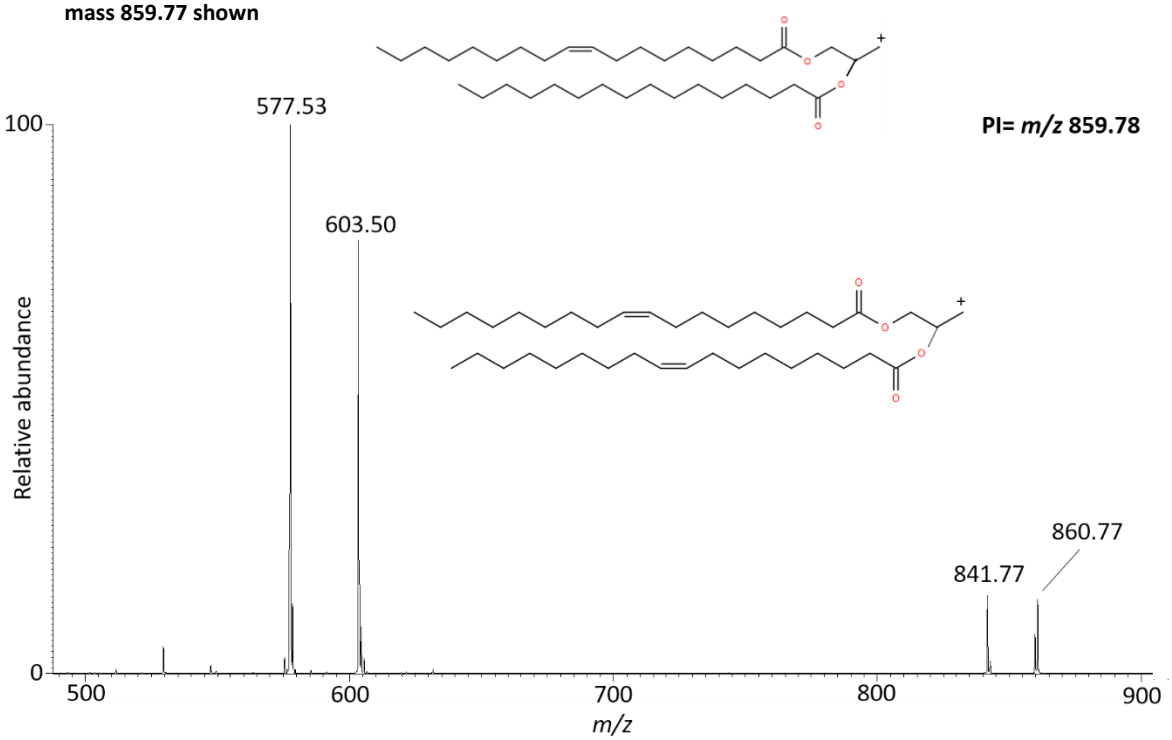

Figure 3.22: MS^2 spectrum from proton adduct ion at *m/z* 859.78 across peak 56 (Table 3.12) (PI=precursor ion). Structure of fragments with mass 577.53 and 603.50 shown

Peak 20 gives a relatively straightforward spectrum with the ammonium adduct ion at *m/z* 628.55 being base peak and three prominent DAG ions at *m/z* 523.47 [PM], *m/z* 383.32 [PC_4] and *m/z* 355.28 [MC_4]. The MS^2 spectrum of the ammonium adduct ion also contains the same three DAG ions as the only major ions. The stereochemistry of the TAG cannot be determined unambiguously, although it is likely that the M acyl group occupies the *sn*-2 position, the [PC_4] DAG having the lowest intensity.

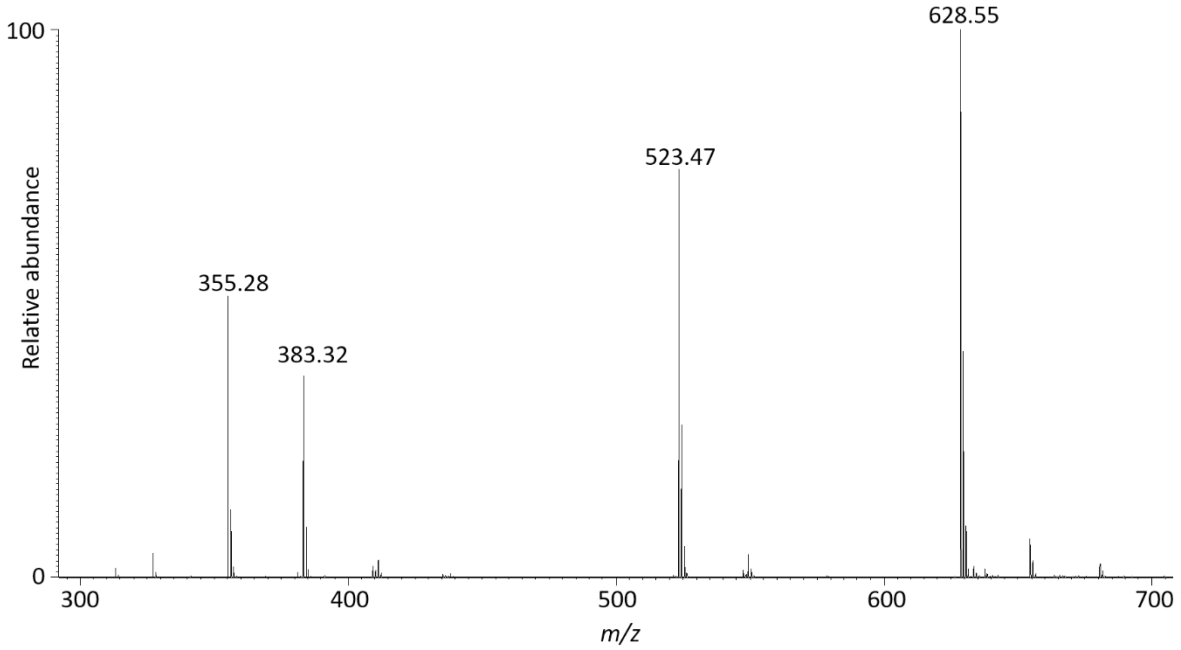

Figure 3.23: APCI-MS spectrum across peak 20 (Table 3.12), apex RT 6.91 (Figure 3.18)

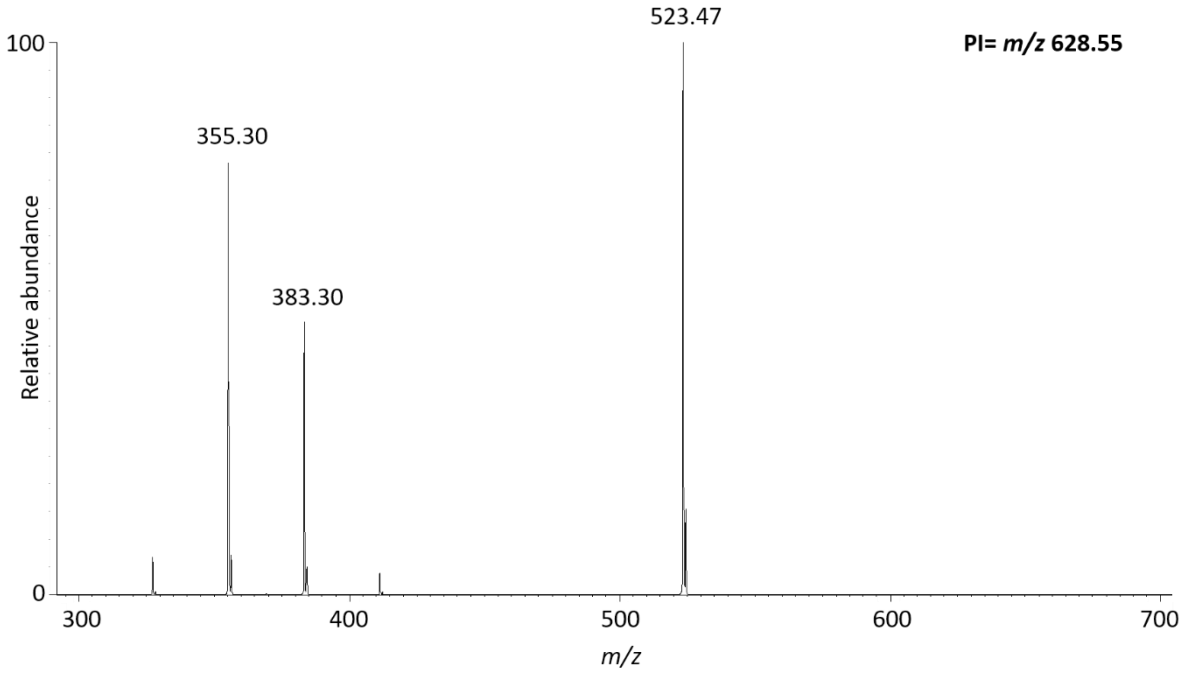

Figure 3.24: MS^2 spectrum from ammonium adduct ion at *m/z* 628.55 across peak 20 (Table 3.12) (PI=precursor ion)

In some cases, more than three DAG ions are present in the MS^2 spectrum of an ammonium or proton adduct ion. This occurs when two or more isobaric TAGs co-elute, as is the case for peak 14. The ammonium adduct ion at *m/z* 600.52 is the largest ion in the MS spectrum with four more ions being present (Figure 3.25). All four ions are also present in the MS^2 spectrum of the ammonium adduct ion which indicates that all four DAG ions come from isobaric TAGs that are structural isomers: a single TAG can have up to three different DAG ions (Figure 3.26). After consideration of all possible combinations of the four DAGs for the ammonium adduct ion two TAGs were identified: MMC4 and PLaC4. Although the presence of both TAGs can be demonstrated, their relative abundances, and for that matter their stereochemistries, cannot be determined owing to the presence of a common DAG ion and the lack of an indication of how much each of the two TAGs contribute to it.

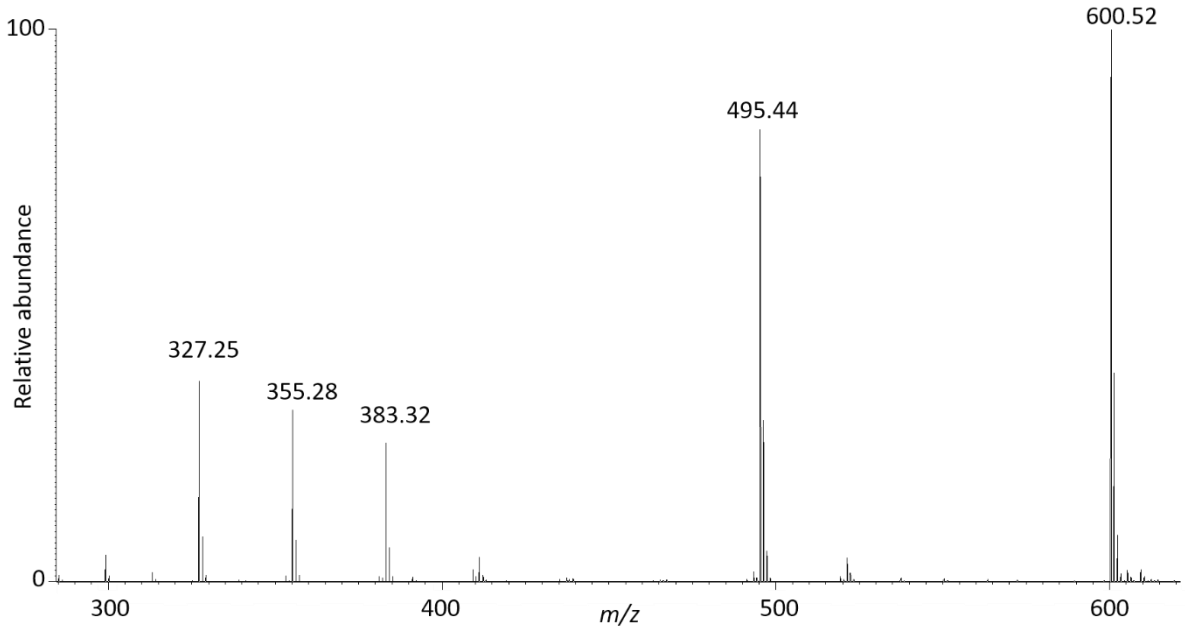

Figure 3.25: APCI-MS spectrum across peak 14 (Table 3.12), apex RT 5.29 (Figure 3.18)

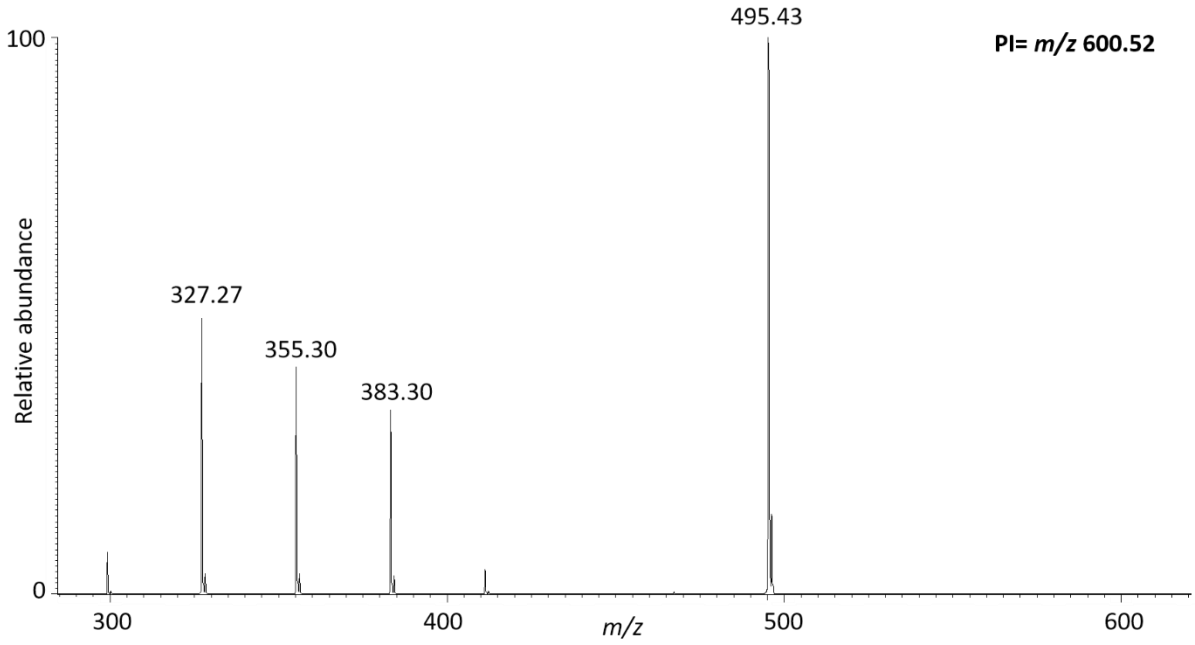

Figure 3.26: MS^2 spectrum from ammonium adduct ion at *m/z* 600.52 across peak 14 (Table 3.12) (PI=precursor ion)

Co-eluting TAGs are not necessarily isobaric or isomeric. Peak 39 is an example where both isobaric and non-isobaric TAGs co-elute within the same peak (Figure 3.27). The ammonium adduct ions, *m/z* 684.62 and 710.63, are both present and across the peak ion *m/z* 684.62 typically has higher relative abundance. Nevertheless, they are time windows where *m/z* 710.63 had higher relative abundance and was selected for dissociation (Figure 3.28 and Figure 3.29). Of all the DAG ions present in the MS spectrum, only *m/z* 551.50, 439.37, 411.37 and 383.33 are present in the tandem spectrum from precursor ion *m/z* 684.62, indicating that the TAGs present are PPC_6 and SMC_6 (Figure 3.28). On the other hand, the MS^2 spectrum from *m/z* 710.63 shows the proton adduct ion at *m/z* 693.60 along with five DAG ions, *m/z* 577.47, 523.47, 465.40, 437.37 and 411.37 indicating the presence of TAGS OPC_6 and $PMC_{10:1}$ (Figure 3.29). Overall, four different TAGs were identified for peak 39.

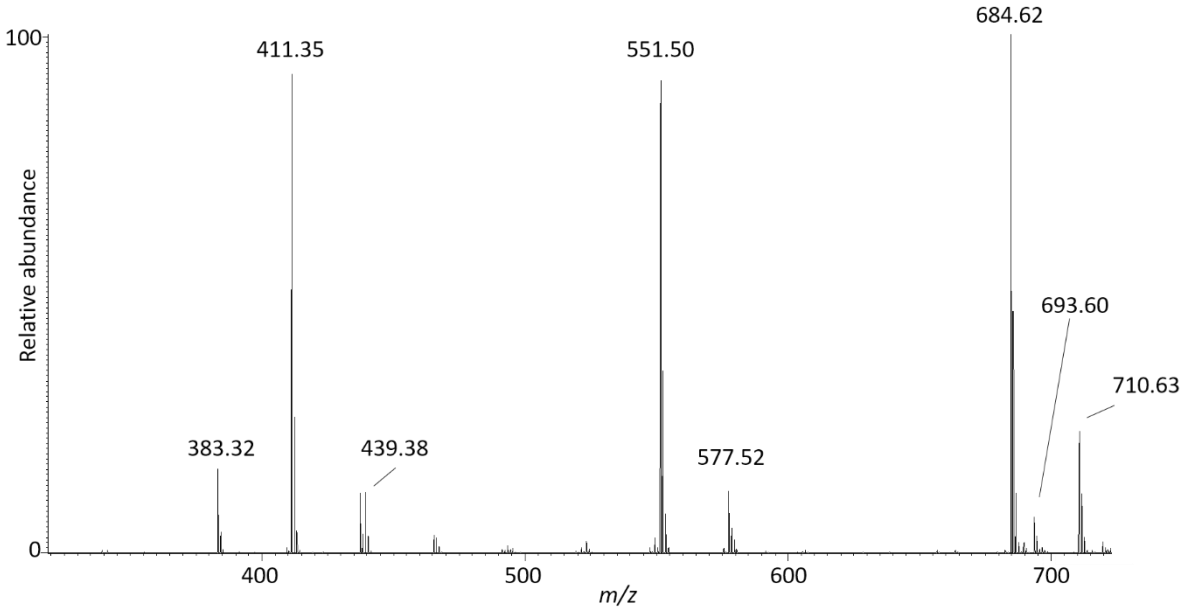

Figure 3.27: APCI-MS spectrum across peak 39 (Table 3.12), apex RT 10.44 (Figure 3.18)

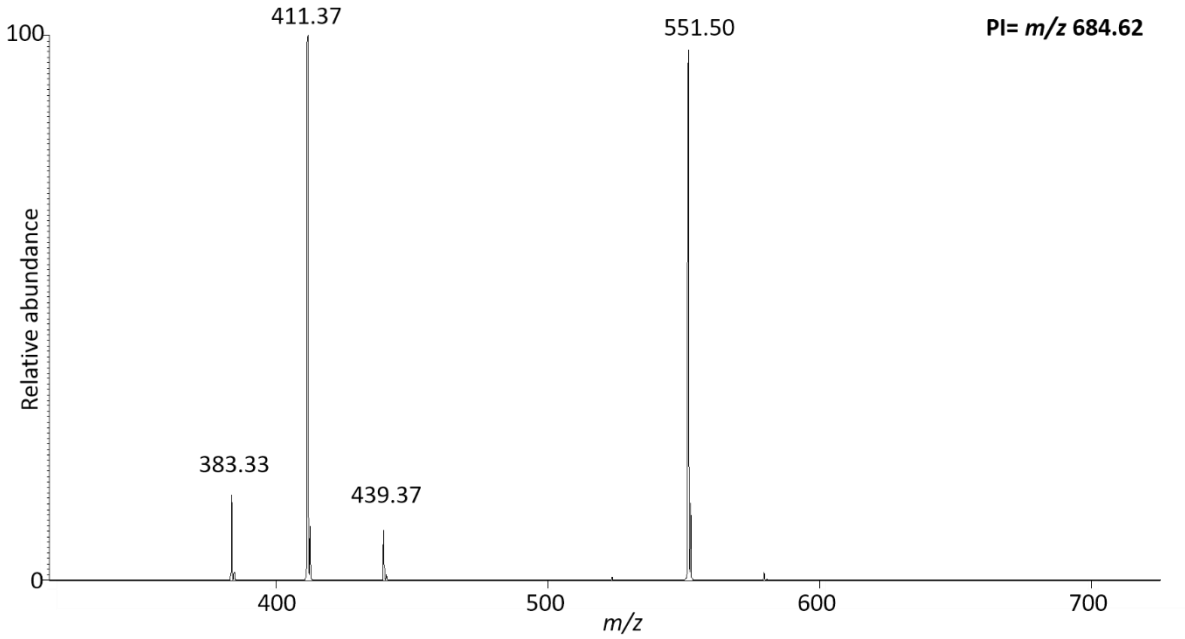

Figure 3.28: MS² spectrum from ammonium adduct ion at *m/z* 684.61 across peak 39 () (PI=precursor ion)

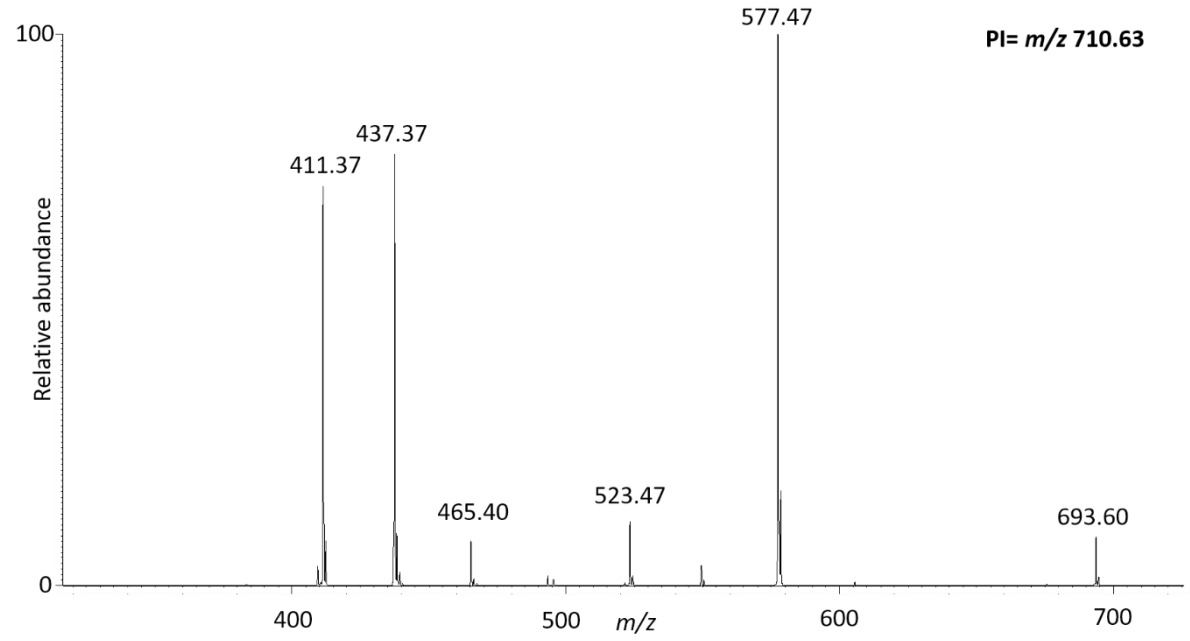

Figure 3.29: MS^2 spectrum from ammonium adduct ion at *m/z* 710.63 across peak 39 (Table 3.12) (PI=precursor ion)

In the previous example, four different TAGs were positively identified in the sample. Unfortunately, this is not always possible for co-eluting TAGs because the combinations of the different DAG ions are too numerous to permit a positive identification. This was the case for peak 45. Two ammonium adduct ions are present (*m/z* 738.66 and 712.65) and one proton adduct ion (*m/z* 721.64) and there are at least seven possible DAG ions, possibly more (Figure 3.30). MS^2 spectra for both ammonium adduct ions are available and can help elucidate the structures of the TAGs. Precursor ion *m/z* 712.65 dissociates to six DAG ions (*m/z* 551.47, 523.47, 495.43, 467.40, 439.37 and 411.37) (Figure 3.31). After examination of different combinations, the TAGs considered most likely are PLaLa (*m/z* 495.43 and 439.38), SMC (*m/z* 551.47, 467.40 and 411.37), PMCa (*m/z* 523.47, 467.40 and 439.37) and PPC (*m/z* 551.47 and 439.37). Even though some DAG ions are present in more than one TAG, all the TAGs listed need to be present for this combination of DAGs to appear on the MS^2 spectrum, with the exception of PPC. The two DAG ions that indicate PPC are present in other TAGs as well, but their higher relative abundance compared to the other ions indicates that PPC is present and contributing more than the other TAGS. As before, quantification and identification of isomers is not possible in this case. The second MS^2 spectrum, from precursor ion *m/z* 738.66 includes the proton adduct ion (*m/z* 721.64) and eight possible DAG ions (*m/z* 577.50, 549.47, 521.47, 495.43, 493.40, 467.43, 465.40 and 439.37) (Figure 3.32). The possible TAGs that would fragment to give these DAG ions are OMCa (*m/z* 549.47, 493.40 and 439.37), PPoCa (*m/z* 549.47, 467.43 and 465.40), OLaLa (*m/z* 521.47 and 439.37), OPC (*m/z* 577.50, 465.40 and 439.40) and MMMy (*m/z* 495.43 and 493.40). Not all of these suspected TAGs need to be present though, because of the overlaps of DAGs between different TAGs. Specifically, TAG

OMCa could be present since all the DAGs that could result from its dissociation are present. Nevertheless, the DAGs in the MS^2 spectrum could also result from dissociation of the other TAGs, precluding definitive assignment. Thus, the TAGs confirmed to be present in peak 45 are PLaLa, SMC, PPC, PMCa, PPoCa, OLaLa, OPC, MMMy and it is possible that OMCa is also present.

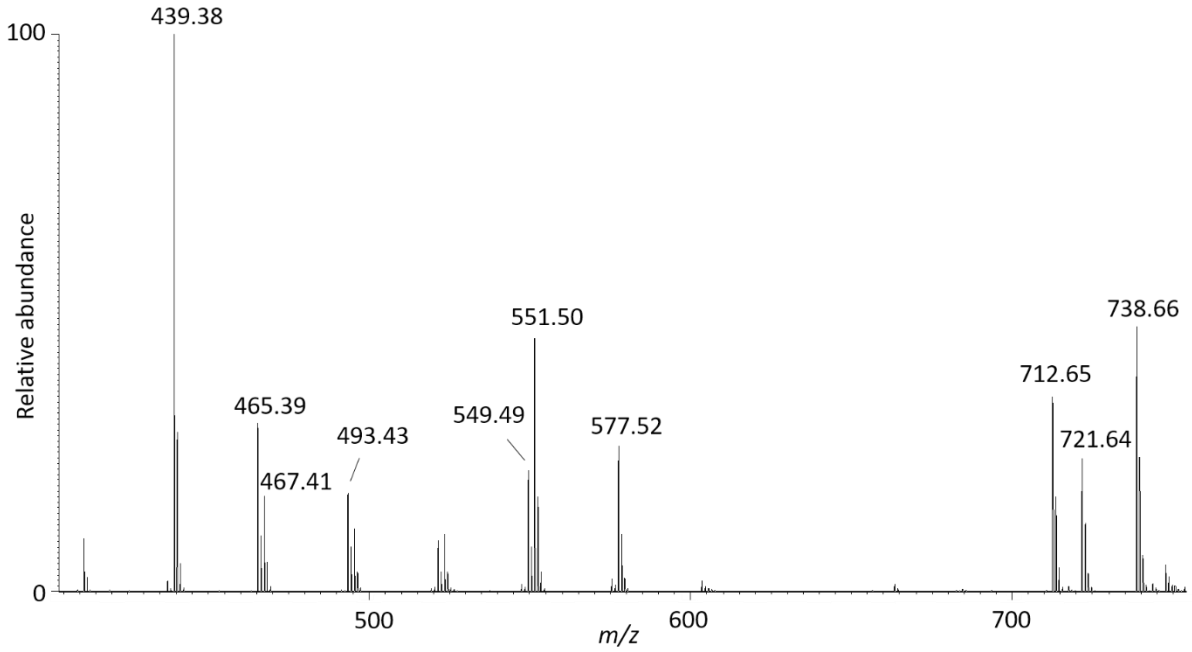

Figure 3.30: APCI-MS spectrum across peak 45 (Table 3.12), apex RT 12.53 (Figure 3.18)

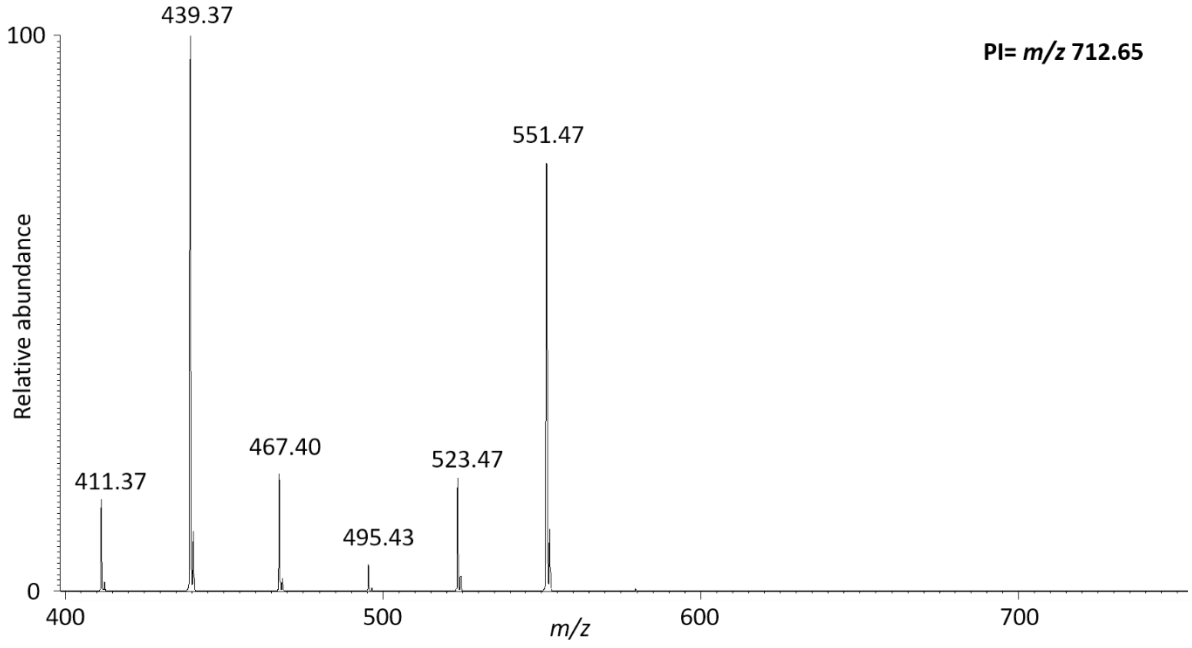

Figure 3.31: MS^2 spectrum from ammonium adduct ion at *m/z* 712.65 across peak 45 (Table 3.12) (PI=precursor ion)

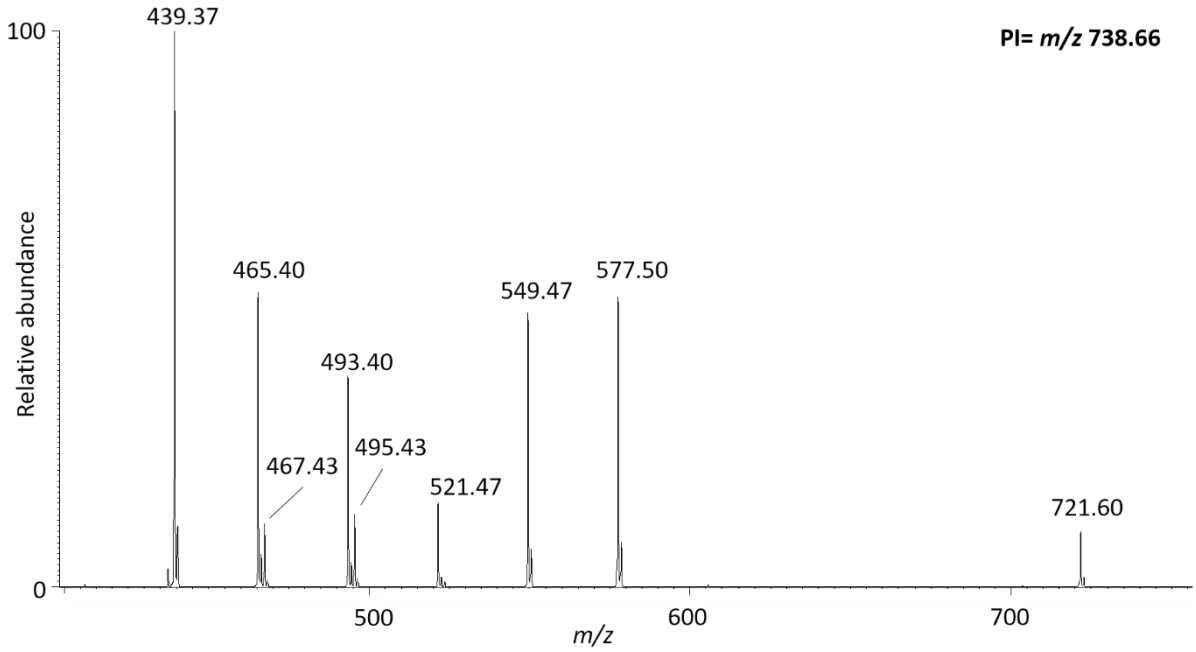

Figure 3.32: MS^2 spectrum from ammonium adduct ion at *m/z* 738.66 across peak 45 (Table 3.12) (PI=precursor ion)

Lastly, there were some cases where an MS^2 spectrum was not available for either the ammonium or proton adduct ion, making the identification of TAGs difficult. For example, peak 67 is a small peak and the ammonium adduct ion at *m/z* 908.86 was not abundant enough to be selected for MS^2 analysis (Figure 3.33). This creates an issue, since a number of the peaks that could be attributed to different DAG ions (*m/z* 635.60, 579.54 and 551.50) have similar or lower intensity to an interference ion present throughout the chromatograph (*m/z* 663.45) and without the MS^2 data, it is impossible to determine if those peaks are DAG ions or part of the background noise. Hence, TAG SSS is positively identified in peak 67 and TAGs SPC20 and PPC22 are suspected to be present but cannot be confirmed without MS^2 data.

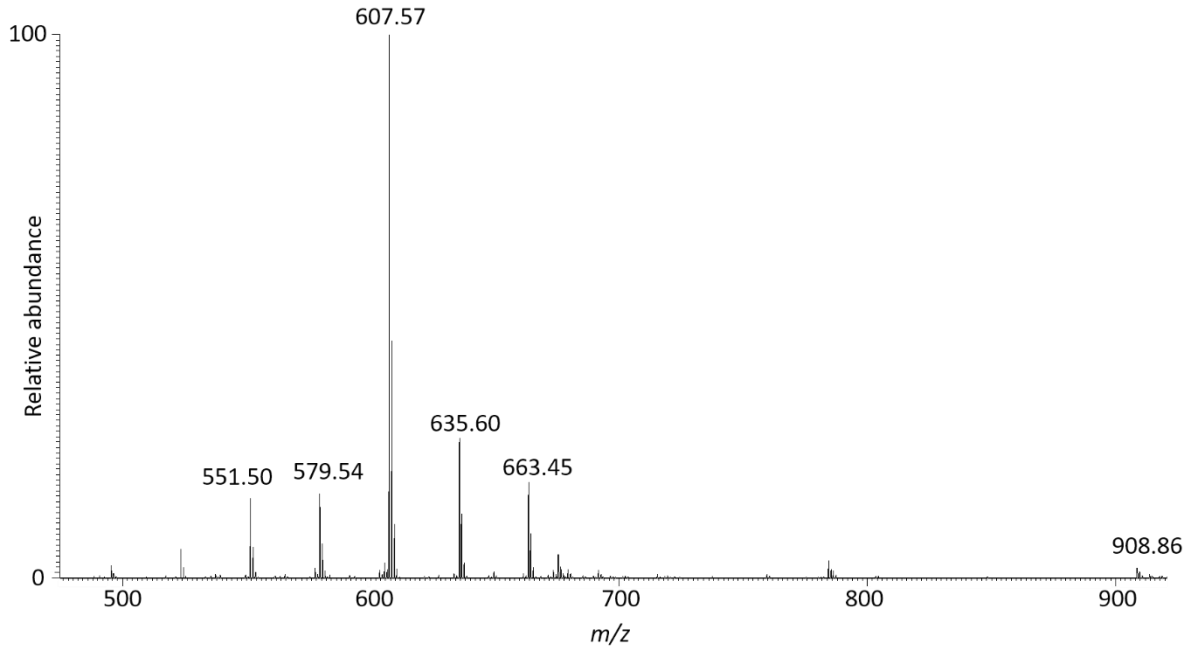

Figure 3.33: APCI-MS spectrum across peak 67 (Table 3.12), apex RT 21.71 (Figure 3.18)

Differences in response for selected ammonium and proton adduct ions awere observed in the course of this work. Proton adducts ions of TAGs with no double bonds gave either very low abundance ions or were absent in this study. This is in agreement with results from previous research that showed that more polar TAGs result in proton adduct ions with higher abundance (Byrdwell and Emken, 1995; Jakab et al., 2002; Hasan, 2010). Notably, it was observed that the protonation of TAGs is affected by structural features: with the exception of OOO, the presence of three double bonds in a TAG gives rise to spectra in which the proton adduct ion is base peak. In the case of OOO the proton adduct ion is still a major ion, though not base peak (Figure 3.34). There are some discrepancies to what would be expected when two double bonds are present in the TAG with proton adduct ions having lower abundances than what is expected. Specifically, when both double bonds are present in one of the acyl group chains (for example in L, linoleyl group) the abundance of the proton adduct ion is lower than in cases where there is one double bond in two of the acyl chains. Seven such cases were noted. Other discrepancies from the expected abundances of proton adduct ions can be explained by the presence of more than one TAG in the peak being examined, because when TAGs co-elute the relative abundances of the proton adduct ion peaks are not dependent only on the degree of saturation of each TAG, but also on the amount of each TAG present in the peak and their relative contribution to it.

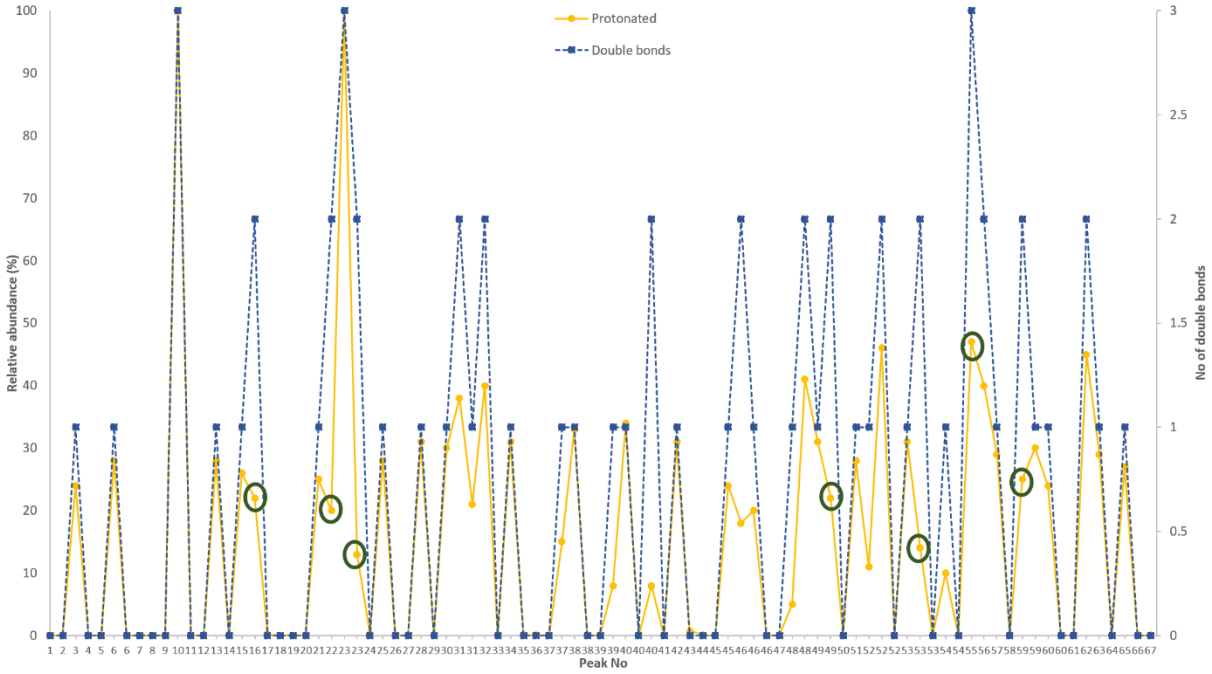

Figure 3.34: Correlation between the relative abundance of the proton adduct ion of a peak and the number of double bonds of the TAG suspected to elute. The circled data points represent TAGs that exhibited proton adduct ion peaks smaller than expected from the literature and the number of double bonds present. 1) LMC4 2) LPC4 and OPoC4 3) LPC4 4) LPP 5) OPMo 6) OOO and 7) OOMa

The ammonium acetate introduced through the methanol solvent was not sufficient to produce ammonium adduct ions after the point in the separation where methanol was ≤ 5% (Figure 3.35). Keeping the ammonium acetate constant throughout the separation is important because the presence of ammonium adduct ions with high abundance is imperative for the generation of MS^2 spectra that provide structural and compositional information on TAGs.

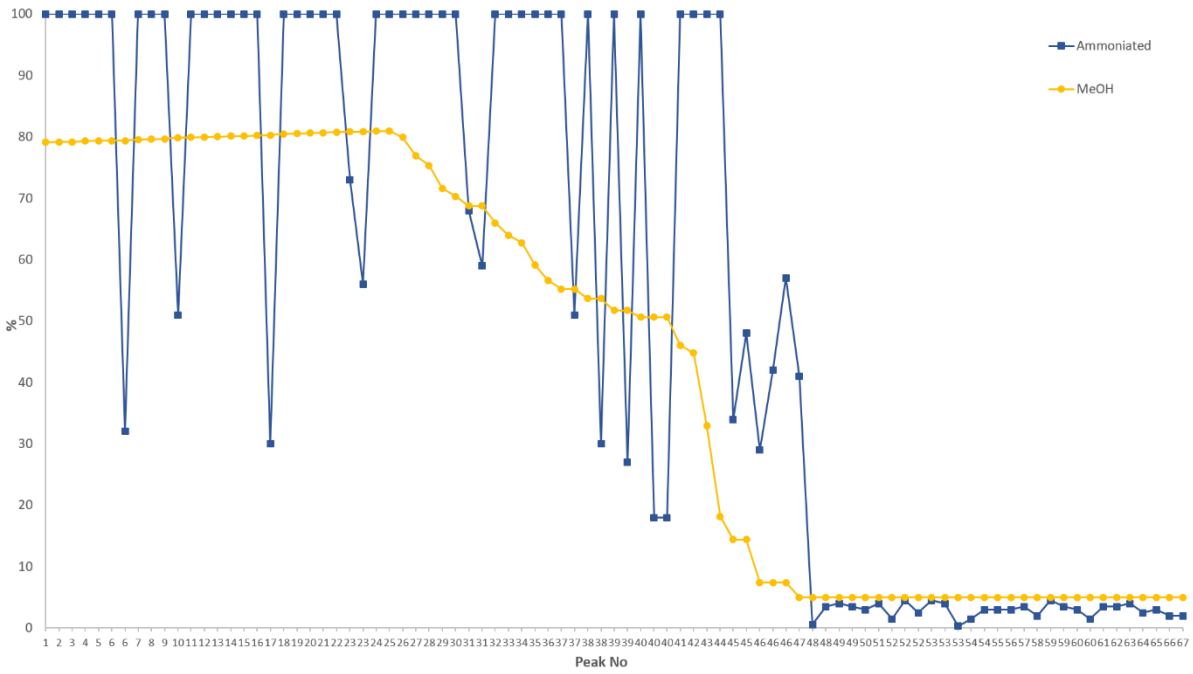

Figure 3.35: Correlation between the percentage of Solvent A (Methanol (90%) and ammonium acetate in methanol (10 mM; 10%; Table 3.11) in the mobile phase and the relative abundance of the ammonium adduct ion detected in the MS spectrum of the peak.

The TAGs identified with Method S (this chapter) were compared with those identified by Beccaria *et al.* (2014) (Table 3.13). A total of 166 TAGs were identified between both studies, 88 TAGs were identified in both studies while 51 were only present in Beccaria *et al.* (2014) and 27 were only identified in this work. Out of the 51 not identified in this study, 24 TAGs were in the region of ECN 42 and 44, where separation was very limited in this study. Of the 27 TAGs identified in this study but not in Beccaria *et al.* (2014), 17 were positively identified, while 10 are only suspected to be present. Furthermore, 19 TAGs were identified only in cow milk and not in goat milk, human milk and mozzarella by Beccaria *et al.* (2014) and so can play an important role in discriminating cow milk samples from other types of milk. Of those 19, six were also identified in the present study ($LnMC_4$, LMC_4, OMC_6, SMC_6, $SPtC_6$, SOPt) and could be used for the identification of samples.

Table 3.13: TAGs identified in Beccaria et al. (2014) **and in the present study. No positional isomers were identified in Beccaria et al.** (2014)**.**

TAG No	TAGs identified by Beccaria et al.	TAGs identified in current study	ECN
1	$LaCaC_4$		26
2	MCC_4	MCC_4	26
3	OC_6C_4	PC_6C_4	26
4	PC_6C_4	OC_6C_4	26
5	$LaCaC_6$	MCC_6	28
6	MCC_6	$LaCaC_6$	28
7	OCC_4	$MCaC_4$	28
8	$MCaC_4$	OCC_4	28
9	PCC_4	PCC_4	28
10	CaCaCa		30
11	$MCaC_6$	$MCaC_6$	30
12	PCC_6	PCC_6	30
13	$OCaC_4$		30
14	$PCaC_4$	$PCaC_4$	30
15	$MLaC_4$	$MLaC_4$	30
16	$LnMC_4$	$LnMC_4$	30
17	LaCaCa	LaCaCa	32
18	$PoLaC_6$	MCaC	32
19	$OCaC_6$	$OCaC_6$	32
20	$PCaC_6$	$PCaC_6$	32
21	OC_4La	$OLaC_4$	32
22	LLC_4		32
23	$OLnC_4$		32
24	LMC_4	LMC_4	32
25	$PMyC_4$	$PMyC_4$	32
26	MMC_4	MMC_4	32
27	$PLaC_4$	$PLaC_4$	32
28		PCC	32
29		$MLaC_6$	32
30		$PoMC_4$	32
31	$PtMC_4$	$PtMC_4$	33
32	MCaCa	[MCaCa]	34
33	LMC_6		34
34	PCaC	PCaC	34
35	OLC_4	OLC_4	34
36	$OPoC_4$	$OPoC_4$	34
37	MMC_6	MMC_6	34
38	$PLaC_6$	$PLaC_6$	34
39	$PPoC_4$	$PPoC_4$	34
40	OMC_4	OMC_4	34
41	PMC_4	PMC_4	34
83	SPC_4	SPC_4	38

TAG No	TAGs identified by Beccaria et al.	TAGs identified in current study	ECN
42	$SLaC_4$		34
43		[LaLaCa]	34
44		[MLaC]	34
45		LPC_4	34
46	PtCaCa		35
47	$OPtC_4$	$OPtC_4$	35
48	$PPtC_4$	$PPtC_4$	35
49	$MaMC_4$		35
50		$MoPC_4$	35
51	OCaCa		36
52	OLC_6		36
53	OMyC		36
54	OLaC		36
55	$PPoC_6$	$PPoC_6$	36
56	PCaCa	PCaCa	36
57	OOC_4	OOC_4	36
58	OMC_6	OMC_6	36
59	OPC_4	OPC_4	36
60	PPC_4	PPC_4	36
61	SMC_4		36
62		MMC	36
63		[MLaCa]	36
64		PMC_6	36
65		SLC_4	36
66	$PPtC_6$	$PPtC_6$	37
67		$OMaC_4$	37
68		$OPtC_6$	37
69		$MoPC_6$	37
70	OOC_6	OOC_6	38
71	OLaCa	OLaCa	38
72	OMC	OMC	38
73		[MLaLa]	38
74	$SPtC_4$	$SPtC_4$	37
75	$MaPC_4$	$MaPC_4$	37
76	MMCa	[MMCa]	38
77	PLaCa	PLaCa	38
78	PMC	PMC	38
79	OPC_6	OPC_6	38
80	PPC_6	PPC_6	38
81	SMC_6	SMC_6	38
82	SOC_4	SOC_4	38
125	SMLa		44

TAG No	TAGs identified by Beccaria et al.	TAGs identified in current study	ECN
84	$MaPC_6$	$MaPC_6$	39
85	$SPtC_6$	$SPtC_6$	39
86		$SMaC_4$	39
87	OOC	OOC	40
88	$OOC_{10:1}$		40
89	$OPoC_{12:1}$		40
90	LPCa	LPCa	40
91	OMCa	[OMCa]	40
92	PPoCa	[PPoCa]	40
93	OPC	OPC	40
94	SOC_6	SOC_6	40
95	MMLa	MMLa	40
96	SMC	SMC	40
97	PPC	PPC	40
98	SPC_6	SPC_6	40
99	SSC_4	SSC_4	40
100		PMCa	40
101		OLaLa	40
102		[MMMy]	40
103		$PPC_{10:1}$	40
104	OOCa		42
105	$OOC_{12:1}$		42
106	OPoMy		42
107	PoPoM		42
108	OMLa		42
109	PMMy		42
110	SPoCa		42
111	PPCa		42
112	SMCa		42
113	SLaLa		42
114	SPC		42
115	SSC_6		42
116	OLL		44
117	OLM		44
118	OLnP		44
119	OOLa		44
120	LMP		44
121	OPLa		44
122	SOCa		44
123	SPCa		44
124	PPLa		44

TAG No	TAGs identified by Beccaria et al.	TAGs identified in current study	ECN
126	PMM		44
127	SSC		44
128	OOL		46
129	PPtM		45
130	OLP		46
131	OOM	OOM	46
132	SPoPo		46
133	LPP	[LPP]	46
134	SLM		46
135	OPM	[OPM]	46
136	SOLa		46
137	SMM	[SMM]	46
138	PPM	[PPM]	46
139	SPLa		46
140		OPPo	46
141	OOO	OOO	48
142	PPPt	[PPPt]	47
143		OPPt	47
144		[OOPt]	47
145		[OPMo]	47
146		[MaPM]	47
147	OOP	OOP*	48
148	SLP		48
149	OPP	OPP*	48
150	SOM		48
151	OOMa	[OOMa]	49
152	PPP		48
153	SMP	SPM	48
154	OMaP	[OMaP]	49
155	SPPt	[SPPt]	49
156	MaPP	[MaPP]	49
157	SOO	SOO*	50
158	SOPt	[SOPt]	49
159	SPO	SPO*	50
160	SSM		50
161	SPP	SPP*	50
162	SSO	SSO*	52
163	SSP	SSP*	52
164	SSS	SSS	54
165		$[SPC_{20}]$	54
166		$[PPC_{22}]$	54

3.3 Conclusions

An ultra high performance liquid chromatography (UHPLC) method was developed using a Waters Acquity UPLC BEH C18 1.7 µm column. The method enables the rapid analysis of milk samples, which contain a wide range of TAGs with long and short, saturated and unsaturated acyl group chains. The wide range of TAG polarities necessitated the use of a number of different solvents to achieve the required solubility and change in eluotropic strength during gradient elution. Elution of the more polar components (ECNs 28-38) was achieved using mixtures of methanol with water as a polar modifier whereas elution of apolar components (ECN 40 and higher) was achieved using an apolar mobile phase, consisting mainly of acetonitrile and dichloromethane. The inclusion of dichloromethane was found to give better solubilisation of apolar components than was achieved with other solvents. This method allowed the clear separation of TAGs according to their ECNs and in most cases allowed the separation of TAGs with the same ECN. TAGs with ECN 42 or 44 did not separate and only one broad peak eluted for each of the ECNs. Notably, this partially compromised region of the chromatogram represents the point at which the mobile phase changes fairly rapidly from mainly methanol to acetonitrile and dichloromethane. That could signify that components with ECN 42 and 44 are too apolar to elute in a mixture of methanol and water and the change in eluotropic strength on introduction of the less polar mobile phase composition was too severe, leading to rapid elution of the ECN 42 and 44 TAGs, reducing their interaction with the stationary phase. A more gradual elution could solve this problem but would significantly increase the analysis time.

The use of mass spectrometry allowed the identification of TAGs even in some cases where they were co-eluting. MS^2 spectra enabled the identification of TAGs with greater confidence and in some cases allowed assignment of positional isomers of TAGs. No other published work on TAGs of milk samples has discussed TAG positional isomers and this is an area where this work demonstrates a particular improvement. The presence of ammonium adduct ions is critical for obtaining MS^2 spectra that can be used to identify TAGs and positional isomers. Because of the presence of only four solvent reservoirs in the UHPLC system, ammonium acetate was added to the sample via the methanol component of the mobile phase. Consequently, the decrease of methanol during the later part of the separation led to a decrease in the abundance of ammonium adduct ions. This needs to be addressed by addition of ammonium acetate throughout the analysis, either pre- or post-column. A correlation between the number of double bonds and the relative abundance of the proton adduct ions has been recorded in the literature before and was also observed in this work. Notably, additional observations made in this study reveal the critical role played by the positions of the

double bonds within the acyl moieties. This is an interesting aspect that could contribute to structural assignment though it was beyond the scope of this study to examine it further.

In total, 105 TAGs were positively identified in this study with a method that is of 25 min duration. This compares favourably with the identification of 139 TAGs by Beccaria *et al.* (2014) using a method of more than 150 min duration. Not all TAGs identified in this study were identified in Beccaria *et al.* (2014), possibly indicating a wider diversity in TAG occurrences even in samples of common origin. Clearly there is a need for the characterisation of the TAG profiles in a greater number of samples in order that the profiles can be used in a diagnostic manner. The method developed here shows potential as a fast screening method for characterisation of TAG profiles.

4 Development of two stage separation method for TAGs

4.1 Introduction

The final version of the UHPLC method for separating and identifying TAGs in milk, Method S, presented in Chapter 3 is under 25 min duration, representing a significant improvement compared with existing methods in the literature. Nevertheless, Method S exhibits a number of limitations that could be targeted in attempts to improve the method. Most importantly, the individual components of the TAGs with ECNs 42 and 44 were not separated: each ECN was represented as a single broad peak. A number of other components also co-elute, leading to varying degrees of success in their identification. One of the difficulties in identifying co-eluting TAGs results from the low efficiency of formation of ammonium adduct ions for some of the TAGs with higher ECNs. In some cases, this prevented the collection of the MS^2 data required to determine the structures of the various TAGs present.

The reason why UHPLC didn't work equally well for all samples with Method S was the wide range of ECNs that the components had and the big differences in polarities and solubilities which meant big differences in eluent composition were needed to obtain good separation. But, changing eluent composition too fast, doesn't allow for good separation.

A solution to this would be to separate and collect fractions of TAGs according to their ECNs and then analyse each fraction with the eluent composition determined to be optimal by UHPLC.

The potential for a multi-stage approach is explored in this chapter. The aim of the work was to continue utilising the speed of UHPLC analysis, while at the same time addressing the reasons for the poor separation of TAGs in specific ECN regions that proved more problematic. In particular, the development of different methods of separation for different groups of TAGs with similar ECNs and polarities was targeted in order to develop a better understanding of the factors limiting their separation and hence to develop a multi-stage approach. Additional samples were analysed with the multi-stage approach to provide an initial evaluation of the method's effectiveness in characterising samples of different biological origins.

4.2 Results and discussion

4.2.1 Method development

4.2.1.1 Two stage separation

The initial method development, to explore the potential of this approach before applying it to milk samples, was performed using olive oil samples which are simpler and require less preparation time. The fraction collection method was adapted from methods developed previously (Dugo et al., 2006; Hasan, 2010) with a Waters XBRIDGE C18 column (4.6 mm x 150 mm, 5 µm, 18% C loading) and a mobile phase of acetonitrile and isopropanol (Table 4.1). The experimental details of the fraction collection are described in Chapter 2. There were nine fractions collected, with TAGs of different ECNs collected in separate fractions (Table 4.2; Figure 4.1).

Table 4.1: Mobile phase gradient of fraction collection method for HPLC separation of TAGs and collection of fractions. Flow rate 1 mL/min.

Time (min)	% acetonitrile	% isopropanol
0	70	30
15	60	40
25	45	55
38	30	70
45	30	70

Table 4.2: Fraction numbers and the corresponding ECN of TAGs collected.

Fraction No	Corresponding ECN
1	-
2	-
3	42
4	44
5	46
6	48
7	50
8	52
9	54

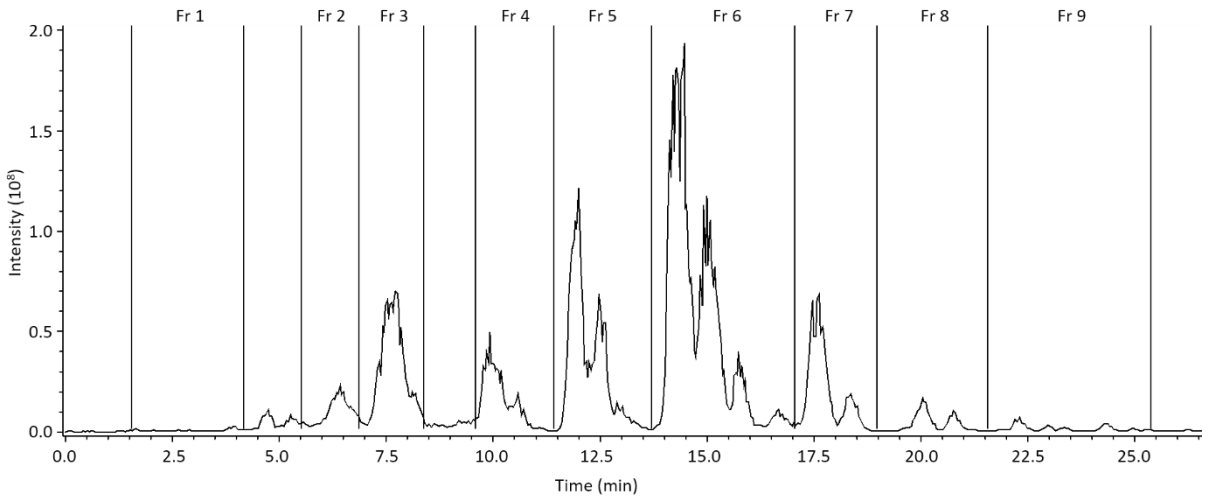

Figure 4.1: Partial base peak RP LC-APCI MS chromatogram of olive oil sample analysed with fraction collection method (Table 2.3). Regions represent fractions collected (Table 2.5).

The olive oil sample was first analysed with Method S to enable comparison of any improvements achieved during the development of the new method (Figure 4.2). The separation of TAGs with ECNs 42, 44, 46 and 48 was incomplete and identification of all of the different TAG components was not possible. The retention times of the peaks corresponding to different ECNs were used to determine the eluent composition required for elution of these components (Table 4.3), for use as a starting point for the method development of the separation for the corresponding fraction.

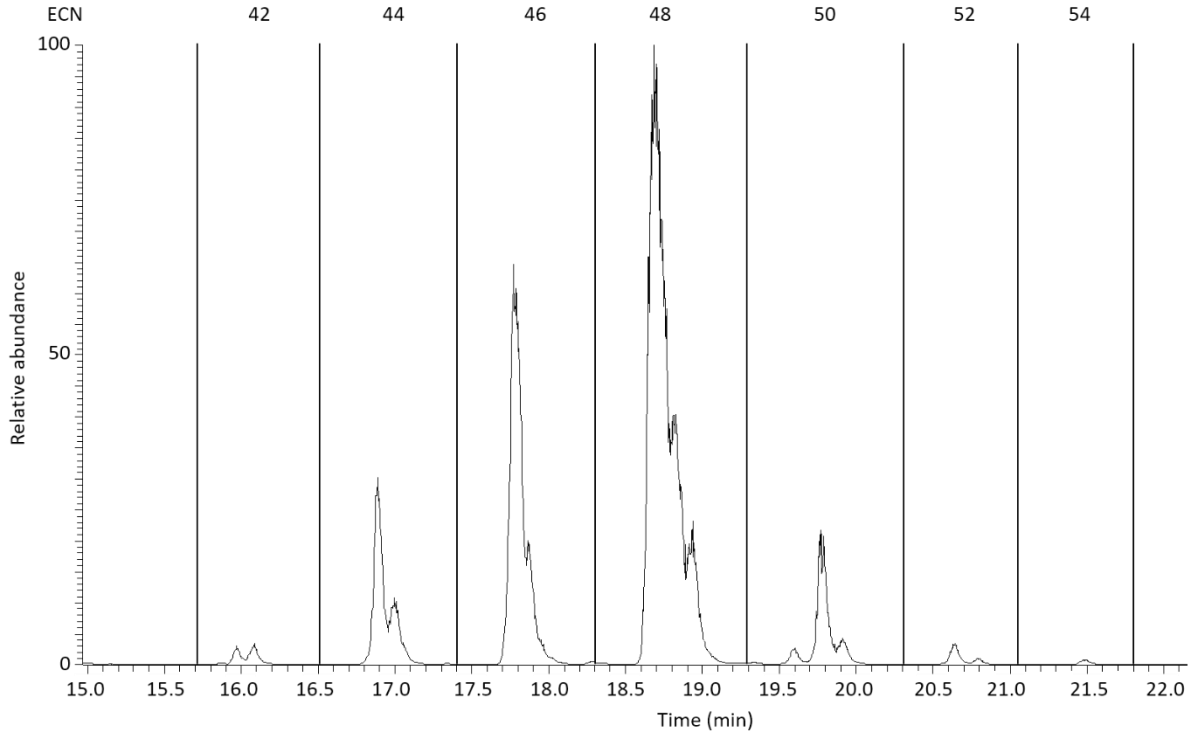

Figure 4.2: Partial RP UHPLC-APCI MS base peak chromatogram of olive oil sample analysed with Method S (Table 3.11). Regions are assigned according to ECN.

Table 4.3: Eluent composition of Method S at the retention time windows for components of different ECNS regions where separation of TAGs was incomplete, i.e. ECNs 42, 44, 46 and 48.

Equivalent carbon number of eluting components	Acetonitrile solvent (%)	Dichloromethane (%)	Methanol (90%) and ammonium acetate in methanol (10 mM; 10%) (%)
42	71-69	24-26	5
44	68-67	27-28	5
46	66-65.5	29-29.5	5
48	65	30	5

Fraction 6 (ECN 48) was the first to be examined. The eluent used for the first method tested, Method ECN48_A, comprising acetonitrile (70%), dichloromethane (25%) and ammonium acetate in methanol (10 mM; 10%) was based on the mobile phase composition of Method S when components with ECN 48 eluted (Table 4.3). A slightly more polar composition (25% dichloromethane instead of 30%) to allow components to separate more gradually in an attempt to avoid co-elution. Four TAGs were separated and identified; TAGs OOO, OOP and OPP with ECN 48 and TAG OOG with ECN 50 (Figure 4.3). The comparison of Methods ECN48_A (Figure 4.3) and S (Figure 4.2) show greatly improved separation in a short time period with the new method. Three peaks are clearly separated and not co-eluting or appearing as shoulders, as was the case with Method S.

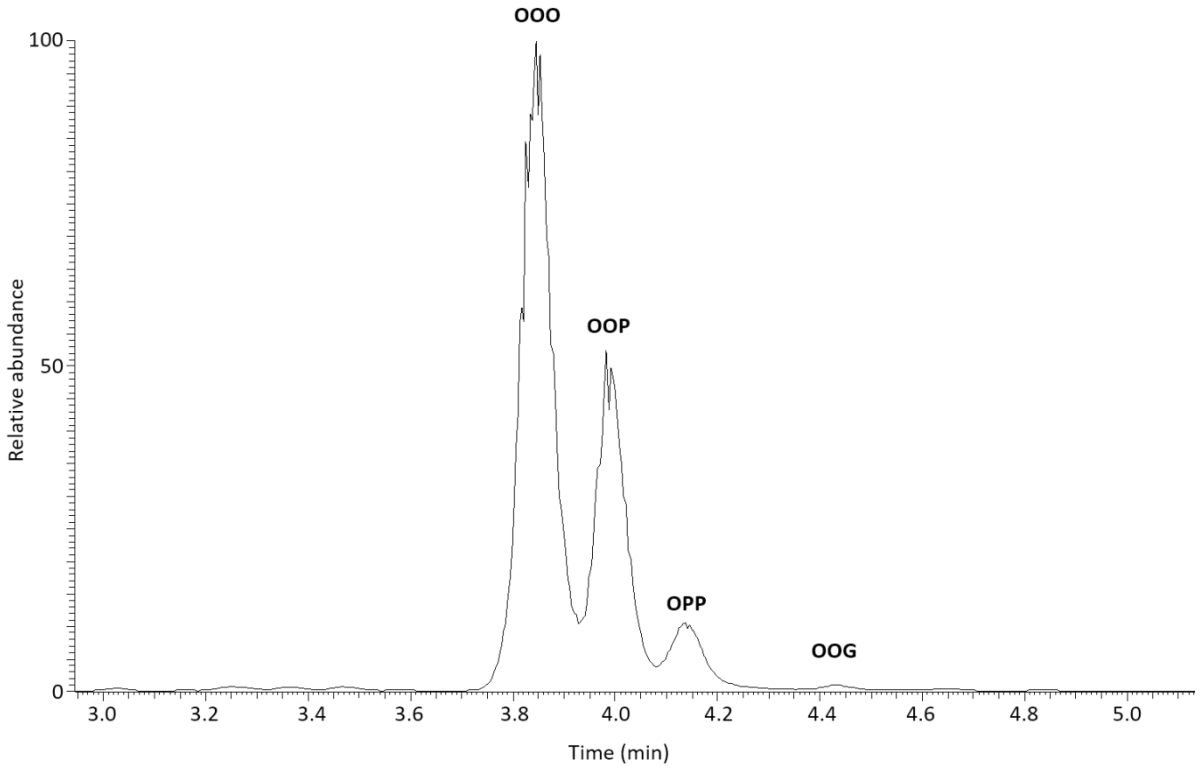

Figure 4.3: Partial RP UHPLC-APCI MS base peak chromatogram of fraction 6 (Table 2.5) of olive oil sample analysed with Method ECN48_A (isocratic elution, acetonitrile (70%), dichloromethane (25%) and ammonium acetate in methanol (10 mM; 10%) (5%), temperature 50°C, flow rate: 0.45 mL/min). TAGs OOO, OOP, OPP and OOG were identified with MS and the peaks are labelled accordingly.

The backpressure that was an issue with Method S was mainly caused by the presence of water in the mix of solvents. Since this method was not using water, the flow rate could be increased to 0.65 mL/min to further decrease the retention time (Figure 4.4), something that was not possible with the previous method due to the high backpressure. However, this also caused the separation of the peaks to reduce.

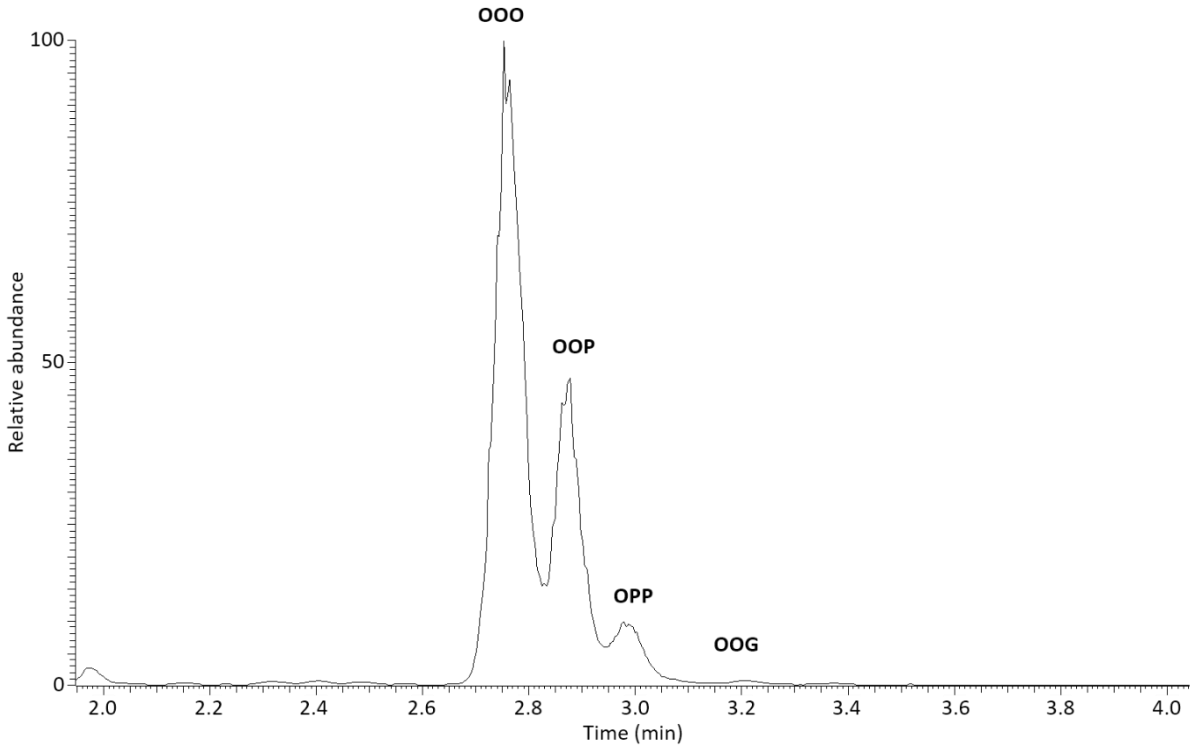

Figure 4.4: Partial RP UHPLC-APCI MS base peak chromatogram of fraction 6 (Table 2.5) of olive oil sample analysed with Method ECN48_B (isocratic elution, acetonitrile (70%), dichloromethane (25%) and ammonium acetate in methanol (10 mM; 10%) (5%), temperature 50°C, flow rate: 0.65 mL/min). TAGs OOO, OOP, OPP and OOG were identified with MS and the peaks are labelled accordingly.

The flow rate was lowered to 0.45 mL/min and the temperature to 40°C (Figure 4.5). The lower temperature had a positive impact on the separation of the peaks, resulting to almost baseline separation between all four peaks. The overall time for the method increased to 7.3 min for all components to elute.

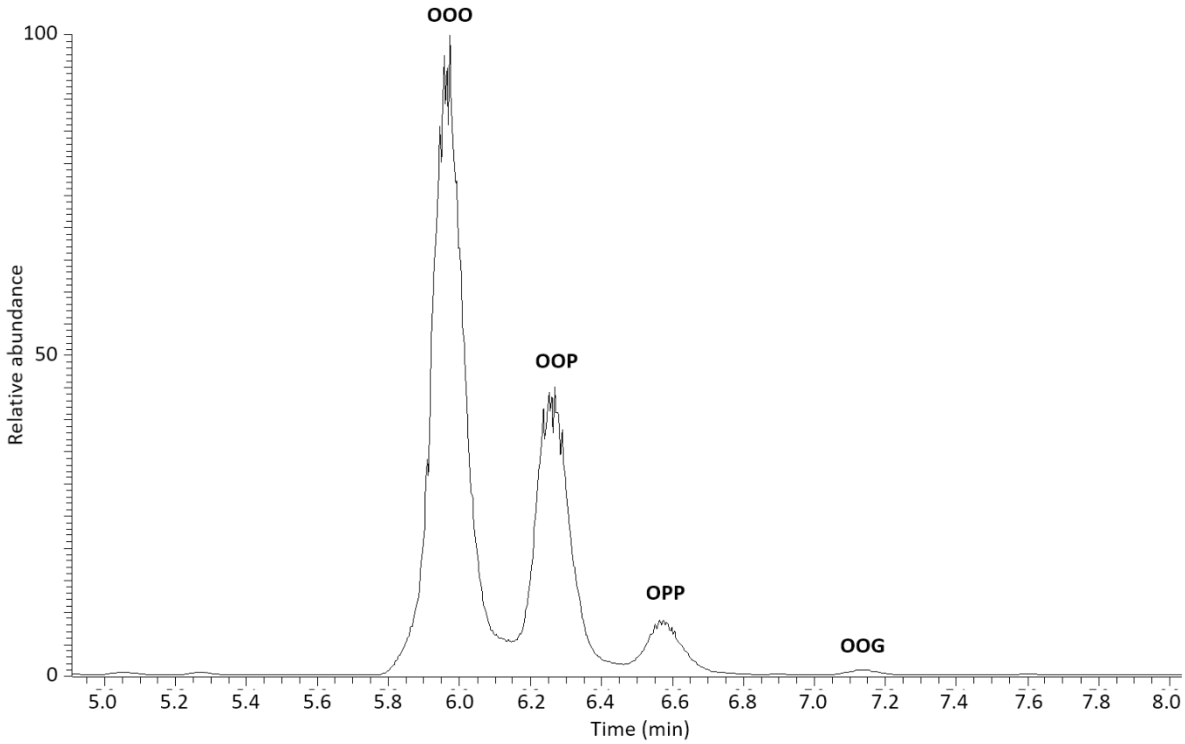

Figure 4.5: Partial RP UHPLC-APCI MS base peak chromatogram of fraction 6 (Table 2.5) of olive oil sample analysed with Method ECN48_C (isocratic elution, acetonitrile (70%), dichloromethane (25%) and ammonium acetate in methanol (10 mM; 10%) (5%), temperature 40°C, flow rate: 0.45 mL/min). TAGs OOO, OOP, OPP and OOG were identified with MS and the peaks are labelled accordingly.

By increasing the flow rate to 0.6 mL/min the retention times of the peaks were reduced good separation maintained with backpressure remaining within the instrument limitations (Figure 4.6). The resolution of peaks OOO and OOP for Method ECN48_A was 1.1 compared with resolution for Methods ECN48_C and ECN48_D of 1.7 and 1.5 respectively. Hence, both methods have greatly improved resolution but the last method is significantly faster, so that one would be optimal to use.

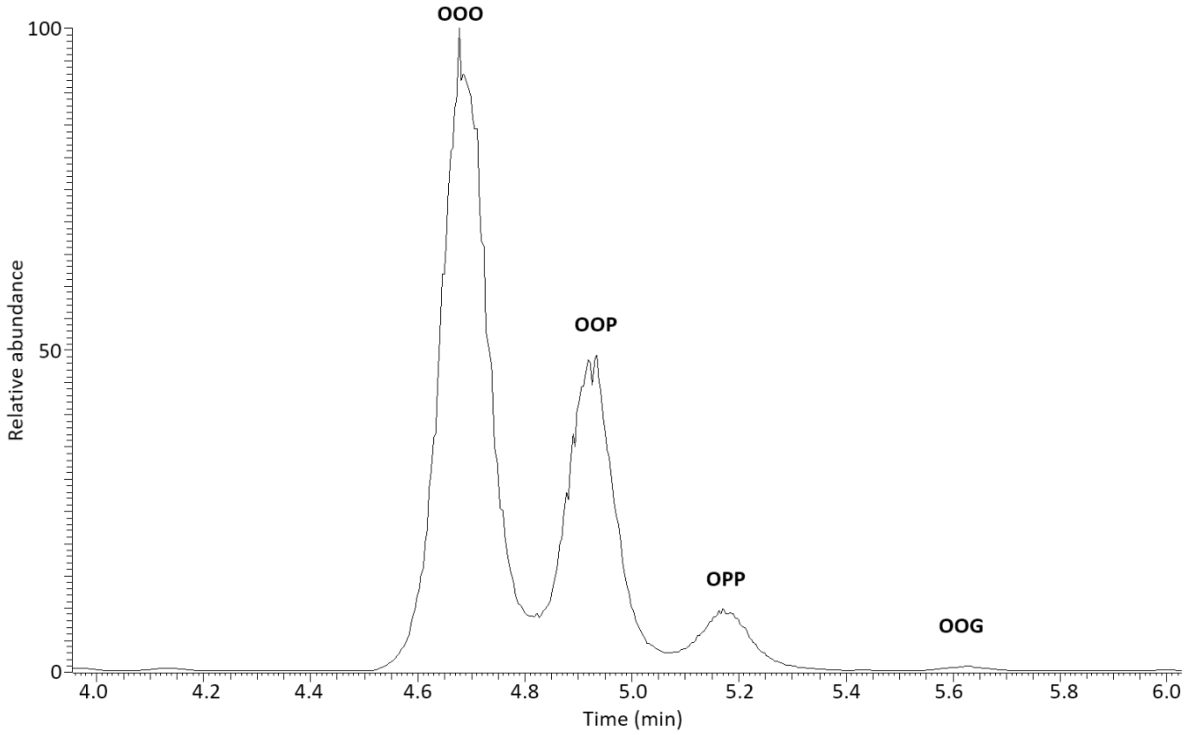

Figure 4.6: Partial RP UHPLC-APCI MS base peak chromatogram of fraction 6 (Table 2.5) of olive oil sample analysed with Method ECN48_D (isocratic elution, acetonitrile (70%), dichloromethane (25%) and ammonium acetate in methanol (10 mM; 10%) (5%), temperature 40^{o}C, flow rate: 0.60 mL/min). TAGs OOO, OOP, OPP and OOG were identified with MS and the peaks are labelled accordingly.

The method tested for separation of Fraction 4 (ECN 44) used a more polar eluent composition (75% acetonitrile and 20% dichloromethane) than that in which it eluted with Method S (Figure 4.7). TAGs LLO, LnOO and LnOP were identified and the three peaks were partially separated in 5.2 minutes.

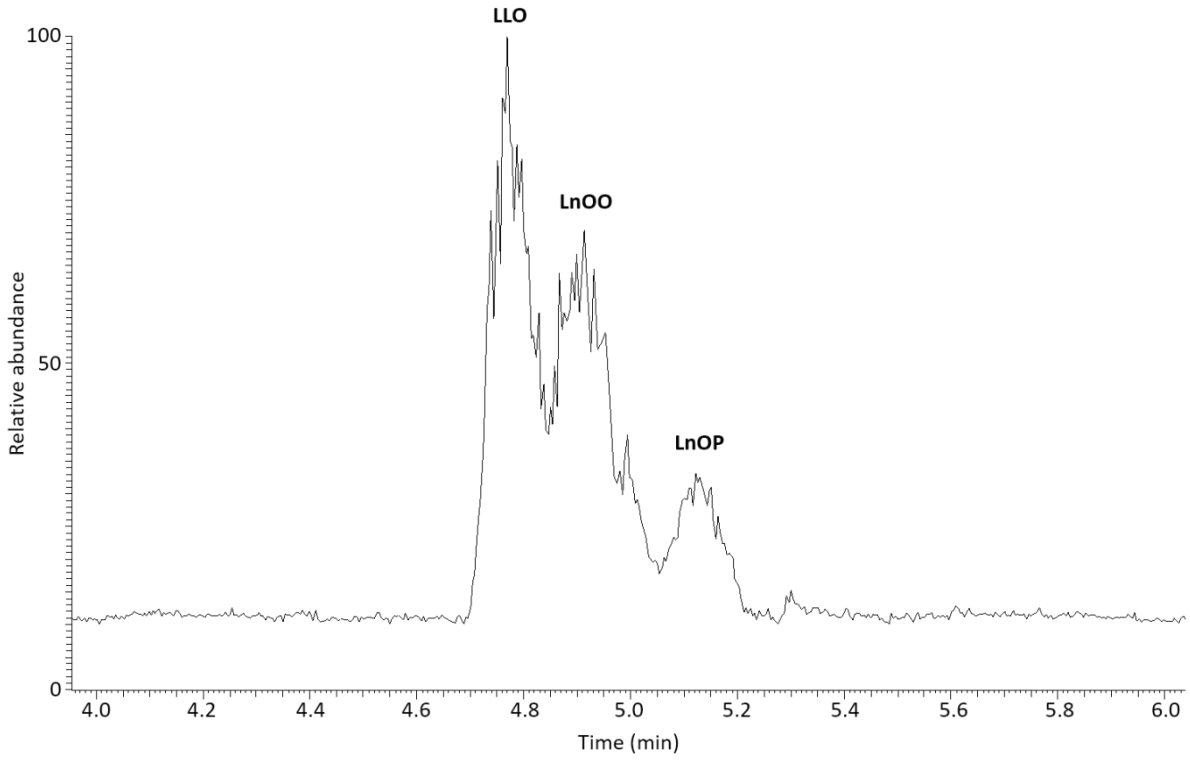

Figure 4.7: Partial RP UHPLC-APCI MS base peak chromatogram of fraction 4 (Table 2.5) of olive oil sample analysed with Method ECN44_A (isocratic elution, acetonitrile (75%), dichloromethane (20%) and ammonium acetate in methanol (10 mM; 10%) (5%), temperature 40°C, flow rate: 0.55 mL/min). TAGs LLO, LnOO and LnOP were identified with MS and the peaks are labelled accordingly.

The polarity of the eluent was further increased by increasing the amount of methanol present (10% from 5% previously) (Figure 4.8). Although the resulting separation was improved retention increased with the elution of the last component complete at around 7.4 min.

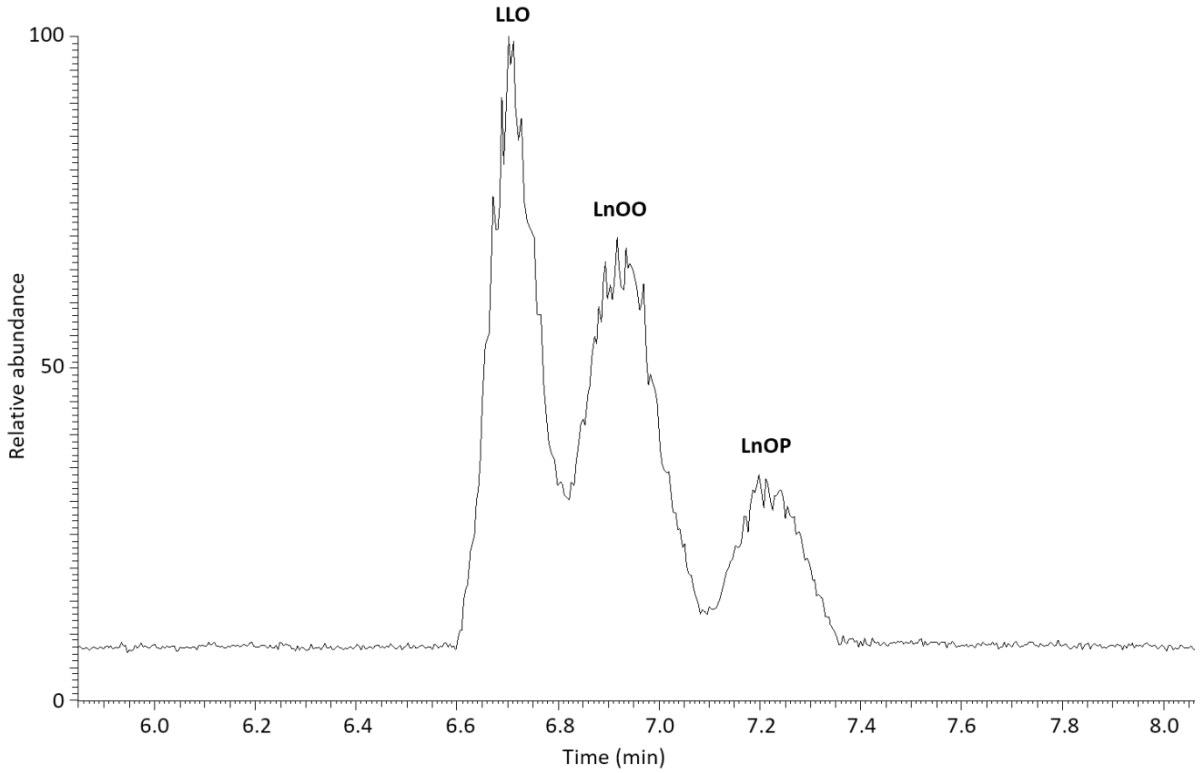

Figure 4.8: Partial RP UHPLC-APCI MS base peak chromatogram of fraction 4 (Table 2.5) of olive oil sample analysed with Method ECN44_B (isocratic elution, acetonitrile (75%), dichloromethane (15%) and ammonium acetate in methanol (10 mM; 10%) (10%), temperature 40°C, flow rate: 0.55 mL/min). TAGs LLO, LnOO and LnOP were identified with MS and the peaks are labelled accordingly.

Increasing the amount of dichloromethane (25% from 15% previously) resulted in loss of separation (TAGs LLO and LnOO co-eluted and the peak for LnOP was not separated as well as with the previous methods.

Different flow rates and temperatures were tested to separate the TAGs of fraction 3 (ECN 42) and the eluent composition was set to 70% acetonitrile, 20% DCM and 10% ammonium acetate in methanol to make the eluent more polar (Figure 4.9). Three TAGs were identified and separated, LLL, OLLn and PLLn, though their very low concentrations resulted in high noise levels in the MS signal. Another peak was present in the chromatogram which could not be identified using MS. Its presence can be attributed to the low concentration of TAGs and high interference of contamination. This proves a disadvantage for this approach since the preparatory stage for the fractions would need to be adjusted to collect enough of the fraction to avoid high levels of noise and interference.

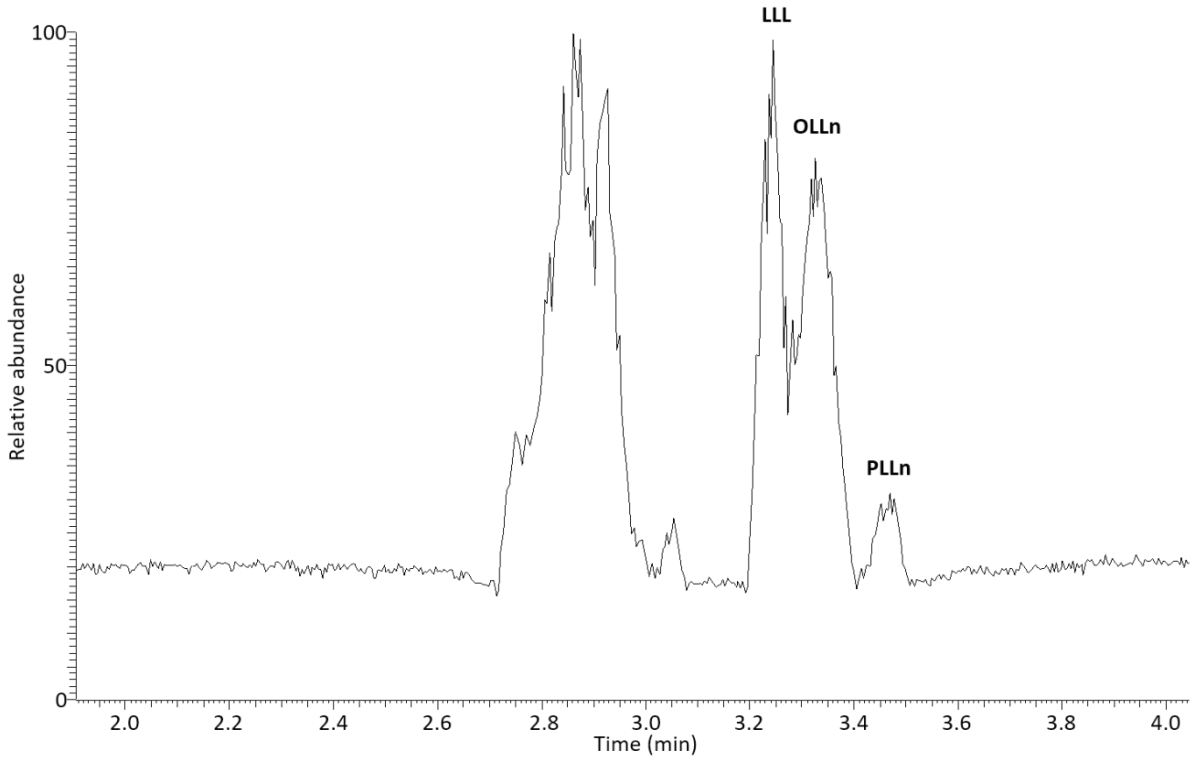

Figure 4.9: Partial RP UHPLC-APCI MS base peak chromatogram of fraction 3 (Table 2.5) of olive oil sample analysed with Method ECN42_A (isocratic elution, acetonitrile (70%), dichloromethane (20%) and ammonium acetate in methanol (10 mM; 10%) (10%), temperature 40°C, flow rate: 0.60 mL/min). TAGs LLL, OLLn and PLLn were identified with MS and the peaks are labelled accordingly.

Lastly, a number of methods were tested for the separation of components of fraction 5 (ECN 46) (Figure 4.10 and Figure 4.11). TAGs OOL, OOPo and OLP were detected with both methods, but OOPo and OLP coeluted with Method ECN46_A. The more polar eluent composition (Method ECN46_B) improved the separation of OLP from OOPo and the presence of another component (PPL) became evident though separation was not achieved (PPL, Figure 4.11). Despite the improvements achieved OOPo and PPL exhibit partial co-elution and baseline separation was not achieved for any of the peaks in the chromatogram.

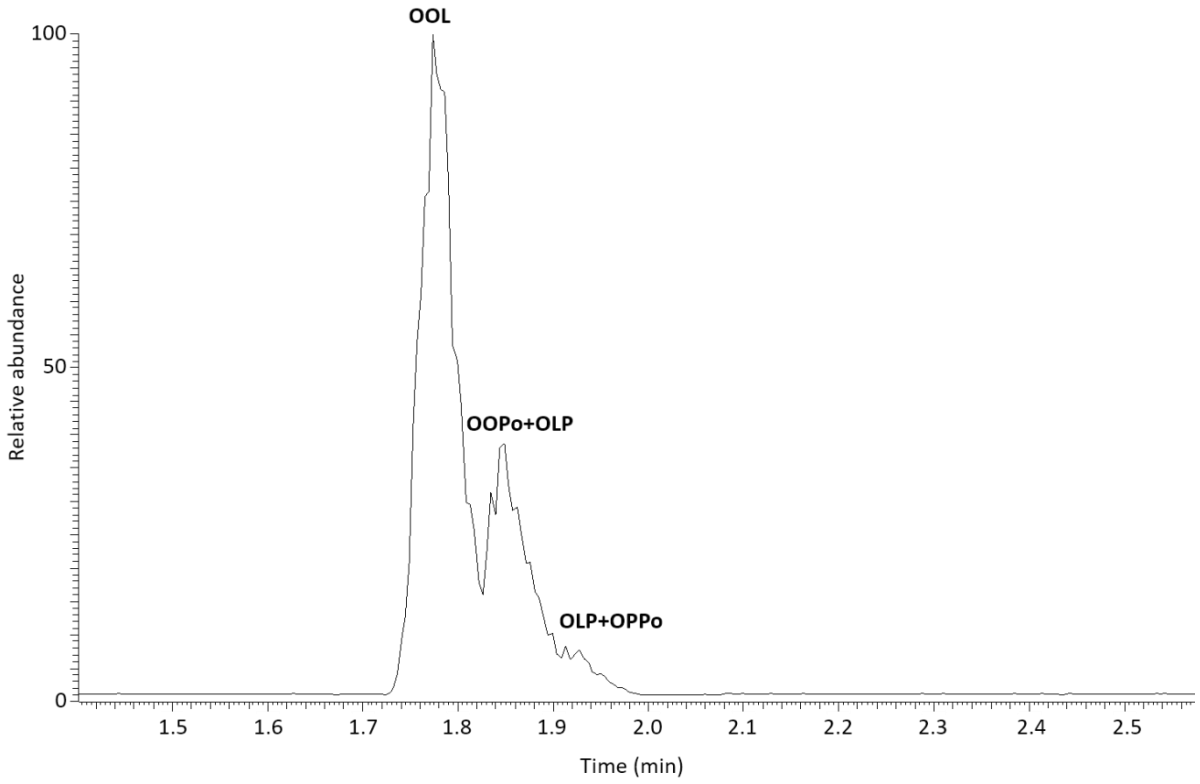

Figure 4.10: Partial RP UHPLC-APCI MS base peak chromatogram of fraction 5 (Table 2.5) of olive oil sample analysed with Method ECN46_A (isocratic elution, acetonitrile (60%), dichloromethane (35%) and ammonium acetate in methanol (10 mM; 10%) (5%), temperature 40°C, flow rate: 0.60 mL/min). TAGs OOL, OOPo, OLP and OPPo were identified with MS and the peaks are labelled accordingly. TAG OLP co-elutes with OOPo at peak with apex RT 1.85 min and with OPPo at peak with apex RT 1.92 min.

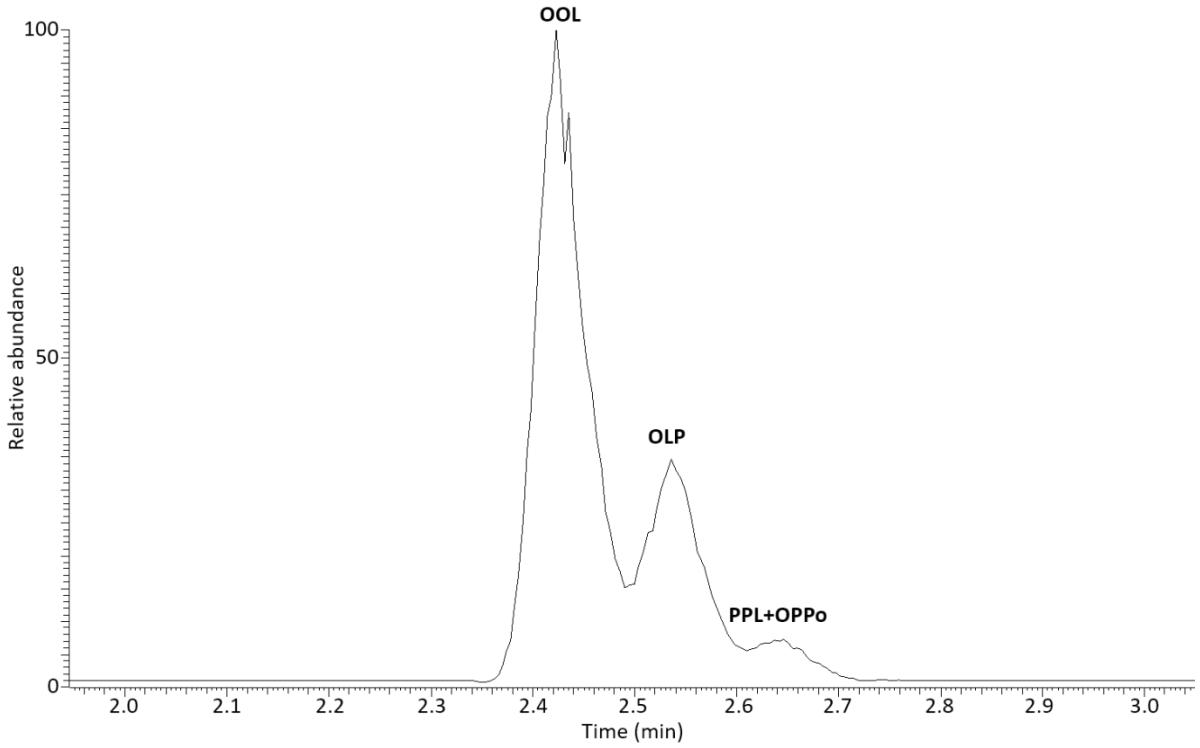

Figure 4.11: Partial RP UHPLC-APCI MS base peak chromatogram of fraction 5 (Table 2.5) of olive oil sample analysed with Method ECN46_B (isocratic elution, acetonitrile (65%), dichloromethane (30%) and ammonium acetate in methanol (10 mM; 10%) (5%), temperature 40°C, flow rate: 0.60 mL/min). TAGs OOL, OLP, PPL and OPPo were identified with MS and the peaks are labelled accordingly. TAGs PPL and OPPo co-elute.

4.2.1.2 UHPLC separation in two stages

The eluent compositions of the methods developed for separation of fractions with different ECNs were very similar. In the context of the development of a method that could be operated in a fully or semi-automated and high-throughput manner it is unlikely that this approach would be suitable. Separating and collecting fractions is time intensive in itself and the second stage separation of all fractions would need to be shorter than the retention time of the components in the first stage of the method. Hence, a different approach was considered. The main issue with the single stage separation (Chapter 3) was the abrupt change of eluent composition associated mainly with reducing methanol to 5% from 65% and increasing acetonitrile from 15% to 70%. TAGs with ECNs up to 40 were separated better with methanol and water present whereas TAGs with higher ECNs separated better in the absence of water and lower proportions of methanol. The approach considered was to employ two different separation for each sample: one to separate and identify TAGs with ECNs lower or equal to 40 and one for TAGs with ECNs of 42 and higher.

Separation of apolar TAGs

Methods for separating TAGs of ECNs higher than 42 were tested first. The absence of water and low concentration of methanol in the eluent allowed a lower temperature and higher flow

rate to be used than for Method S, both factors leading to improvement in separation in the analysis of the fractions. The olive oil sample was analysed using two methods (Table 4.4) which differ in the solvent composition, with Method ECN42-56_A being more polar than Method ECN42-56 due to the increased amount of methanol present. Similar separation was achieved with both methods, though with a much shorter analysis time for Method ECN42-56_A (Figure 4.12). The two methods were also applied to the analysis of a sample of cow's milk (Figure 4.13). In this case, Method ECN42-56 provided much better separation. The cow's milk sample contains a much larger number of components with more likelihood of co-elution, consequently a longer analysis time was found to be necessary. This method represents a clear improvement in separation compared with Method S. This is especially evident for TAGs with ECN 42, 44 and 46 which appeared as unresolved peaks with Method S, whereas three, four and seven peaks, respectively were separated with Method ECN42-56. The separation of peaks with ECNs 48 and 50 was also improved.

The cow's milk sample was not fractionated prior to analysis because the elution of earlier components was not found to affect the components being targeted in the analysis (TAGs with ECN≥42). TAGs with ECNs between 32 and 40 were partially separated, and where not identified with this method since the intention was to develop a separate method for their analysis.

Table 4.4: Mobile phase gradient of Methods ECN42-56_A and ECN42-56 for UHPLC separation of TAGs. Flow rate 0.55 mL/min. Temperature controlled at 40°C. The solvents used were A: Acetonitrile, B: Dichloromethane and C: Ammonium acetate in methanol (10 mM; 10%).

Method ECN42-56_A	**Time (min)**	0	4	10	20		
	Solvent A %	80	70	65	65		
	Solvent B %	10	20	30	30		
	Solvent C %	10	10	5	5		
Method ECN42-56	**Time (min)**	0	15	18	20	21	26
	Solvent A %	85	70	65	60	85	85
	Solvent B %	10	25	30	35	10	10
	Solvent C %	5	5	5	5	5	5

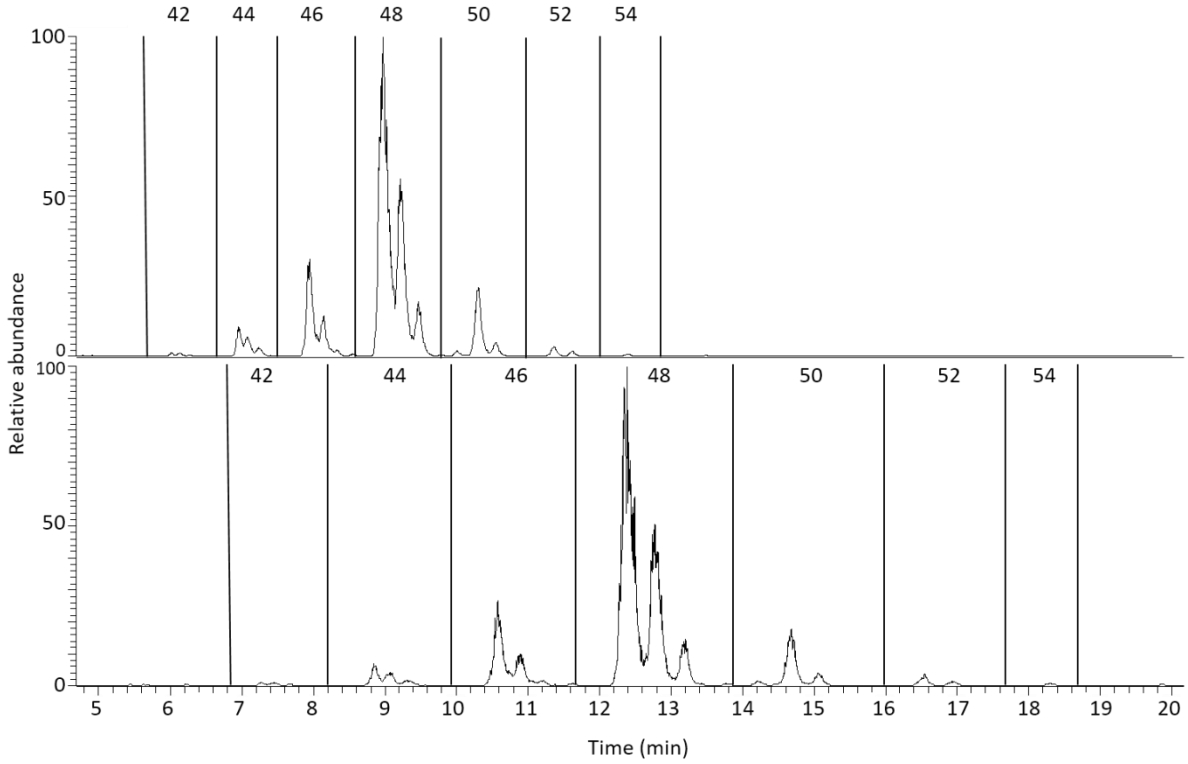

Figure 4.12: Partial RP UHPLC-APCI MS base peak chromatograms of olive oil sample analysed with Methods ECN42-56_A (top) and ECN42-56 (bottom) (Table 4.4).

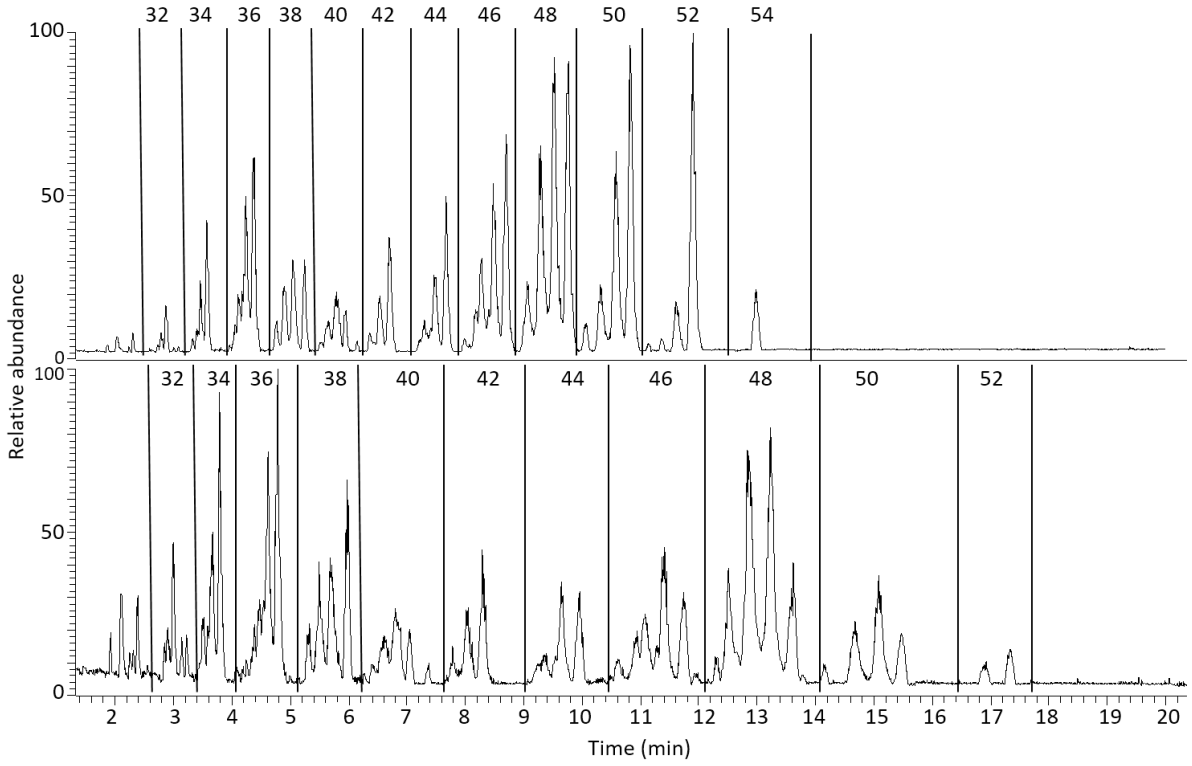

Figure 4.13: Partial RP UHPLC-APCI MS base peak chromatograms of cow milk sample analysed with Methods ECN42-56_A (top) and ECN42-56 (bottom) (Table 4.4).

Separation of polar TAGs

Method S provided a relatively good separation of components with ECNs lower than 40, hence the eluent composition, temperature and flow rate of that method was used as the basis for the development of the method for those components (Table 4.5). With the analysis being developed in two stages, the separation of TAGs with higher ECNs was not of interest in this stage. Thus, acetonitrile was maintained at 15% and the proportion of dichloromethane increased at the end of the analysis to elute those components rapidly prior to reconditioning of the column before the next sample.

Table 4.5: Mobile phase gradient of Methods ECN26-40_A, ECN26-40_B and ECN26-40 for UHPLC separation of TAGs. Flow rate 0.45 mL/min. Temperature controlled at 40°C for ECN26-40_A and at 50°C for ECN26-40_B and ECN26-40. The solvents used were A: Methanol (90%) and ammonium acetate in methanol (10 mM; 10%), B: Acetonitrile, C: Dichloromethane and D: Water

Method ECN26-40_A	**Time (min)**	0	2	11	13	18	24	25	35
	Solvent A %	79	79	68	65	55	55	79	79
	Solvent B %	15	15	15	15	15	15	15	15
	Solvent C %	3	3	3	20	30	30	3	3
	Solvent D %	3	3	0	0	0	0	3	3
Method ECN26-40_B	**Time (min)**	0	2	11	13	18	24	25	35
	Solvent A %	79	79	68	65	55	55	79	79
	Solvent B %	15	15	15	15	15	15	15	15
	Solvent C %	3	3	3	20	30	30	3	3
	Solvent D %	3	3	0	0	0	0	3	3
Method ECN26-40	**Time (min)**	0	11	13	18	24	25	30	
	Solvent A %	79	79	62	52	52	79	79	
	Solvent B %	15	15	15	15	15	15	15	
	Solvent C %	3	3	20	30	30	3	3	
	Solvent D %	3	3	3	3	0	3	3	

Method ECN26-40 provided the best separation of TAGs. Peaks in regions corresponding mainly to ECN 34 and 36 were separated better than with the other methods, including Method S, and a greater number of peaks were detected in for ECN 38 and 40 (eight and six respectively, compared to six and four with Method S) (Figure 4.14).

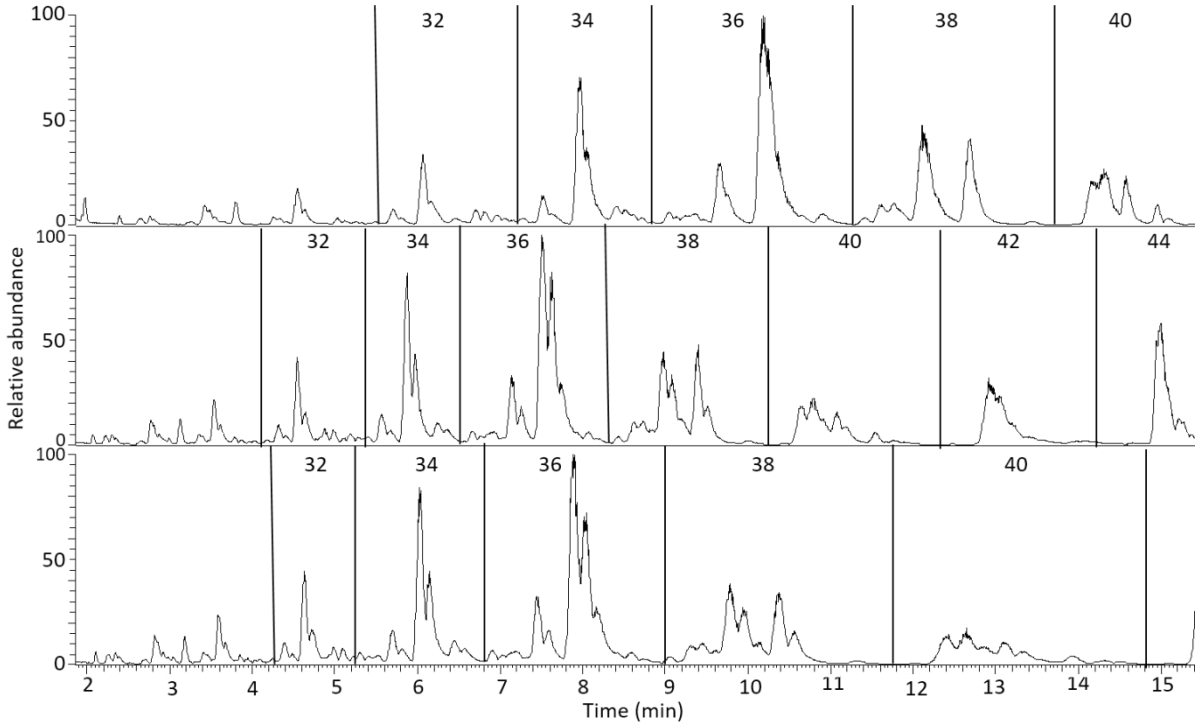

Figure 4.14: Partial RP UHPLC-APCI MS base peak chromatograms of cow milk sample analysed with Methods ECN26-40_A (top) ECN26-40_B (middle) and ECN26-40 (bottom) (Table 4.5).

4.2.2 Separation of cow's milk TAGs with methods ECN26-40 and ECN42-56

Mass spectrometry was used to identify TAGs in the milk sample for both methods. As previously discussed (3.2.2), the Thermo Orbitrap was used because of its short duty cycle, which is important because of the narrow peak widths of the chromatogram, and its ability to scan ions with the Orbitrap detector at the same time as isolating a precursor ion in quadrupole mode and generating collision- induced dissociation MS^n spectra rapidly, which is crucial for the identification of the different acyl groups present in each TAG identified. A precursor ion *m*/*z* range was selected to ensure that appropriate ions were selected for dissociation. The *m*/*z* values of the ammonium adduct ions for the milk TAGs range from *m*/*z* 516.43 to *m*/*z* 908.87 as stated previously (3.2.2). Precursor scan ranges were set at *m*/*z* 490-790 for 0-15 min and *m*/*z* 720-940 for 15 to 30 min for Method ECN 26-40 and at *m*/*z* 490-790 for 0-7.5 min and *m*/*z* 720-940 for 7.5 to 26 min for Method ECN 42-56 (Table 2.9 and Table 2.10 respectively, Chapter 2) reflecting the mass of the adducts eluted during each time period. All ammonium adduct ions were present in significant abundance and were correctly selected for MS^2 analysis, something that wasn't achieved with Method S and caused uncertainty in the identification of TAGs.

A total of 58 distinct peaks were recognised (Table 4.6), 25 of which correspond to single TAGs and 33 show evidence of coelution. The MS^2 spectra enabled identification of a total of 89 TAGs (25 separated and 64 coeluting) and a further 34 were identified tentatively.

Table 4.6: TAGs identified in cow milk analysed using Methods ECN26-40 (Table 4.5, Figure 4.14) and ECN42-56 (Table 4.4, Figure 4.13) giving m/z values of ammonium adduct ions, [M+NH4]+, proton adduct ions, [M+H]+, and DAG product ions, [M-RCO2]+. Tentative TAG identifications are enclosed in brackets. Multiple positional isomers of the TAGs could not be distinguished apart from a small number of cases where the TAG in question is labelled as ABC*, meaning the acyl group in position sn-2 is B and positions sn-1 and sn-3 are occupied by either A or C. The abbreviations used for the acyl groups are explained in Abbreviations

Peak No	Method	Apex RT min	$[M\text{-}RCO_2]^+$ *m/z*	$[M+NH_4]^+$ *m/z*	$[M+H]^+$ *m/z*	TAG identification	ECN
1	26-40	2.31	299, 355, 383 299, 327, 411 271, 355, 411 327, 355 327, 383	516	499	$[LaCC_6]$ $[LaCaC_4]$ MCC_4 [CaCC] $[CaCaC_6]$	26
2	26-40	2.39	243, 383, 411 243, 409, 437 297, 355, 437	516 542	499 525	PC_6C_4 OC_4C_6 $MC_4C_{10:1}$	
3	26-40	2.92	271, 383, 439 299, 355, 439 271, 437	544 570	527 553	PCC_4 $MCaC_4$ OC_6C_6	28
4	26-40	3.53	299, 411, 439 327, 383, 439 355, 439	572	555	PCC_6 $MCaC_6$ $LaLaC_6$	
5	26-40	3.72	299, 383, 467 327, 355, 467	572	555	$PCaC_4$ $MLaC_4$	30
6	26-40	3.81	299, 409, 493	598	581	$OCaC_4$	
7	26-40	4.58	327, 411, 467 355, 383, 467	600	583	$PCaC_6$ $MLaC_6$	
8	26-40	4.69	327, 437, 493 381, 383, 493 327, 465	626	609	$OCaC_6$ $MMyC_6$ OCC	
9	26-40	4.84	327, 383, 495 355, 495	600	583	$PLaC_4$ MMC_4	32
10	26-40	4.95	327, 409, 521 353, 383, 521 355, 381, 521	626	609	$OLaC_4$ $PMyC_4$ $MPoC_4$	
11	26-40	5.82	355, 439, 467 383, 411, 467 383, 439 411, 439	628	611	PCCa [MCLa] [MCaCa] [CaLaLa]	34
12	26-40	6.02	355, 411, 495 383, 495	628	611	$PLaC_6$ MMC_6	

Peak No	Method	Apex min	RT	$[M-RCO_2]^+$ *m/z*	$[M+NH_4]^+$ *m/z*	$[M+H]^+$ *m/z*	TAG identification	ECN
13	26-40	6.14		355, 437, 521 381, 411, 521	654	637	$OLaC_6$ $PMyC_6$	
14	26-40	6.38		355, 383, 523	628	611	PMC_4	
15	26-40	6.48		355, 409, 549 381, 383, 549	654	637	OMC_4 $PPoC_4$	
16	26-40	6.81		383, 407, 575	680	663	LPC_4	
17	26-40	6.97		407, 409, 601	706	689	OLC_4	
18	26-40	7.33		369, 383, 537	642	625	$PPtC_4$	35
19	26-40	7.66		383, 439, 495 383, 467 411, 495 411, 439, 467 439	656	639	[PLaC] [PCaCa] [MMC] [MLaCa] [LaLaLa]	
20	26-40	7.93		383, 411, 523	656	639	PMC_6	
21	26-40	8.12		383, 437, 549 409, 411, 549	682	665	OMC_6 $PPoC_6$	36
22	26-40	8.42		383, 551	656	639	PPC_4	
23	26-40	8.57		383, 409, 577	682	665	OPC_4	
24	26-40	8.76		409, 603 383, 409, 577	708 682	691 665	OOC_4 OPC_4	
25	26-40	9.17		369, 411, 565 383, 397, 565 397, 411, 537	670	653	$SPtC_4$ $PMaC_4$ $PPtC_6$	37
26	26-40	9.99		411, 467, 495 439, 495 439, 467	684	667	PLaCa [MMCa] [MLaLa]	
27	26-40	10.14		411, 467, 495 411, 439, 523	684	667	PLaCa PMC	
28	26-40	10.49		411, 551	684	667	PPC_6	38
29	26-40	10.73		411, 437, 577	710	693	OPC_6	
30	26-40	11.13		383, 411, 579	684	667	SPC_4	
31	26-40	11.35		409, 411, 605	710	693	SOC_4	
32	26-40	13.23		439, 467, 523 439, 495	712	695	PMCa PLaLa	40

Peak No	Method	Apex min	RT	$[M\text{-}RCO_2]^+$ *m/z*	$[M+NH_4]^+$ *m/z*	$[M+H]^+$ *m/z*	TAG identification	ECN
33	26-40	13.56		439, 551	712	695	PPC	
34	26-40	13.81		439, 465, 577	738	721	OPC	
35	26-40	14.05		411, 439, 579	712	695	SPC_6	
36	26-40	14.24		437, 439, 605 465, 551	738	721	SOC_6 $PPC_{10:1}$	
37	42-56	7.7		493, 603 493, 521, 575 493, 547, 549	792	775	OOCa OPoLa OMMy	
38	42-56	7.94		467, 493, 577 467, 521, 549 493, 521, 523 465, 467, 605 493, 495, 549	766	749	OPCa [OMLa] PMMy OSC PPoLa	42
39	42-56	8.21		439, 467, 579 439, 495, 551 495 439, 523 467, 551 467, 495, 523	740	723	SPC [SMCa] [MMM] [SLaLa] [PPCa] [PMLa]	42
40	42-56	9.26		521, 603 521, 547, 577 521, 549, 575 547, 549	820	803	OOLa OPMy OMPo [PPoPo]	
41	42-56	9.56		493, 495, 605 493, 523, 577 493, 549, 551 495, 521, 577 495, 549 521, 551 521, 523, 549	794	777	OSCa [SPoLa] [SMMy] [OPLa] [OMM] [PPMy] [MPPo]	44
42	42-56	9.85		467, 523, 551 467, 495, 579 495, 551 495, 523	768	751	[SMLa] SPCa [PPLa] [PMM]	
43	42-56	10.98		549, 603 549, 575, 577	848	831	OOM OPPo	
44	42-56	11.16		549, 603 551, 575 549, 575, 577 523, 549, 577	848 822	831 805	OOM LPP [OPPo] OPM	46

Peak No	Method	Apex RT min	$[M-RCO_2]^+$ *m/z*	$[M+NH_4]^+$ *m/z*	$[M+H]^+$ *m/z*	TAG identification	ECN
45	42-56	11.27	523, 549, 577	822	805	OPM	
46	42-56	11.61	523, 551 495, 551 495, 523, 579 551, 579	796	779	[PPM] [SMM] [SPLa] [SPP]	
47	42-56	11.84	577, 563, 537 603, 563 589, 577, 563	836 862	819 845	OPPt OOPt OPMo	47
48	42-56	12.17	577, 563, 537	836	819	OPPt	
49	42-56	12.38	603	902	885	OOO	
50	42-56	12.75	577, 603	876	859	OPO*	
51	42-56	13.08	551, 577 549, 551, 605	850	833	OPP* SMO	48
52	42-56	13.45	523, 551, 579	824	807	SPM	
53	42-56	14.02	565, 577, 591 605, 565, 563 537, 565, 579 551, 565	864 838	847 821	OMaP SOPt SPPt MaPP	49
54	42-56	14.52	603, 605	904	887	SOO*	
55	42-56	14.93	577, 579, 605	878	861	SPO*	50
56	42-56	15.31	551, 579	852	835	SPP*	
57	42-56	16.71	605, 607	906	889	SSO*	
58	42-56	17.14	579, 607	880	863	SPS*	52

The two stage method approach with a combination of Methods ECN26-40 and ECN42-56 achieved the identification of a number of different TAGs not identified by the single stage approach of Method S, especially for ECN 42 and 44. A number of TAGs identified by Method S were not identified with this new approach. That is for the most part a result of improved use of tandem mass spectrometry (MS^2) which allowed the discrimination of DAGs that were products of dissociation of a specific TAG from other mass peaks in the mass spectra. The separation of peaks (Figure 4.15) and identification of TAGs for ECN 38 (Table 4.7) are provided as an example of the improvement of the two stage approach compared to Method S. Peaks 28 and 29 for Method ECN26-40 correspond to peaks 39 and 40 for Method S and the separation between the two is improved significantly (Figure 4.15). The same is true for peaks

30 and 31 for Method ECN26-40 which correspond to peaks 41 and 42 for Method S (Figure 4.15).

Overall, the TAGs identified with Method S were 117 while the two stage approach identified 125 TAGs. Method S identified 41 TAGs that were not identified by the two stage method, while the two stage method identified 49 TAGs that were not previously identified (Table 4.8).

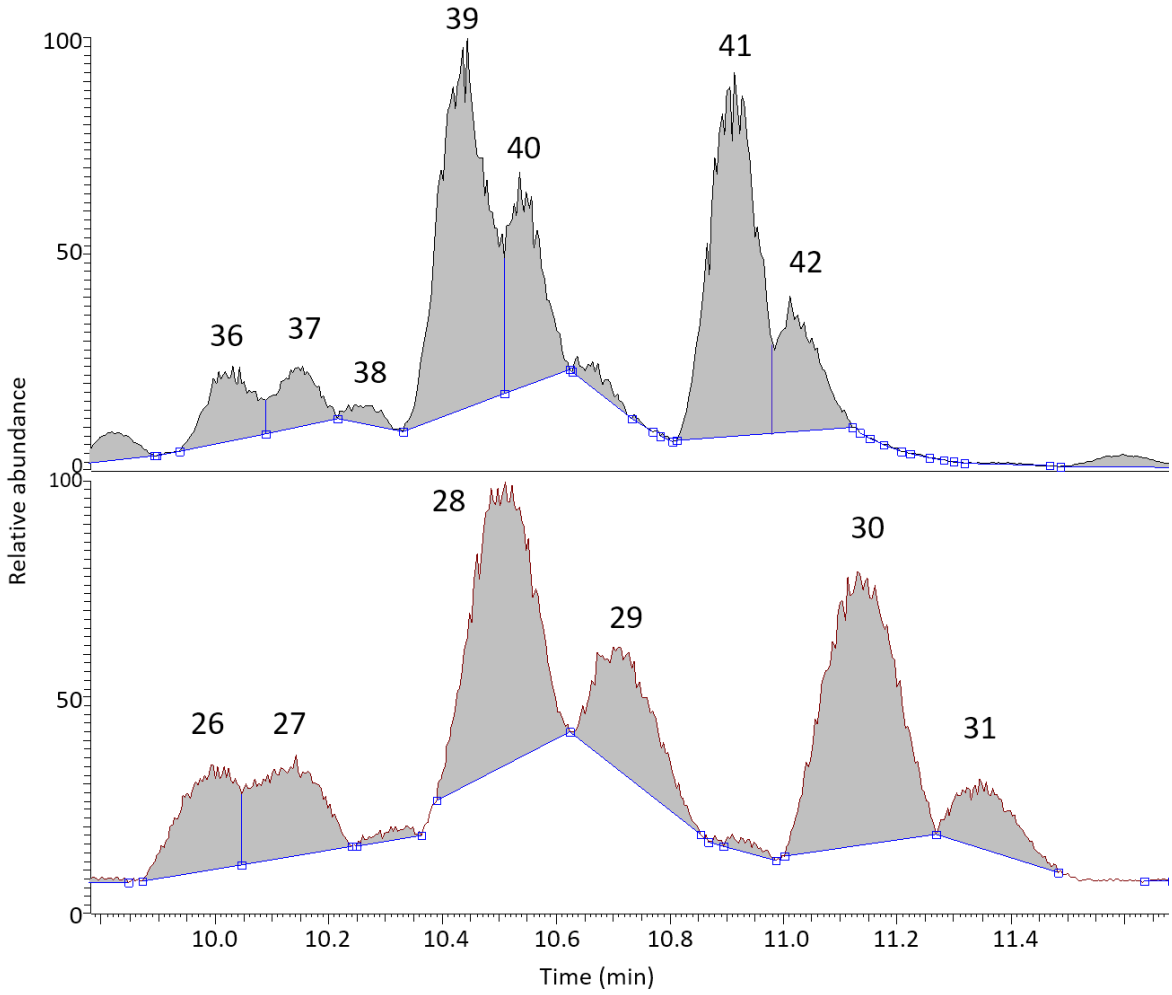

Figure 4.15: Partial RP UHPLC-APCI MS base peak chromatograms of cow milk sample analysed with Methods S (Table 3.11) (top) and ECN26-40 (Table 4.5) (bottom) (Table 4.5). The region depicted in both chromatograms shows the peaks attributed to TAGs with ECN 38 and the integration of the peaks is shown as well. The numbers above each peak correspond to the identification of the TAGs of each peak with can be found in Table 3.12 for Method S (top) and in Table 4.6 for Method ECN26-40 (bottom).

Table 4.7: TAG identification for peaks of Figure 4.15.

Method	Peak No	$[M\text{-}RCO_2]^+$ *m/z*	$[M+NH_4]^+$ *m/z*	$[M+H]^+$ *m/z*	TAG identification
S	36	467, 439 495, 439 495, 467, 411	684	667	[MLaLa] [MMCa] PLaCa
S	37	523, 439, 411 521, 493, 411	684 710	667 693	PMC OLaCa
S	38	549, 465, 411 523., 439, 411	710 684	693 667	OMC PMC
S	39	551, 411 551, 439, 383 577, 437, 411 523, 465, 437	684 710 	667 693 	PPC_6 SMC_6 OPC_6 $PMC_{10:1}$
S	40	577, 437, 411 551, 411 603, 437	710 684 736	693 - 719	OPC_6 PPC_6 OOC_6
S	41	579, 411, 383	684	667	SPC_4
S	42	605, 411, 409	710	693	SOC_4
ECN26-40	26	495, 467, 411 495, 439 467, 439	684	667	PLaCa [MMCa] [MLaLa]
ECN26-40	27	495, 467, 411 523, 439, 411	684	667	PLaCa PMC
ECN26-40	28	551, 411	684	667	PPC_6
ECN26-40	29	577, 437, 411	710	693	OPC_6
ECN26-40	30	579, 411, 383	684	667	SPC_4
ECN26-40	31	605, 411, 409	710	693	SOC_4

Table 4.8: TAGs identified with Method S and TAGs identified with the two stage approach.

Method S	*Method ECN26-40*	*ECN*	*Method S*	*Method ECN26-40*	*ECN*	*Method S*	*Method ECN26-40*	*ECN*	*Method S*	*Method ECN26-40*	*ECN*
MCC_4	MCC_4	26	LMC_4	-	32	-	$PMyC_6$	34	PLaCa	PLaCa	38
PC_6C_4	PC_6C_4	26	$MLaC_6$	$MLaC_6$	32	$PPtC_4$	$PPtC_4$	35	PMC	PMC	38
OC_6C_4	OC_4C_6	26	$PCaC_6$	$PCaC_6$	32	$OPtC_4$	-	35	PPC_6	PPC_6	38
-	[CaCC]	26	$OCaC_6$	$OCaC_6$	32	$MoPC_4$	-	35	OPC_6	OPC_6	38
-	$[CaCaC_6]$	26	MMC_4	MMC_4	32	PCaCa	[PCaCa]	36	SPC_4	SPC_4	38
-	$[LaCC_6]$	26	$PLaC_4$	$PLaC_4$	32	MMC	[MMC]	36	SOC_4	SOC_4	38
-	$[LaCaC_4]$	26	$OLaC_4$	$OLaC_4$	32	MLaCa	[MLaCa]	36	OLaCa	-	38
-	$MC_4C_{10:1}$	26	$PMyC_4$	$PMyC_4$	32	PMC_6	PMC_6	36	OMC	-	38
MCC_6	-	28	-	$MMyC_6$	32	$PPoC_6$	$PPoC_6$	36	SMC_6	-	38
$LaCaC_6$	-	28	-	OCC	32	OMC_6	OMC_6	36	$PMC_{10:1}$	-	38
OCC_4	-	28	-	$MPoC_4$	32	PPC_4	PPC_4	36	OOC_6	-	38
$MCaC_4$	$MCaC_4$	28	$PtMC_4$	-	33	OPC_4	OPC_4	36	$MaPC_6$	-	39
PCC_4	PCC_4	28	[MCaCa]	[MCaCa]	34	OOC_4	OOC_4	36	$SPtC_6$	-	39
	OC_6C_6	28	PCaC	PCCa	34	SMC_4	-	36	$SMaC_4$	-	39
$MCaC_6$	$MCaC_6$	30	[LaLaCa]	[CaLaLa]	34	SLC_4	-	36	PMCa	PMCa	40
PCC_6	PCC_6	30	[MLaC]	[MCLa]	34	-	[LaLaLa]	36	PPC	PPC	40
$PCaC_4$	$PCaC_4$	30	MMC_6	MMC_6	34	-	[PLaC]	36	OPC	OPC	40
$MLaC_4$	$MLaC_4$	30	$PLaC_6$	$PLaC_6$	34	$PPtC_6$	$PPtC_6$	37	SOC_6	SOC_6	40
$LnMC_4$		30	PMC_4	PMC_4	34	$SPtC_4$	$SPtC_4$	37	$PPC_{10:1}$	$PPC_{10:1}$	40
-	$OCaC_4$	30	$PPoC_4$	$PPoC_4$	34	$MaPC_4$	$PMaC_4$	37	SPC_6	SPC_6	40
-	$LaLaC_6$	30	OMC_4	OMC_4	34	$OMaC_4$	-	37	MMLa	-	40
LaCaCa	-	32	LPC_4	LPC_4	34	$OPtC_6$	-	37	SMC	-	40
MCaC	-	32	OLC_4	OLC_4	34	$MoPC_6$	-	37	[OMCa]	-	40
PCC	-	32	$OPoC_4$	-	34	[MLaLa]	[MLaLa]	38	PPoCa	-	40
$PoMC_4$	-	32	-	$OLaC_6$	34	[MMCa]	[MMCa]	38	OLaLa	-	40

Method S	*Method ECN26-40*	*ECN*
MMMy	-	40
OOC	-	40
LPCa	-	40
SSC_4	-	40
-	PLaLa	40

Method S	*Method ECN42-56*	*ECN*
-	OOCa	42
-	OPoLa	42
-	OMMy	42
-	OPCa	42
-	[OMLa]	42
-	PMMy	42
-	OSC	42
-	PPoLa	42
-	SPC	42
-	[SMCa]	42
-	[MMM]	42
-	[SLaLa]	42
-	[PPCa]	42
-	[PMLa]	42
-	OOLa	44
-	OPMy	44
-	OMPo	44
-	[PPoPo]	44
-	OSCa	44
-	[SPoLa]	44
-	[SMMy]	44
-	[OPLa]	44
-	[OMM]	44
-	[PPMy]	44
-	[MPPo]	44

Method S	*Method ECN42-56*	*ECN*
-	[SMLa]	44
-	SPCa	44
-	[PPLa]	44
-	[PMM]	44
[OPM]	OPM	46
OOM	OOM	46
OPPo	OPPo	46
[LPP]	LPP	46
[SMM]	[SMM]	46
[PPM]	[PPM]	46
-	[OPPo]	46
-	[SPLa]	46
-	[SPP]	46
OPPt	OPPt	47
[OOPt]	OOPt	47
[OPMo]	OPMo	47
[MaPM]	-	47
[PPPt]	-	47
OOO	OOO	48
OOP*	OOP*	48
OPP*	OPP*	48
SPM	SPM	48
-	SMO	48
[OMaP]	OMaP	49
[SOPt]	SOPt	49

Method S	*Method ECN42-56*	*ECN*
[SPPt]	SPPt	49
[MaPP]	MaPP	49
[OOMa]	-	49
SOO*	SOO*	50
SPO*	SPO*	50
SPP*	SPP*	50
SSO*	SSO*	52
SSP*	SSP*	52
SSS	-	54
$[SPC_{20}]$	-	54
$[PPC_{22}]$	-	54

4.2.3 PCA of results

The relative peak areas of 72 individual TAGs in five samples of cows milk and one sample of goats milk were determined from the base peak chromatogram. The data, though comprising a small dataset, were processed by principal components analysis to give an indication of the potential of the separation method in identifying TAGs and correctly assigning sample origin Samples were produced by extraction of the lipophilic fraction from shop bought liquid milks: CM01 to CM03 from full fat cows milk; sample CM04 from skimmed cows milk; sample CM05 from semi-skimmed cows milk and sample GM01 from goats milk.

A total of 144 different variables were considered in the data matrix for each sample: the presence or absence of the 72 different TAGs and their relative base peak abundances. Principal components analysis (PCA) allows the representation of results in fewer dimensions by calculating principle components which are used as new variables. Principle components are ordered in terms of how much of the variance they account for, i.e. principle component 1 (PC1) represents the highest amount of variance in the data. The original variables, TAG identity and ion abundance in this study, contribute different amounts to the various different principle components, the extent of those contribution being represented by loadings. The first two principle components are usually used to visualise the data in two dimensions, while still maintaining most of the information in the data. In this work, the eigenvalues of each of the principle components were presented in scree plots used to determine the statistically significant components (Appendix C).

An important consideration in PCA analysis is whether to use scaled or unscaled data, both approaches were explored to determine which TAGs are the most important in identifying samples. For the former, auto-scaling was used in this study: the mean value of each variable was subtracted and the result divided by the standard deviation. This way, all variables will have a mean of zero unit variance, making all variables equally important. Using scaling with HPLC data means that components with smaller relative peak areas can still influence the characterisation of samples. This is not desirable in TAG analysis with HPLC data, because the most abundant TAGs in oils and fats are indicative of different origin and TAGs in much smaller amounts don't always inform the identification of samples. Furthermore, the auto-scaling can increase the influence of noise peaks in the data analysis.

The unscaled data produced the results in Figure 4.16, with goat milk being clearly separated from cow's milk. PC1 and PC2 contributed more than 89% of the overall variance, indicating that the TAGs that contribute the most to these two principal components are critical TAGs in the distinction of the samples. The TAGs that contributed to PC1 negatively were mainly PMCa and also OPCa, OOM, OLP, OOCa, PCaCa, PPCa and TAGs that contributed positively were mainly PPC_4 and then also PPM, PMLa, PMC_4, OPPo, SPM. Larger contributions of Ca acyl groups in TAGs is a characteristic of goat's milk.

PC2 separated the milk samples into two sub-groups, CM02, CM03, CM04 and CM01, CM05. TAGs that contributed to PC2 negatively were mainly OPC4 and also OMC4, OOP, OPPo, OOO, SOO and TAGs that contributed positively were SPM, OPP, PMLa, SPCa, PPCa. This grouping did not appear to reflect variance related to any specific property; all samples are cow milk, full fat samples appear in both groups and all samples were bought from different shops at different times. This leads to the conclusion that there were not two separate groups of cow milk samples, the variance simply reflecting the natural variation between milks from different sources.

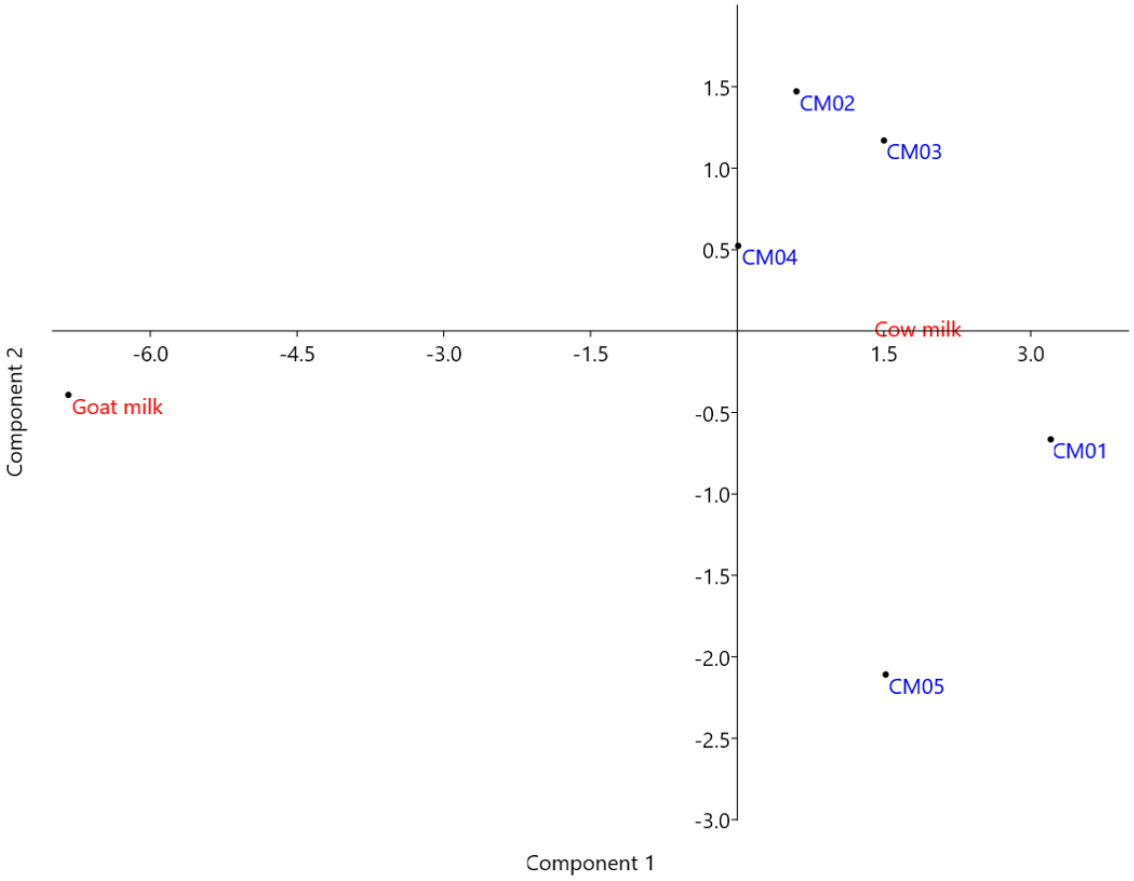

Figure 4.16: PCA plot of unscaled data for milk samples. PC1 contribution to variance 80.8%. PC2 contribution to variance 8.9%. GM01 is a goat milk sample and CM01-CM05 are cow milk samples. More details on all samples can be found in Appendix B. Scree plot and loading plots can be found in Appendix C (pages 151, 154 and 155).

The scaled data (Figure 4.17) also separated cow and goat milk and the two subgroups of cow milk are present. The fact that the scaled data did not reveal any additional differences between the samples indicates that smaller peaks are not crucial for the identification of different types of samples. This is in accordance with previous observations from HPLC data analysis, hence unscaled data were used from this point onwards.

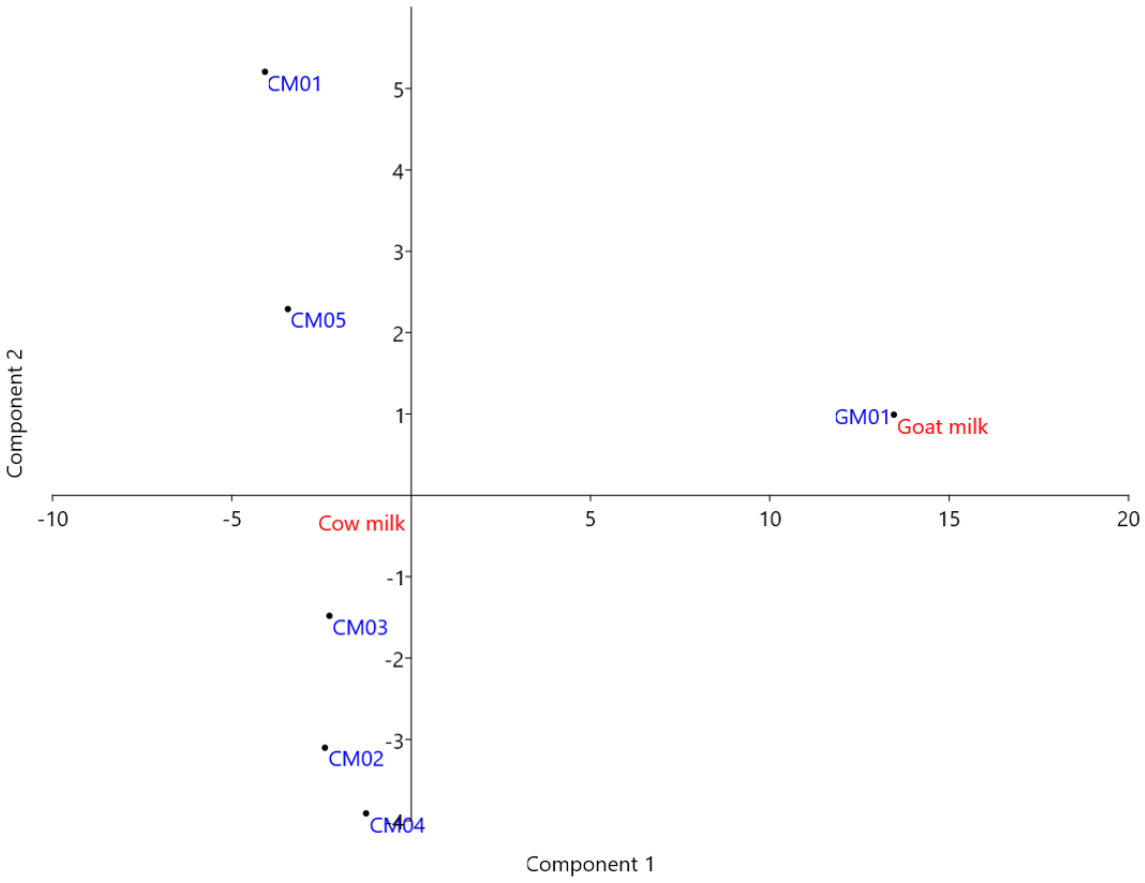

Figure 4.17: PCA plot of scaled data for milk samples. PC1 contribution to variance 61.7%. PC2 contribution to variance 16.8%. GM01 is a goat milk sample and CM01-CM05 are cow milk samples. More details on all samples can be found in Appendix B.

Cluster analysis is a way to discover groupings between samples, without any prior knowledge or assumptions about the data. The technique of hierarchical clustering was employed in this work, specifically agglomative clustering. Agglomative clustering is a type of clustering where each object or sample is considered its own cluster and clusters are merged with each other according to similarity so that the final results merges all objects in a single cluster.

The degree of similarity between clusters in this study was calculated using the Euclidean distance between single samples or in the case of clusters the Euclidean distance between the centroids of the two clusters. The clustering starts with the samples that are the closest matches to each other. This can be determined with the use of a distance matrix where the distances between all the different samples are plotted using the variables of each sample as

coordinates to calculate the Euclidean distance. The two closest ones are merged into a cluster and a new distance matrix is created, where the two samples are now replaced by the centroid of the newly created cluster. This process continues until all samples are part of one cluster. The results of the agglomative clustering can be displayed in a dendrogram.

Cluster analysis for the milk samples is presented in the dendrogram below (Figure 4.18). The samples most similar with each other are CM02 and CM03, two of the full fat cow milk samples. These two samples cluster together with sampleCM04, the skimmed cow milk, and then with CM05, the semi-skimmed milk. The remaining full fat cow milk sample, CM01, is the most different in this cluster of cow milk samples. The small number of samples analysed does not allow for a clear interpretation of the reason for its difference. It is possible all the differences between sample CM01-CM05 are due to natural variance in cow milk samples or other factors, such as geographic origin or processing, could affect the analysis. The goat milk sample, GM01, is the last to be included in the cluster and indicates a genuine difference from the cow milk samples. Specifically, the distance between the goat milk sample and the cow's milk samples is more than 10 units, while the distance between the different cow milk samples ranges from 2 to 4 units.

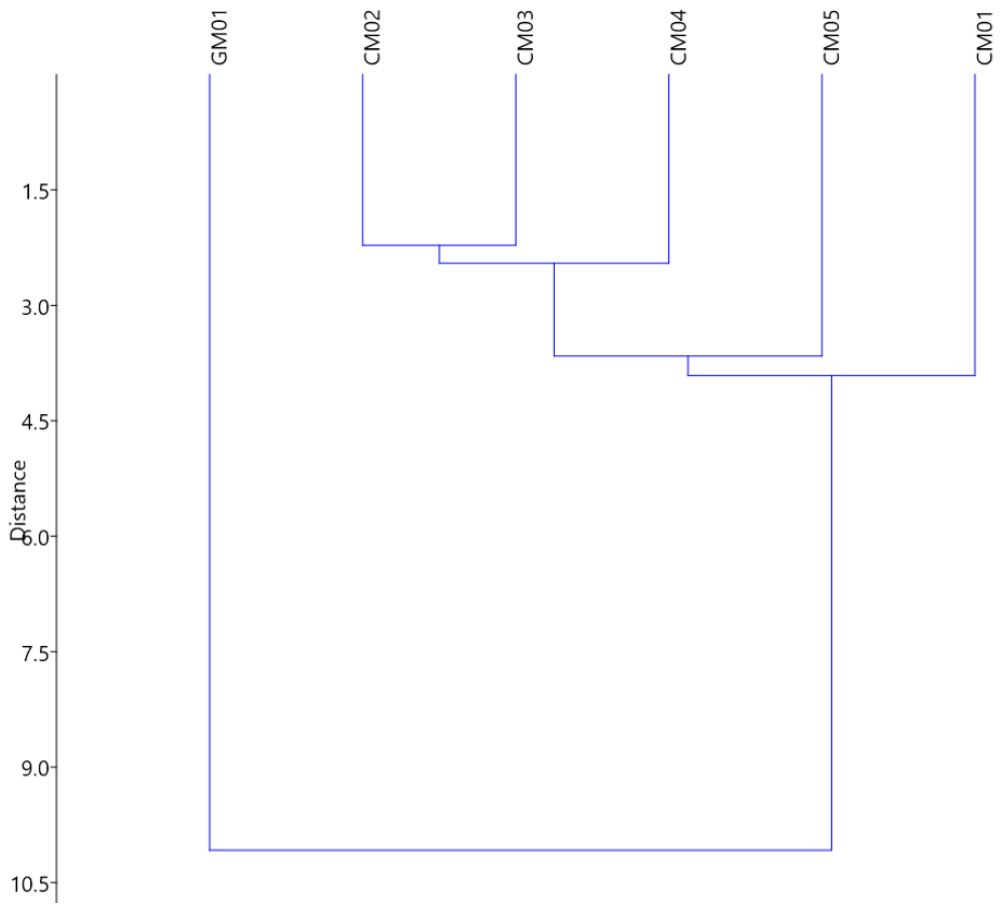

Figure 4.18: Dendrogram of milk samples. GM01 is a goat milk sample and CM01-CM05 are cow milk samples. More details on all samples can be found in Appendix B.

4.3 Conclusions

A two stage method was developed for the separation of TAGs in milk samples. Both stages of the method employ ultra high performance liquid chromatography (UHPLC) with the solvent system, the temperature of the column and the flow rate of the mobile phase changing between the two stages. The different solvent systems achieve better separation of TAGs with major differences in their polarities; the mobile phase for one stage of the separation is optimised for the elution and separation of TAGs with ECNs between 26 and 40, while the mobile phase of the other stage for TAGs with ECNs between 42 and 56. There is significant improvement compared to Method S developed in Chapter 3 for the separation of TAGs, especially for ECNs 42 and 44 which were problematic with that method and were separated very distinctly with the two stage approach.

The use of tandem mass spectrometry (MS^2) allowed the identification of TAGs with greater confidence than previously. The issues with low abundance of ammonium adducts present in Method S were resolved and MS^2 spectra were obtained for all peaks. The result is higher confidence in the identification of TAGs. Notably, a total of 117 TAGs were identified with Method S while 125 were identified with the two stage approach, 49 of which were not identified with Method S. The 41 TAGs that were identified with Method S but not with the two stage approach can be in most cases attributed to mistaken assignments due to the lack of MS^2 spectra. The two stage approach requires no further preparation of samples between the two stages like multidimensional methods usually do. The total time needed for the analysis of a sample with the two stage approach is 56 min, compared to 25 min for Method S and more than 150 min for the method by Beccaria et al. (2014), meaning that higher accuracy in the identification of TAGs was achieved while still taking one third of the time previously needed for the analysis.

The two stage approach was used to characterise 5 cow and 1 goat milk samples and PCA analysis of the data was employed to determine if the method can discriminate samples from different origins. The results were promising even though a small number of samples was used, so the method should be applied to more samples to test its capabilities further. Furthermore, the second part of the approach, Method ECN42-56, was used to analyse olive oil successfully, so the method can be applied to oil and potentially fat samples. The two stage approach has the potential to be a universal screening method for any sample containing TAGs.

5 Application of RP UHPLC separation of TAGs to fat and oil samples

5.1 Introduction

Adulteration of food products with animal fats is important to the food industry but also to consumers who observe a specific diet, especially for religious reasons, and the full characterisation of beef fat can enable the recognition of such adulterations (Vaclavik et al., 2011; Rohman and Che Man, 2012). A number of studies have reported results for the TAG or FA composition of beef fat, some using gas chromatography and mass spectrometry methods (Kallio et al., 2001; Indrasti et al., 2010) and others using HPLC methods, (Fauconnot et al., 2004; Marikkar et al., 2005; Dugo et al., 2006) but only two of these studies have reported HPLC chromatograms with identified TAGs corresponding to labelled peaks (Fauconnot et al., 2004; Dugo et al., 2006).

The work presented in this chapter aims to evaluate the use of the RP UHPLC Method ECN42-56, presented in Chapter 4, to identify and differentiate between a wide range of oils and fats of plant and animal origin and to identify TAGs that can act as specific markers for oils and fats from particular biological sources and hence which can be targeted as markers for differentiating samples with otherwise very similar lipids compositions.

5.2 Results and discussion

The oils and fats were analysed in this chapter with one part of the two stage approach, Method ECN42-56. The reason for this was that only a small number of components where found in the region analysed by Method ECN26-40 on a small number of samples that were tested with it. This agrees with the literature that does not report TAGs in oils and fats with small ECNs. The small number of components that are present were still able to be separated and identified with Method ECN42-56.

5.2.1 Chromatograms of vegetable oils

All the samples analysed were edible oils or vegetable "milks" purchased from local supermarkets. Vegetable oils that were tested include olive oil, rapeseed oil, sunflower oil, sesame seed oil and others and one chromatogram of each type of oil is presented bellow (Figure 5.1, Figure 5.2 and Figure 5.3).

A lot of the oils and "milks" presented similar characteristics. Peaks in the regions for ECNs 42 and 44 dominated the chromatograms for rice milk, corn oil, walnut oil, grapeseed oil, soya milk, sesame seed oil and sunflower oil samples. ECN regions 44, 46 and 48 included the more prominent peaks for almond milk and groundnut oil samples. Rapeseed oil, mixed vegetable oil and rice bran oil samples had intense peaks in the regions of ECN 42, 44, 46 and 48. The dominant features in the olive oil samples' chromatograms were found in the region of ECN 48. The coconut milk sample was the one with the most noticeable differences since most of its peaks were found in the region for ECNs 32, 34, 36 and 38. The earlier eluting peaks in regions for ECN lower than 40 for all other samples were found to be DAGs.

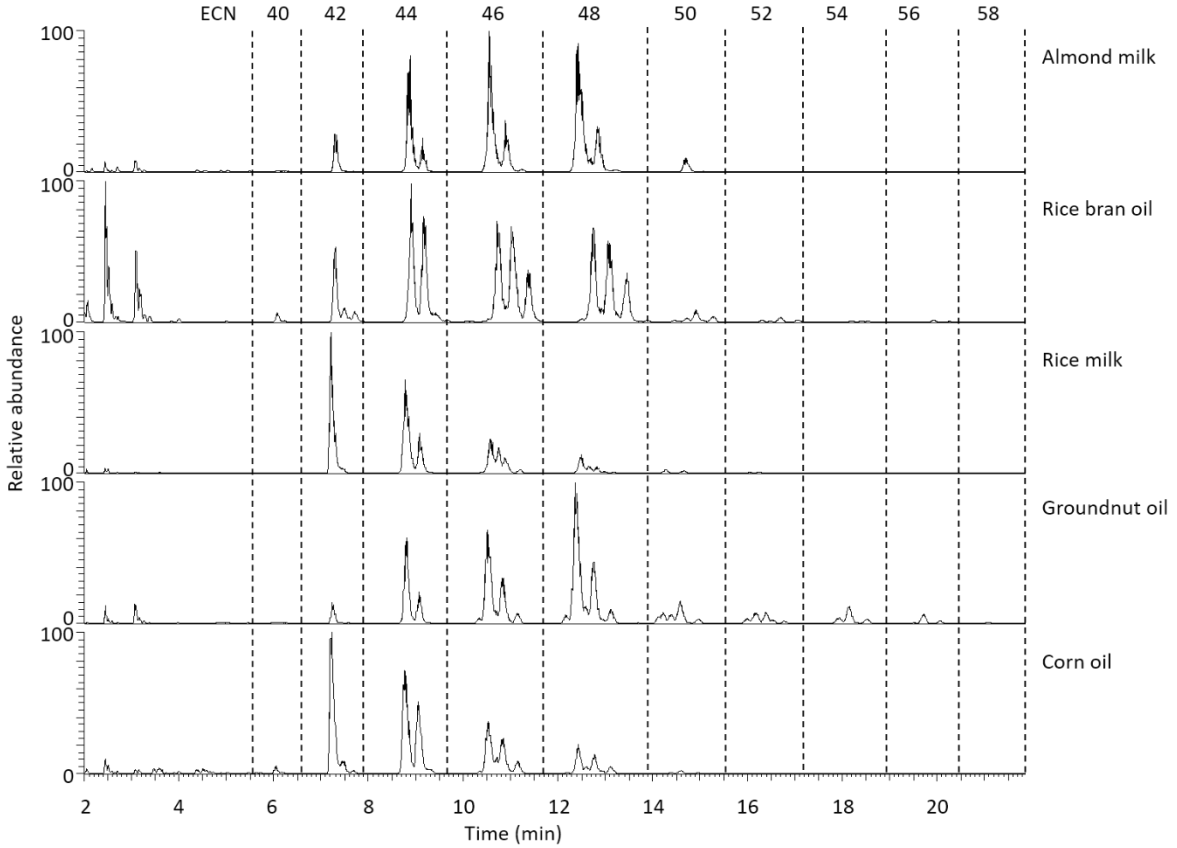

Figure 5.1: Partial RP UHPLC-APCI MS base peak chromatograms of almond milk, rice bran oil, rice milk, groundnut oil and corn oil samples analysed with Method ECN42-56 (Table 4.4). Regions are assigned according to ECN.

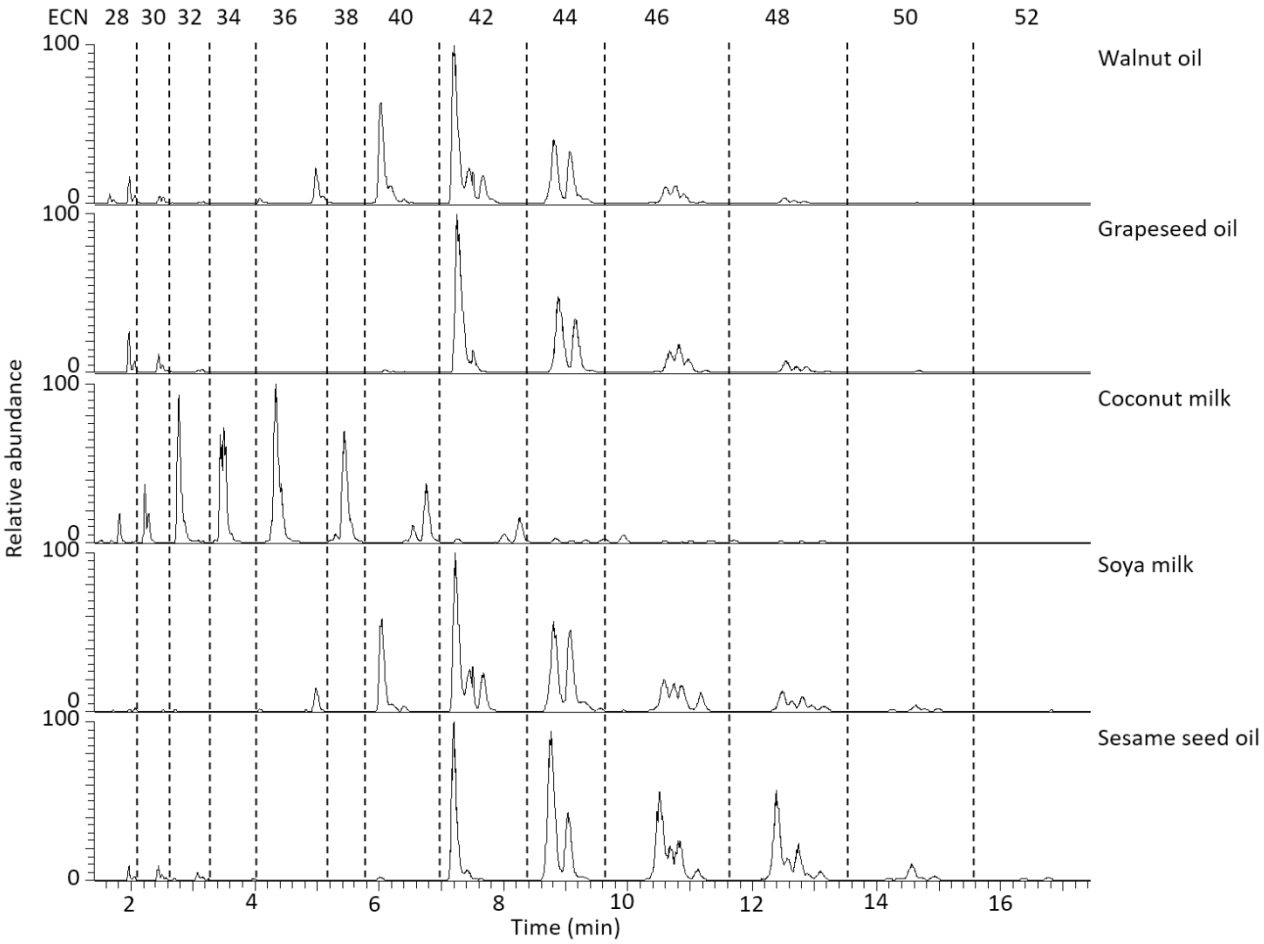

Figure 5.2: Partial RP UHPLC-APCI MS base peak chromatograms of walnut oil, grapeseed oil, coconut milk, soya milk and sesame seed oil samples analysed with Method ECN42-56 (Table 4.4). Regions are assigned according to ECN.

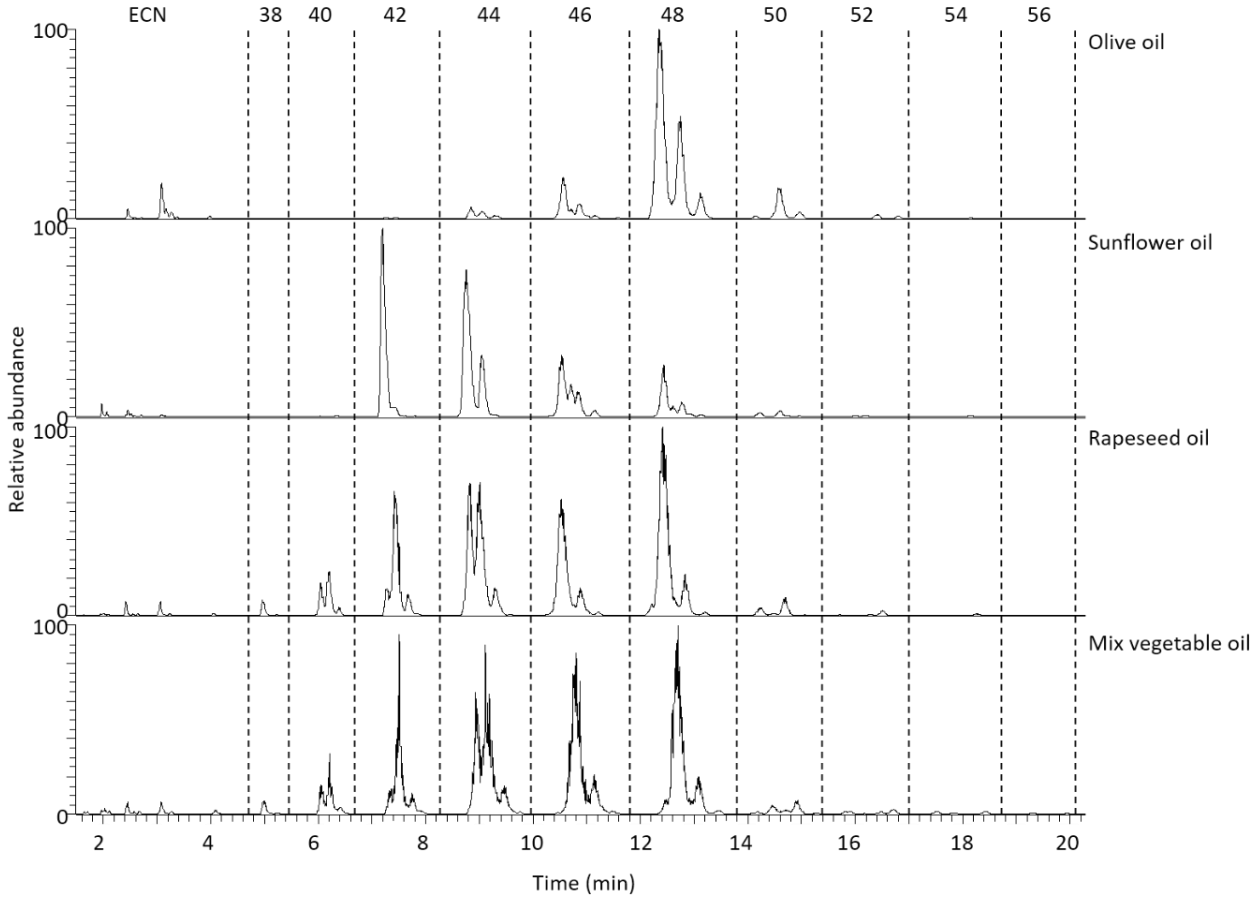

Figure 5.3: Partial RP UHPLC-APCI MS base peak chromatograms of olive oil, sunflower oil, rapeseed oil and mix vegetable oil analysed with Method ECN42-56 (Table 4.4). Regions are assigned according to ECN.

TAGs identified ranged from 28 to 58 ECN (Table 5.1). A number of TAGs were found in all the samples with a range of peak abundances. TAGs LLL, LLO and LLP were found in all samples with significantly high amounts present in corn oil, grapeseed oil and soya milk. TAGs OOL*, OOO and OOP* were found in all samples and were present in high amounts in almond oil, rapeseed oil, sesame seed oil and especially olive oil samples. TAGs LPO, PPO* and OOS were also found in most samples but in significantly smaller amounts.

Table 5.1: TAGs identified in different products of plant origin using in base peakchromatographs using Method ECN42-56 (Table 4.4). The TAGs are listed in retention time order. The relative abundance of peaks corresponding to TAGs identified was used as a second component for the identification of samples. The values given in the table below are averages for the relative abundance of the same peak for samples of the same type. Only TAGs corresponding to peaks with relative abundances higher than 0.1 are listed.

TAGs	Relative abundance (%)													
	Corn	Groundnut	Grapeseed	Coconut	Almond	Rice milk	Soya	Olive	Rapeseed	Rice oil	Sunflower	Sesame	Mix veg blend	Walnut
CCLa				1.87										
LaLaC				15.40										
LaLaCa				10.41										
CLaM				0.10										
LnLnLn									0.20					
LaLaLa				21.41										
LLnLn							2.78		0.95				1.13	5.59
LaLaM				15.62										
LLLn	1.13		0.60			0.15	12.36		1.86	0.73		1.16	2.20	15.89
OLaLa				2.07										
OLnLn									3.61				3.36	
PLnLn							0.58						0.30	
LLL	24.63	2.48	35.15	0.55	5.35	30.30	22.52	0.35	1.00	5.60	31.13	18.46	0.95	27.39
OLLn	1.19		1.82				4.87	0.34	12.40	0.89		1.15	10.86	4.72
OLaM				1.26										
LLnP*	0.28						5.11	0.12	0.65	0.76		0.16	1.04	4.67
LLO	20.55	11.84	18.92	0.62	17.06	27.56	13.88	2.61	9.82	10.72	26.24	22.70	8.00	12.29
LnOO								1.54	12.06				11.37	
LLP	13.48	3.80	12.77	0.24	3.47	9.84	11.25			9.92	10.61	10.02		8.67

TAGs	Relative abundance (%)													
	Corn	Groundnut	Grapeseed	Coconut	Almond	Rice milk	Soya	Olive	Rapeseed	Rice oil	Sunflower	Sesame	Mix veg blend	Walnut
LnOP							0.56	0.65	2.25				2.01	
OOLa				0.31										
LnPP*							0.36							
PLnP*													0.10	
MaLL			0.13				0.17							
LLG	0.15	0.39	0.26											0.19
OOL*	9.22	14.19	4.96	0.19	21.08	8.13	4.65	11.39	16.63	9.70	8.26	11.92	20.92	3.37
LLS			6.70			3.40	3.58					2.43		3.61
LPO	5.49	6.63	3.02		6.95	3.04	3.69	3.79	1.44	10.23	3.87	4.92	2.98	1.68
OPPo												1.37		
PPL*	2.04	1.49	0.48		0.46	1.07	2.48	0.38		5.38	0.71			0.35
MoOO								0.22						
GLO	0.13	0.79							0.45	0.18			0.47	
OOO	4.88	23.35	2.32	0.19	25.40	4.39	2.52	42.91	22.71	8.57	4.89	9.46	19.51	1.09
OLS	0.52	0.50	0.75		0.45	1.09	0.98				1.15	2.13	0.13	0.49
OOP*	3.16	9.27	1.08	0.21	7.56	1.24	1.48	16.91	3.46	9.05	0.97	3.80	3.38	0.38
LPS						0.32	0.69							
PPO*	1.23	1.95	0.36	0.27	0.46	0.36	0.68	3.61	0.05	4.83	0.24	1.16	0.33	0.10
SMP				0.10										
PPP										0.15				
OOMa		0.11						0.11						
OOG								0.44	0.84	0.19			0.81	

TAGs	Relative abundance (%)													
	Corn	Groundnut	Grapeseed	Coconut	Almond	Rice milk	Soya	Olive	Rapeseed	Rice oil	Sunflower	Sesame	Mix veg blend	Walnut
OLC_{20}	0.17	0.76							0.17	0.28		0.14		
LLC_{22}						1.13	0.31				0.97			
OOS	0.55	3.30	0.44		2.83	0.76	0.75	6.01	1.50	0.99	0.68	2.36	1.36	0.22
LSS	0.23	0.66	0.10		0.13		0.27					0.13		
SOP*						0.17	0.32			0.59			0.13	
SPO*								1.01	0.02		0.11	0.62		
$OLC_{24:1}$									0.14					
LLC_{24}	0.13	0.52				0.30				0.17	0.27			
OLC_{22}		1.52				0.35			0.09	0.46	0.27		0.18	
OOC_{20}	0.14	1.36						0.89	0.47			0.25	0.53	
OPC_{20}		0.36								0.21				
SOS*							0.15							
SSO*								0.42				0.37		
OLC_{24}		0.75				0.12				0.16				
$LC_{22:1}C_{22:1}$									0.08				0.28	
$OOC_{24:1}$									0.07					
OOC_{22}		2.57				0.23		0.29	0.26	0.12	0.20	0.02	0.30	
OPC_{22}		0.65												
$OC_{22:1}C_{22:1}$									0.05				0.18	
OOC24		1.25						0.12	0.02	0.20	0.10		0.13	
OPC_{24}		0.32												
OOC_{26}		0.20												

5.2.2 Chromatograms of animal fats

Animal fats that were tested include pork, beef and lamb and others and one chromatogram of each type of fat is presented bellow (Figure 5.4 and Figure 5.5).

Animal fat components are generally more saturated and apolar than vegetable oil ones. The main component peaks for animal fats elute later in the chromatogram. Specifically, the major peaks for beef and lamb appear at ECN ranges 48 and 50, while for pork and chicken they appear slightly earlier at ECN ranges 44, 46 and 48. Duck and goose samples exhibited major component peaks mainly at ECN range 48 displaying more apolar behaviour than chicken samples.

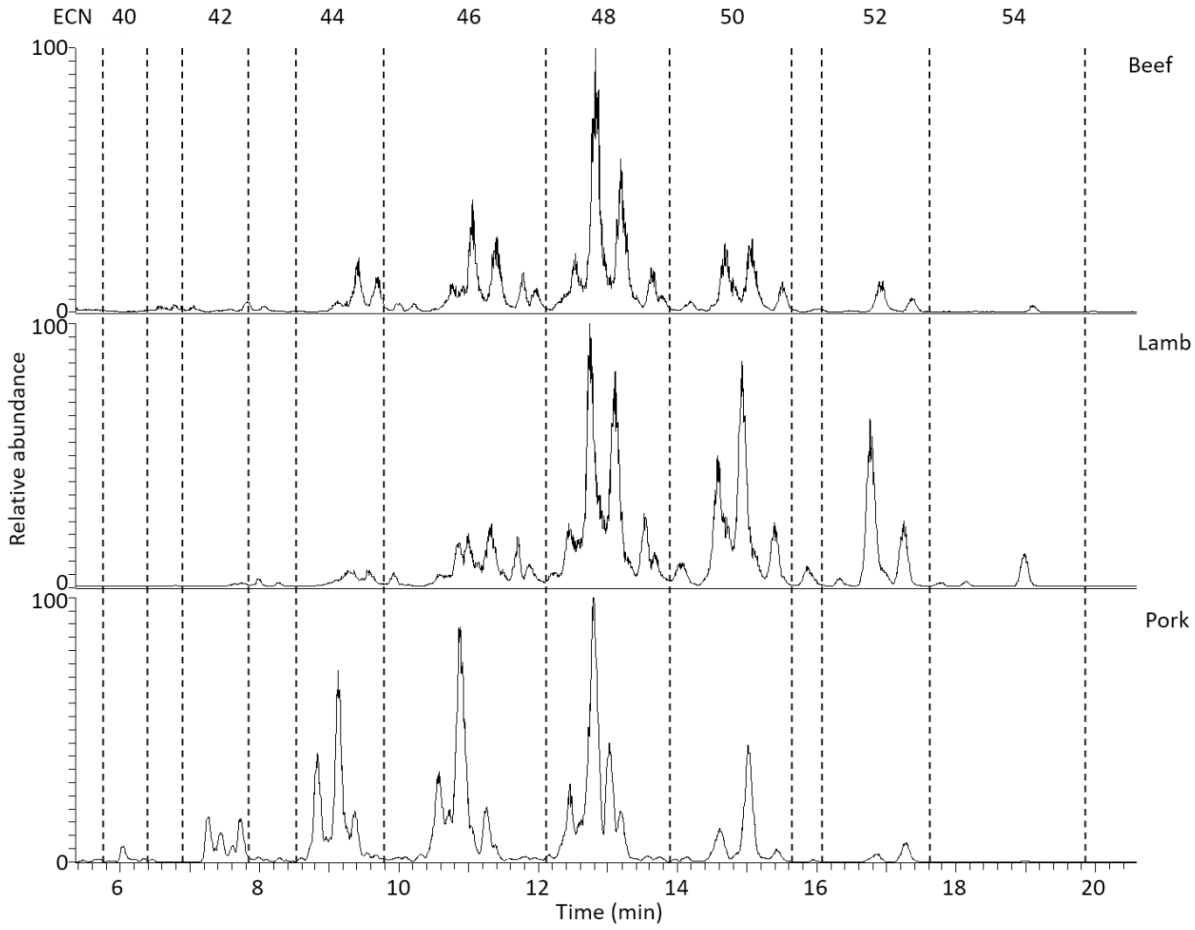

Figure 5.4: Partial RP UHPLC-APCI MS base peak chromatograms of beef, lamb and pork fat samples analysed with Method ECN42-56 (Table 4.4). Regions are assigned according to ECN.

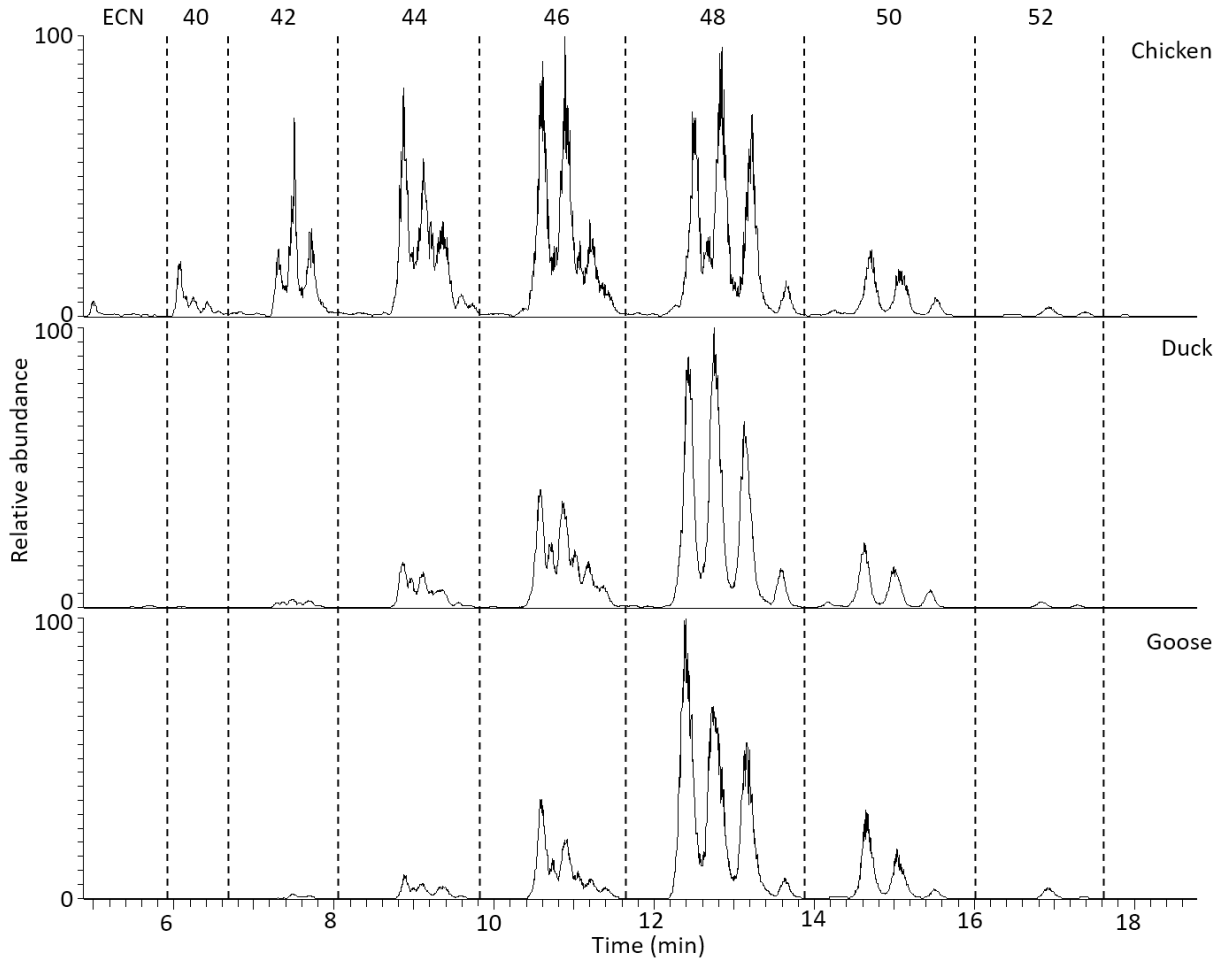

Figure 5.5: Partial RP UHPLC-APCI MS base peak chromatograms of chicken, duck and goose fat samples analysed with Method ECN42-56 (Table 4.4). Regions are assigned according to ECN.

TAGs identified ranged from 40 to 54 ECN (Table 5.2) so there is a much smaller range of TAGs in animal fats than in both milk fats and vegetable oils. A number of TAGs are of interest because their presence or absence can help identify samples. TAGs LLO and OOL* were only found in the pork and poultry samples, while LPO was found in all samples but the abundance of its peak was significantly higher for pork and poultry compare to beef and lamb samples. TAG isomers SOP*, OOP* and POP* were not found in pork, but they were represented by significant peaks for all other samples, while isomers PPO* and SPO* were only found in pork samples and as small peaks in lamb samples and isomer OPO* was found only in pork samples. TAG isomer SOS* was only found in beef and lamb samples, while isomer SSO* was present in all samples except for beef samples. Lastly, TAG SSS was found mostly in beef and lamb samples. These results are consistent with those of Hasan (2010) and Dugo et al. (2006) who also reported different isomers present in beef, pork, lamb and chicken samples.

Table 5.2: TAGs identified in different products of plant origin using in base peakchromatographs using Method ECN42-56 (Table 4.4). The TAGs are listed in retention time order. The relative abundance of peaks corresponding to TAGs identified was used as a second component for the identification of samples. The values given in the table below are averages for the relative abundance of the same peak for samples of the same type. Only TAGs corresponding to peaks with relative abundances higher than 0.1 are listed.

TAGs	Beef	Lamb	Pork	Chicken	Duck	Goose
LLLn			0.05	1.72	0.41	0.15
LLL			0.48	2.24	1.18	0.66
LLPo					0.13	
OLLn			0.56	3.97	1.52	0.95
LLM			0.21			
LLnP*			0.89	2.62	1.34	0.52
PMM		1.35	0.21			
LLO			2.44	9.05	6.56	3.62
OLPo				0.42	0.38	0.32
LLP			6.52	4.69	3.82	1.80
LnOP				3.22	1.91	1.28
OOL*		1.07	3.11	10.91	9.78	10.06
OOPo	1.46		0.32	0.26	0.53	0.61
LPO	1.27	2.72	14.49	9.04	6.20	7.83
OPPo	5.04			0.41	2.86	0.38
PPL*			2.12	3.04	3.48	1.09
POM*	4.94	3.73		0.34	0.30	0.33
PMO*		0.31				
PPM	1.46	2.72				
OPMo		0.91				
OPPt		0.52				
OOO	7.71	5.46	5.76	10.48	13.43	21.39
OOP*	21.13	12.72		12.77	15.83	18.62
OPO*			23.77			
LPS			3.27			
POP*	11.22	9.97		8.90	12.25	11.75
PPO*		0.58	2.78			
SMP	2.54	3.17	0.63			
PPP				1.85	1.54	1.66
OOMa	1.62					
OPMa*	1.17	1.19	0.23			
OMaP*		0.98				
OOG				0.27	0.26	0.22
OOS	10.06	15.55	3.96	3.44	4.10	5.90
SOP*	7.26	9.85		2.67	3.16	3.82
SPO*		0.60	13.08			
PPS	2.16	2.41	1.50	1.08	0.72	0.91
SMaO	0.67	0.97				
SPMa	0.12	0.28				
SOS*	4.57	8.90				
SSO*		0.15	1.13	0.56	0.60	0.90

TAGs	Beef	Lamb	Pork	Chicken	Duck	Goose
SPS	1.39	2.06	2.62	0.26	0.10	0.41
SSMa	0.05	0.33				
SPC20			0.21			
SSS	0.45	0.92				0.05

5.2.3 PCA of oils and fats

Vegetable oils and "milks"

Principal components analysis was performed for 37 samples of vegetable origin, 32 of which were vegetable oils and 5 were "milks", extracts of protein and fat from vegetables meant to substitute cow milk for lactose intolerant individuals. 63 different TAGs were used meaning a total of 126 different variables were considered in the data matrix for each sample. PC1, PC2 and PC3 contributed to 91.80% of the variance found in the samples. The TAGs contributing the most are OOO, OOP*, LLL, LLO, LLP, OLLn, LnOO and OOL*, which range between ECN 42 and 48. A number of clear groups emerged from the analysis (Figure 5.6). All the olive oil samples are in the first quadrant of the graph, which means they have the most positive PC1 and PC2 values, OOO and OOP* being the TAGs that most influence their position. Samples O05 and O06 are distanced from the rest of the olive oils and looking at the origin of the samples, those were the only two olive oils that were not produced in Spain (they were Greek and Italian respectively). A definite conclusion cannot be reached with the number of samples available, but this is a noticeable trend that could be further investigated to establish whether this method can distinguish between geographical origins of different samples. Rapeseed oil samples cluster in the fourth quadrant of the graph, with TAGs OLLn, LnOO and OOL* affecting it the most. Sunflower and sesame seed samples cluster in the second quadrant in two distinct groups. The TAGs that most affect that quadrant are LLO, LLL and LLP. The two soya milk samples and the walnut oil cluster together in the third quadrant and almond milk and groundnut oil are positioned in the first quadrant, close to each other. Corn oil is positioned between the sunflower oil and sesame seed oil groups, but it is clearly separated from either. Rice bran oil and coconut milk both have only slightly negative PC1 values and negative PC2 values, coconut milk much more than rice bran milk. The TAGs that contribute to negative PC2 values are mainly OLLn, LnOO and LaLaLa. The three remaining samples cluster with samples that are not necessarily closely related with them taxonomically, the vegetable mixed oil is inside the rapeseed oil group and the grapeseed oil and rice milk are clustered with the sunflower oil group. There are a number of reasons for why that would happen. The fact that there are only individual or a couple of samples of each type means that these samples could be outliers or that the TAGs important for their discrimination are not present in other samples

and were not taken into consideration by the principal component analysis. In the case of the mixed vegetable oil, it is possible that most of the mix was rapeseed oil and that is the reason for clustering with that group. Furthermore, the significant difference between rice bran oil and rice milk could be a reflection of the manufacturing procedure and the parts of the rice plant used for the production.

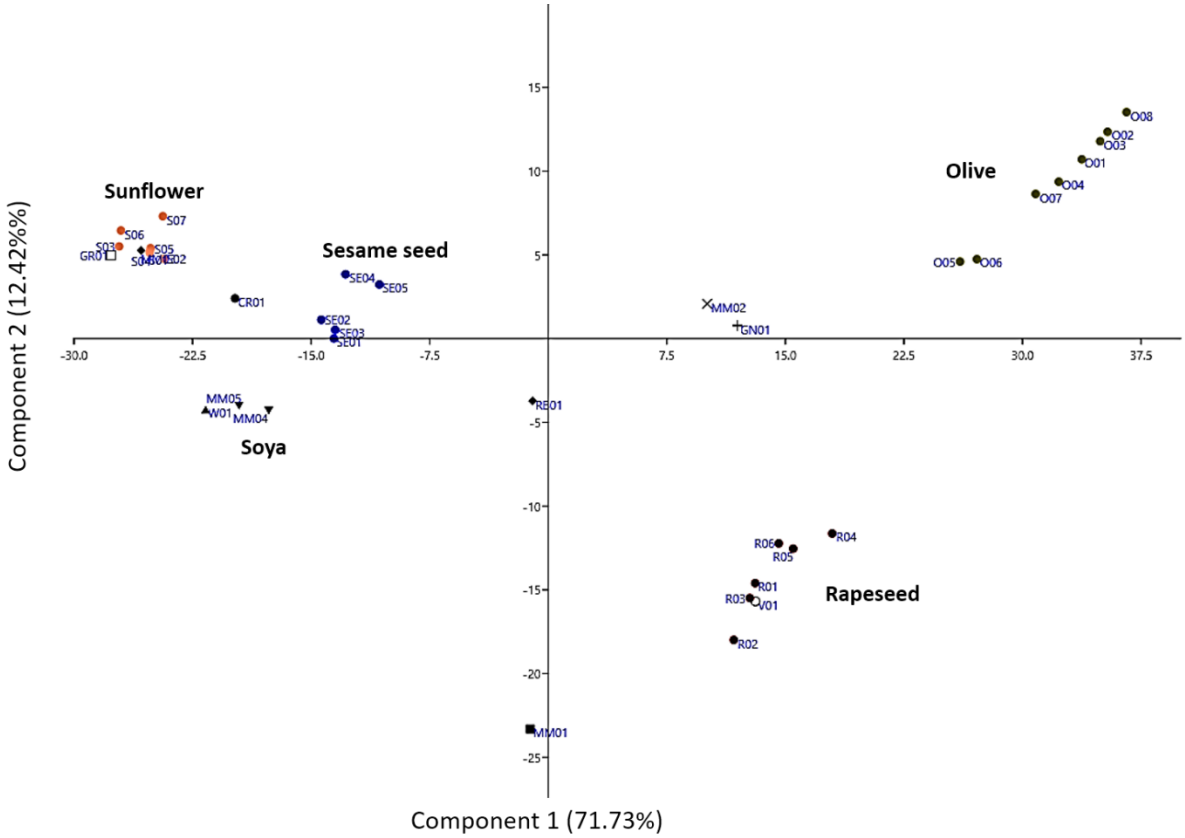

Figure 5.6: PCA plot of unscaled data for oils and fats from products of plant origin. PC1 contribution to variance 71.7%. PC2 contribution to variance 12.4%. Samples O01-O08 are olive oil samples, S01-S07 are sunflower oil samples, R01-R06 are rapeseed oil samples, SE01-SE05 are sesame seed oil samples, MM01-MM05 are milk products of plant origin, CR01 is corn oil sample, GN01 is groundnut oil, GR01 is grapeseed oil, RB01 is rice bran oil, V01 is a mix blend of vegetable oils and W01 is walnut oil. More details on all samples can be found in Appendix B. Scree plot and loading plots can be found in Appendix C (pages 151, 156 and 157).

The dendrogram confirms the groupings indicated by the principal components analysis (Figure 5.7). Olive oils group together, with O05 and O06 having closer affinity to each other than the other olive oil samples. Rapeseed oils group together with the mixed vegetable oil as well. Upon further examination of the labels of the samples, it was determined that the only ingredient listed in the mixed vegetable oil was rapeseed oil. The sesame seed oils all cluster within a single group with no clear distinction between toasted sesame seed oil (SE03-SE05) and raw sesame seed oil (SE01-SE02). The two soya milks (MM04 and MM05) are closest to each other and then to the walnut oil sample (W01). Ground nut (GN01) and almond oil (MM02) cluster closely and exhibit the greatest similarity to rice bran oil (RB01). Rice milk (MM03) and corn oil (CR01) group together with different sunflower oils (S01-S07), with rice

milk having the most affinity to S01, followed by S02-S03 and S05-S07 and corn oil having the most affinity to S04 and then to all other sunflower oil samples and rice milk. Grapeseed oil (GR01) is most similar to the group containing sunflower oil, rice milk and corn oil samples. Coconut milk (MM01) is the sample with the least similarities with any other sample.

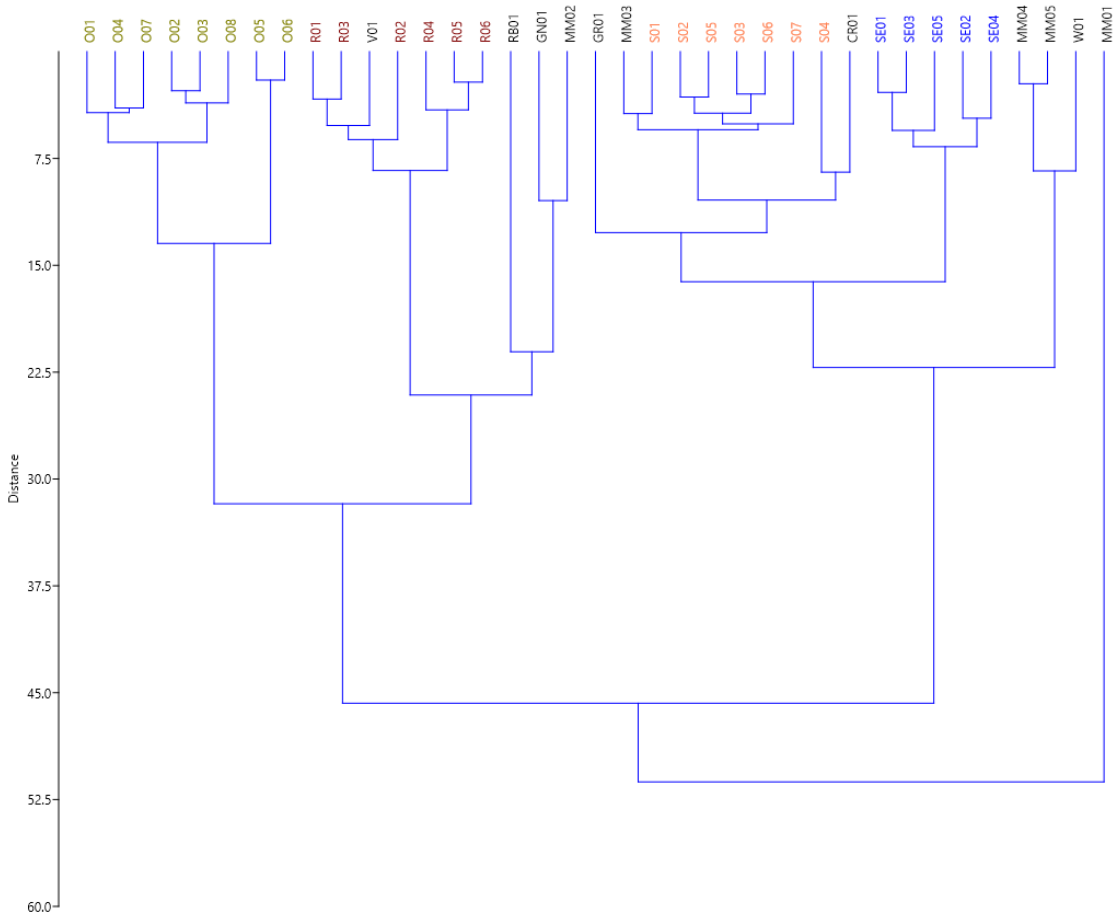

Figure 5.7: Dendrogram of vegetable oil samples. Samples O01-O08 are olive oil samples, S01-S07 are sunflower oil samples, R01-R06 are rapeseed oil samples, SE01-SE05 are sesame seed oil samples, MM01-MM05 are milk products of plant origin, CR01 is corn oil sample, GN01 is groundnut oil, GR01 is grapeseed oil, RB01 is rice bran oil, V01 is a mix blend of vegetable oils and W01 is walnut oil More details on all samples can be found in Appendix B.

Animal fats

Principal components analysis was executed for 37 samples of animal origin, including pork, beef, lamb, chicken, duck and goose fat. 45 different TAGs were used meaning a total of 90 different variables were considered in the data matrix for each sample. PC1, PC2 and PC3 contributed to 92.45% of the variance found in the samples. The TAGs contributing the most are OOP*, OPO*, SPO*, POP*, LPO, OOL*, LLO, OOS, OOO, SOS*, SOP*, LLP and LPS, which range between ECN 44 and 52. A number of clear groups emerged from the analysis (Figure 5.8). Pork samples group in the second and third quadrant of the graph, meaning they had negative PC1 values and a wider range of PC2 values. The TAGs that most influence their position were OPO*, SPO* and LPO. Chicken, duck and goose samples appear on the first quadrant of the graph. The four chicken samples cluster closely together while the duck and goose samples exhibit a larger range. Chicken samples tend to have higher PC2 values, meaning TAGs OOL*, LLO and OOO are present in higher concentrations in chicken samples than all other meat samples. The duck and goose samples have generally lower PC2 values and higher PC1 values. The increased PC1 values mean that these samples have higher concentrations of TAGs POP* and OOP* than chicken samples. Beef and lamb samples both appear at the fourth quadrant, with positive PC1 values and negative PC2 values. Beef samples exhibit higher PC1 values than lamb, higher concentrations of TAGs OOP*, OPPo and POP* contributing to this. On the other hand, lamb samples generally exhibit lower values of PC2, higher concentrations of TAGs OOS, SOS* and SOP* contributing to this. Due to using unscaled data for the PCA analysis, smaller peaks affect the variance of the samples less. One of the main differences of the beef and lamb samples is the presence of the PPO* and SPO* isomers in lamb but not in beef. Nevertheless, the peaks corresponding to those two TAGs in the lamb sample chromatograms have quite low abundances and do not affect the variance of the samples enough to completely separate lamb and beef. Using scaled data and PC1 and PC3 (Figure 5.9), beef and lamb can be quite clearly separated, but unfortunately the rest of the samples are not. The unscaled approach is the one that identifies the most samples in the appropriate groups and the one recommended for use in TAG analysis, so this will be the approach moving forward. Nevertheless, the scaled approach can be used for samples where ambiguity between beef and lamb identification exists.

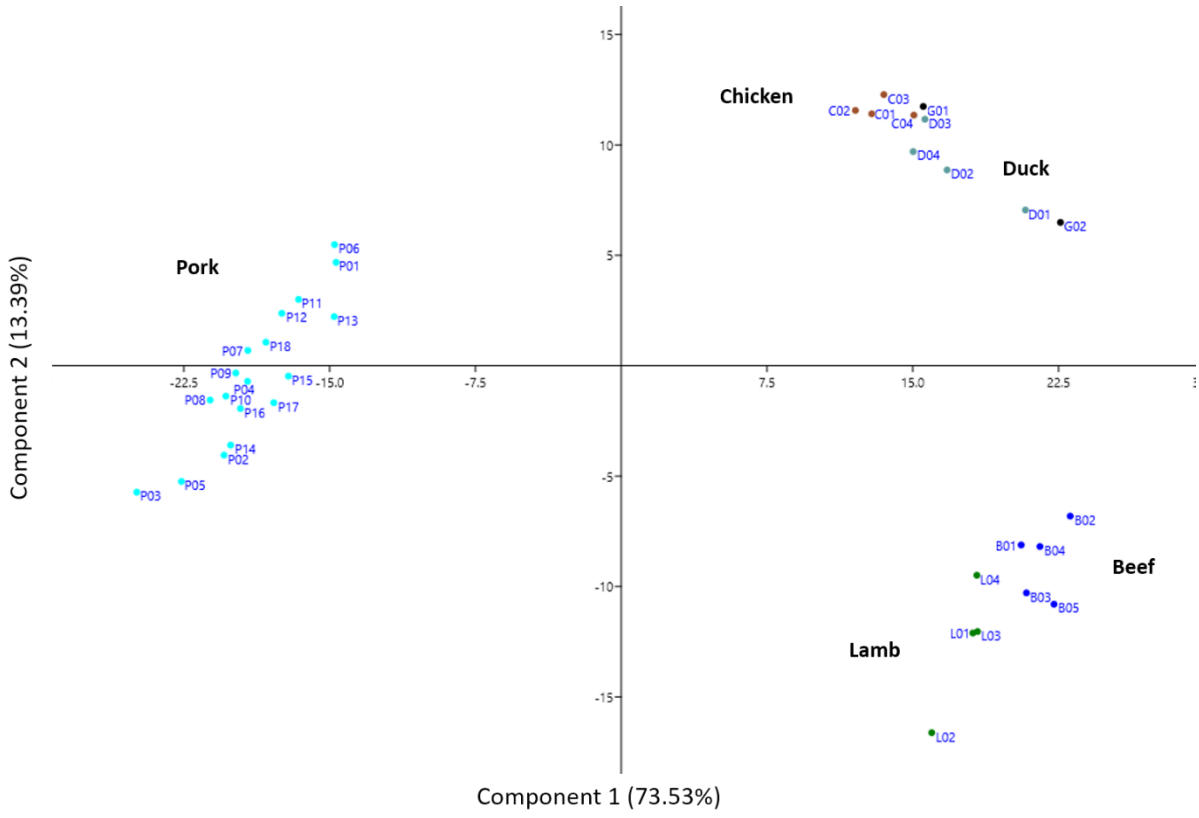

Figure 5.8: PCA plot of unscaled data for fats from products of animal origin. PC1 contribution to variance 73.5%. PC2 contribution to variance 13.4%. Samples P01-P18 are pork fat samples, B01-B05 are beef fat samples, L01 to L04 are lamb fat samples, C01-C04 are chicken fat samples, D01 to D04 are duck fat samples and G01 and G02 are goose fat samples. More details on all samples can be found in Appendix B. Scree plots and loading plots can be found in Appendix C (pages 152, 158 and 159).

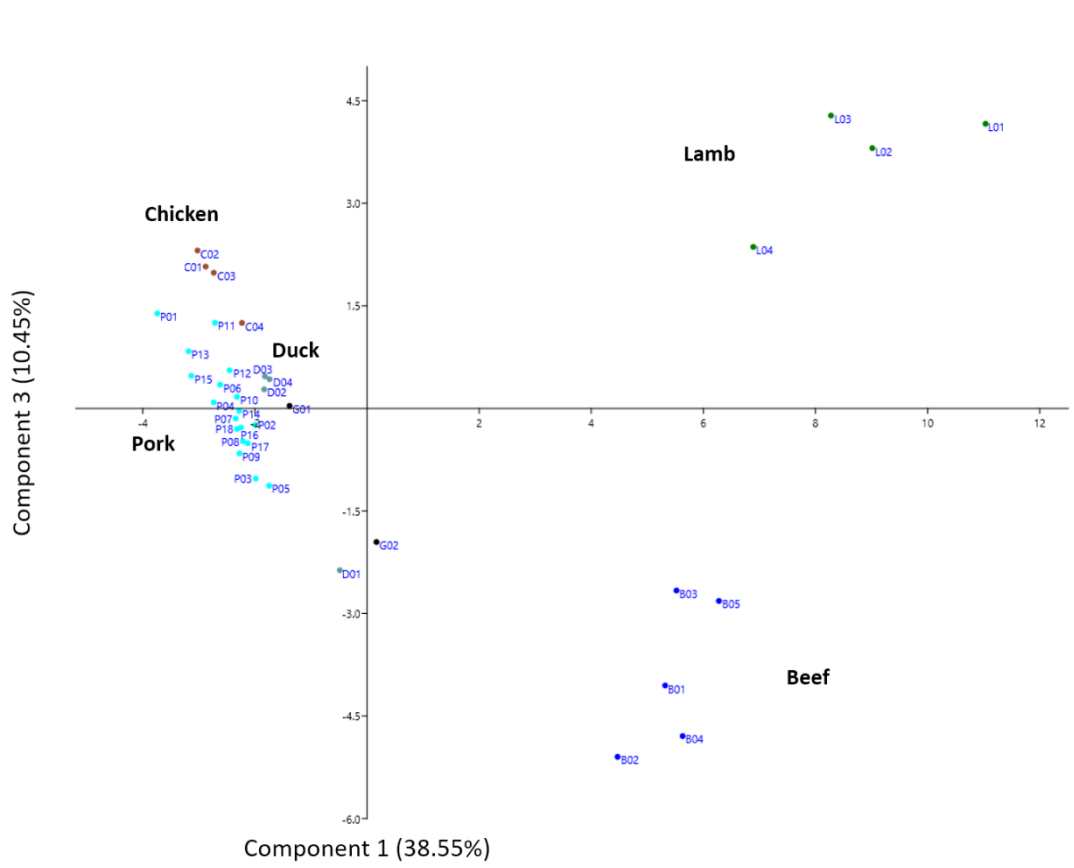

Figure 5.9: PCA plot of unscaled data for fats from products of animal origin. PC1 contribution to variance 38.6%. PC3 contribution to variance 10.4%. Samples P01-P18 are pork fat samples, B01-B05 are beef fat samples, L01 to L04 are lamb fat samples, C01-C04 are chicken fat samples, D01 to D04 are duck fat samples and G01 and G02 are goose fat samples. More details on all samples can be found in Appendix B. Scree plots and loading plots can be found in Appendix C (pages 152, 158 and 160).

The separation of the different groups of samples is more obvious in the dendrogram (Figure 5.10). All pork samples group together before connecting to any of the other groups. Lamb and beef group together, but the two subgroups contain only one type of sample, one sub-group for all lamb samples and one sub-group for all beef samples. Finally, all fowl samples group together, with the four chicken samples being closest to each other. But the duck and goose samples are not separated from each other.

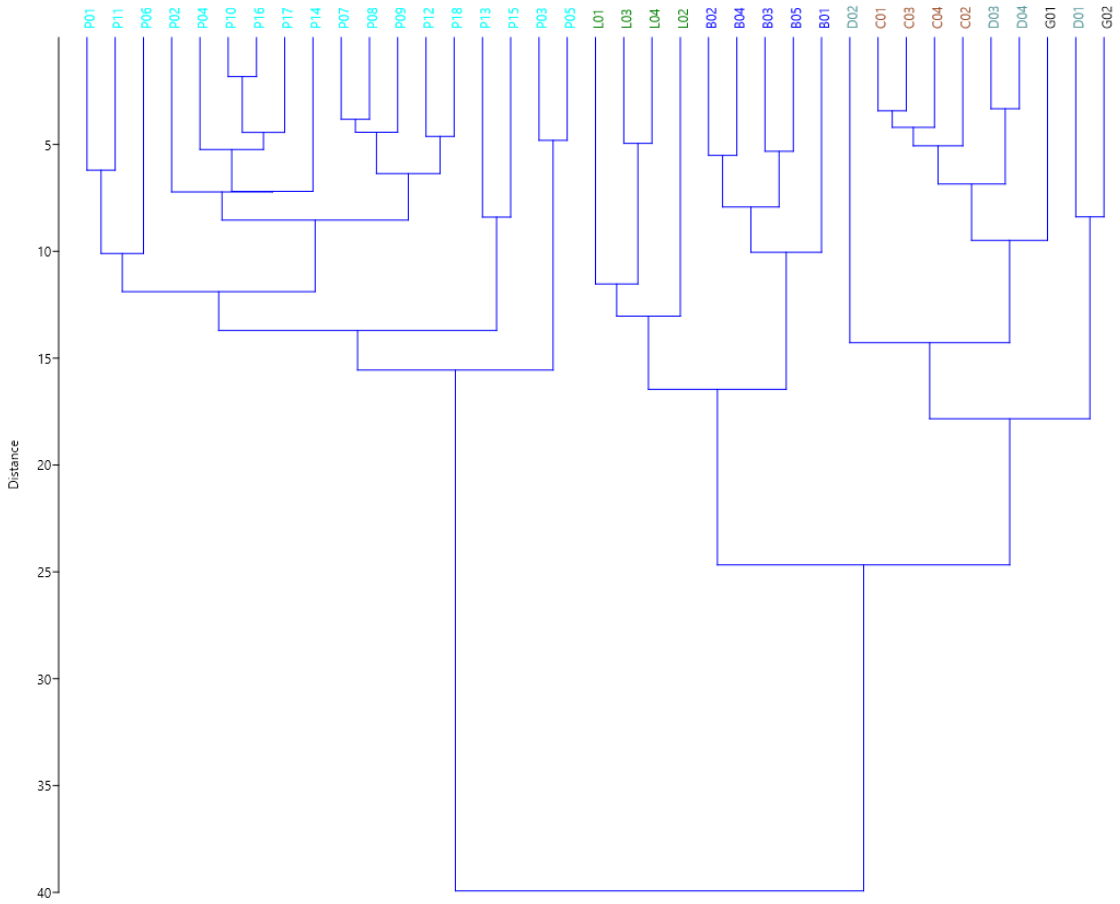

Figure 5.10: Dendrogram of fats from products of animal origin. Samples P01-P18 are pork fat samples, B01-B05 are beef fat samples, L01 to L04 are lamb fat samples, C01-C04 are chicken fat samples, D01 to D04 are duck fat samples and G01 and G02 are goose fat samples. More details on all samples can be found in Appendix B.

The pork samples came from specific anatomical positions (leg, loin, shoulder and belly; Figure 5.11), types of fat (subcutaneous and intramuscular; Figure 5.12) and from three distinct pigs (A, B and C; Figure 5.13). The pork samples were labelled with different colours according to the anatomical locations, types of fat and individual animals they were extracted from, in order to assess whether they could be separated based on those characteristics. After observing the plots (Figure 5.11Figure 5.12 and Figure 5.13) the conclusion was that there cannot be distinction between them based on the available data.

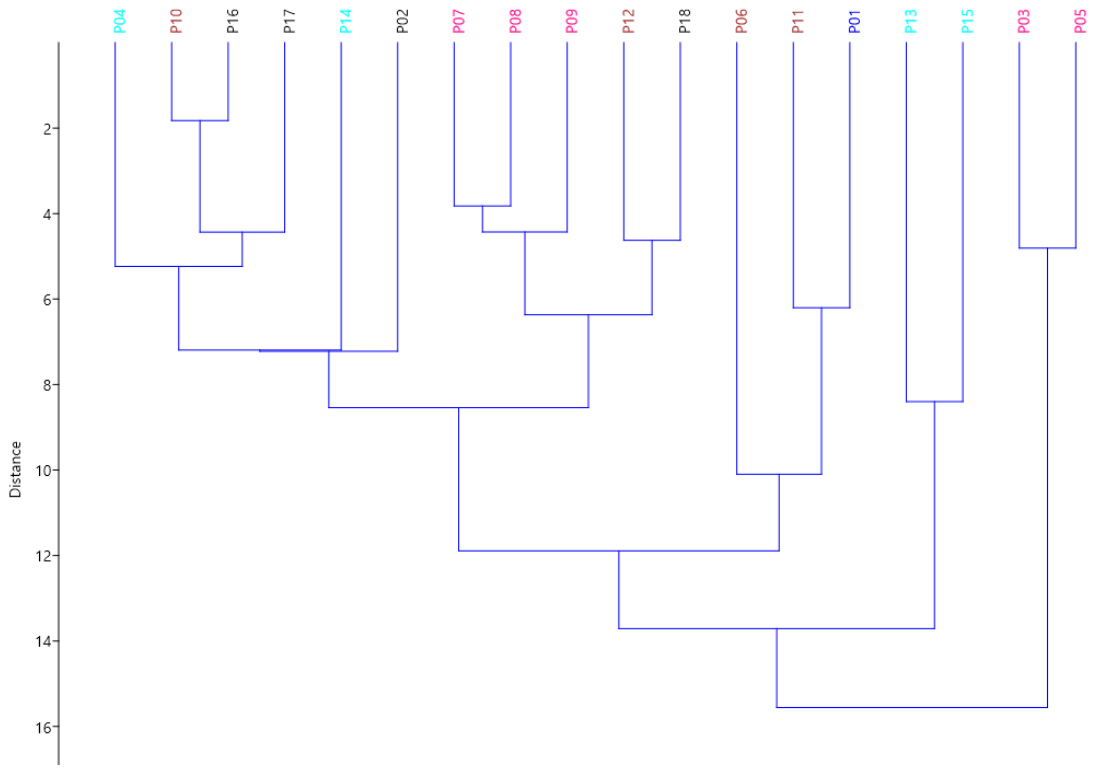

Figure 5.11: Dendrogram of pork fat samples from different anatomical positions. Pink: leg, Black: shoulder, Blue: unknown, Aqua: belly, Brown: loin

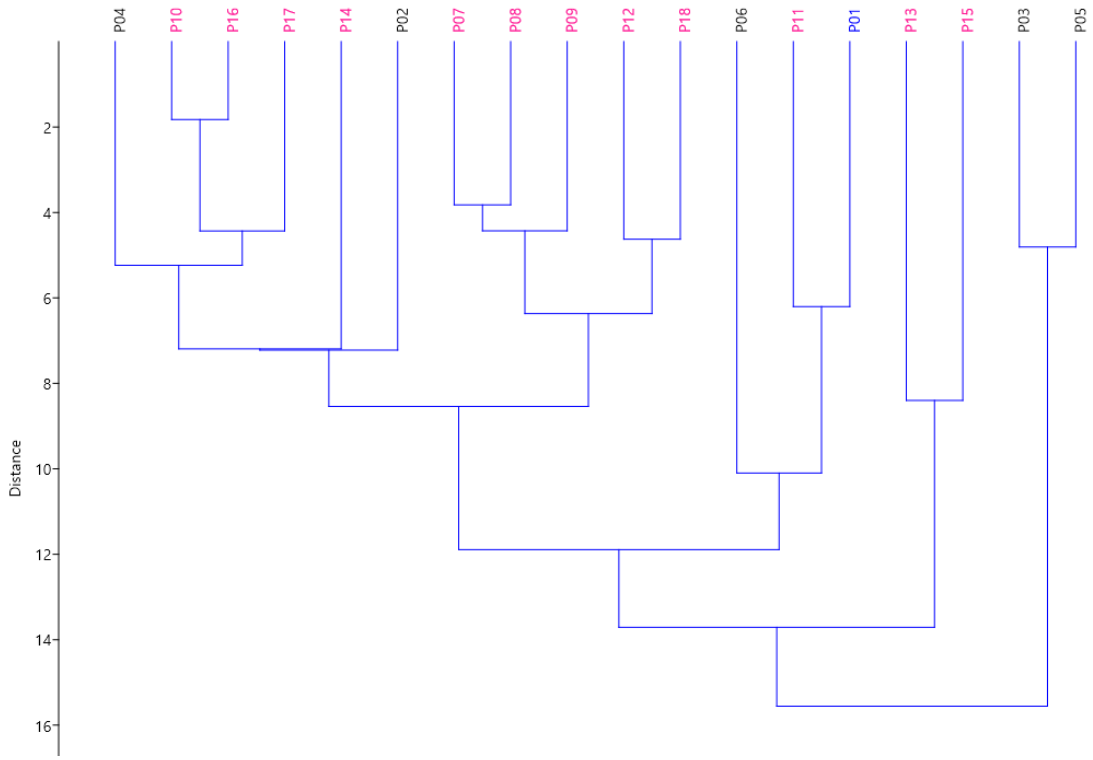

Figure 5.12: Dendrogram of pork fat samples from different types of fat. Blue: unknown, Black: subcutaneous, Pink: intramuscular

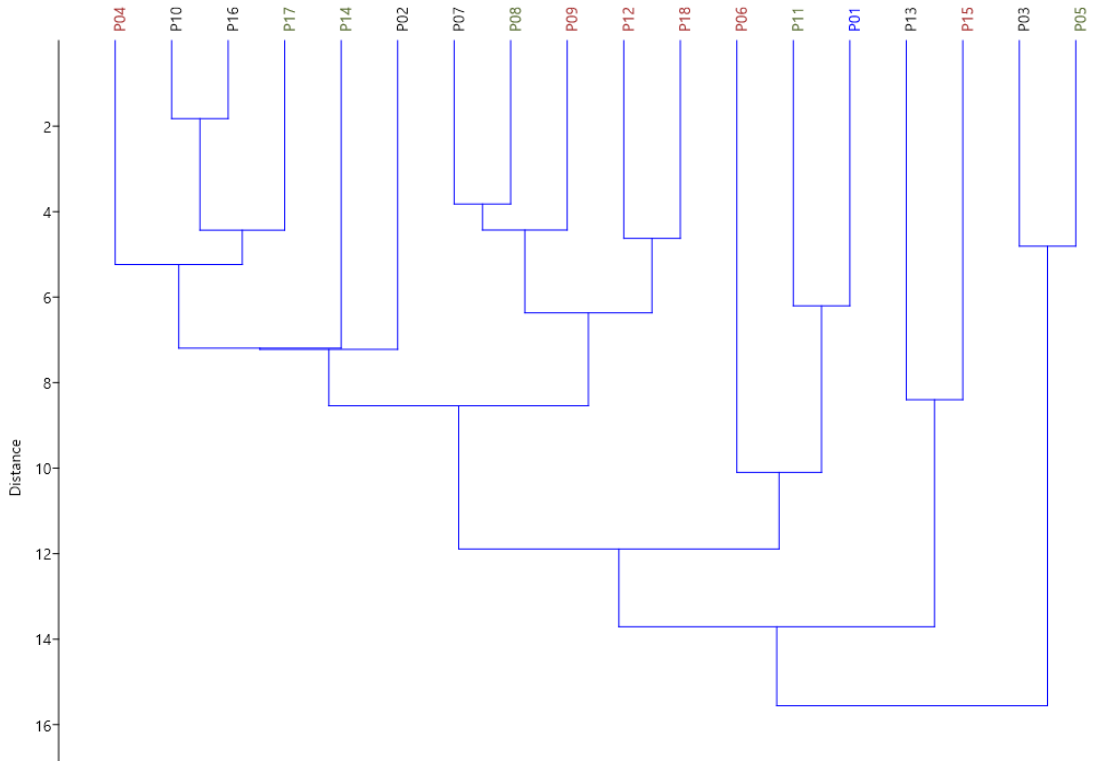

Figure 5.13: Dendrogram of pork fat samples from different pigs. Blue: unknown, Black: pig A, Green: pig B, Brown: pig C

5.2.4 PCA of vegetable oils, animal fats and milk samples

The results from both Chapter 4 and Chapter 5 can be analysed together to determine if the separation of the different types of samples is possible when having a sample whose origin cannot be narrowed down to vegetable, animal or dairy.

Data from all samples was analysed using PCA of 138 different TAGs identified and relative abundances of peaks measured. There was a wider range of variance because of the number of samples and variables, which meant that more principal components needed to be examined. PC1, PC2, PC3, PC4 and PC5 contributed to 90.84% of the variance between samples. TAGs contributing the most were OOO, LLL, LLO, LLP, OPO*, SPO*, LPO, POP*, SOP*, OOP*, OOS, OLLn, LnOO and OOL*, which range between ECN 42 and 50. The different groups of samples remain separate as well as they had been previously (Figure 5.14). Chicken samples are between rapeseed and beef sample, which correlates well with Hasan results.

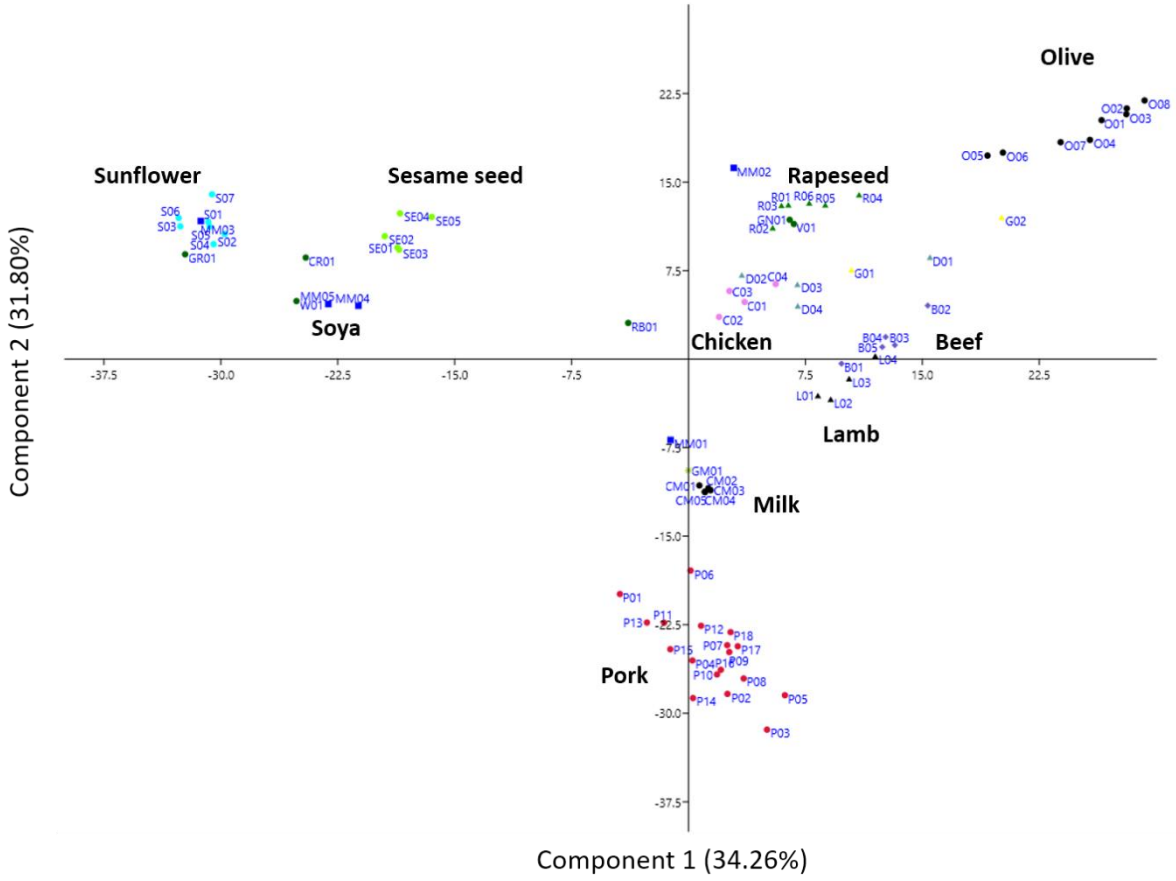

Figure 5.14: PCA plot of unscaled data for oils and fats from products of plant and animal origin including milks. PC1 contribution to variance 34.3%. PC2 contribution to variance 31.8%. Sample codes as previously. More details on all samples can be found in Appendix B. Scree plots and loading plots can be found in Appendix C (pages 152, 161, 162 and 163).

This is clearer to see in the dendrogram (Figure 5.15). Goat milk and cow milk, although closer to each other than other samples, are still grouped separately. Beef and lamb samples are still separated and the rest of the samples are in groups as they were previously.

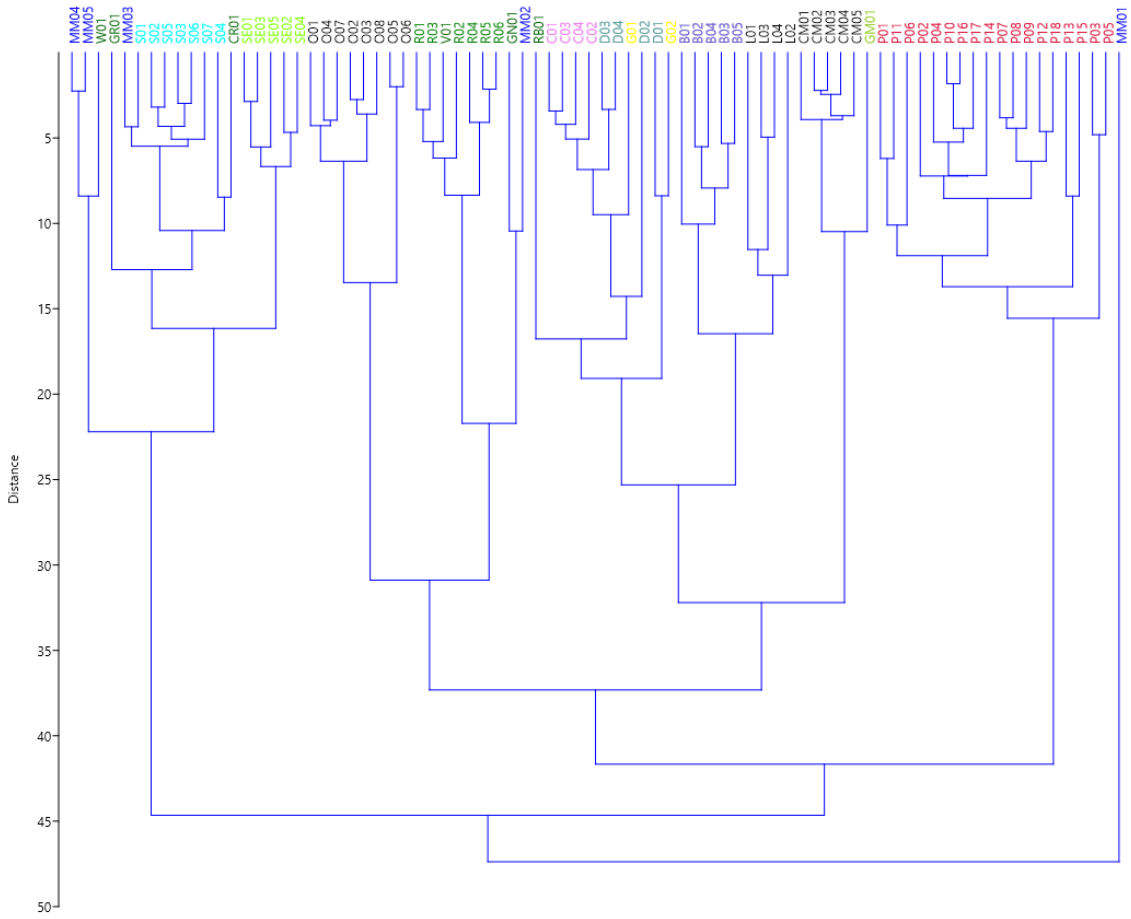

Figure 5.15: Dendogram of oils and fats from products of plant and animal origin including milks. Sample codes as previously. More details on all samples can be found in Appendix B.

5.3 Chapter conclusions/overview

The two stage method developed previously (Chapter 4) was used to identify TAGs present in a wider number and type of samples than previously, including vegetable oils and milks and animal fats. Only the second stage of the method was used for the analysis of these samples because the ECN range of the TAGs present were covered by Method ECN42-56.

Including the samples from Chapter 4, a total of 80 samples were analysed with the two stage method. A few assumptions for the future identification of samples can be derived from the identification of TAGs for each type of sample. Chromatograms of olive oil samples have really abundant peaks corresponding to TAGs OOO and OOP*, while peaks for TAGs OLLn, LnOO and OOL* are more intense for rapeseed oil chromatograms. Both sunflower and sesame seed oil chromatograms display intense peaks for TAGs LLO, LLL and LLP. Positional isomers of TAGs play an important role in the correct identification of animal fats. For example, isomer OPO* is only found in pork samples, while all the other animal fat samples examined contained the OOP* isomer. Beef samples contain the SOS* isomer exclusively while lamb samples contain both SOS* and SSO* isomers and the rest of the animal fat samples contain only SSO*. Furthermore, isomers PPO* and SPO* appear in pork and lamb samples, while isomers POP* and SOP* appear in beef, lamb and all the poultry samples analysed.

The statistical analysis of the results with PCA and dendrograms showed that samples of the same origin group together and in most cases there is clear discrimination from samples that are different taxonomically, even after adding the milk samples analysed previously in the PCA analysis. More than 86% of the variance observed in the 80 samples were attributed to 14 TAGs, OOO, LLL, LLO, LLP, OPO*, SPO*, LPO, POP*, SOP*, OOP*, OOS, OLLn, LnOO and OOL*, with ECNs between 42 and 50. This means that even milk samples could be analysed only with Method ECN42-56 and still be separated from other types of samples. The two stage approach would be very useful for full identifications of all TAGs in a sample, but for faster screening of samples of completely unknown origins, the use of Method ECN42-56 can give very accurate results in 26 min. Examining additional samples of each type of oil and fat would improve the results and the groupings of samples.

6 Application of two stage method on forensic case

6.1 Introduction

Analysis of lipids and specifically TAGs has applications in fields other than food analysis, such as archaeology and forensic science. Lipid residues in samples of archaeological and forensic context could be remains of foodstuff or other materials such as cosmetics, pharmaceuticals and other products that contained oils or animal fats, especially from previous centuries when such products could not be synthesised in labs.

In archaeological contexts, identifying the lipids present in samples and determining their origin can provide valuable information on the diet of ancient civilisations, the use of different vessels and artefacts, the culture and practices of the time. Lipid residues have been extracted from pottery, soils, human remains and other types of archaeological remains. Lipid analysis of mummified tissue has provided important insights in the process of mummification. The characteristic lipid composition of human tissue has led to the application of lipid analysis in forensics contexts, such as identifying potential grave sites or locations of decomposed bodies.

Both forensic and archaeological samples provide unique difficulties when analysing, with the most important hurdle being the degradation of lipids and TAGs which does not allow their direct comparison with modern data. The degree of degradation can depend on the age of the sample and the method of preservation (whether the sample was found buried or it was exposed to environmental conditions), but nevertheless, no sample can be perfectly preserved.

The aim of the work described in this chapter was to explore whether the methods developed could be employed in archaeological or forensic contexts.

The samples described on this chapter are from a real case and were delivered to our lab by the police for analysis. The details of the case pertinent to the analysis are as follow:

- Medical staff attending the scene of an unexplained infant death noted that the clothing was very wet.
- Police officers seized the clothing for evidence in consideration of a possible case of neglect.
- The possibility of prop-feeding causing the infant death could be supported by the identification of the liquid that soaked the clothing as infant milk of the brand found at the scene.

6.2 Results and discussion

6.2.1 Forensic case, baby gro experiment

Wet infant clothing was stored frozen from the time of seizure by the police until it was sampled for analysis. Six samples of cloth (*c.* 4 x 4 cm) were cut from six different positions on the garment (Figure 6.1). An empty feed bottle containing some residues was also found close to the infant and a powder infant milk formula, Cow & Gate infant milk 1, was found in the house. The same brand of infant milk was used for producing experimental samples of similar nature to the forensic samples. The infant milk was poured over two different infant garments and one sample of cloth was taken from each of them.

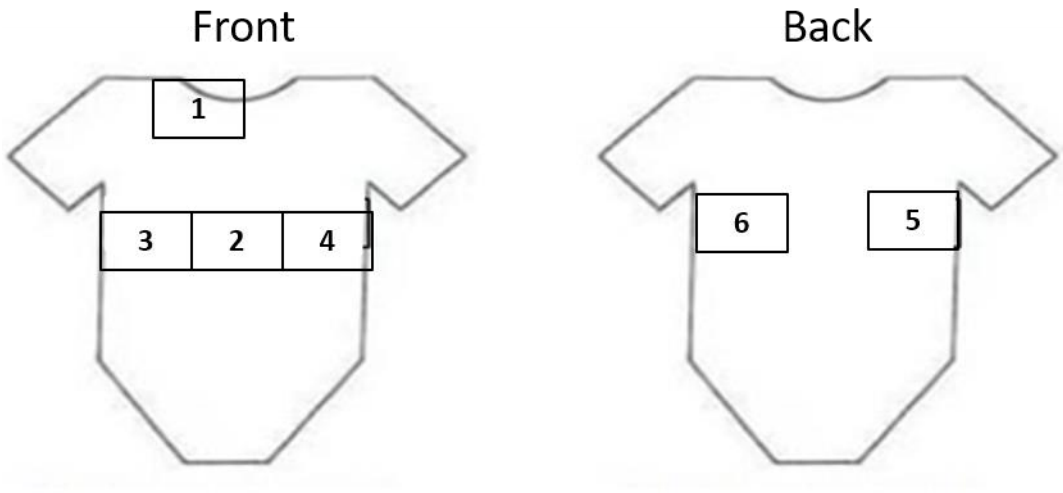

Figure 6.1: Sampling positions for forensic samples IM01 to IM06.

The cloth samples were each weighed prior to extraction by submerging in solvent (DCM: MeOH, 2:1 v/v, *c.* 100 mL) for 24 h. The extract was filtered through cellulose filtered paper into labelled vials (Table 6.1). Hexane (5 mL) was used to dissolve each extract and the solution was washed with of H_2O (4 mL). The organic phase was collected, filtered through DCM washed cotton wool and the solvent was removed under N_2 flow.

Table 6.1: Weight of sample extracted from each sampling position that was consequently dissolved in appropriate organic solvent for analysis.

Sample	Extract /mg
IM01	115.02
IM02	30.80
IM03	9.97
IM04	8.67
IM05	13.62
IM06	11.53
IM07	25.60
IM08	25.60

The two stage RP-UHPLC/MS method developed previously (Chapter 4) was used to analyse the six samples taken from the infant clothing (IM01-IM06), two samples from infant clothing soaked in infant milk in the lab (IM07-IM08) and two samples of commercial infant milk, one of the brand found in the house (IM09) and one other brand (IM10) (more details on samples found in Appendix B).

For comparison of the forensic samples, the experimental samples and the two samples of two different infant formula brands, only chromatograms of samples IM01 (forensic sample), IM07 (experimental sample), IM09 (sample from same brand infant formula as the one found in the house with the forensic samples) and IM10 (sample from another infant formula brand) are presented in Figure 6.2 and Figure 6.3. There are some differences in the samples, especially in the regions for ECN 34, 40, 44 and 46.

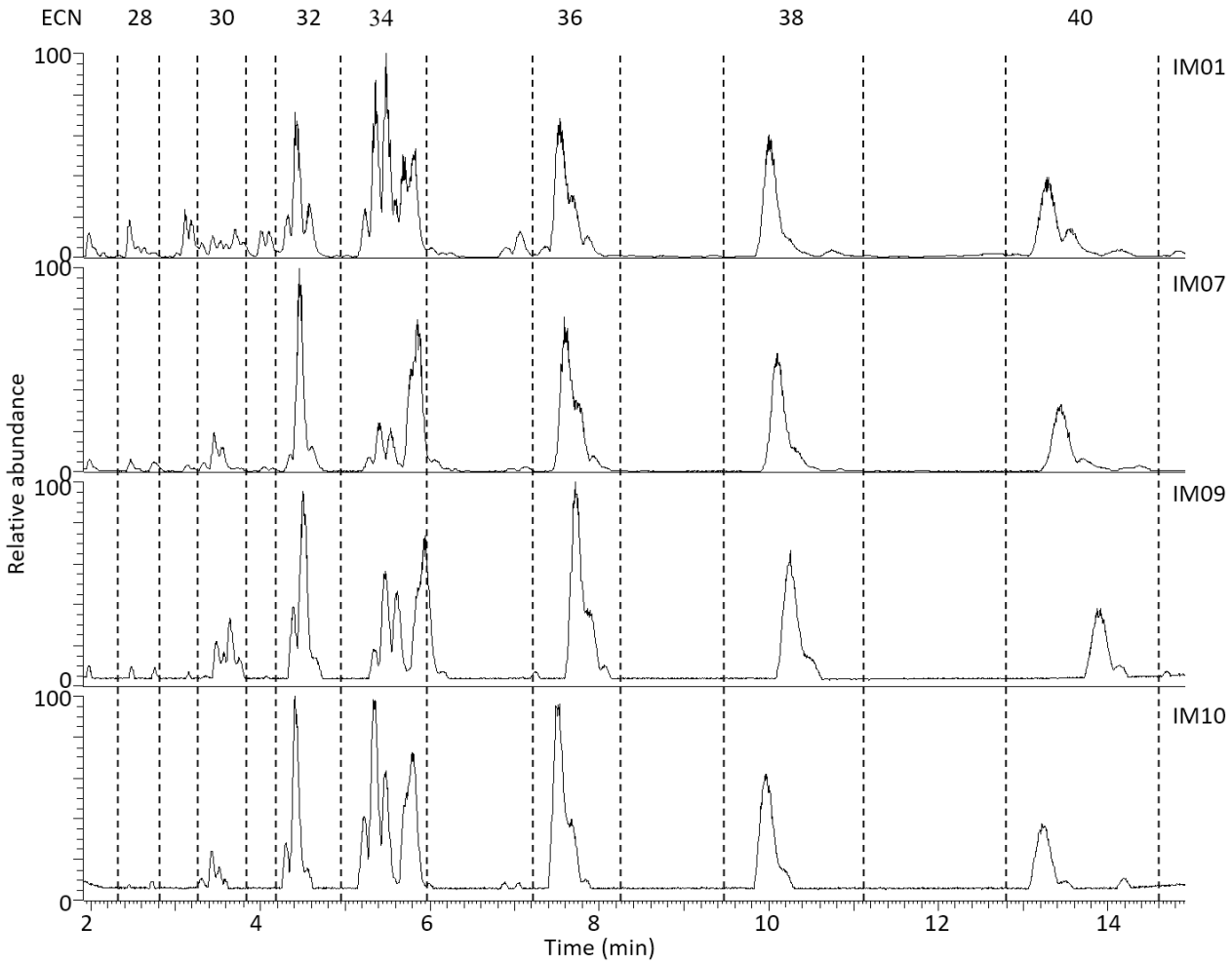

Figure 6.2: Partial RP UHPLC-APCI MS base peak chromatograms of infant milk samples analysed with Method ECN28-40 (Table 4.5). IM01 is the forensic sample from sampling point 1, IM07 is the experimental sample created in the lab, IM09 and IM10 are two commercial brands of infant milk. Regions are assigned according to ECN.

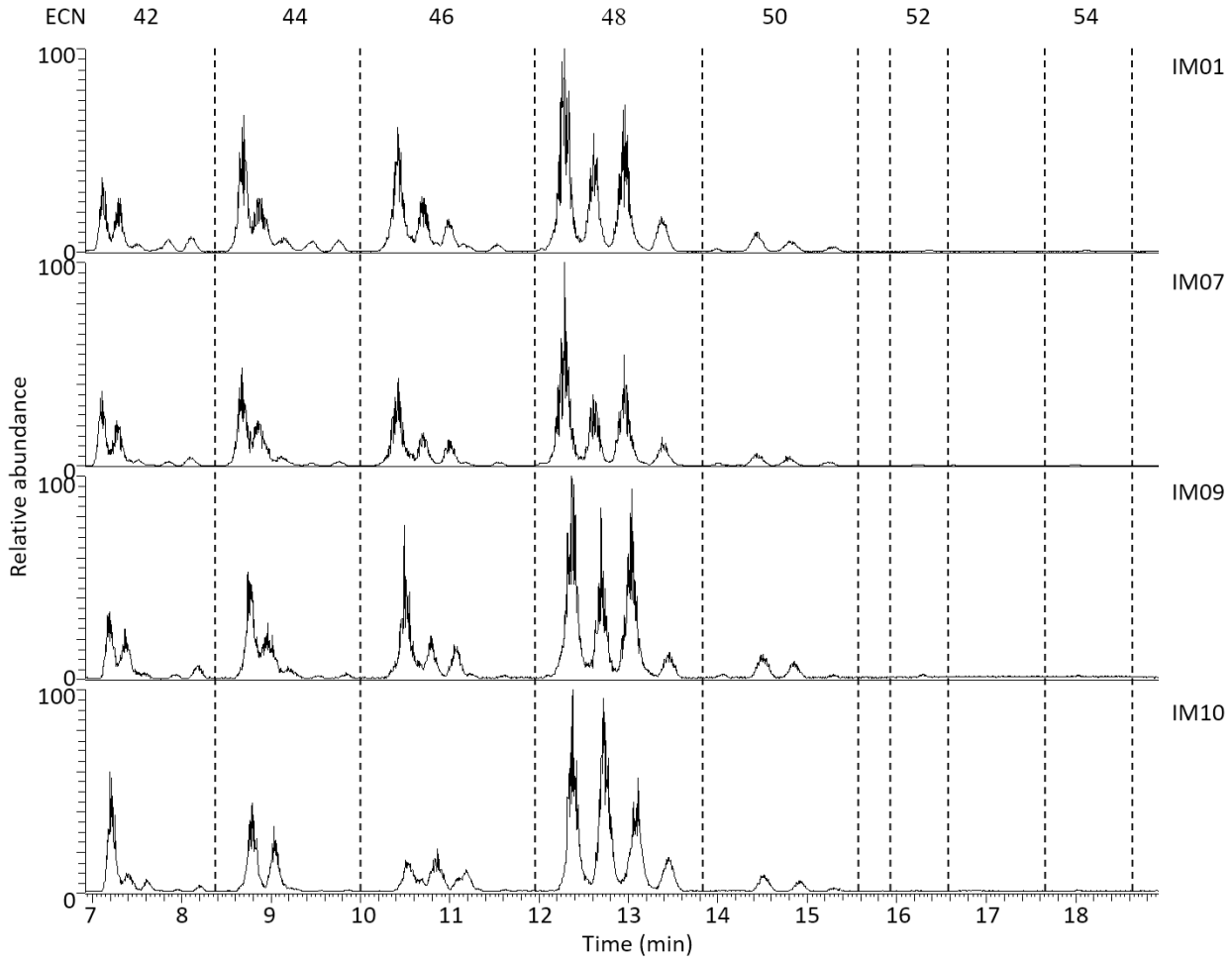

Figure 6.3: Partial RP UHPLC-APCI MS base peak chromatograms of infant milk samples samples analysed with Method ECN42-56 (Table 4.4). IM01 is the forensic sample from sampling point 1, IM07 is the experimental sample created in the lab, IM09 and IM10 are two commercial brands of infant milk. Regions are assigned according to ECN.

40 different TAGs with a relative abundance higher than 0.1% were identified for samples IM01 to IM10 (Table 6.2). Samples IM09 and IM10 are freshly extracted samples, so no degradation is expected, and the extraction was done according to the method described in section 2.2.1. The two samples are infant formula milks from two different brands. Most of the TAGs are present in both samples, except for POP*, PPO* and PLP*. The isomer POP* is present in sample IM09 while the isomer PPO* is present in sample IM10. Additionally, PLP* is present in IM10 but not in IM09. Samples IM07 and IM08 were the experimental samples extracted from cloth soaked in infant formula milk of the same brand as IM09. Both these samples contain all the TAGs identified in IM09, including isomer POP*, and the sample doesn't appear degraded. They do not contain PPO* or PLP* which were found in sample IM10.

Table 6.2: TAGs identified in infant milk samples in base peakchromatographs Methods ECN26-40 (Table 4.5, Figure 4.14) and ECN42-56 (Table 4.4, Figure 4.13). The TAGs are listed in retention time order. The relative abundance of peaks corresponding to TAGs identified was used as a second component for the identification of samples. Only TAGs corresponding to peaks with relative abundances higher than 0.1 are listed.

TAGs	IM01	IM02	IM03	IM04	IM05	IM06	IM07	IM08	IM09	IM10
CCLa							0.27	0.18	0.14	
CaLaC	0.3	0.1			0.19		0.69	0.96	0.51	0.3
$LaLaC_6$	0.13				0.13		0.44	0.59	0.27	0.14
LaLaC	3.27				1.5		4.64	5.33	3.65	2.32
$MLaC_6$							0.17	0.22	0.43	0.19
LaLaCa							2.22	1.53	1.24	0.84
CLaM	2.54	0.87	0.08		1.51		4.03	5.34	2.7	2.01
LaLaLa	3.46	1.96	1.8	0.71	3.13	0.7	5.75	7.1	4.84	3.78
PLaC	0.51	0.79	0.42		1.14		2.07	1.83	1.57	0.62
OLaC	0.3	0.17	0.1		0.18		0.2	0.22	0.12	0.05
LaLaM	3.91	1.9	1.72	0.72	2.38	0.88	4.21	4.92	2.98	2.09
SCaC							0.1	0.12	0.16	0.08
LaLaL	0.23	0.22	0.06							
MMLa	2.6	1.52	1.21	0.51	1.91	0.85	2.5	2.85	2.33	1.49
OLaLa	0.57	0.43	0.39	0.93	0.32		0.22	0.22	0.18	0.09
PMLa	0.94	0.88	0.51	0.84	1.56		0.89	0.96	0.89	0.52
LLL	2.93	3.56	1.78	0.93	3.71	1.19	5.48	4.99	3.39	7.38
OLLn	2.2	2.48	1.44	0.77	2.42	0.71	3.72	3.16	2.17	1.1
PLLn*	0.28	0.53	0.5	0.11	0.22	0.28	0.25	0.26	0.22	0.89
OLaM	0.83	0.87	0.46	0.36	0.75		0.38	0.38	0.25	0.18
LLO	5.6	5.22	3.55	2.46	4.77	1.35	6.56	6.31	5.54	6.43
LLP	0.67	0.87	0.45	0.32	0.5	0.49	0.63	0.57	0.96	4.15
OOLa			0.74	0.26						
OPLa	0.71	0.71	0.49	0.32	0.8					
OLO*	5.64	5.12	3.61	2.85	5.05	1.03	6.5	5.99	6.29	3.35
LPO	2.78	2.61	1.83	0.97	2.17	0.46	2.75	2.61	2.33	3.12
PLP*										0.88
PPL*	1.66	1.8	1.33	0.61	1.89	0.44	2.4	2.53	2.34	1.56
POM*	0.28	0.29	0.39	0.96	1	1.77	0.12	0.1	0.15	0.09
OOO	10.1	10.86	7.69	6.32	11.61	5.49	13.52	14.48	11.12	14.31
OOP*	5.42	5.83	4.62	4.06	6.42	3.16	5.92	6.14	7.03	16.03
POP*	7.31	8.55	5.61	5.03	8.85	3.27	8.31	8.36	10.77	
PPO*										8.77
PPP	2.37	2.62	2.36	2.64	3.89	3.08	2.26	1.34	1.95	3.69
OOG	0.17	0.14			0.26		0.28	0.27	0.29	
OOS	1.36	1.37	1.1	0.47	1.74	0.61	1.24	1.23	2.09	1.86
SOP*	0.75	0.92	0.53		1.09	0.44	0.93	0.84	1.17	1.2
PPS	0.33	0.38	0.17	0.1	0.56	0.5	0.39	0.19	0.19	0.38
OOC_{20}	0.12	0.16					0.21	0.2	0.21	0.07
OOC_{22}	0.1	0.14			0.15		0.18	0.17	0.13	0.12

Samples IM01 to IM06 contain some of the TAGs present in the other samples and some TAGs not found in the other samples. The three most abundant TAGs in sample IM09 are OOO, POP* and OOP* and the three most abundant TAGs in sample IM10 are OOO, PPO* and OOP*. All of the forensic samples (IM01 to IM06) contain significant amounts of OOO, POP* and OOP*. Furthermore, sample IM10 contains PLP* and none of the forensic samples contain this TAG. The analysis up to this point reinforces the hypothesis that the liquid on the clothing was infant formula milk and possibly of the brand found in the house.

6.2.2 PCA of samples

The forensic samples were found to have great similarity with each other and the samples prepared in lab (IM07 and IM08), and to be distinctly different to cow and goat milk (CM01-CM05 and GM01) and also from the other brand of infant milk (IM10) (Figure 6.4). 102 different TAGs were used for this analysis and PC1, PC2 and PC3 contributed to 94.94% of the variance between samples. The TAGs contributing the most to the variance are PPC_4, OOO, PMC_4, OLO, LLO, OOP, PPO, POP, LLL, LaLaC, LaLaLa and CLaM, with ECNs ranging between 32 and 48. The variance across PC1 separates cow and goat milk from the forensic and infant milks and the TAGs that contribute the most to that are PPC_4 and PMC_4 that are elevated for cow and goat milk and OOO which is elevated for infant milks. The infant milks are separated across the PC2 axis, with IM10 having much higher responses for TAGs OOP and PPO*, while the rest of the samples group around IM09 with higher POP* responses.

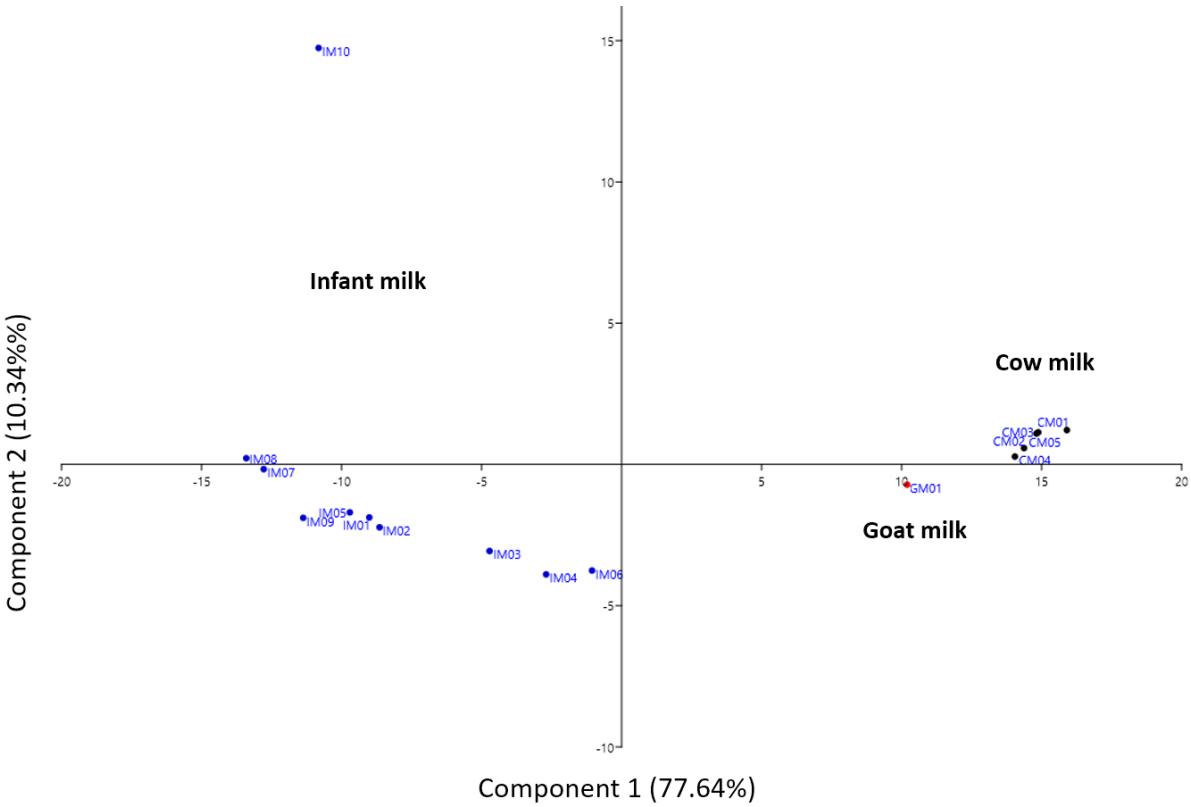

Figure 6.4: PCA plot of unscaled data for milks and infant milks. PC1 contribution to variance 77.6%. PC2 contribution to variance 10.3%. More details on all samples can be found in Appendix B.

These conclusions are confirmed by the dendrogram (Figure 6.5). Sample IM10 is the furthest from all the infant milk samples. Similarly, goat milk is still in a different group from the cow milk samples. It is also interesting how the two samples extracted from cloth in the lab group together (IM07 and IM08) while the sample extracted from bottled infant milk clusters closer to forensic samples (IM01, IM02 and IM05), which are also the samples that had the highest mass extracted.

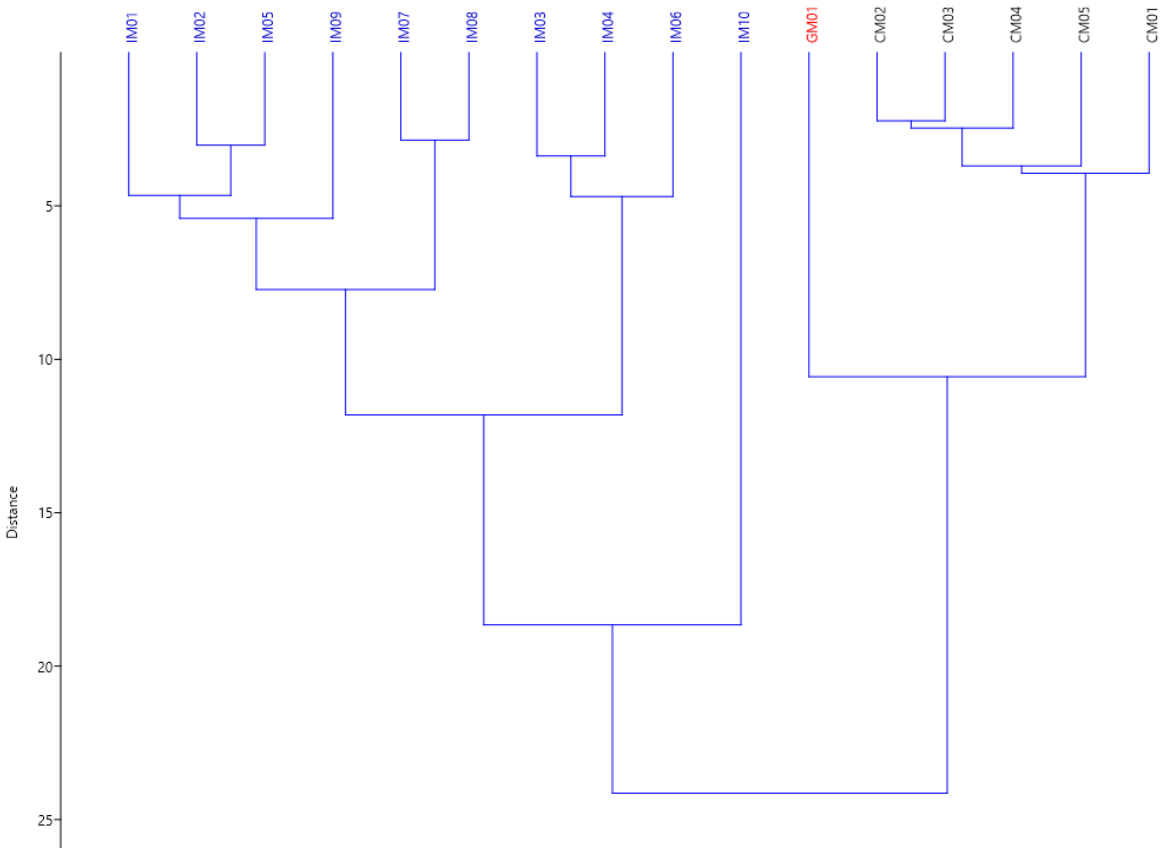

Figure 6.5: Dendogram of milk and infant milk samples.

6.2.3 PCA of results from all chapters

149 different TAGs were used for the PCA of all the samples from the different chapters. Principal components 1 to 6 contributed to 91.70% of the variance between the samples. The TAGs responsible for the variance are: CLaM, LaLaC, LaLaCa, LaLaLa, LaLaM, LLL, LLO, LLP, LnOO, LnOP, LPO, OLLn, OLO, OOL, OOO, OOP, OOS, OPO, PMC_4, POP, PPC_4, PPL, PPM, PPO, PPP, SMP, SOP, SOS and SPO, with ECNs ranging between 32 and 52. Separation could be achieved using only these 29 TAGs. The groups identified in previous chapters are still present and separated when all samples are analysed together (Figure 6.6).

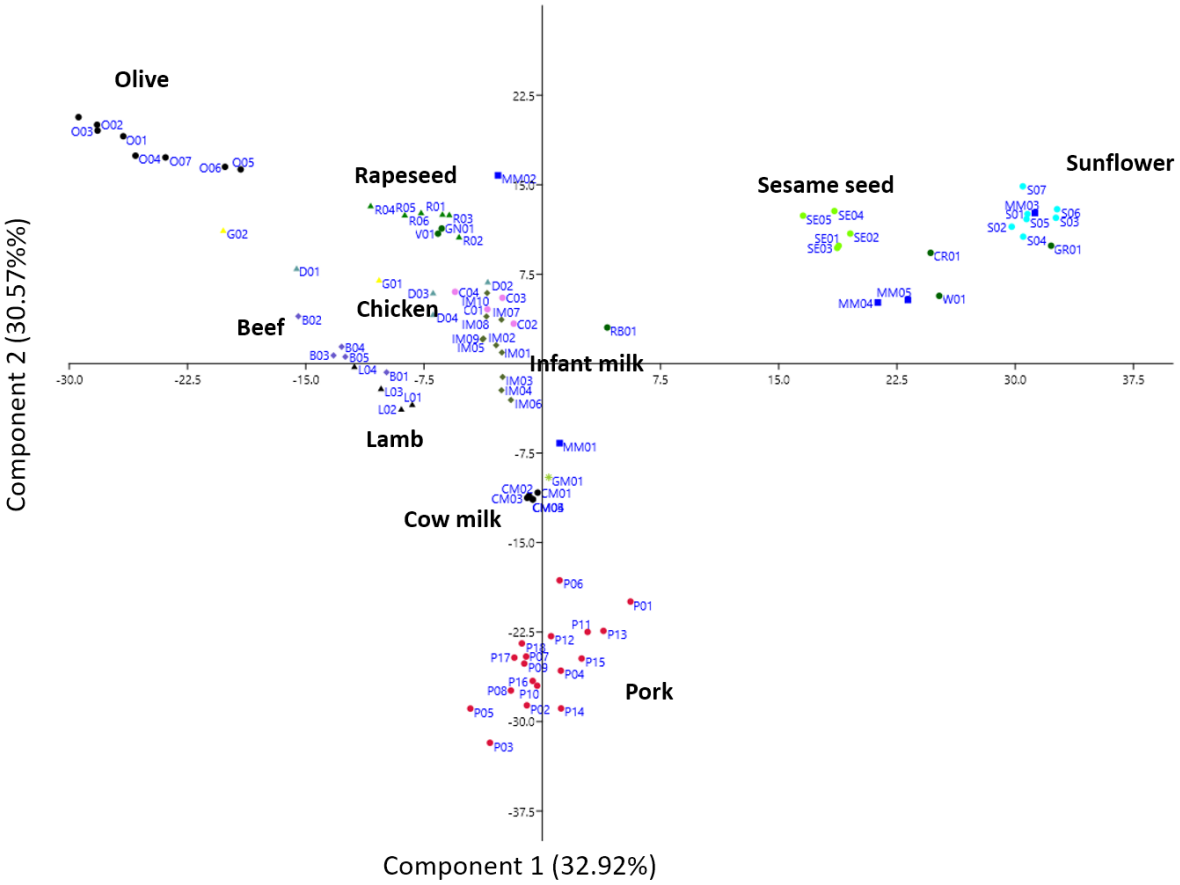

Figure 6.6: PCA plot of unscaled data for oils and fats from products of plant and animal origin including milks and infant milks. PC1 contribution to variance 32.9%. PC2 contribution to variance 30.6%. Sample codes as previously. More details on all samples can be found in Appendix B. Scree plots and loading plots can be found in Appendix C (pages 153, 164, 165, 166 and 167).

The dendrogram presents the similarities between samples by grouping them together (Figure 6.7). Samples are grouped together according to type, with the exception of the single oil samples that group with other types. All the forensic and infant formula samples are in the same group, with sample IM10 having the largest distance from the other samples, indicating it is the most different in the group. The similarities between the forensic and infant formula samples and the clear distinction between them and all the other samples analysed in this work indicates that the liquid absorbed in the baby clothes was infant formula milk.

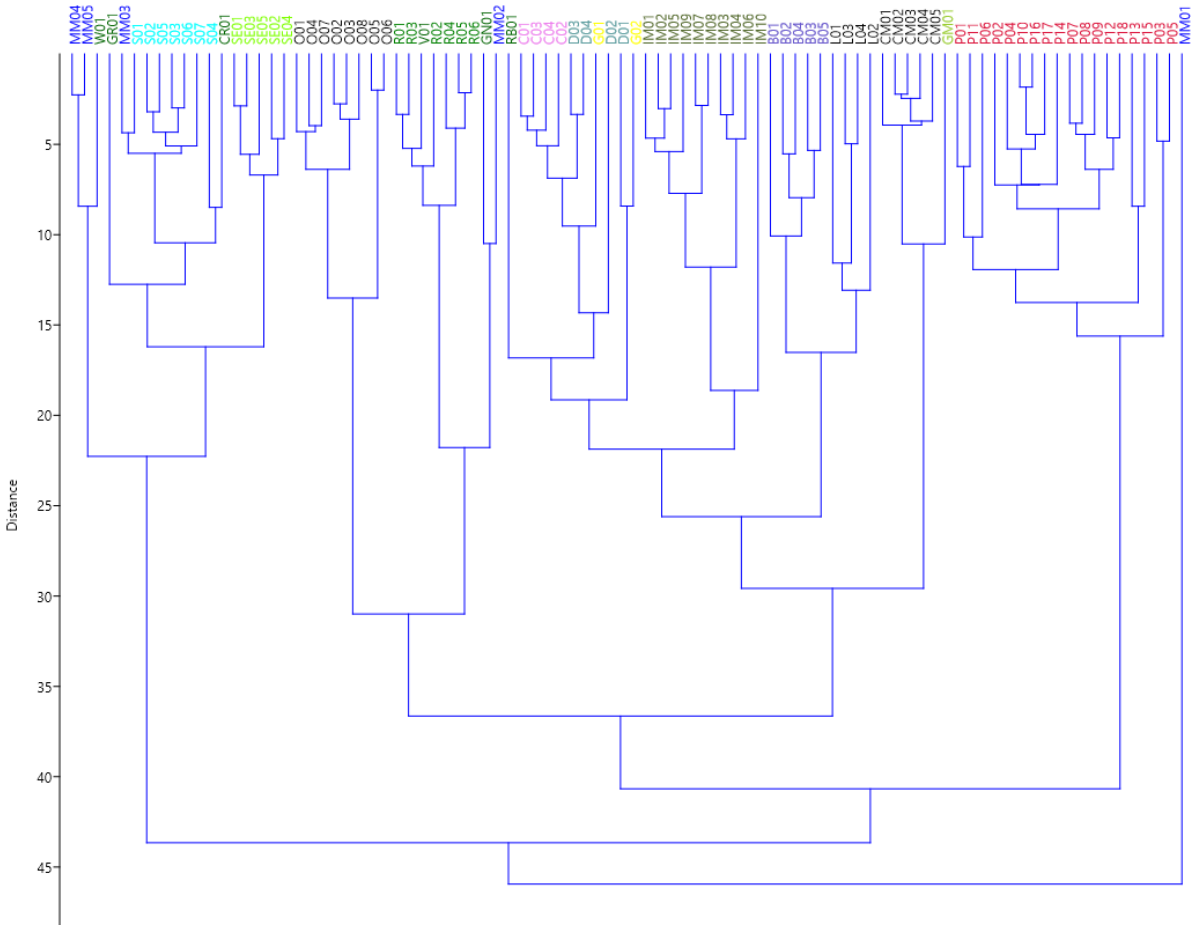

Figure 6.7: Dendogram of samples of oils and fats from products of plant and animal origin including milks and infant milks. More details on all samples can be found in Appendix B.

6.3 Chapter conclusions/overview

From the samples available in this work, the forensic samples collected by the police and sent to our lab for analysis, have the most similarities to infant milk formula samples, especially to one of the two brands analysed. This approach can at the moment only give indications on the origin of forensic samples, because of the limited pool of samples analysed here. In the case of infant formula, analysis of samples from other brands, with multiple samples for each brand, would help increase the confidence in identifying the forensic sample.

This work has shown that samples of different origin, plant or animal, extracted with different methods, from food material or from clothing, can be analysed with the method developed and produce comparable data that can be used to group similar samples together. Higher numbers and more types of samples are needed to be able to apply this method in more contexts with higher confidence.

Furthermore, the PCA analysis has shown that this level of separation can be achieved without complete identification of all TAGs present in a sample, something that is time and cost consuming in many cases, especially for more complicated samples, such as milk. This work has shown that identifying key TAGs and their relative abundancies in a sample can be sufficient to correctly identify the origin of the sample in terms of type of plant or animal the oil or fat came from.

7 Conclusions and further work

The aim of this work was to develop a TAG separation and identification method that could be applied to a wide range of samples, provide enough information for identification and have potential for application in forensic or archaeological contexts, while also minimising the run time of the method.

7.1 Conclusions

A rapid UHPLC method for the analysis of milk samples was initially developed (Method S, Table 3.11). Milk was selected because of its complexity as a matrix and the large number of TAGs present. The method did not achieve complete separation of all components. Nevertheless, a significant number of TAGs were identified, comparable to similar studies. The advantages of this method lie in the short run time of 25 min, a sixth of the run time of the Beccaria *et al.* method (2014), and the separation and identification of positional isomers, something that has not previously been reported for milk samples.

A multi-stage method approach was implemented in an effort to overcome the limitations of the UHPLC Method S in separating and identifying all components. An off-line two dimensional method was considered too time-consuming, with potential for introducing errors during multiple stages of preparation for the samples. Using the same UHPLC column for both stages allowed the use of the same sample with no need for changing sample solvent or preparing two different extracts. All the TAGs contained in the sample were introduced in both stages of the method, but the selection of solvent system, temperature and flow rate resulted in the two stages focusing in different ECN ranges. So there was one method used for better separation and identification of TAGs with ECNs between 26 and 40 (Method ECN26-40, Table 4.5) and a second one for the separation and identification of TAGs with ECNs between 42 and 56 (Method ECN42-56, Table 4.4). The two methods have run times of 21 and 25 minutes respectively, so even though there is no additional sample preparation needed the overall run time is increased. Statistical analysis, PCA and dendrograms, were used on 6 milk samples, 5 cow milk and 1 goat milk, to determine whether the method could successfully discriminate between the two types of samples. Even though this was a small number of samples, the results were positive enough to warrant further study. An interesting outcome of the statistical analysis was that most of the variance between the milk samples was due to 13 TAGs, 10 of which had ECNs between 40 and 48, indicating that only using the second stage of the method could be sufficient to identify sample type. The number of samples was too small to make this assumption, so further analysis of more samples was needed.

Partially degraded forensic samples were also analysed and identified with a significant degree of confidence.

7.2 Further work

The scope for future work based on this method is great and a number of issues could be addressed to improve it.

a) More samples of the types already examined in this study need to be analysed along with samples from other species that were not part of this study. It would also be interesting to include other dairy products such as different types of cheese, butter, yogurt etc. This would improve the quality of the results of the PCA analysis and potentially allow unsupervised analysis of unknown samples and their correct identification.
b) Degraded samples from forensic and archaeological contexts need to be examined further. This method provides both detailed identification and also high- throughput time that can benefit studies in those areas.
c) Cooked samples of oils and fats can be analysed with this method both for food safety and identification studies, but also for studies into the degradation and transformations of TAGs during cooking.
d) Samples of human breast milk and other commercial types of infant milks can be examined with this method to give a better understanding on the unique composition of breast milk and how better to reproduce it for replacement milks.

Appendix A

UHPLC method name in lab book	UHPLC method name in thesis
R60(2)_3	A
T4	B
T5	C
T8	D
T10	E
T11	F
T12	G
T13	H
T13a	I
T14	J
T14c	K
T16	L
T19	M
T20	N
T21	O
T28	P
T30	Q
T36	R
T36a	R_a
T36b	R_b
T36c	R_c
T42	S
UPLC TAG ECN 48_A	ECN48_A
UPLC TAG ECN 48_A2	ECN48_B
UPLC TAG ECN 48_H	ECN48_C
UPLC TAG ECN 48_J	ECN48_D
UPLC TAG ECN 42-46_A	ECN44_A
UPLC TAG ECN 42-46_E	ECN44_B
UPLC TAG ECN 42-46_I	ECN44_C
UPLC TAG ECN 42-46_M	ECN42_A
UPLC TAG ECN 48_N	ECN46_A
UPLC TAG ECN 48_L	ECN46_B
Aa35	Fraction Collection
Half_T36b_2	ECN42-56_A
ECN42-56_D2	ECN42-56
ECN26-40_a	ECN26-40_A
ECN26-40_b	ECN26-40_B
ECN26-40_c	ECN26-40

Appendix B

No	PCA name	File name	Type	Fat type	Brand (if available)
1	CR01	Pure corn oil	Corn	vegetable	
2	GN01	Groundnut oil	Groundnut	vegetable	
3	GR01	Grapeseed oil	Grapeseed	vegetable	
4	MM01	Coconut milk	Coconut	vegetable	
5	MM02	Almond milk	Almond	vegetable	
6	MM03	Rice milk	Rice bran	vegetable	
7	MM04	Soya milk	Soya	vegetable	
8	MM05	Wholebean soya milk	Soya	vegetable	
9	O01	Vegoil2	Olive	vegetable	Tesco
10	O02	Vegoil6	Olive	vegetable	Napolina, extra virgin
11	O03	Vegoil8	Olive	vegetable	Tesco, extra virgin, blend
12	O04	Vegoil12	Olive	vegetable	Bella Ricetta, extra virgin
13	O05	Vegoil13	Olive	vegetable	Thasos, Greece, extra virgin
14	O06	Vegoil15	Olive	vegetable	Sicily, Italy
15	O07	Vegoil20	Olive	vegetable	Waitrose
16	O08	Olive oil	Olive	vegetable	
17	R01	Vegoil4	Rapeseed	vegetable	Pura Refined
18	R02	Vegoil7	Rapeseed	vegetable	Yorkshire original Yors, extra virgin, cold pressed
19	R03	Vegoil19	Rapeseed	vegetable	Crisp 'n Dry
20	R04	Vegoil23	Rapeseed	vegetable	McHughs, extra virgin
21	R05	Vegoil24	Rapeseed	vegetable	Tesco Finest, cold pressed
22	R06	Rapeseed oil	Rapeseed	vegetable	
23	RB01	Rice bran oil	Rice bran	vegetable	
24	S01	Vegoil1	Sunflower	vegetable	Flora, pure, with Vitamin E
25	S02	Vegoil5	Sunflower	vegetable	Morrisons
26	S03	Vegoil10	Sunflower	vegetable	Tesco, pure
27	S04	Vegoil11	Sunflower	vegetable	Flora, pure, with Vitamin E
28	S05	Vegoil14	Sunflower	vegetable	Tesco
29	S06	Vegoil18	Sunflower	vegetable	Sainsburys
30	S07	Sunflower oil	Sunflower	vegetable	
31	SE01	Vegoil9	Sesame	vegetable	Lee Kum Kee, pure
32	SE02	Vegoil21	Sesame	vegetable	Blue Dragon
33	SE03	Vegoil3	Toasted sesame	vegetable	Morrisons
34	SE04	Vegoil22	Toasted sesame	vegetable	Tesco
35	SE05	Toasted Sesame seed oil	Toasted sesame	vegetable	
36	V01	Vegoil17	Mix blend	vegetable	
37	W01	Walnut oil	Walnut	vegetable	

No	PCA name	File name	Type	Fat type	Brand (if available)
38	CM01	CM1	Cow milk	Milk	
39	CM02	CM2	Cow milk	Milk	
40	CM03	CM3	Cow milk	Milk	
41	CM04	Skimmed	Cow milk	Milk	
42	CM05	Semi	Cow milk	Milk	
43	GM01	Goat milk	Goat milk	Milk	
44	IM01	A048317.1	Forensic	Milk	
45	IM02	A048317.2	Forensic	Milk	
46	IM03	A048317.3	Forensic	Milk	
47	IM04	A048317.4	Forensic	Milk	
48	IM05	A048317.5	Forensic	Milk	
49	IM06	A048317.6	Forensic	Milk	
50	IM07	Sample 1	Infant milk	Milk	Cow & Gate, on baby gro
51	IM08	Sample 2	Infant milk	Milk	Cow & Gate, on baby gro
52	IM09	CowGate	Infant milk	Milk	Cow & Gate, ready to drink
53	IM10	SMA	Infant milk	Milk	SMA, ready to drink
54	B01	Beef	Beef	animal	
55	B02	Beef rump	Beef	animal	
56	B03	Meat1	Beef	animal	Butcher
57	B04	Meat2	Beef	animal	Butcher
58	B05	Meat5	Beef	animal	
59	C01	Chicken	Chicken	animal	
60	C02	Chicken 305	Chicken	animal	
61	C03	Chicken thighs A	Chicken	animal	
62	C04	Chicken thighs B	Chicken	animal	
63	D01	Duck	Duck	animal	
64	D02	Duckleg A	Duck	animal	
65	D03	Duckleg B	Duck	animal	
66	D04	Duckleg C	Duck	animal	
67	G01	Goose fat	Goose	animal	Morrisons The Best
68	G02	Goose fat BJK	Goose	animal	
69	L01	LambA	Lamb	animal	
70	L02	Meat3	Lamb	animal	Butcher
71	L03	Meat4	Lamb	animal	Butcher
72	L04	Meat6	Lamb	animal	
73	P01	Pork	Pork	animal	
74	P02	A shoulder S	Pork	animal	Subcutaneous
75	P03	A leg S	Pork	animal	Subcutaneous
76	P04	C belly S	Pork	animal	Subcutaneous
77	P05	B leg S	Pork	animal	Subcutaneous
78	P06	C loin S	Pork	animal	Subcutaneous
79	P07	A leg IM	Pork	animal	Intramuscular
80	P08	B leg IM	Pork	animal	Intramuscular
81	P09	C leg IM	Pork	animal	Intramuscular

No	PCA name	File name	Type	Fat type	Brand (if available)
82	P10	A loin IM	Pork	animal	Intramuscular
83	P11	B loin IM	Pork	animal	Intramuscular
84	P12	C loin IM	Pork	animal	Intramuscular
85	P13	A belly IM	Pork	animal	Intramuscular
86	P14	B belly IM	Pork	animal	Intramuscular
87	P15	C belly IM	Pork	animal	Intramuscular
88	P16	A shoulder IM	Pork	animal	Intramuscular
89	P17	B shoulder IM	Pork	animal	Intramuscular
90	P18	C shoulder IM	Pork	animal	Intramuscular

Appendix C

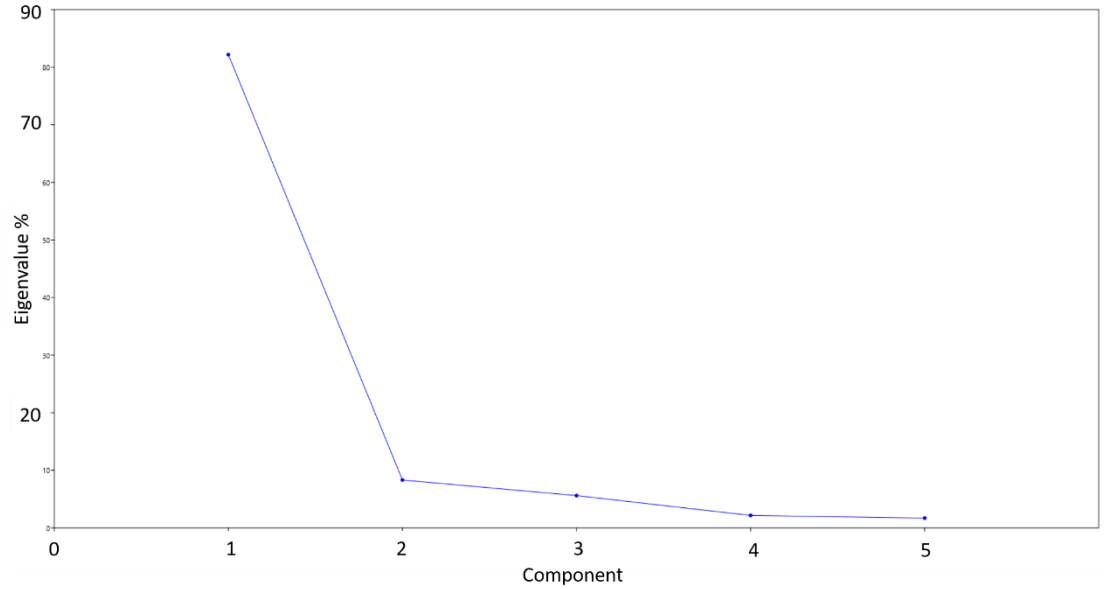

Figure C 1: Scree plot of principal components against eigenvalue for PCA Figure 4.16

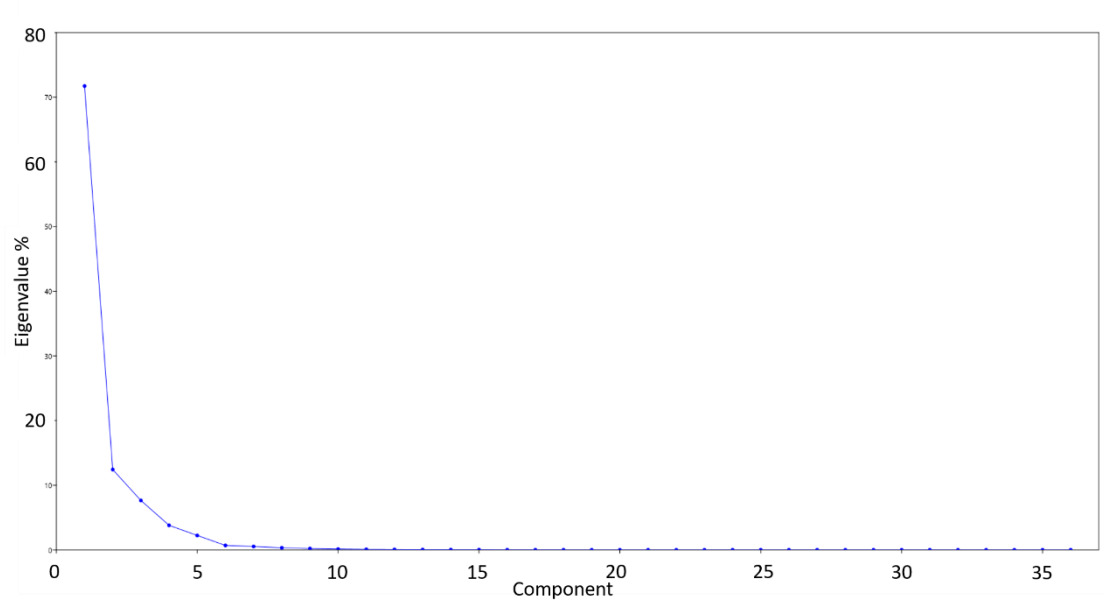

Figure C 2: Scree plot of principal components against eigenvalue for PCA Figure 5.6

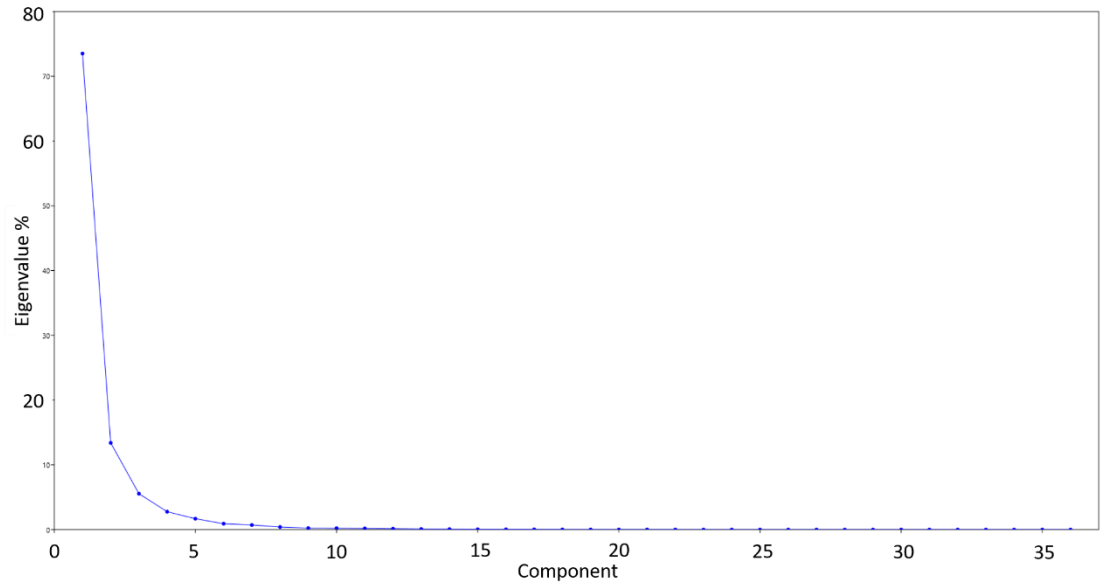

Figure C 3: Scree plot of principal components against eigenvalue for PCA Figure 5.8 and Figure 5.9

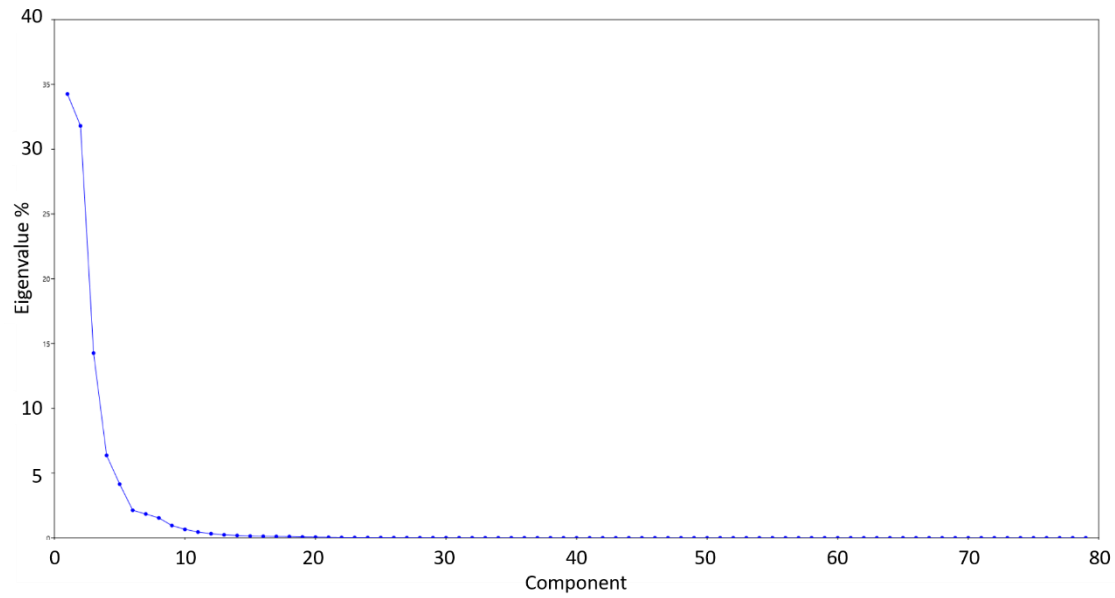

Figure C 4: Scree plot of principal components against eigenvalue for PCA Figure 5.14

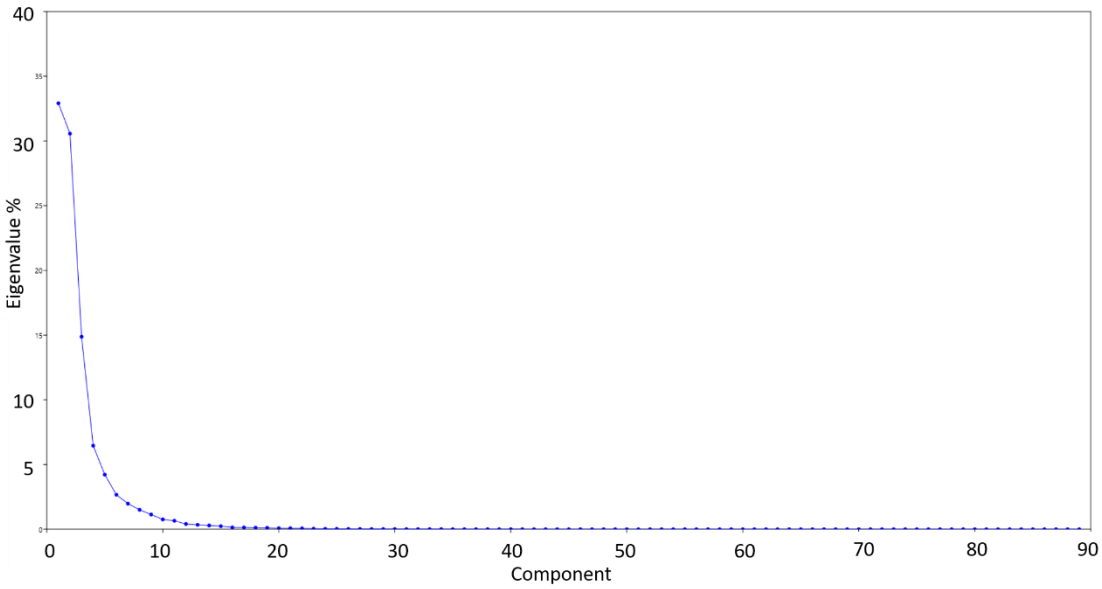

Figure C 5: Scree plot of principal components against eigenvalue for PCA Figure 6.6

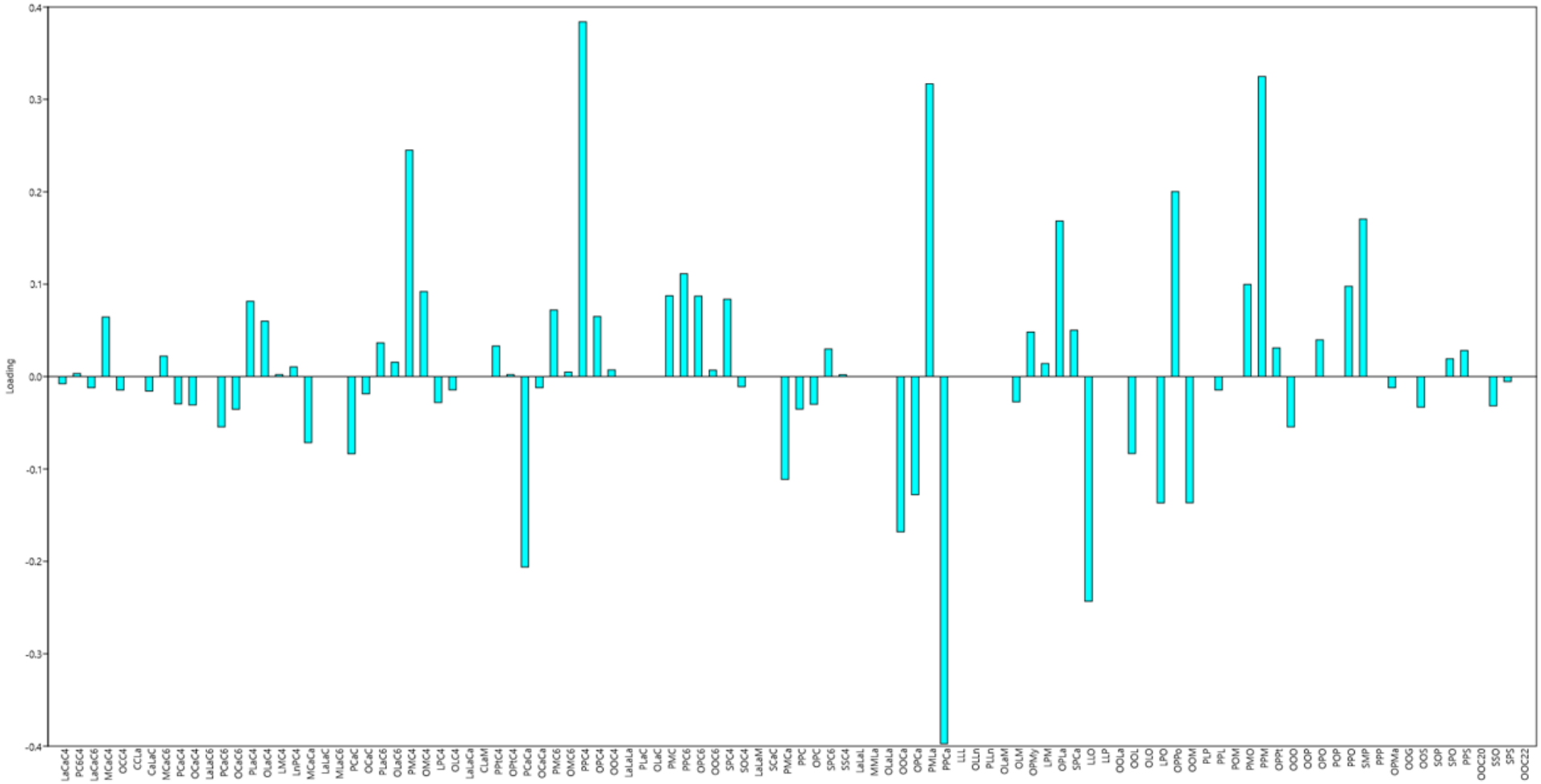

Figure C 6: PC1 loadings plot for Figure 4.16

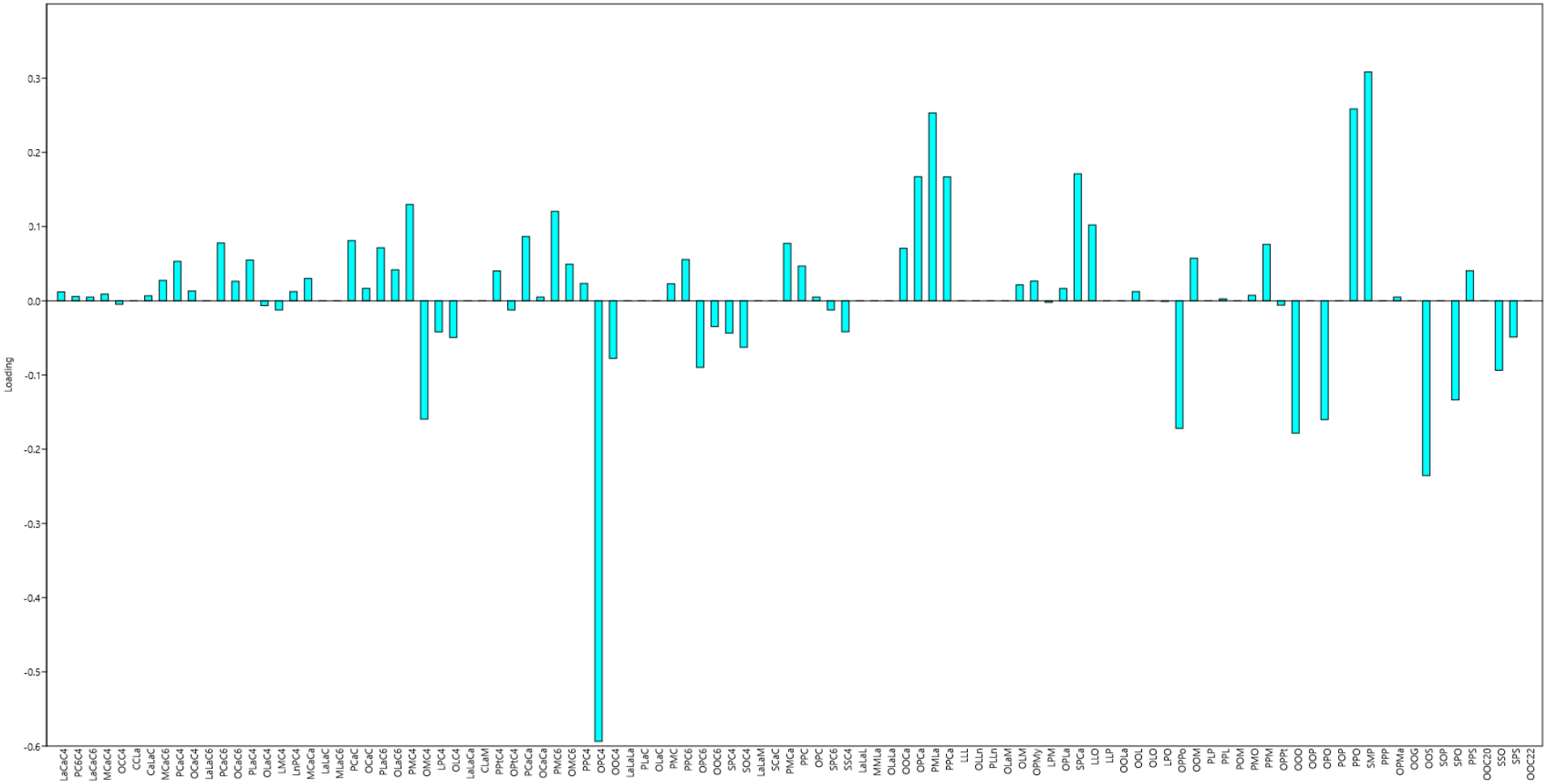

Figure C 7: PC2 loadings plot for Figure 4.16

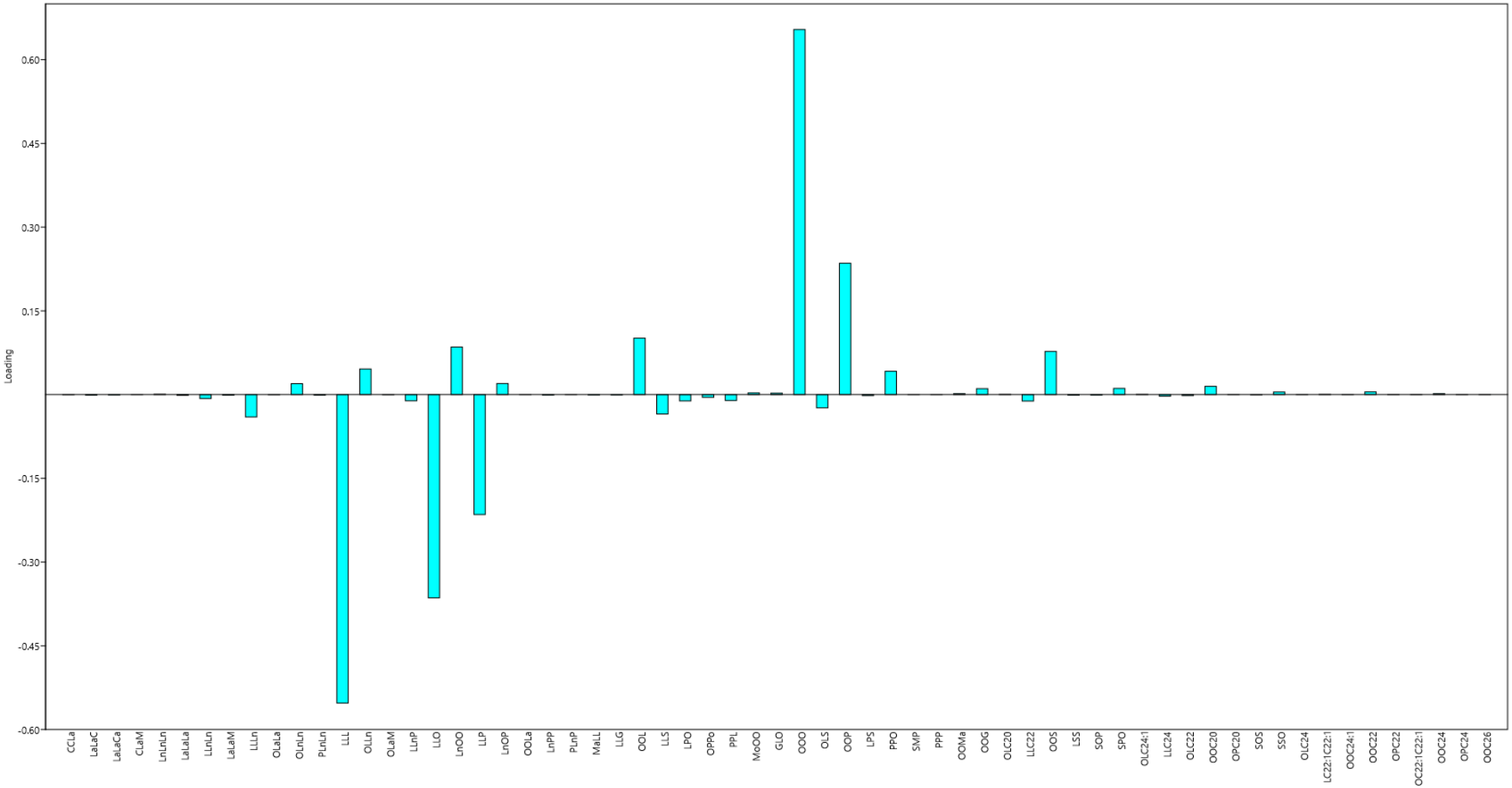

Figure C 8: PC1 loadings plot for Figure 5.6

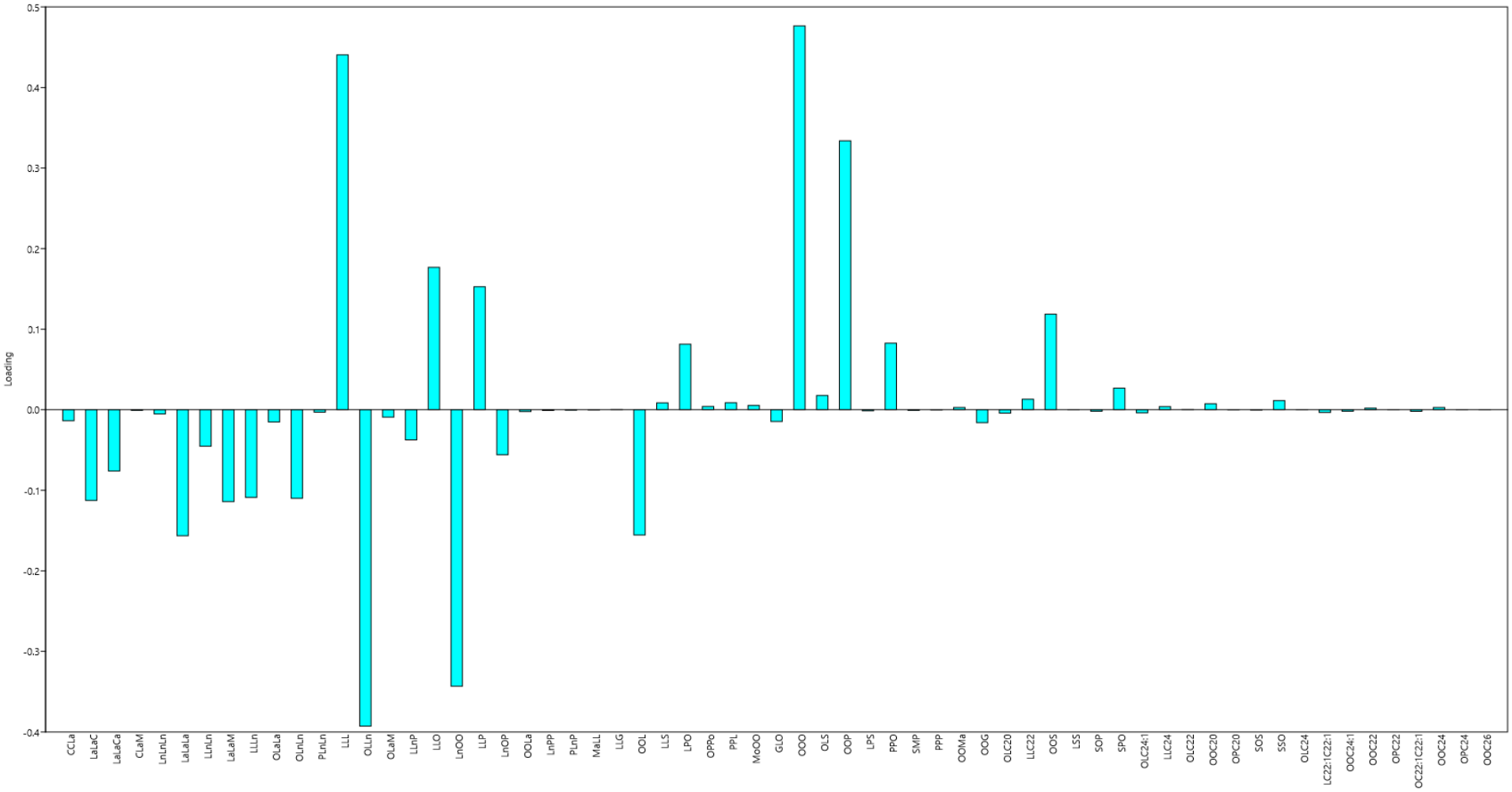

Figure C 9: PC2 loadings plot for Figure 5.6

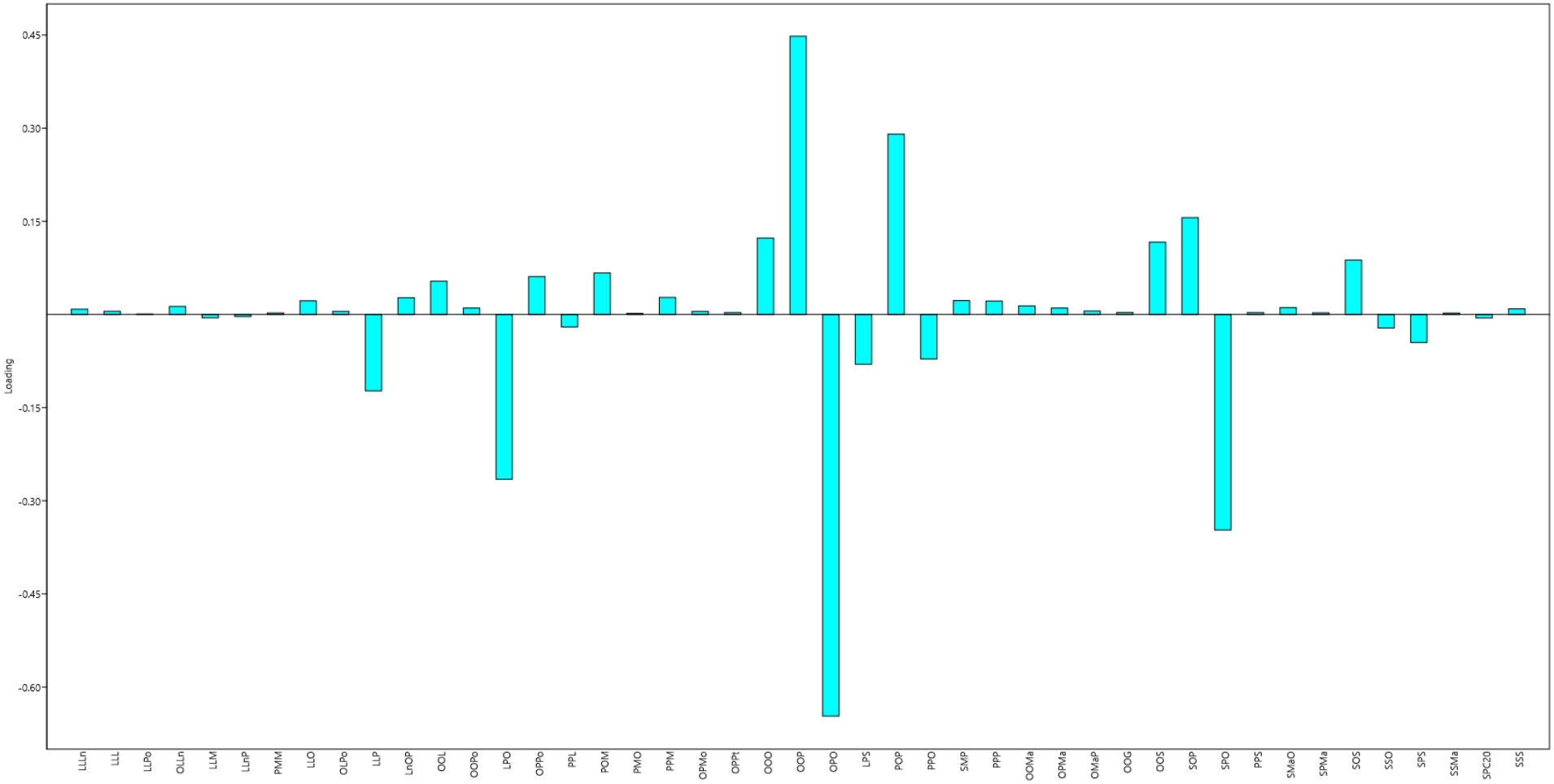

Figure C 10: PC1 loadings plot for Figure 5.8 and Figure 5.9

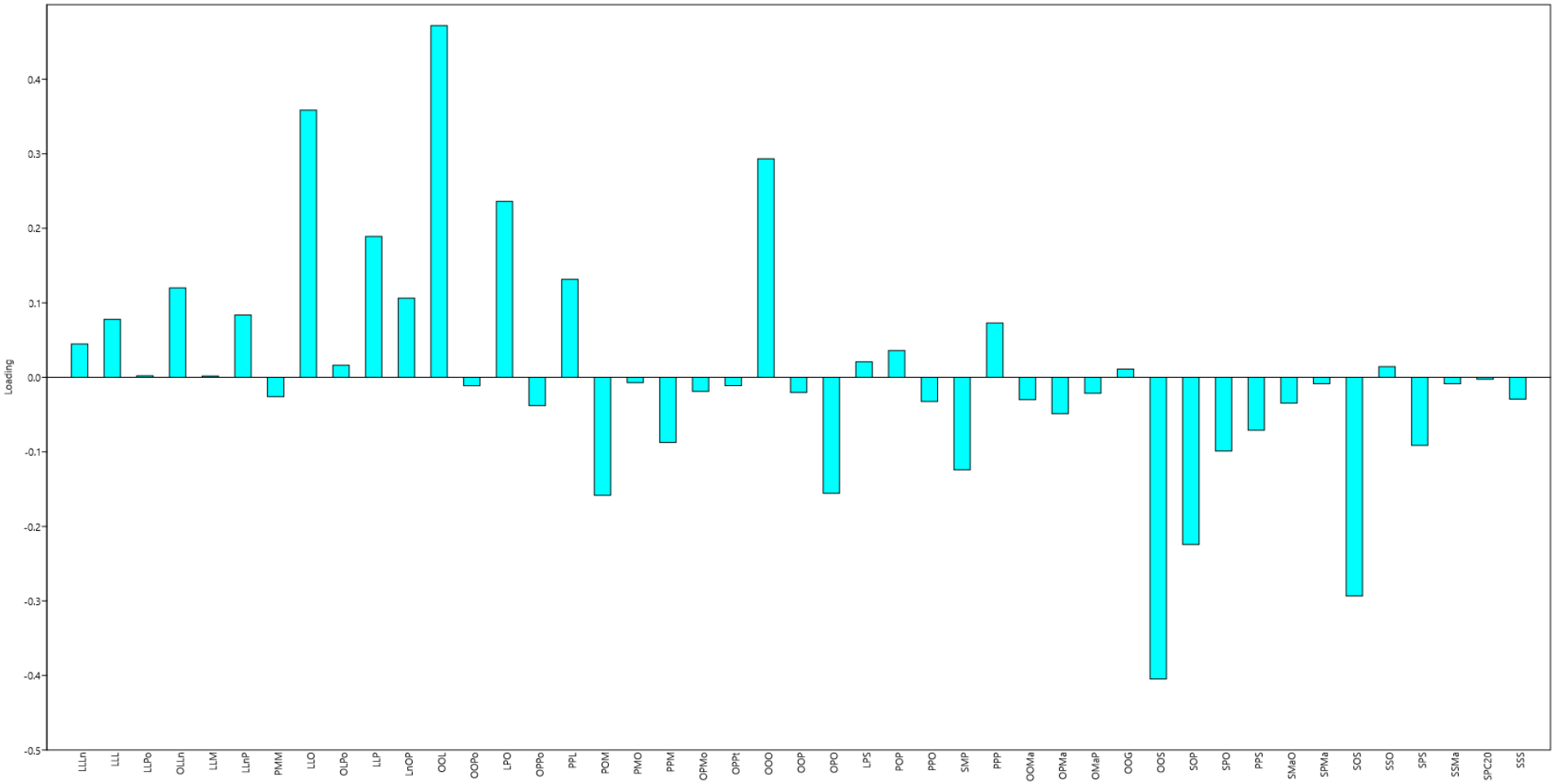

Figure C 11: PC2 loadings plot for Figure 5.8

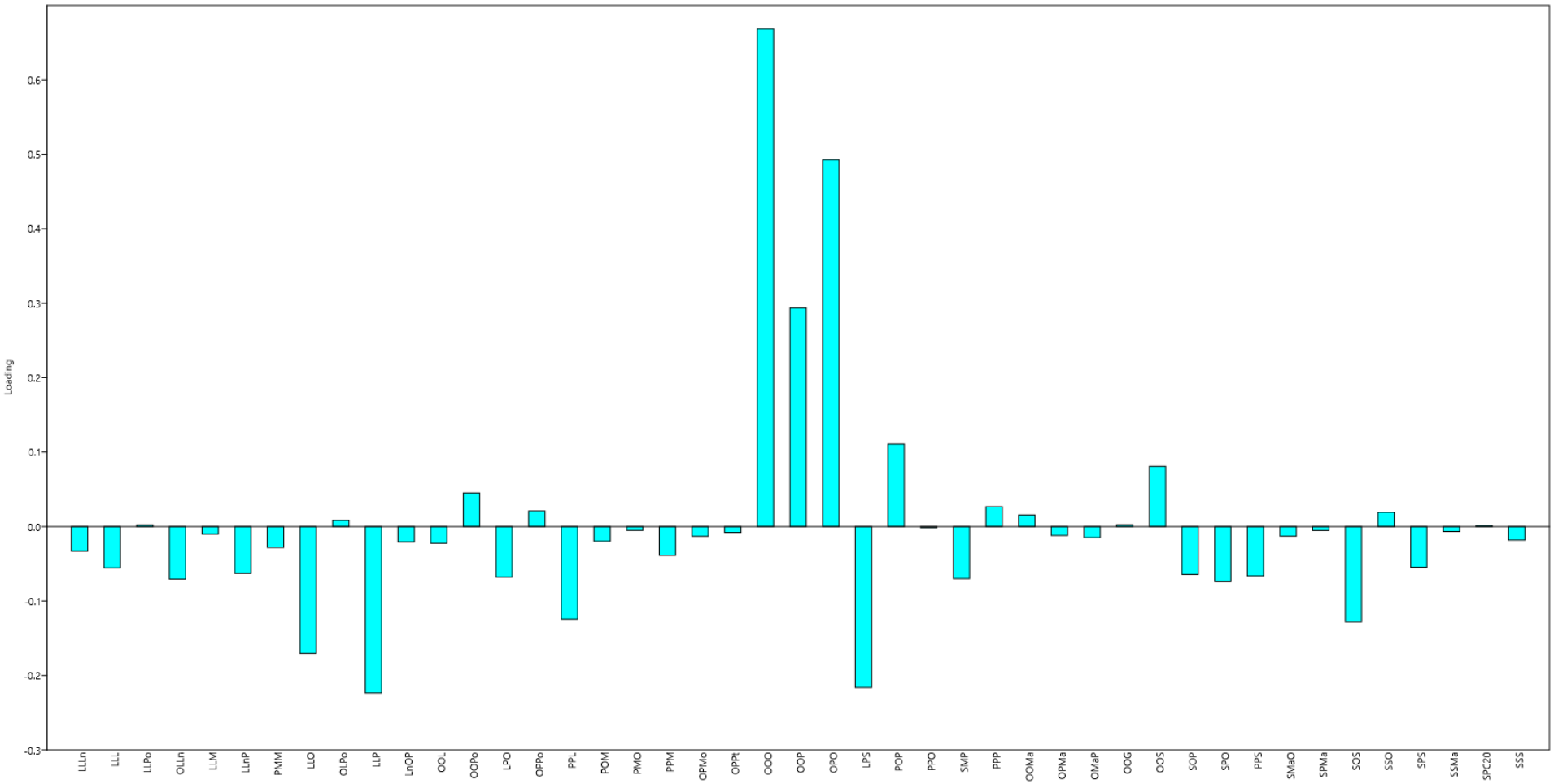

Figure C 12: PC3 loadings plot for Figure 5.8

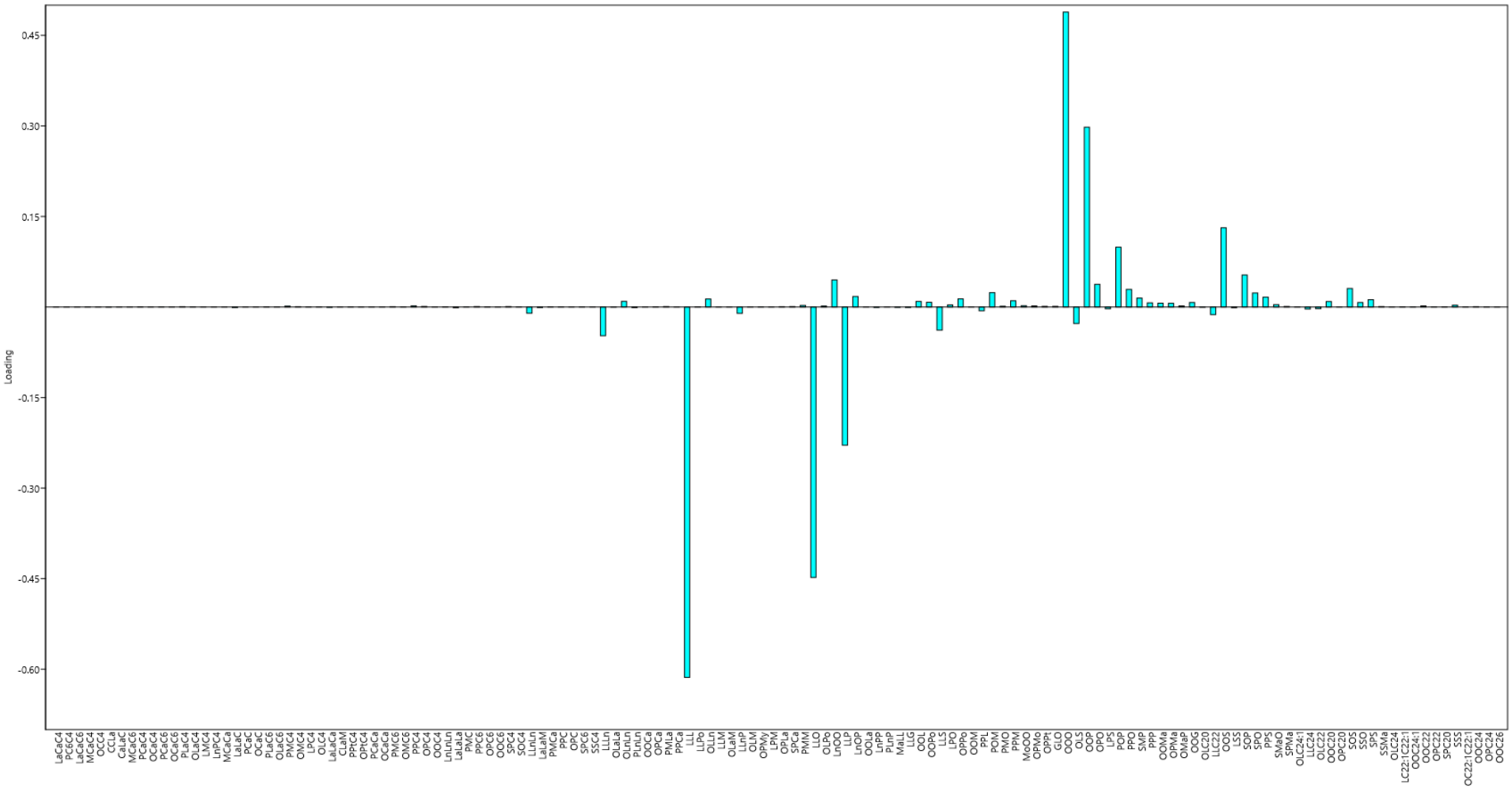

Figure C 13: PC1 loadings plot for Figure 5.14

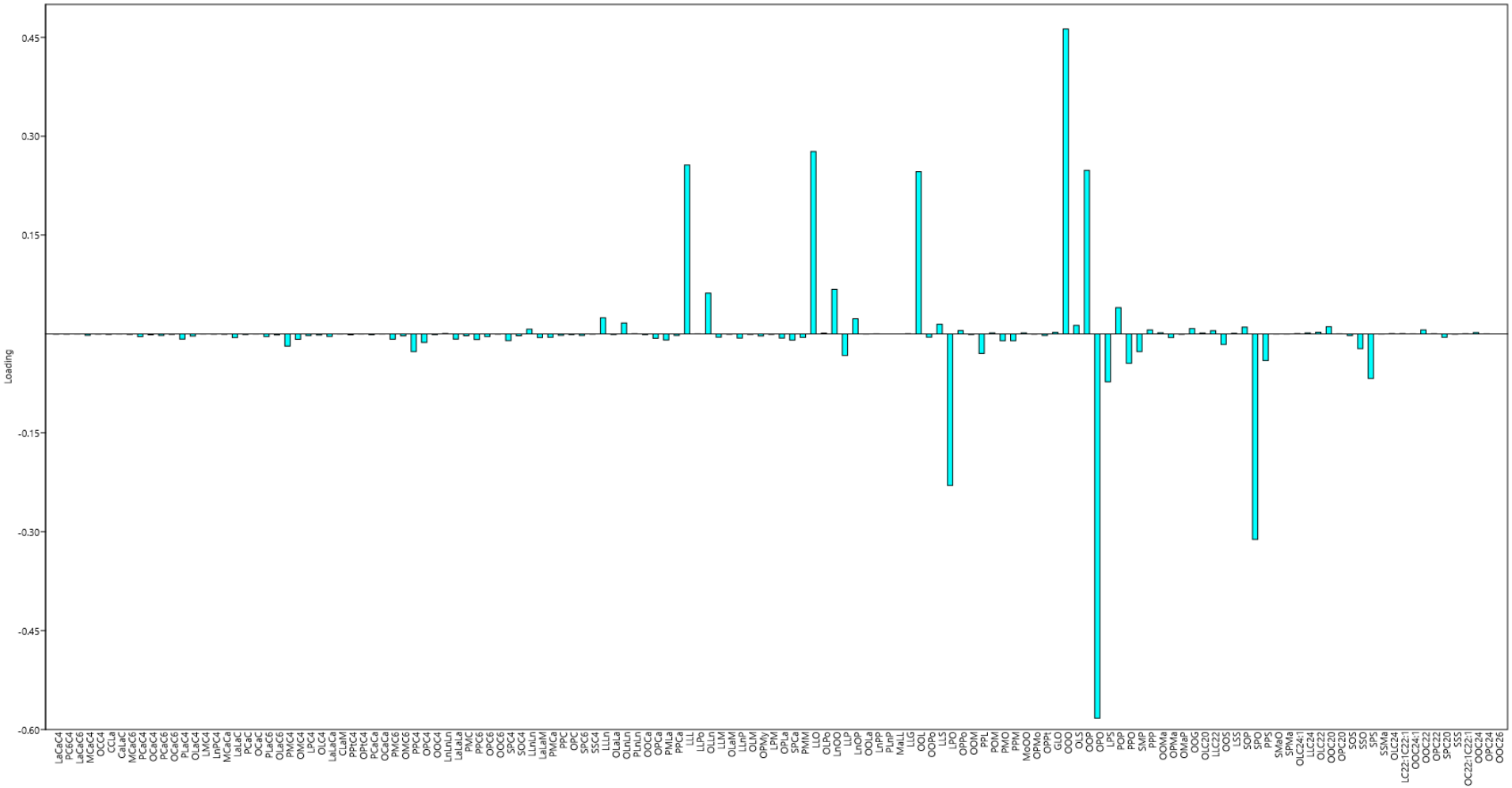

Figure C 14: PC2 loadings plot for Figure 5.14

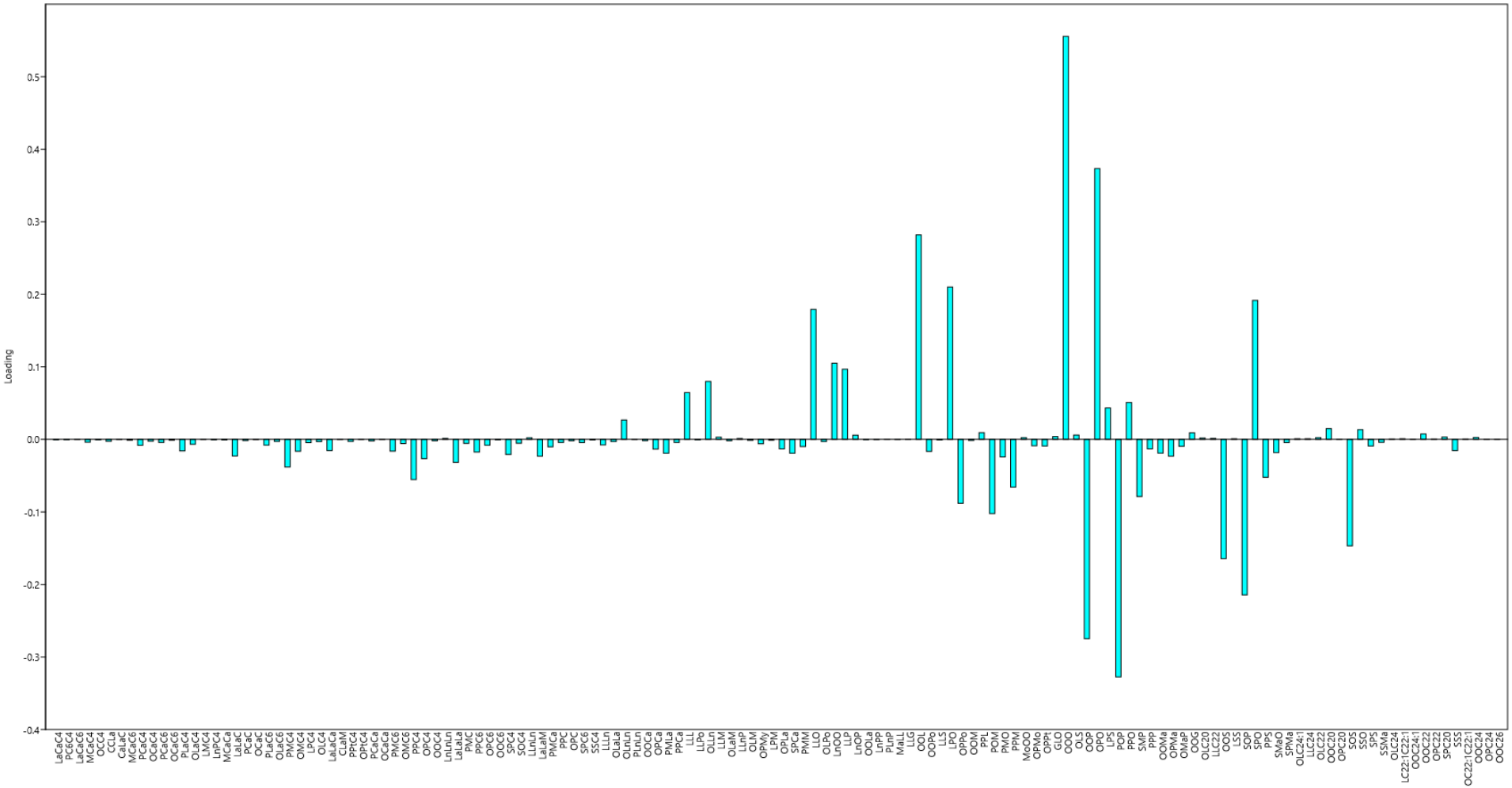

Figure C 15: PC3 loadings plot for Figure 5.14

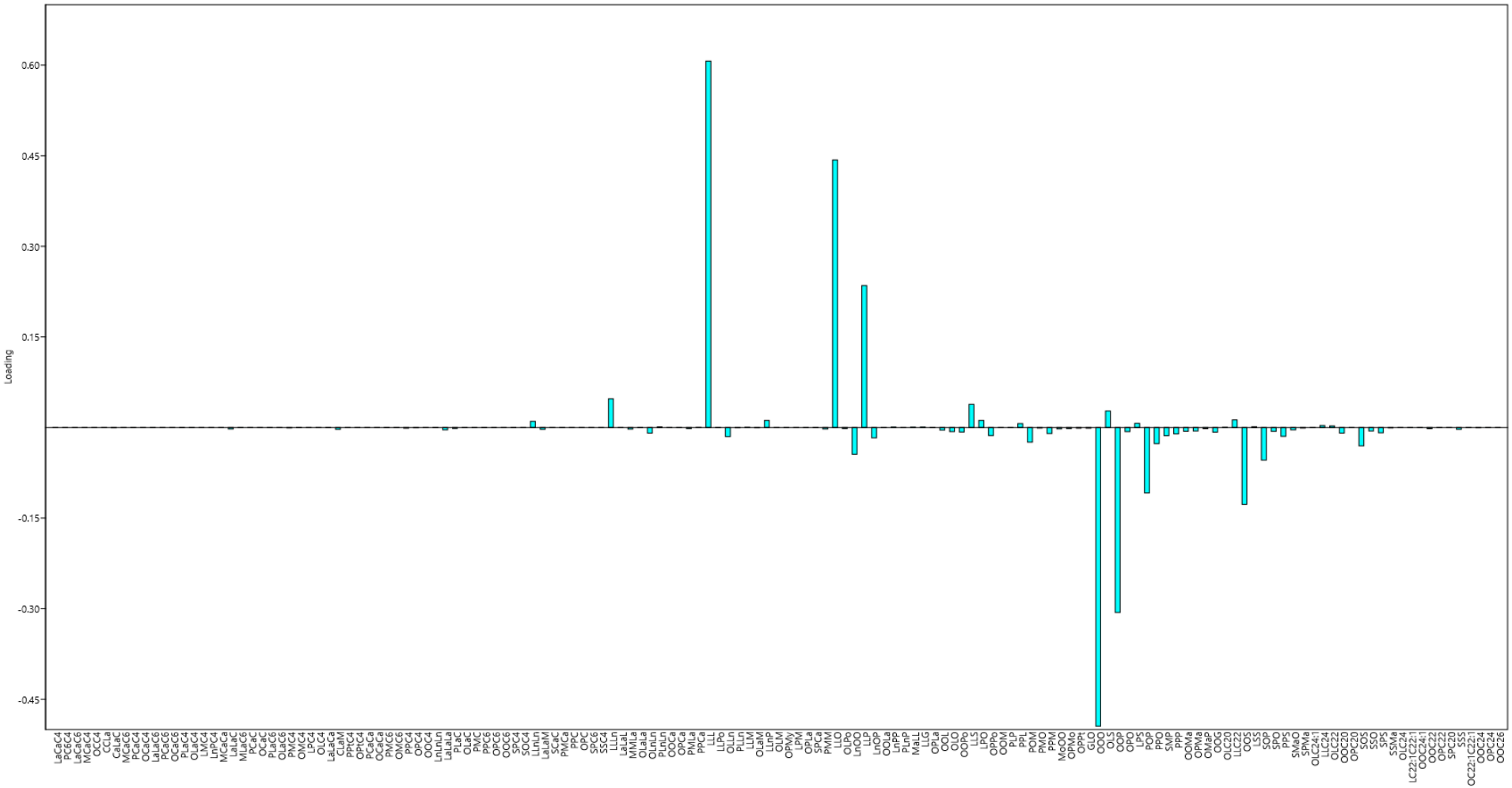

Figure C 16: PC1 loadings plot for Figure 6.6

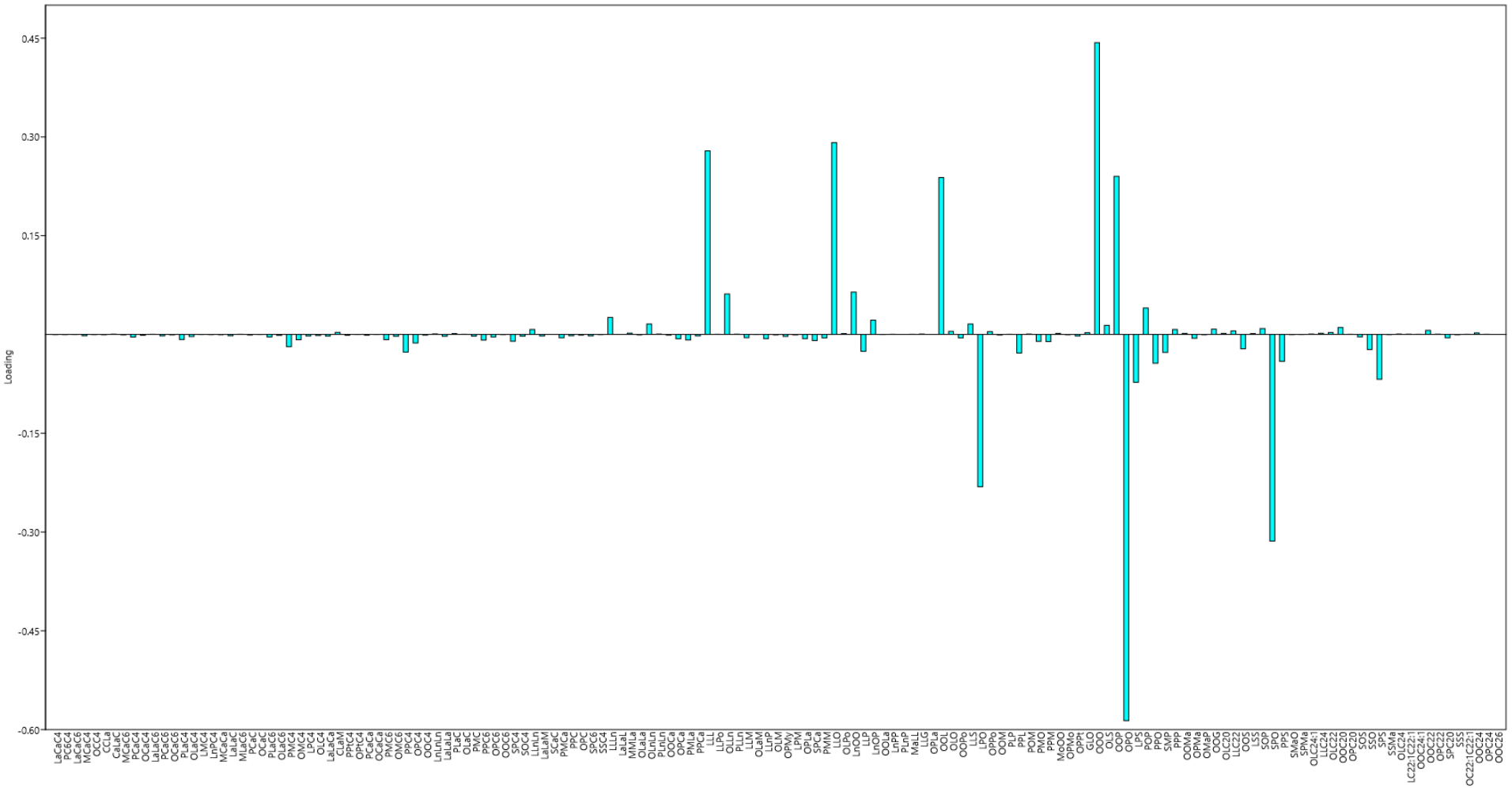

Figure C 17: PC2 loadings plot for Figure 6.6

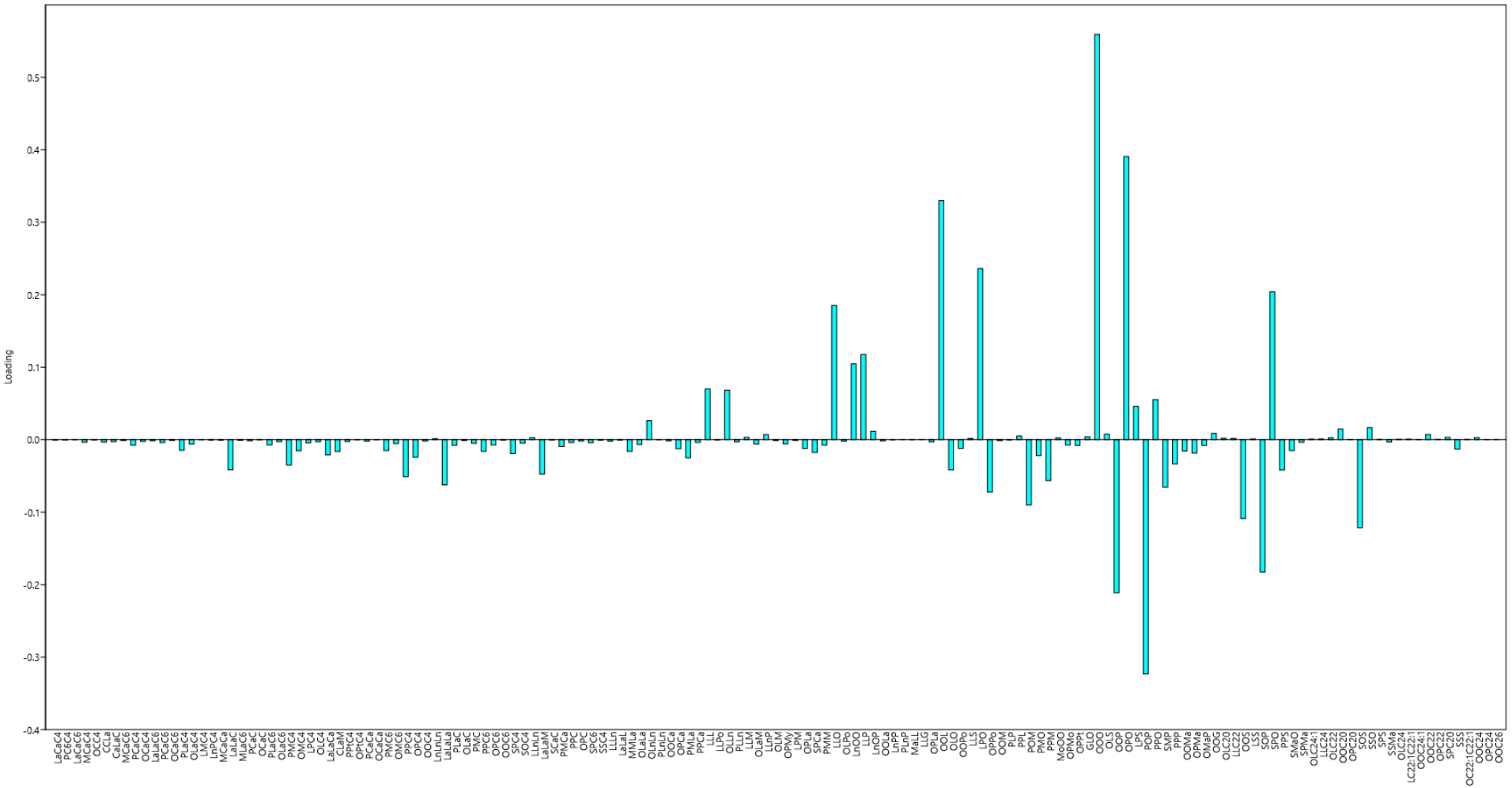

Figure C 18: PC3 loadings plot for Figure 6.6

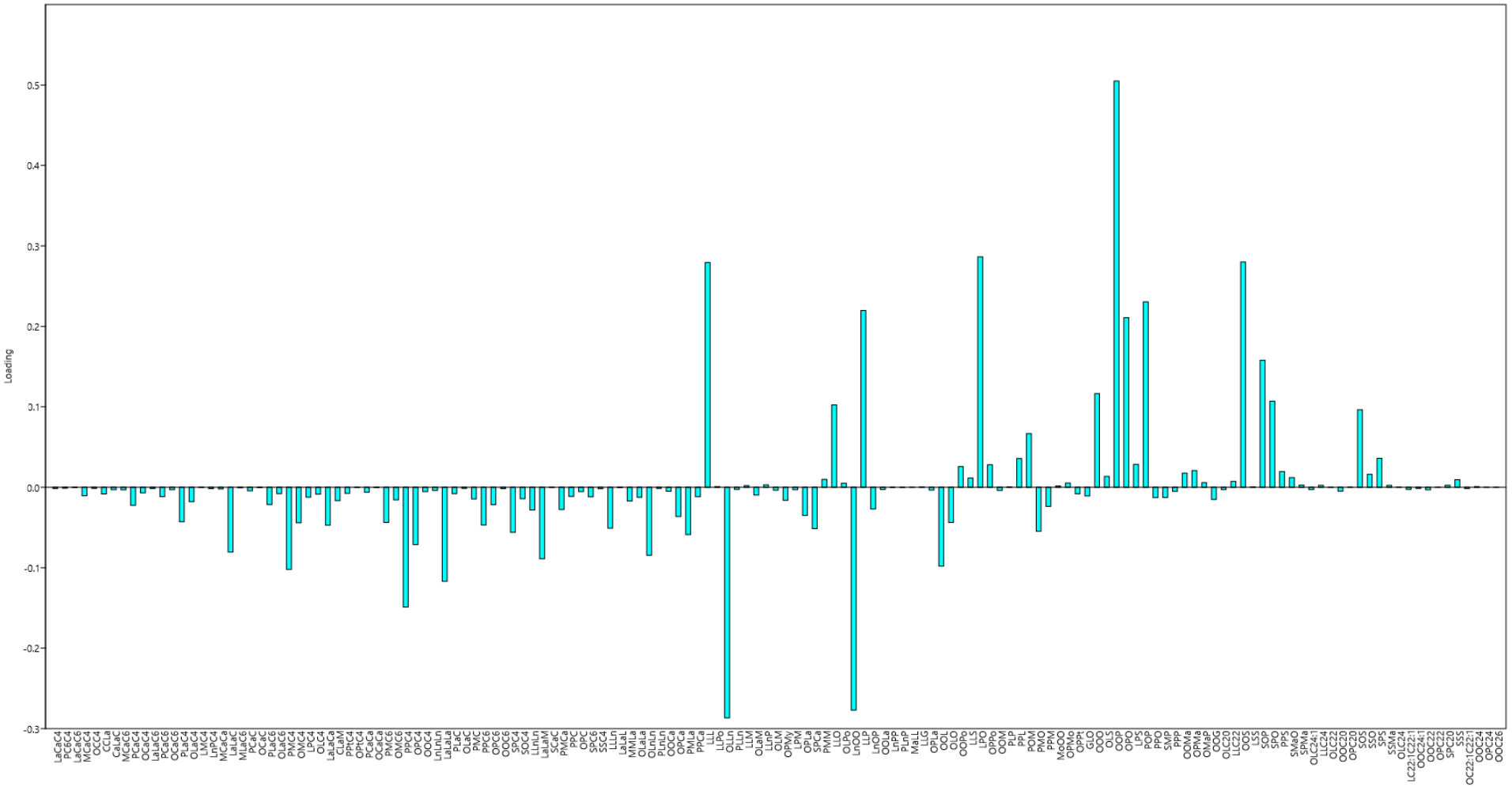

Figure C 19: PC4 loadings plot for Figure 6.6

Abbreviations

APCI atmospheric pressure chemical ionisation

BPC base peak chromatogram

CAD charged aerosol detector

CID collision induced dissociation

DAG diacylglycerols

DB double bond number

ECN equivalent carbon number

FA fatty acid

GC gas chromatography

HPLC high performance liquid chromatography

MS mass spectrometry

MS/MS tandem mass spectrometry

MS^n multistage tandem mass spectrometry

m/*z* mass to charge ratio

NARP non aqueous reverse phase

NP normal phase

PI precursor ion

PCA principal components analysis

RP reverse phase

TAG triacylglycerol

TIC total ion chromatogram

UHPLC ultra high performance liquid chromatography

References

Abrahim, A., Al-Sayah, M., Skrdla, P., Bereznitski, Y., Chen, Y., Wu, N., 2010. Practical comparison of 2.7 µm fused-core silica particles and porous sub-2 µm particles for fast separations in pharmaceutical process development. Journal of Pharmaceutical and Biomedical Analysis 51, 131–137.

Barron, L.J.R., Hierro, M.T.G., Santa-María, G., 1990. HPLC and GLC analysis of the triglyceride composition of bovine, ovine and caprine milk fat. Journal of Dairy Research 57, 517.

Beccaria, M., Oteri, M., Micalizzi, G., Bonaccorsi, I.L., Purcaro, G., Dugo, P., Mondello, L., 2016. Reuse of dairy product: evaluation of the lipid profile evolution during and after their shelf-life. Food Analytical Methods 9, 3143–3154.

Beccaria, M., Sullini, G., Cacciola, F., Donato, P., Dugo, P., Mondello, L., 2014. High performance characterization of triacylglycerols in milk and milk-related samples by liquid chromatography and mass spectrometry. Journal of chromatography. A 1360, 172–87.

Belitz, H.-D., Grosch, W., Schieberle, P., 2009. Food Chemistry. Springer Berlin Heidelberg, Berlin, Heidelberg.

Bosque-Sendra, J.M., Cuadros-Rodríguez, L., Ruiz-Samblás, C., de la Mata, A.P., 2012. Combining chromatography and chemometrics for the characterization and authentication of fats and oils from triacylglycerol compositional data--a review. Analytica chimica acta 724, 1–11.

Bravo-Lamas, L., Aldai, N., Kramer, J.K.G., Barron, L.J.R., 2018. Case study using commercial dairy sheep flocks: Comparison of the fat nutritional quality of milk produced in mountain and valley farms. LWT - Food Science and Technology 89, 374–380.

Byrdwell, W.C., Emken, E.A., 1995. Analysis of triglycerides using atmospheric pressure chemical ionization mass spectrometry. Lipids 30, 173–175.

Byrdwell, W.C., Neff, W.E., 2002. Dual parallel electrospray ionization and atmospheric pressure chemical ionization mass spectrometry (MS), MS/MS and MS/MS/MS for the analysis of triacylglycerols and triacylglycerol oxidation products. Rapid Communications in Mass Spectrometry 16, 300-319.

Coultate, T., Davies, J., 2001. Triglycerides, in: Food : The Chemistry of Its Components. Royal Society of Chemistry, Cambridge, pp. 101–102.

Dugo, P., Beccaria, M., Fawzy, N., Donato, P., Cacciola, F., Mondello, L., 2012. Mass spectrometric elucidation of triacylglycerol content of Brevoortia tyrannus (menhaden) oil using non-aqueous reversed-phase liquid chromatography under ultra high pressure conditions. Journal of chromatography. A 1259, 227–36.

Dugo, P., Fawzy, N., Cichello, F., Cacciola, F., Donato, P., Mondello, L., 2013. Stop-flow comprehensive two-dimensional liquid chromatography combined with mass spectrometric detection for phospholipid analysis. Journal of chromatography. A 1278, 46–53.

Dugo, P., Kumm, T., Cacciola, F., Dugo, G., Mondello, L., 2008. Multidimensional Liquid Chromatographic Separations Applied to the Analysis of Food Samples. Journal of Liquid Chromatography & Related Technologies 31, 1758–1807.

Dugo, P., Kumm, T., Fazio, A., Dugo, G., Mondello, L., 2006. Determination of beef tallow in lard through a multidimensional off-line non-aqueous reversed phase–argentation LC method coupled to mass spectrometry. Journal of Separation Science 29, 567–575.

Dugo, P., Kumm, T., Lo Presti, M., Chiofalo, B., Salimei, E., Fazio, A., Cotroneo, A., Mondello, L., 2005. Determination of triacylglycerols in donkey milk by using high performance liquid chromatography coupled with atmospheric pressure chemical ionization mass spectrometry. Journal of Separation Science 28, 1023–1030.

Evershed, R.P., Dudd, S.N., Copley, M.S., Berstan, R., Stott, A.W., Mottram, H., Buckley, S.A., Crossman, Z., 2002. Chemistry of archaeological animal fats. Accounts of chemical research 35, 660–8.

Fauconnot, L., Hau, J., Aeschlimann, J.-M., Fay, L.-B., Dionisi, F., 2004. Quantitative analysis of triacylglycerol regioisomers in fats and oils using reversed-phase high-performance liquid chromatography and atmospheric pressure chemical ionization mass spectrometry. Rapid communications in mass spectrometry : RCM 18, 218–224.

Gastaldi, D., Medana, C., Giancotti, V., Aigotti, R., Dal Bello, F., Baiocchi, C., 2011. HPLC-APCI analysis of triacylglycerols in milk fat from different sources. European Journal of Lipid Science and Technology 113, 197–207.

Gotoh, N., Matsumoto, Y., Nagai, T., Mizobe, H., Otake, I., Ichioka, K., Kuroda, I., Watanabe, H., Noguchi, N., Wada, S., 2011. Actual ratios of triacylglycerol positional isomers consisting of saturated and highly unsaturated fatty acids in fishes and marine mammals. Food Chemistry 127, 467-472,

Harkewicz, R., Dennis, E.A., 2011. Applications of mass spectrometry to lipids and membranes. Annual review of biochemistry 80, 301–325.

Hasan, H., 2010. Development of an LC-MS / MS method for the analysis of triacylglycerols from meat and application in the discrimination of cooked meat products. Thesis at University of York.

Herrero, M., Ibáñez, E., Cifuentes, A., Bernal, J., 2009. Multidimensional chromatography in food analysis. Journal of chromatography. A 1216, 7110–29.

Holcapek, M., Jandera, P., Zderadicka, P., Hrubá, L., 2003. Characterization of triacylglycerol and diacylglycerol composition of plant oils using high-performance liquid chromatography-atmospheric pressure chemical ionization mass spectrometry. Journal of Chromatography. A 1010, 195-215.

Holčapek, M., Lísa, M., Jandera, P., Kabátová, N., 2005. Quantitation of triacylglycerols in plant oils using HPLC with APCI-MS, evaporative light-scattering, and UV detection. Journal of Separation Science 28, 1315–1333.

Indrasti, D., Che Man, Y.B., Mustafa, S., Hashim, D.M., 2010. Lard detection based on fatty acids profile using comprehensive gas chromatography hyphenated with time-of-flight mass spectrometry. Food Chemistry 122, 1273–1277.

Jakab, A., Nagy, K., Héberger, K., Vékey, K., Forgács, E., 2002. Differentiation of vegetable oils by mass spectrometry combined with statistical analysis. Rapid communications in mass spectrometry : RCM 16, 2291–7.

Kallio, H., Yli-Jokipii, K., Kurvinen, J.P., Sjövall, O., Tahvonen, R., 2001. Regioisomerism of triacylglycerols in lard, tallow, yolk, chicken skin, palm oil, palm olein, palm stearin, and a transesterified blend of palm stearin and coconut oil analyzed by tandem mass spectrometry. Journal of Agricultural and Food Chemistry 49, 3363–3369.

Kalo, P., Kemppinen, A., Ollilainen, V., Kuksis, A., 2004. Regiospecific determination of short-chain triacylglycerols in butterfat by normal-phase HPLC with on-line electrospray-tandem mass spectrometry. Lipids 39, 915–28.

Kalo, P.J., Kemppinen, A., 2012. Regiospecific analysis of TAGs using chromatography, MS, and chromatography-MS. European Journal of Lipid Science and Technology 114, 399–411.

Koletzko, B., Rodriguez-Palmero, M., Demmelmair, H., Fidler, N., Jensen, R., Sauerwald, T., 2001. Physiological aspects of human milk lipids. Early Human Development 65, S3–S18.

Kuksis, A., Itabashi, Y., 2005. Regio- and stereospecific analysis of glycerolipids. Methods (San Diego, Calif.) 36, 172–85.

Linderborg, K.M., Kalpio, M., Mäkelä, J., Niinikoski, H., Kallio, H.P., Lagström, H., 2014. Tandem mass spectrometric analysis of human milk triacylglycerols from normal weight and overweight mothers on different diets. Food chemistry 146, 583–90.

Lísa, M., Lynen, F., Holcapek, M., Sandra, P., 2007. Quantitation of triacylglycerols from plant oils using charged aerosol detection with gradient compensation. Journal of chromatography. A 1176, 135–42.

Lísa, M., Netušilová, K., Franěk, L., Dvořáková, H., Vrkoslav, V., Holčapek, M., 2011. Characterization of fatty acid and triacylglycerol composition in animal fats using silver-ion and non-aqueous reversed-phase high-performance liquid chromatography/mass spectrometry and gas chromatography/flame ionization detection. Journal of chromatography. A 1218, 7499–510.

Liu, Z., Rochfort, S., Cocks, B., 2018. Milk lipidomics: What we know and what we don't. Progress in Lipid Research 71, 70-85.

Long, A.C., Kaiser, J.L., Katz, G.E., 2013. Lipids in infant formulas: Current and future innovations. Lipid Technology 25, 127–129.

Lopez, C., Briard-Bion, V., Bourgaux, C., Pérez, J., 2013. Solid triacylglycerols within human fat globules: β crystals with a melting point above in-body temperature of infants, formed upon storage of breast milk at low temperature. Food Research International 54, 1541–1552.

Makarov, A., Scigelova, M., 2010. Coupling liquid chromatography to Orbitrap mass spectrometry. Journal of Chromatography A 1217, 3938-45.

Marikkar, J.M.N., Ghazali, H.M., Che Man, Y.B., Peiris, T.S.G., Lai, O.M., 2005. Distinguishing lard from other animal fats in admixtures of some vegetable oils using liquid chromatographic data coupled with multivariate data analysis. Food Chemistry 91, 5–14.

Mirabaud, S., Rolando, C., Regert, M., 2007. Molecular criteria for discriminating adipose fat and milk from different species by NanoESI MS and MS/MS of their triacylglycerols: application to archaeological remains. Analytical chemistry 79, 6182–92.

Morera, S., Castellote, A.I., Jauregui, O., Casals, I., López-Sabater, M.C., 2003. Triacylglycerol markers of mature human milk. European journal of clinical nutrition 57, 1621–6.

Mottram, H.R., Evershed, R.P., 1996. Structure analysis of triacylglycerol positional isomers using atmospheric pressure chemical ionisation mass spectrometry. Tetrahedron Letters 37, 8593-8596.

Mottram, H.R., Crossman, Z.M., Evershed, R.P., 2001. Regiospecific characterisation of the triacylglycerols in animal fats using high performance liquid chromatography-atmospheric pressure chemical ionisation mass spectrometry. The Analyst 126, 1018–1024.

Mottram, H.R., Evershed, R.P., 2001. Elucidation of the composition of bovine milk fat triacylglycerols using high-performance liquid chromatography–atmospheric pressure chemical ionisation mass spectrometry. Journal of Chromatography A 926, 239–253.

Nájera, A.I., Barcina, Y., de Renobales, M., Barron, L.J.R., 1998. Determination of triacylglycerol composition of idiazabal cheese. Chromatographia 47, 579–586.

Nájera, A.I., Barcina, Y., de Renobales, M., Barron, L.J.R., 1998. Changes in Triacylglycerols during the Ripening of Idiazabal Cheese. Journal of Agricultural and Food Chemistry 46, 3252–3256.

Núñez, O., Gallart-Ayala, H., Martins, C. P. B, Lucci, 2012. New Trends in Fast Liquid Chromatography for Food and Environmental Analysis. Journal of chromatography. A 1228, 298-323.

Pande, G., Sabir, J.S.M., Baeshen, N.A., Akoh, C.C., 2013. Synthesis of Infant Formula Fat Analogs Enriched with DHA from Extra Virgin Olive Oil and Tripalmitin. Journal of the American Oil Chemists' Society 90, 1311–1318.

Pickering, M. D., Ghislandi, S., Usai, M. R., Wilson, C., Connelly, P., Brothwell, D. R., Keely, B. J., 2018. Signatures of degraded body tissues and environmental conditions in grave soils from a Roman and an Anglo-Scandinavian age burial from Hungate, York. Journal of Archaeological Science 99, 87-98.

Regert, M., 2011. Analytical strategies for discriminating archeological fatty substances from animal origin. Mass spectrometry reviews 30, 177–220.

Rodriguez-Aller, M., Gurny, R., Veuthey, J., Guillarme, D., 2013. Coupling Ultra High-pressure Liquid Chromatography with Mass Spectrometry: Constraints and Possible Applications. Journal of Chromatography A 1292, 2-18.

Rohman, A., Che Man, Y.B., 2012. Analysis of Pig Derivatives for Halal Authentication Studies. Food Reviews International 28, 97–112.

Romeu-Nadal, M., Morera-Pons, S., Castellote, A., López-Sabater, M., 2004. Comparison of two methods for the extraction of fat from human milk. Analytica Chimica Acta 513, 457–461.

Ruiz-Gutiérrez, V., Barron, L.J.R., 1995. Methods for the analysis of triacylglycerols. Journal of Chromatography B: Biomedical Sciences and Applications 671, 133–168.

Sala-Vila, A., Castellote, A.I., Rodriguez-Palmero, M., Campoy, C., López-Sabater, M.C., 2005. Lipid composition in human breast milk from Granada (Spain): changes during lactation. Nutrition (Burbank, Los Angeles County, Calif.) 21, 467–73.

Saliu, F., Modugno, F., Orlandi, M., Colombini, M.P., 2011. HPLC-APCI-MS analysis of triacylglycerols (TAGs) in historical pharmaceutical ointments from the eighteenth century. Analytical and bioanalytical chemistry 401, 1785–800.

Smit, E.N., Martini, I.A., Mulder, H., Boersma, E.R., Muskiet, F.A.J., 2002. Estimated biological variation of the mature human milk fatty acid composition. Prostaglandins, Leukotrienes and Essential Fatty Acids 66, 549–555.

Sun, C., Wei, W., Zou, X., Huang, J., Jin, Q., Wang, X., 2018. Evaluation of sn-2 fatty acid composition in commercial infant formulas on the Chinese market: A comparative study based on fat source and stage. Food Chemistry 252, 154–162.

Ten-Doménech, I., Beltrán-Iturat, E., Herrero-Martínez, J.M., Sancho-Llopis, J.V., Simo-Alfonso, E.F., 2015. Triacylglycerol Analysis in Human Milk and Other Mammalian Species: Small-Scale Sample Preparation, Characterization and Statistical Classification Using HPLC-ELSD Profiles. Journal of Agricultural and Food Chemistry 63, 5761-70.

Tu, A., Ma, Q., Bai, H., Du, Z., 2017. A comparative study of triacylglycerol composition in Chinese human milk within different lactation stages and imported infant formula by SFC coupled with Q-TOF-MS. Food Chemistry 221, 555–567.

Vaclavik, L., Hrbek, V., Cajka, T., Rohlik, B.-A., Pipek, P., Hajslova, J., 2011. Authentication of animal fats using direct analysis in real time (DART) ionization-mass spectrometry and chemometric tools. Journal of Agricultural and Food Chemistry 59, 5919–26.

Vehovec, T., Obreza, A., 2010. Review of operating principle and applications of the charged aerosol detector. Journal of chromatography. A 1217, 1549-56.

Villaseñor, A., Garcia-Perez, I., Garcia, A., Posma, J.M., Fernández-López, M., Nicholas, A.J., Modi, N., Holmes, E., Barbas, C., 2014. Breast milk metabolome characterization in a single-phase extraction, multiplatform analytical approach. Analytical chemistry 86,

8245–52.

Zou, X.-Q., Huang, J.-H., Jin, Q.-Z., Guo, Z., Liu, Y.-F., Cheong, L.-Z., Xu, X.-B., Wang, X.-G., 2013. Model for Human Milk Fat Substitute Evaluation Based on Triacylglycerol Composition Profile. Journal of Agricultural and Food Chemistry 61, 167–175.

Zou, X., Huang, J., Jin, Q., Guo, Z., Liu, Y., Cheong, L., Xu, X., Wang, X., 2013a. Characterization and Oxidative Stability of Human Milk Fat Substitutes Enzymatically Produced from Palm Stearin. Journal of the American Oil Chemists' Society 91, 481–495.

Zou, X., Huang, J., Jin, Q., Guo, Z., Liu, Y., Cheong, L., Xu, X., Wang, X., 2013b. Lipid composition analysis of milk fats from different mammalian species: potential for use as human milk fat substitutes. Journal of agricultural and food chemistry 61, 7070–80.